INCLUSION PROPERTIES OF HYDROXY HOST COMPOUNDS.

Thesis submitted to the

University of Cape Town

for the degree of

Doctor of Philosophy.

Susan Ann Bourne

Department of Chemistry
University of Cape Town
Rondebosch
7700
South Africa

September 1991

ACKNOWLEDGEMENTS.

My thanks go to :

Professor L. Nassimbeni for constant guidance and for many interesting chemical and non-chemical discussions.

Dr Margi Niven for her help and advice.

"This work would not have been possible without the incisive guidance and loving kinship of Louise Johnson and Janet Scott. To them I extend my fondest thanks."

My mother for worrying about me.

The Foundation for Research Development and the University of Cape Town for financial support.

PUBLICATIONS AND CONFERENCE PROCEEDINGS.

Parts of this thesis have been published :

1. "Complexation with Diol Host Compounds Part 2. Structures of 1,1,2,2-Tetraphenylethane-1,2-diol and its 1:2 Molecular Inclusion Complex with Dimethylsulphoxide." D. R. Bond; S. A. Bourne; L. R. Nassimbeni; F. Toda. *J. Crystallogr. Spectrosc. Res.* **19(5)**, 809, (1989).

2. "Selective Inclusion of Ethanol by Triphenylsilanol. Crystal structure and Thermal Analysis." S. A. Bourne; L. R. Nassimbeni; K. Skobridis; E. Weber. *J. Chem. Soc., Chem. Commun.* 282, (1991).

3. "Complexation with Diol Host Compounds, Part 7. Structures and Thermal Analysis of 1,1,2,2-Tetraphenylethane-1,2-diol with Lutidine guests." S. A. Bourne; L. R. Nassimbeni; F. Toda. *J. Chem. Soc., Perkin Trans. II.* in Press.

4. "Complexation with Hydroxy Host Compounds, Part 3. Structures and Thermal Analysis of the Inclusion Compounds of Tri-1-naphthylsilanol with Toluene, *o*-Xylene, *m*-Xylene and *p*-Xylene." S. A. Bourne; L. R. Nassimbeni; K. Skobridis; E. Weber. In preparation.

5. "Complexation with Hydroxy Host Compounds, Part 4. Structures and Thermal Stabilities of Inclusion Compounds with dioxane as guest." S. A. Bourne; L. Johnson; C. Marais; L. R. Nassimbeni; K. Skobridis; E. Weber; F. Toda. *J. Chem. Soc., Perkin Trans. II.* in Press.

Parts of this thesis have been presented at the following :

9th International Conference on the Chemistry of the Organic Solid State, Como, Italy, 2 - 7 July 1989.

South African Chemical Institute Young Chemist's meeting, Fine Chemicals Corp. (Pty) Ltd., Cape Town, 17 May 1990.

XVth Congress of the International Union of Crystallography, Bordeaux, France, 19 - 28 July 1990.

31st South African Chemical Institute Convention, Grahamstown, 23 - 27 June 1991.

ABSTRACT

Inclusion compounds can be defined as those in which one type of molecule is able to enclose another molecule (usually smaller) within its structure, leaving the bonding systems of both components unchanged. The molecular network and the enclosed species are usually referred to as the "host" and "guest" respectively.

The ability of four hydroxyl-containing molecules to form inclusion compounds was studied. Each of these molecules has a tetrahedral carbon or silicon atom bonded to an hydroxyl group and shielded by two or three aromatic moieties. The bulkiness of these molecules prevents them from crystallizing in a close-packed fashion while the hydroxyl groups enable them to participate in hydrogen bonding.

The formation and characterisation by single crystal X-ray diffraction methods of two non-porous α-phase compounds and eighteen inclusion compounds have been described. The inclusion compounds were divided into four classes :

Class A consisted of compounds of 1,1,2,2-tetraphenylethane-1,2-diol,
Class B consisted of compounds of triphenylmethanol,
Class C consisted of compounds of triphenylsilanol and
Class D consisted of compounds of tri-1-naphthylsilanol.

A number of guest compounds were chosen. Most had at least one atom which could act as an acceptor in a hydrogen bond. Hydrogen bonding (host-host, host-guest or a combination of these) proved to be the greatest stabilizing force in these compounds.

The shape and size of the cavities available for guests were analysed by means of volume calculations.

The thermal decomposition of the inclusion compounds was studied by Thermogravimetry (TG) and Differential Scanning Calorimetry (DSC), to determine the forces holding the guest within the structure and the changes in the host lattice as the guest was desorbed. X-ray powder diffraction methods were also used to confirm phase changes that occurred with guest loss. In addition, Thermogravimetry was used to determine the activation energy of the guest desorption process.

1,1,2,2-Tetraphenylethane-1,2-diol was shown to include 3,5-lutidine preferentially from mixtures of 2,6- and 3,5-lutidine, provided that the mole fraction of 3,5-lutidine exceeded 0.30. Triphenylsilanol was selective to ethanol from equimolar mixtures of ethanol and other simple alcohols. Ethanolic solutions of up to 40%(w/w) water also yielded only the 4:1 triphenylsilanol•ethanol complex.

Host-guest interactions were quantified using the method of atom-pair potentials. The position of the guest molecule was varied to allow a minimum potential energy to be calculated. Comparison across a series of related inclusion compounds showed a qualitative correlation between the enthalpy of guest release, ΔH (measured by DSC), and the minimum potential energy of the guest within the crystal structure.

ABBREVIATIONS.

H	Host
G	Guest
e.s.d.	estimated standard deviation
s.o.f.	site occupancy factor
TG	Thermogravimetry
DSC	Differential Scanning Calorimetry
m.p.	melting point
b.p.	boiling point
XRD	X-ray powder diffraction

TABLE OF CONTENTS.

CHAPTER 1 : INTRODUCTION.

Inclusion compounds were first described more than one hundred years prior to their nature being understood. In 1811 Davy[1.1] observed a chlorine clathrate hydrate whose preparation was confirmed by Faraday[1.2] in 1823. Furthermore, graphite intercalates,[1.3] the β-quinol • H_2S clathrate,[1.4] the Hofmann clathrate with benzene[1.5] and cyclodextrin inclusion compounds[1.6] were all prepared during the nineteenth century. More inclusion compounds prepared and described during the first half of the twentieth century were those of triphenylmethane,[1.7] Dianin's compound,[1.8] phenol,[1.9] urea,[1.10] amylose[1.11] and deoxycholic acid.[1.12]

Some authors commented on the fact that many of these compounds seemed to be of variable composition but no explanation was proposed to account for this until 1948. During the X-ray determination of the structure of the β-quinol complex with sulphur dioxide, Palin and Powell[1.13] found that the SO_2 molecule was enclosed in a "cage" made up of the molecules of quinol with no chemical bond existing between the two components. Powell[1.14] coined the term "clathrate" to describe compounds where one component is enclosed within the framework of another. The recognition that non-stoichiometric compounds of this type could be described in a satisfactory manner led chemists to reexamine many of the inclusion compounds previously reported. The increasing availability of X-ray crystallographic methods aided this process as the determination of the spatial arrangements within a crystal structure helped the understanding of the nature of inclusion compounds.

Inclusion compounds can thus be defined as those in which one type of molecule is able to enclose another molecule (usually smaller) within its structure, leaving the bonding systems of both components unchanged. The molecular network and the enclosed species are usually referred to as the "host" and "guest" respectively.

Since 1948 the number of host-guest complexes reported has risen dramatically. The importance of this branch of chemistry was recognized in 1987 with the awarding of the Nobel prize to D. J. Cram,[1.15] J-M. Lehn,[1.16] and C. J. Pedersen[1.17] for their work on the design of host compounds, cryptands and crown ethers.

Over the last two or three decades, the emphasis in chemistry has shifted from the methodology of synthesis to the synthesis of particular target molecules which have specific functions. New information on the functioning of biological systems at the molecular level has led to an ever-increasing interest in the mimicking of the highly specific molecular recognition present in biological systems. In addition, new industrial

needs and the need for less polluting industrial processes have kindled further interest in the processes of molecular recognition and inclusion. In an article on the future of organic chemistry, Seebach[1.18] suggests that research should no longer focus on systems which can be treated by simple molecular models. Instead, systems whose structure and properties are governed by non-covalent interactions should become the new target for chemical research.

Applications of Inclusion Compounds.

By their very nature, inclusion compounds employ the processes of molecular recognition between host and guest. This property may in turn be used for the processes of chemical analysis and molecular separation.[1.19] The shape, size and chemical nature of the voids in the host lattice determine which guests are included.[1.20] Selectivity towards a guest on the basis of its size seems at present to be the most promising development on an industrial scale. For separation of compounds with close boiling points, inclusion formation may be a cheaper alternative to distillation. A few pilot plants have been described, such as that of the Union Oil Company[1.21] which employs the selectivity of the Werner clathrate $[Ni(NCS)_2(4\text{-}MePy)_4]$ for *p*-xylene to separate it from a mixture of *m*- and *p*-xylene. The use of liquid clathrates (which require no precipitation or filtration) may overcome some of the technical problems associated with working with inclusion compounds on an industrial scale.[1.20]

Isolation of water soluble materials from aqueous solutions is an expensive and difficult process. If ethanol could be isolated cheaply from an aqueous solution obtained by the fermentation of biomass, it could be an abundant source of energy. Several host compounds have been suggested[1.22] which selectively include ethanol from aqueous solutions, including triphenylsilanol, whose structure with ethanol is described in Chapter 5. Similarly amines, ammonia and alkali metal hydroxides have been isolated from aqueous solutions using the process of inclusion crystallisation.[1.22] If host and guest are both chiral, inclusion formation may be used for optical resolution. Thus, when the host compound is optically active, one enantiomer of a racemic guest mixture should be selectively included. Similarly, an optically active guest could yield the resolved host compound by selective crystal inclusion. An amino acid- and ester-resolving machine has been described[1.23] which makes use of chiral recognition in transport of amino acid or ester salts through lipophilic liquid membranes (see Figure 1.1).

The transport of ions across cell membranes has been studied using crown ethers as transport media.[1.24]

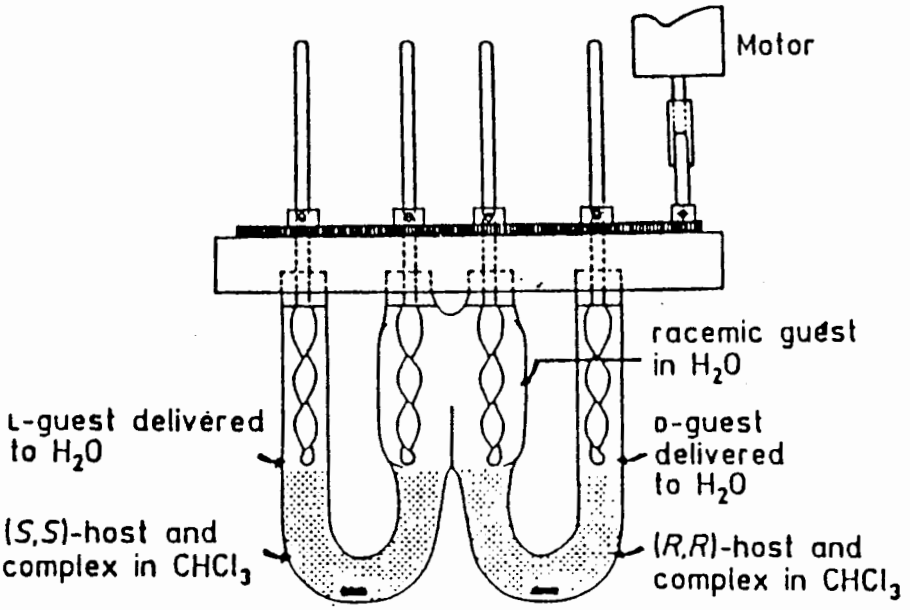

Figure 1.1. Enantiomer resolving machine. The central reservoir contains an aqueous solution of the racemic salt. The L-enantiomer is picked up by the (S,S)-host in the left hand chloroform reservoir and is delivered to the left hand aqueous layer, while the D-enantiomer is transported by the (R,R)-host to the right hand aqueous layer. The thermodynamic driving force for the machine's operation involves the exchange of an energy-lowering entropy of dilution of each enantiomer for an energy-lowering entropy of mixing. To maintain the concentration gradients down which the enantiomers travel in each arm of the W-tube, fresh racemic guest is continuously added to the central reservoir, and L- and D-guest in 86-90% enantiomeric excess are continuously removed from the left and right aqueous reservoirs respectively.
(Figure taken from ref. 1.15)

The topochemistry of inclusion compounds leads to some useful effects. Because crystal lattices are strictly periodical, holes and channels that occur often include guests in a particular orientation with respect to one another. This effect has been used to prepare products which are otherwise difficult to obtain, *eg.* the polymerisation of dienes in the channels of thiourea, which leads to stereoregular polymers.[1.25] Photodimerisation of chalcone in solution and in the solid state leads to a mixture of products. However, irradiation of the 1:2 complex composed of 1,1,6,6-tetraphenylhexa-2,4-diyne-1,6-diol and chalcone gives the *syn*-head-to-tail dimer selectively in 90% yield. (see Figure 1.2).[1.26]

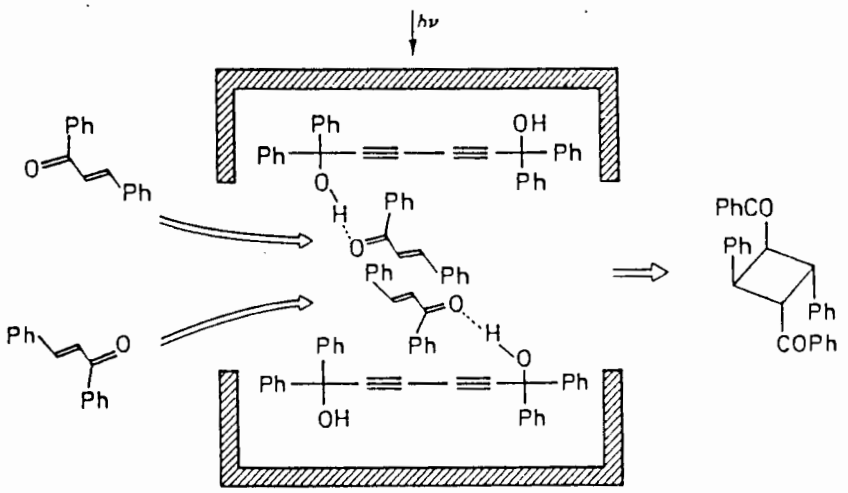

Figure 1.2. Irradiation of a 1:4 mixture of 1,1,6,6-tetraphenylhexa-2,4-diyne-1,6-diol and chalcone gives the product shown in 90% yield. The host can be recycled several times.[1.27]

Photo- or thermal reactivity may be altered on inclusion. It is possible that a molecule be included in a conformation different from that of its free state.[1.28] If the molecule is then able to react within the host lattice, its new conformation can lead to a different reaction path being followed and thus lead to new products. Alternatively, if the reactivity of an included molecule is reduced, the host lattice offers a protective function.

A subject which has received a great deal of attention is the need to store unstable or dangerous compounds. In 1978, Iwamoto *et al*[1.29] produced a number of paramagnetic radicals and examined their stability when included in a Hofmann-type clathrate. Some compounds survived a few hours before decomposing.

Dimethylmercury is a highly toxic environmental pollutant. It has been found[1.30] to form an extremely stable clathrate with 4-*p*-hydroxyphenyl-2,2,4-trimethylthiochroman (a modified form of Dianin's compound) which does not decompose, even on pumping under vacuum for several days. The guest is released when the crystals are crushed.

The two cyclophanes shown below have been suggested[1.31] as storage "vessels" for hydrogen, which is captured in the central torus of the macrocycle at ambient temperature and low pressures.

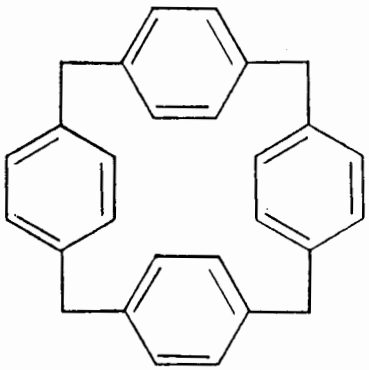

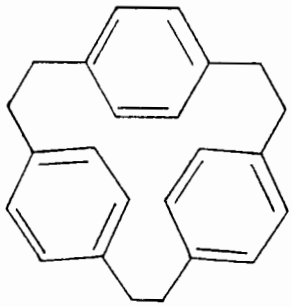

^{85}Kr is a product of ^{235}U fission. Its half-life is approximately ten years. The inclusion of this radioactive isotope in a hydroquinone cage allows it to be finely powdered for safer and easier handling and storage.[1.32] One of the products from the disintegration of plutonium is non-radioactive rhodium, a valuable industrial catalyst and an essential component in car catalytic converters. IBC Advanced Technologies has begun to isolate the rhodium contained in nuclear waste by attaching a host selective for rhodium to a silica gel support and allowing the waste to flow over it.[1.33]

Superconductors have received a great deal of attention over the last twenty years. 2H-tantalum disulphide (2H-TaS_2) is a superconductor at 0.8K. Intercalation of organic compounds[1.34] enhances the superconducting transition temperature (T_c). The intercalation of glycinamide hydrochloride into 2H-TaS_2 raises T_c to 4.1K.[1.35]

A portable refrigeration system based on the adsorption-desorption cycle of zeolites has been suggested for use in developing countries.[1.36] It is illustrated in Figure 1.3. Blackened copper solar panels are filled with a powdered zeolite, and attached to an evaporator and condenser. The evaporator is partially filled with water and the whole system is under a high vacuum. The zeolite absorbs water vapour, so holding the vacuum. It also prompts the water to boil at a low temperature. During the day, the solar panels absorb heat, so water vapour is driven out of the zeolite, into the condenser, and back to the evaporator, where it forms ice, thus keeping the inside of the refrigerator cold. At night, the zeolite reabsorbs water, ready for the next day.

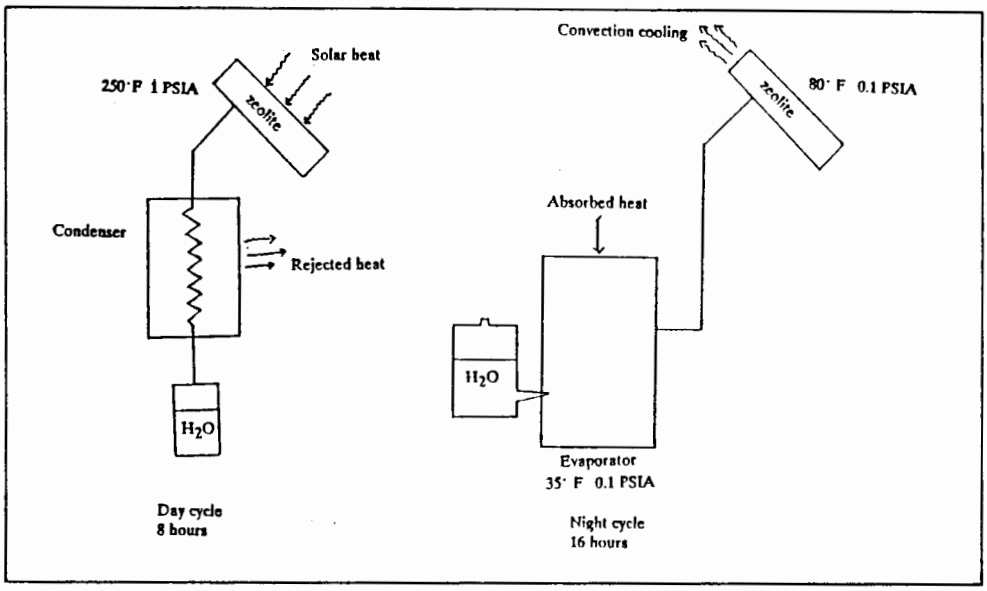

Figure 1.3. Zeolite refrigerator system.[1.36]

Finally, supramolecular chemistry, the binding of substrates to receptors and their subsequent organisation into polymolecular assemblies, appears to hold out hope for the development of devices which operate on a molecular scale. Components and molecular devices (*eg.* molecular wires, resistors, rectifiers, diodes) may be assembled into nanocircuits and combined with organized polymolecular assemblies to give systems capable of performing functions of detection, storage, processing, amplification and transfer of signals and information by means of photons, electrons, protons or molecules.[1.16]

Classification of Inclusion Compounds.

Inclusion compounds were initially classified as cage, channel or layer types.[1.37]
Cages, or true clathrates, were defined as having the guest held in discrete, closed cavities such as those occurring in the β-hydroquinone clathrates.
Channel type compounds enclosed guests in continuous canals *eg.* urea and thiourea compounds.
Layer type inclusion compounds were defined as those that included guests between bands of host structure, *eg.* graphite intercalation compounds. Intermediate structures were also reported, *eg.* some zeolites where cavities are interconnected by channels.

However, as new inclusion compounds were discovered, their classification became very complicated; terms such as loose addition complex, soccer molecule complex, spherands, sepulchrands, octopus molecules and tweezer molecules have all been used. These descriptions, although quite clear pictorially in some cases, have added to the general confusion in the literature since they often apply only to a specific compound. A new system of classification and nomenclature was proposed by Weber and Josel[1.38] in 1983 and has become widely accepted. This system is described below.

The two main criteria which must be defined are :

(a) the host-guest interaction and
(b) the topology of the host-guest aggregate.

(a) Host-guest interactions are divided into :
Complexes (formed by coordinative forces) where the aggregates are formed by coordination between host and guest *eg.* the metal ion complexes of crown ethers.
Clathrates (dominated by crystal lattice forces) where the guest is retained in the aggregate by steric barriers alone *eg.* urea clathrates.

(b) Topologically, the extreme cases can be seen as :
Cavitates : intra-molecular host-guest aggregates in which the guest occupies a cavity inside the host molecule.
Clathrates : extra-molecular inclusion compounds where the guest occupies voids in the host lattice.

Many host-guest compounds however, are formed by both coordinative and crystal lattice forces. Thus "hybrids" are known and defined as follows :
Inclusion compound is a generic term for any undefined cavity.
Coordinatoclathrates have a certain degree of coordinative binding but a predominantly clathrate character. This is the most common form of inclusion compound formed by

hydroxy hosts.

Clathratocomplexes are aggregates in which guest molecules are predominantly bound to the host by weak coordinative forces.

Addition compounds (adducts) have neither coordination nor a cavity.

Figure 1.4 summarizes and relates the different terms.

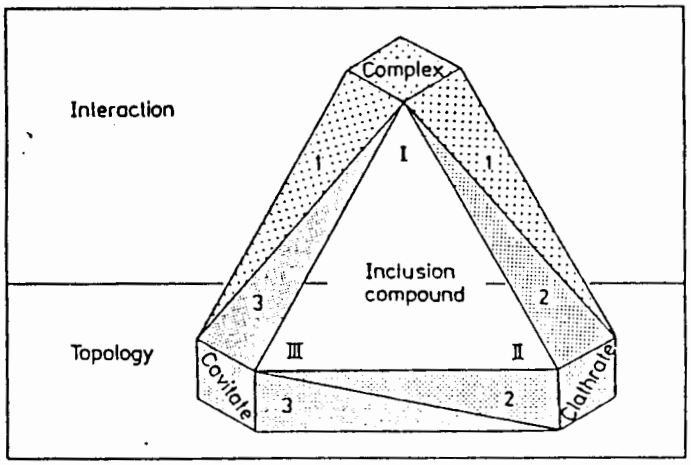

Figure 1.4. Classification of host-guest compounds. (1) coordinative interaction, (2) lattice barrier interaction, (3) mono-molecular shielding interaction; (I) coordination-type inclusion compound (inclusion complex), (II) lattice-type inclusion compound (multi-molecular inclusion compound), (III) cavitate-type compound (mono-molecular inclusion compound).

Further topological features of interest are incorporated by means of prefixes. Thus, intercalates are two-dimensional open layer or sandwich type compounds, while tubulates, aediculates and cryptates describe cavities that are channels, pocket-shaped or cages respectively and coronate and podate are used to describe ring-shaped and open-chain hosts.

The use of this nomenclature allows an illustrative picture of the geometry and interactions within the host-guest unit to be drawn. Different lattice inclusions are drawn diagrammatically below, and are classified as follows :

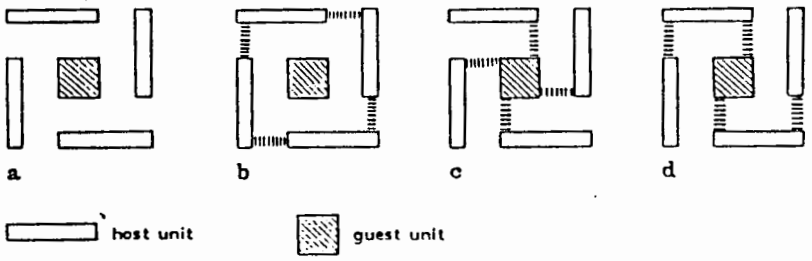

(a) No coordinative interaction (*clathrate*).
(b) Host-host interaction (*coordination-assisted clathrate host lattice*).
(c) Host-guest interaction (*coordinatoclathrate*).
(d) Both host-host and host-guest interaction (*coordinatoclathrate in a coordination-assisted host lattice*).

In addition to the above, the terms "α-phase" for a non-clathrating lattice type and "*β*-phase" for a porous inclusion lattice have been widely adopted[1,39] and are used in this study.

Examples of some Inclusion Compounds.

The field of inclusion compounds increases annually. It would therefore be impossible, in only one chapter, to describe all systems. Instead, a brief survey of some of the inorganic and organometallic inclusion compounds known will be given followed by a more detailed overview of small organic hosts.

Zeolites[1.40] are a large family of aluminosilicates, many of which occur naturally. They are characterized by complex networks of cavities and channels and by their high stabilities. These properties make them industrially attractive.

Hofmann[1.41] and **Werner**[1.42] compounds are two classes of metal coordination complexes which form clathrates with predominantly aromatic guests.

Hofmann compounds have the general formula

$M(NH_3)_2M'(CN)_4 \cdot 2G$

M = Mn, Fe, Co, Ni, Cu
M' = M or Pd, Pt
G = small aromatic molecules.

These compounds have a layered structure of two-dimensional metal complex sheets with ammonia groups protruding above and below the sheets, thus reducing the mobility of the guest molecules which are trapped between adjacent sheets.

Werner clathrates are structurally similar with the general formula

$MX_2A_4 \cdot nG$

M = Fe, Co, Ni, Cu, Zn, Cd, Mn, Hg, Cr
X = NCS^-, NCO^-, CN^-, NO_3^-, NO_2^-, Cl^-, Br^-, I^-
A = neutral substituted pyridines

G = small aromatic molecules.

The host molecules again form layers. Guests are located in the cavities defined by the host complex layers and the anionic groups which protrude into the space between layers.

Only van der Waals interactions between host and guest are possible so these two metal complex host classes form true clathrates.

Organic host molecules.

Urea (1) and thiourea (2) are among the smallest organic molecules known to act as hosts.[1.43]

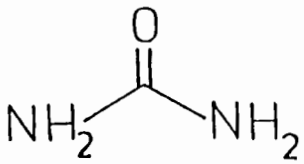

(1)

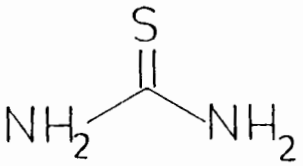

(2)

Urea forms a hexagonal crystal lattice with extended channels. Figure 1.5 shows that for an *n*-alkane inclusion compound, urea forms a helical hydrogen-bonded network involving both the nitrogen and oxygen atoms of each molecule.[1.44]

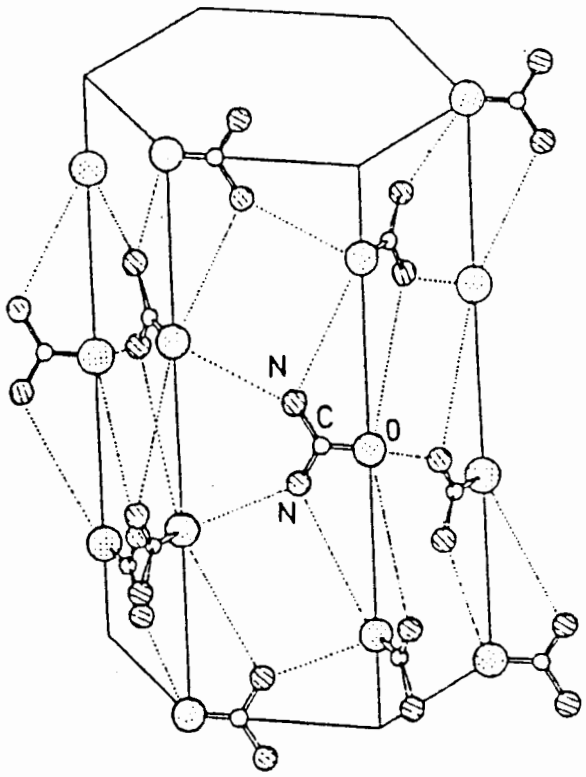

Figure 1.5. The hydrogen-bonded hexagonal channel network of urea (1) for a *n*-hydrocarbon inclusion compound. (Figure taken from ref. 1.82)

Unbranched alkanes are included in this channel and stabilised by van der Waals forces. Urea has been used to separate *n*-alkanes from branched or cyclic compounds.[1.45]

In thiourea compounds, the channel diameter is increased from 5.2 Å (urea) to 6.1 Å. This allows for the inclusion of larger guests. Thiourea has been used to separate benzene and cyclohexane from *n*-heptane.[1.46]

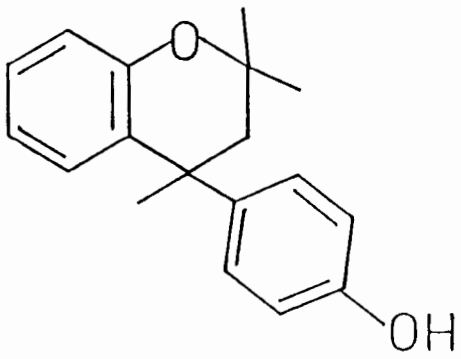

(3)

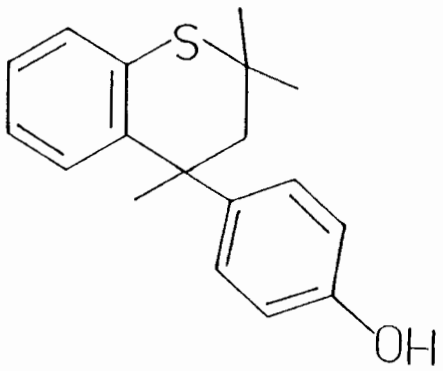

(4)

4-*p*-hydroxyphenyl-2,2,4-trimethylchroman (3) (**Dianin's compound**) has been found to include a wide range of guests.[1.37] Six molecules link by means of hydrogen bonding between their hydroxyl groups so that the oxygen atoms form an irregular hexagon. Alternate molecules of opposite configuration lie on opposite sides of the plane. Two such groups are stacked along the c-axis; their bulky parts interlock to form a cage which has an hour-glass shape of length equal to the c-axis. The packing of Dianin's compound can be represented schematically as shown in Figure 1.6. Modifications of Dianin's compound have resulted in other inclusion compounds of interest. Replacement of the oxygen by a sulphur atom (4) yields a new clathrate with similar inclusion properties to (3). Further substitution of a methyl group at the 8-position of the thia-analogue leads to a major change in the cavity shape, illustrated in Figure 1.7. The change from an 'hour-glass' to a 'chinese-lantern' shaped cavity results in different guests being included.[1.37]

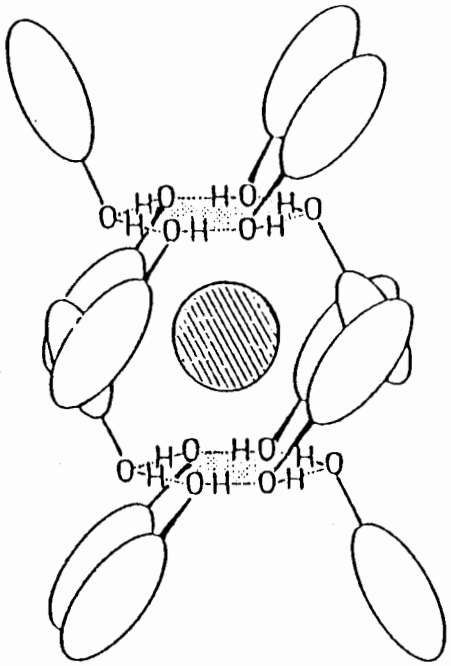

Figure 1.6. Schematic representation of the inclusion matrix of Dianin's compound (**3**). Each molecule is represented by a hydroxy group attached to an ellipse. The hydrogen bonded networks are indicated by shaded hexagons. The hatched circle in the centre of the cavity represents an included guest.[1.66]

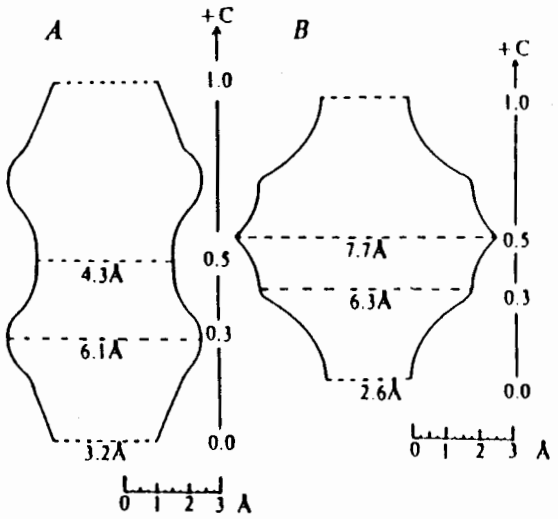

Figure 1.7. Section through the van der Waals surface for (a) (**4**), and (b) the 8-methyl analogue of (**4**), representing the space available for guest inclusion.[1.20]

(5)

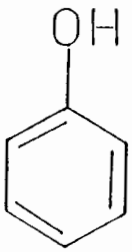

(6)

The inclusion compounds of **hydroquinone** (5) are cage structures in which the floor and roof of the cavity are formed by nearly-planar hexagons of hydrogen bonded oxygen atoms. Molecules point alternately up and down from each hexagon; thus the cages are located between the hexagons as shown in Figure 1.8. The cavity is roughly spherical with a free diameter of ≈4.8 Å. The recognition of the cage-structure of the SO_2 complex of **hydroquinone** by Powell[1.13] led to the introduction of the term *clathrate compound*.[1.14]

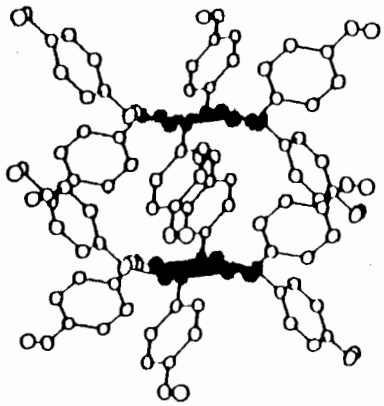

Figure 1.8. The construction of a single cage in unsolvated β-hydroquinone. The hydrogen bonded hexagons are shaded.

Analogous clathrates are formed by **phenol** (6). Two types of cages are formed, one large (length ≈15 Å and 4 - 4.5 Å in free diameter) and one small with free diameter ≈4.5 Å. Both cages are capable of including suitably sized guests.

The analogy between the hydrogen bonded hexamer unit of most phenol-type hosts and a hexa-substituted benzene was used by MacNicol[1.47] to design the first class of hosts which were not related to any known host. These **hexahosts** (general formula (7)) have a number of interesting features.[1.48] The distance between the α-atoms (carbon or other) of the substituents, which are coplanar with the benzene ring, is approximately equal to the distance between the oxygens in the hexagonal hydrogen bonded hydroxyl rings.

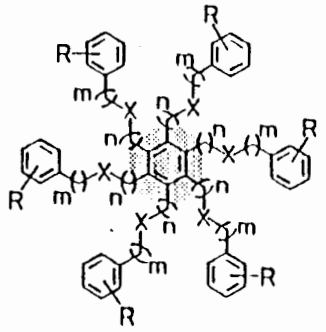

m , n = 0 , 1
X = O , S
R = H , Alkyl, Aryl , Alkoxy , OH , NH_2

(7)(a) m = n = 1, X = S, R = H

Figure 1.9 shows the packing of a typical hexahost clathrate - the dioxane clathrate of (7a) (1:1). An important feature of these hosts is that the shape and size of the cavity is easily altered by changing the substituents on the benzene ring. In this way, highly specific hosts can be prepared.

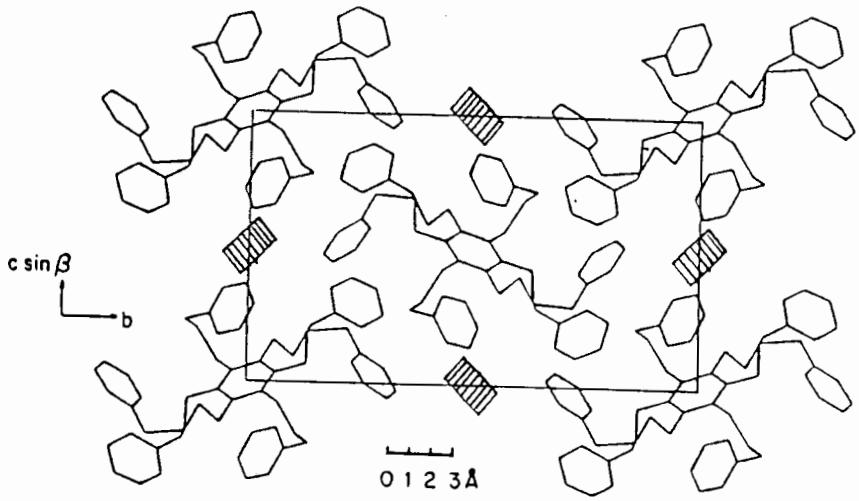

Figure 1.9. Packing diagram of the (7a)·dioxane clathrate. Dioxane molecules are shaded.[1.48]

Trigonal symmetry has been observed in a number of hosts, *eg.* Triphenylmethane (**8**), *trans, anti, trans, anti, trans*-perhydrotriphenylene (**9**).

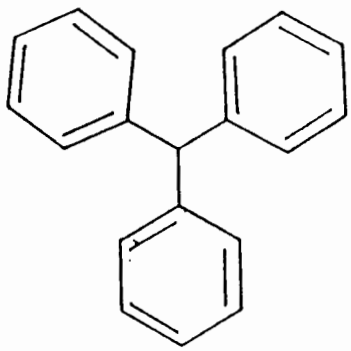

(**8**)

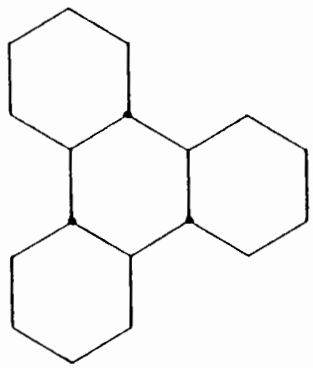

(**9**)

Inclusion compounds formed by these are usually stabilized by van der Waals forces only. The individual host does not always retain exact crystallographic 3-fold symmetry, but trigonal (or hexagonal) lattice symmetry is often found.[1.49] Triphenylmethane (**8**) has been reported to form inclusion compounds with a limited series of guests - benzene, thiophene, aniline and pyrrole (1:1).[1.7] The host adopts a propeller conformation.[1.50]

Other substituted methanes which form inclusion compounds are di(1-naphthyl)phenylmethanol with methanol,[1.51] triphenylmethanol with acetone and carbon tetrachloride[1.52] and triphenylmethanol with methanol and dimethylsulfoxide.[1.53] Packing diagrams of the last two structures are shown in Figure 1.10. The methanol clathrate (Figure 1.10(a)) consists of tetrameric units made up of two hosts and two guests, which are located around the crystallographic centres of inversion. The dmso, on the other hand, (Figure 1.10(b)) is trapped between and hydrogen bonded to two host molecules.

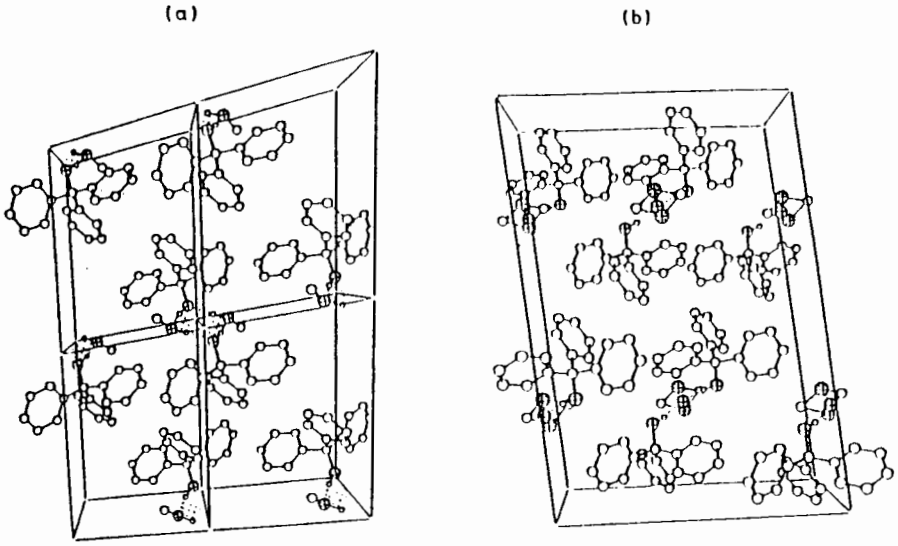

Figure 1.10. (a) Crystal structure of Triphenylmethanol·MeOH (1:1) viewed approximately down the a-axis (b is horizontal).
(b) Crystal structure of Triphenylmethanol·dmso (2:1) viewed approximately down the b-axis (a is horizontal).[1.53]

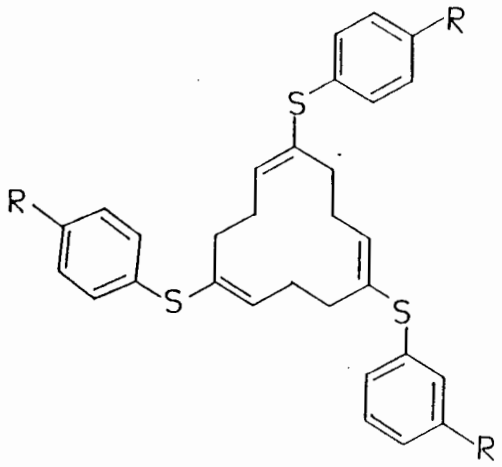

(10) R = H
(11) R = Me

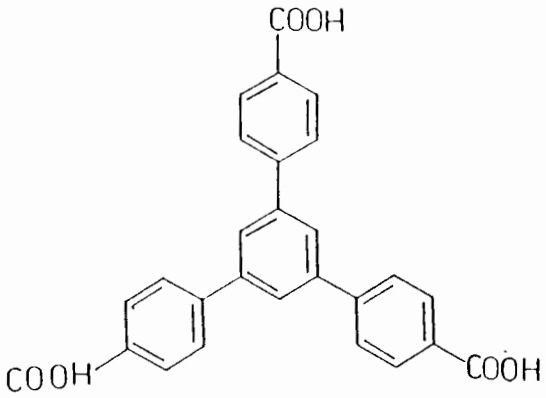

(12)

Using the principle of trigonal symmetry, MacNicol set out to prepare (**10**) and (**11**). Both proved to be hosts for a wide variety of alkanes.[1.48] More recently, Weber *et al.*[1.54] synthesized a series of 1,3,5-triarylsubstituted benzenes, such as (**12**), many of which have proved to be effective hosts.

Deoxycholic acid (13) forms channel-type inclusion compounds by linking host molecules head-to-tail.[1.55] The channels are linked by hydrophobic groups so that guest molecules are held in place by van der Waals forces only. A typical example is shown in Figure 1.11.

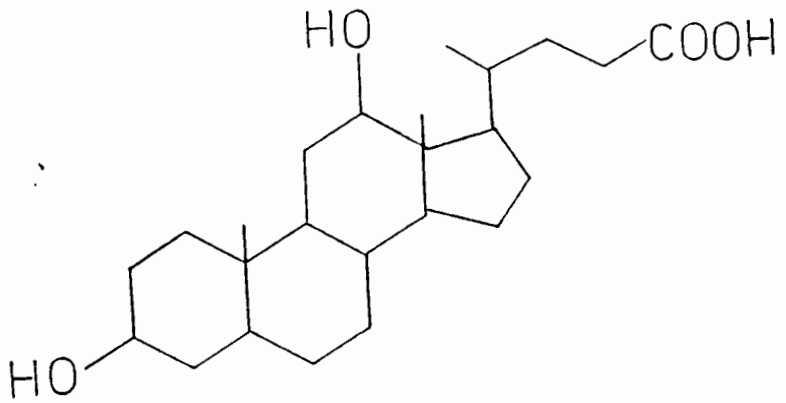

(13)

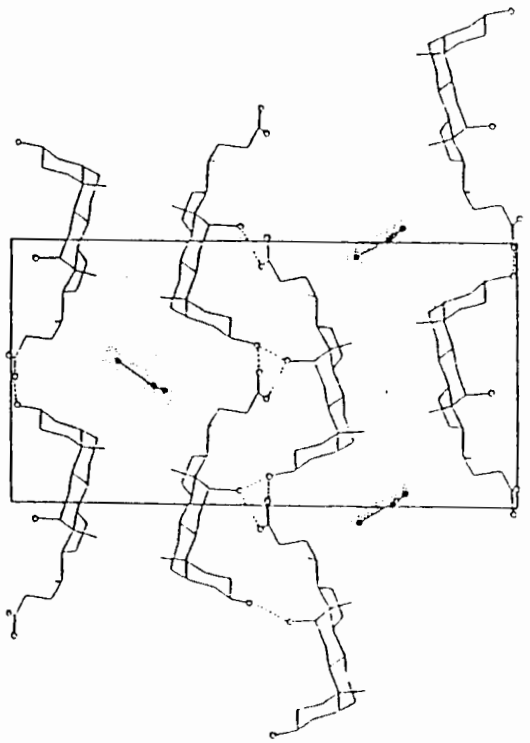

Figure 1.11. Inclusion compound of (13)·acetone showing the head-to-tail hydrogen bonded host molecules. Guests are shaded.[1.82]

The first macrocycle or **cryptate (14)** was synthesized in 1968.[1.59] The general formula for these compounds is that shown below :

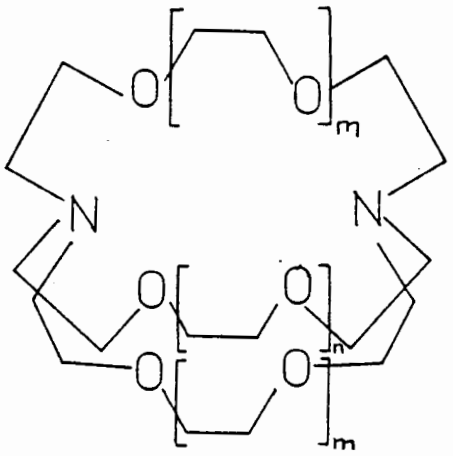

m,n = 0,1,2

(14)

Their uses include enriching precious metals, isotopic separations of cations[1.60] and modelling of the factors in transport of ions across membranes mediated by ionophores.[1.61]

Cyclodextrins[1,56] are torus-shaped molecules made up of linked glucopyranose units. α-, β- and γ-cyclodextrins (CD's) comprise six, seven and eight linked units respectively (Figure 1.12).

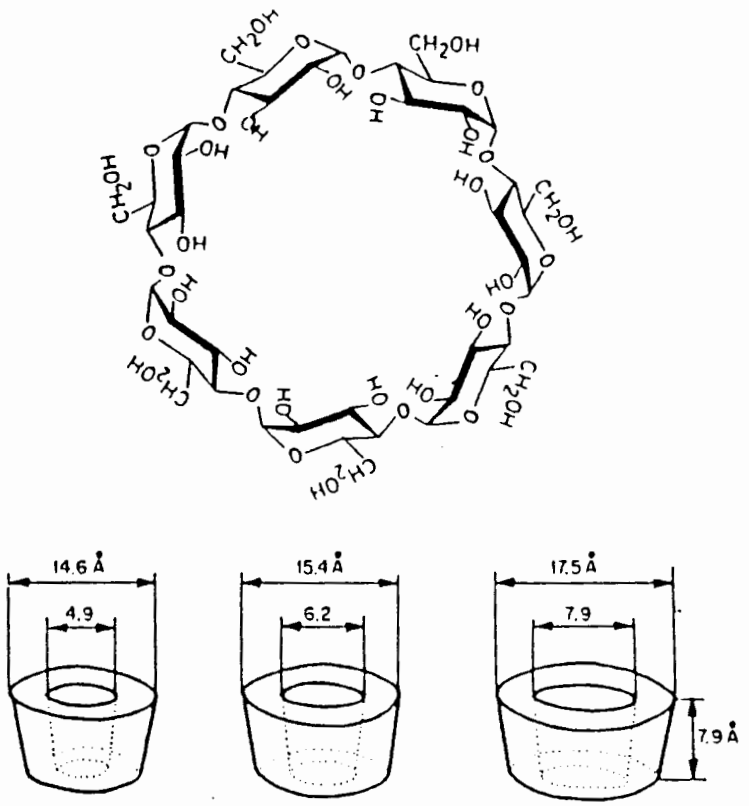

Figure 1.12. Structure of β-cyclodextrin, and molecular dimensions of α-, β- and γ-cyclodextrins.[1,56]

These molecules are unusual in that host-guest chemistry is found in both the solid state and in solution owing to the distribution of hydrophilic and hydrophobic groups on the molecules. The hydroxyls on the rims of the cones render the CD's soluble in aqueous solution while the inside of the cavity is hydrophobic because it is lined by C-H groups and the ether-like oxygens involved in linkages. This enhances the interest that exists in the CD's because of their ability to act as enzyme models.

Two types of crystal structures are seen :
Channel-types : CD molecules are stacked on top of each other, stabilized by hydrogen bonds between units, thus producing "endless" channels.
Cage-types : The cavity of one CD molecule is blocked off on both sides by adjacent CD's.

The macrocyclic polyethers (called **crown ethers** because of the shape of their molecular models) have been used as model compounds in ion-transport, molecular catalysis and stereoselective complexation reactions.[1.57] Examples are shown below (**15**) - (**17**). The trivial names proposed for these compounds by Pedersen[1.58] have become the accepted nomenclature since the IUPAC nomenclature is cumbersome.

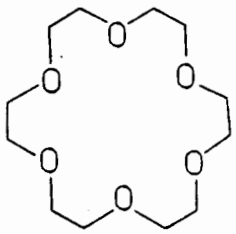

18-crown-6
(**15**)

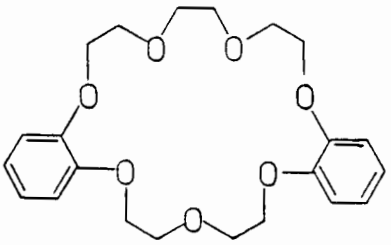

Dibenzo[21]crown-7
(**16**)

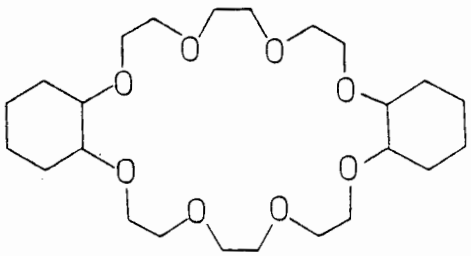

Perhydrodibenzo[24]crown-8
(**17**)

Usually cations *nest* within the cavity of the crown; if they are too large, the cations *perch* above the mean plane of the oxygens.[1.57] However molecular guests are also included. They are usually too large to be included within the crown and coordinate to it instead by means of functional groups. The coordination which occurs in the 1:2 complex of (**15**) with urea is shown in Figure 1.13. These complexes also often retain their host-guest chemistry in solution.

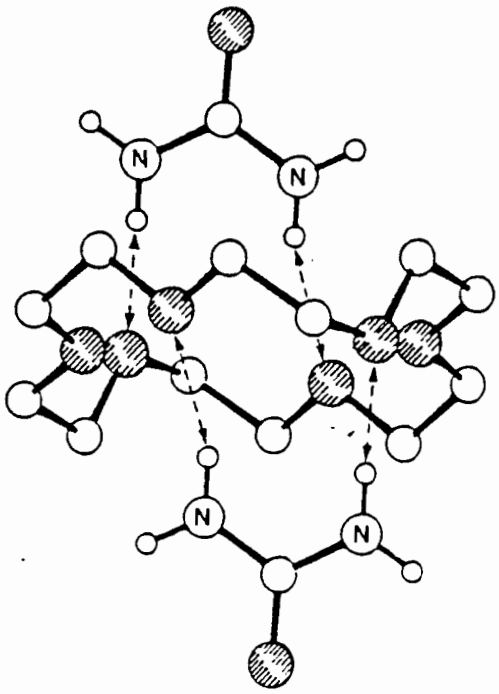

Figure 1.13. The coordination of urea to 18-crown-6 (**15**). Oxygen atoms are shaded.[1.57]

Cyclophanes (cyclic compounds containing non-fused aromatic rings) were developed from work on macrocyclic rings.[1.62] Changing the number of aromatic units and the size and nature of the bridging groups led to the cyclophanes, molecules characterized by intramolecular, neutral cavities.[1.63] Some examples are shown as (**18**) - (**20**).

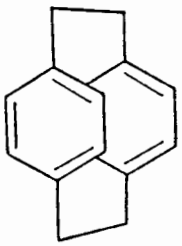

(**18**)

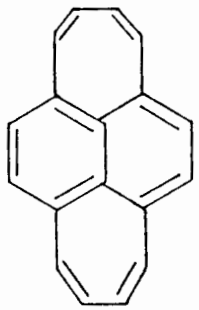

(**19**)

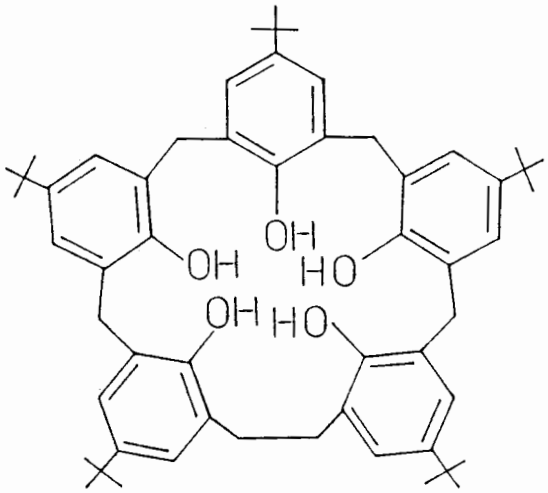

(**20**)

Their ability to include many non-polar molecules with some degree of specificity has led to the cyclophanes being one of the most studied of organic host classes.[1.64]

The **calixarenes** (such as (**20**)) are a subset of the cyclophanes that have been developed specifically as mimics of enzyme activity.[1,65]

Some empirical rules that govern the formation of clathrates have recently been proposed.[1.19, 1.66, 1.67]

The proposed host design includes :
(a) A bulky skeleton to prevent close packing.
(b) Appended functional groups which can coordinate to guest molecules.
The supramolecular systems which are formed in this way are known as **coordinatoclathrates.** They are usually more stable than true clathrates and the hosts are often highly selective.[1.19]

Using these guidelines, a number of new hosts such as the tetraaryl-substituted allenes (**21**),[1.68] "scissor" (**22**)[1.69] and "roof" (**23**)[1.70] shaped molecules and the spirotriphosphazenes (**24**)[1.71] have been designed and tested as potential hosts.

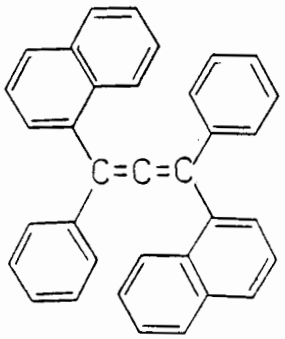

(**21**)

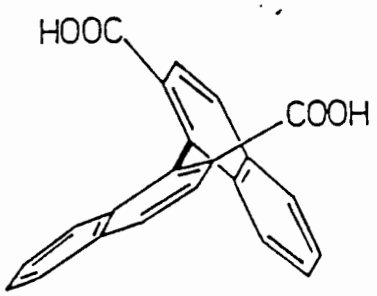

(**22**)

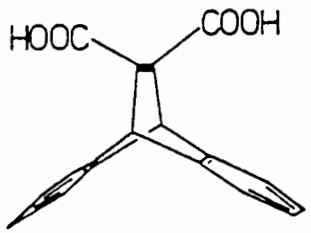

(**23**)

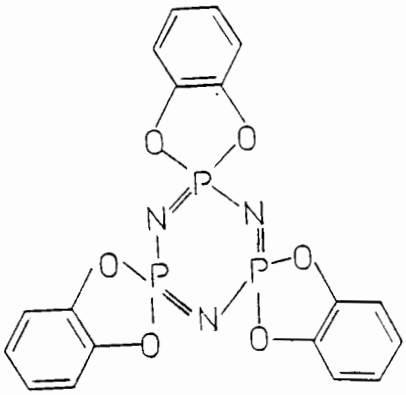

(**24**)

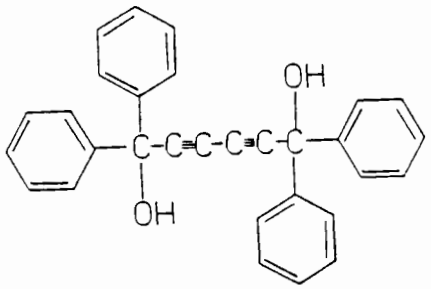

(**25**)

Although Toda[1.72] reported in 1968 that the diacetylenic diol (**25**) formed inclusion compounds with small organic molecules , it was only a decade later that the shape of these molecules was recognised as a likely one to yield further host compounds. Hart *et al.* made a number of new "wheel-and-axle" molecules which proved that the long molecular axis with spacers at either end was an efficient shape for a host molecule.[1.73]

Weber *et al.* extended the concept of a molecular "axis" into a triangle or quadrangle.[1.74] This allows functional groups to be added, allowing adaptations for specific guests to be made. For example, (**26**) includes only EtOH, 2-PrOH and *t*-BuOH (1:1) from a series of alcohols. (**27**) is even more specific, including only MeOH (1:2) from the same series of alcohols.

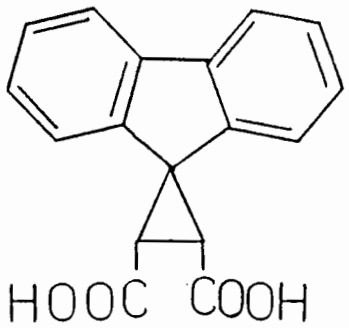

(**26**)

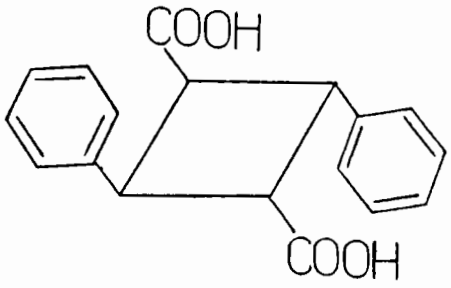

(**27**)

Toda synthesized a number of molecules with an ***anti*-diol** function and some bulky hydrophobic groups which proved to be versatile hosts.[1.22] Some examples are shown below.

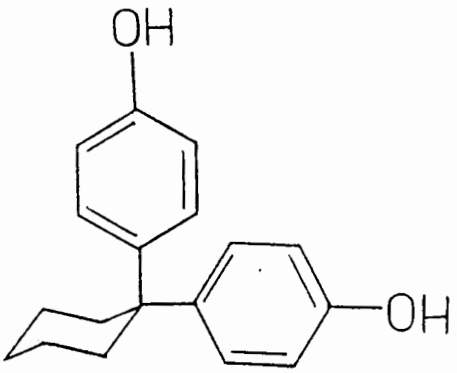

(**28**)

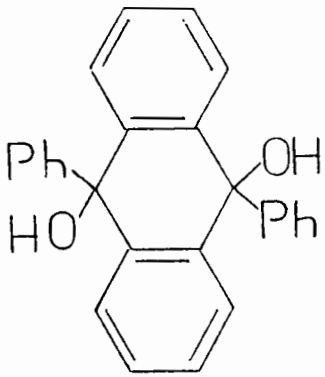

(**29**)

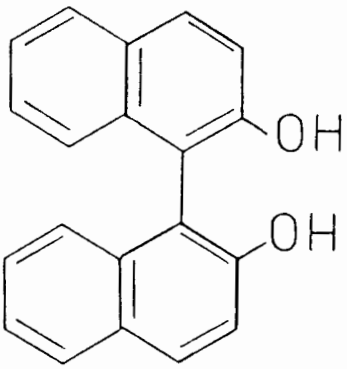

(**30**)

These molecules usually include guests by means of hydrogen bonding[1.75, 1.76, 1.77, 1.78] but non-polar guests may also be included by means of clathration.[1.79]

Some isomers are readily separated by inclusion formation with diol host compounds. Separation of cyclohexanol and cyclohexanone,[1.80] the isolation of *m*-cresol from mixtures of *o*-, *m*- , *p*-cresol and phenol[1.81] and the separation of 3-methylpyridine from the 4-isomer[1.22] have all been reported.

Aim and scope of this project.

The four molecules **A - D** are examples of hosts which are expected to form coordinatoclathrates.

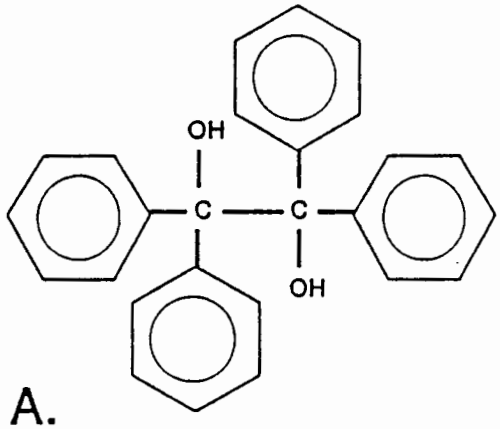

A.

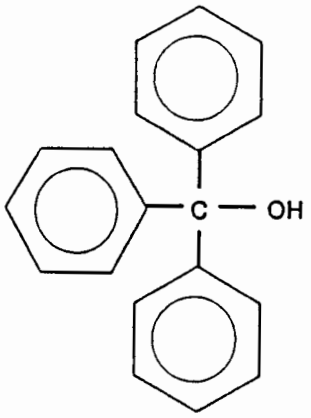

B.

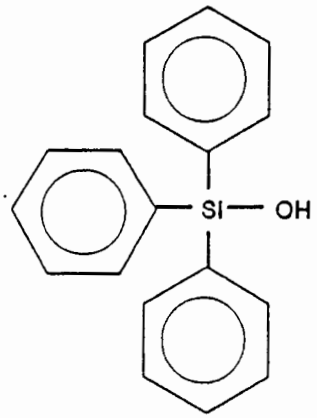

C.

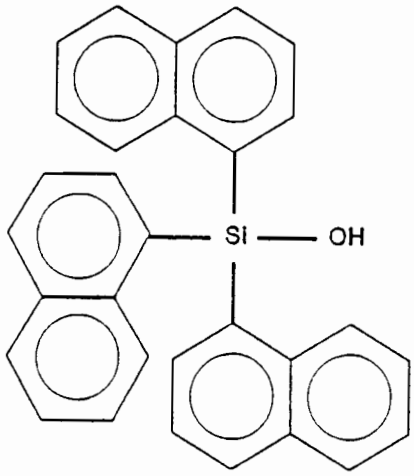

D.

Each has a fairly rigid structure which contains a number of bulky aromatic groups. These should prevent the molecules from finding a close-packed arrangement. Each molecule also has at least one hydroxyl group which can hydrogen bond to suitable guests.

A number of different guest species have been chosen, most of which contain a potential hydrogen bond acceptor atom. Crystal structure analysis has been used to determine the influence of the guests on the host's packing. The thermal decomposition of the inclusion compounds formed has been studied, to determine the forces binding the guest and to gain an understanding of the changes in the host lattice as the guest is desorbed.

References.

1.1. H. Davy. *Philos. Trans. R. Soc. London.* **101**, 1, (1811).

1.2. M. Faraday. *Quart. J. Sci.* **15**, 71, (1823).

1.3. C. Schafhäutl. *J. Prakt. Chem.* **21**, 129, (1841).

1.4. F. Wohler. *Ann. Chem. Leibigs.* **69**, 297, (1849).

1.5. K. A. Hofmann. F. Küspert; *Z. Anorg. Allg. Chem.* **15**, 204, (1891).

1.6. A. Villiers. *C. R. Hebd. Sceances Acad. Sci.* **112**, 536, (1891).

1.7. H. Hartley; N. G. Thomas. *J. Chem. Soc.* 1013, (1906).

1.8. A. P. Dianin. *J. Soc. Phys. Chem. Russe.* **46**, 1310, (1914).

1.9. E. Terres; W. Vollmer. *Z. Petroleum.* **31**, 1, (1935).

1.10. M. F. Bengen. *German Patent Application OZ 123438.* (March 18, 1940).

1.11. F. F. Mikus; R. M. Hixon; R. E. Rundle. *J. Am. Chem. Soc.* **63**, 1115, (1946).

1.12. J. Wieland; H. Sorge. *Z. Physiol. Chem. Hoppe-Seyler's.* **97**, 1, (1916).

1.13. D. E. Palin; H. M. Powell. *J. Chem. Soc.* 208, (1947).

1.14. H. M. Powell. *J. Chem. Soc.* 61, (1948).

1.15. D. J. Cram. *Angew. Chem. Int. Ed. Engl.* **27**, 1009, (1988).

1.16. J. M. Lehn. *Angew. Chem. Int. Ed. Engl.* **27**, 90, (1988).

1.17. C. J. Pedersen. *Angew. Chem. Int. Ed. Engl.* **27**, 1021, (1988).

1.18. D. Seebach. *Angew. Chem. Int. Ed. Engl.* **29**, 1320, (1990).

1.19. E. Weber. 'Molecular Inclusion and Molecular Recognition - Clathrates I and II' in *Topics in Current Chemistry*, **140** and **149**, Springer-Verlag, Berlin Heidelberg, (1987 and 1988).

1.20. J. L. Atwood; J. E. D. Davies; D. D. MacNicol (eds.). *Inclusion Compounds,* **Vol. 1 - 3**, Academic Press, London, (1984).

1.21. P. Strazewski; J. Lipkowski. *Pol. J. Chem.* **53**, 1869, (1979).

1.22. F. Toda. 'Isolation and Optical Resolution of Materials Utilizing Inclusion Crystallization' in *Topics in Current Chemistry*. **140**, 43, Springer-Verlag, Berlin Heidelberg, (1987).

1.23. M. Newcomb; J. L. Toner; R. C. Helgeson; D. J. Cram. *J. Am. Chem. Soc.* **101**, 4941 (1979).

1.24. C. J. Pedersen; H. E. Schroeder. *Curr. Top. Macrocycl. Chem. Jpn.* **1**, 5, (1987).

1.25. J. F. Brown; D. M. White. *J. Am. Chem. Soc.* **82**, 5671, (1960).

1.26. K. Tanaka; F. Toda. *J. Chem. Soc., Chem. Commun.* 593, (1983).

1.27. F. Toda. 'Reaction Control of Guest Compounds in Host-Guest Inclusion Compounds.' in *Topics in Current Chemistry.* **149**, 211, Springer-Verlag, Berlin Heidelberg, (1988).

1.28. R. Arad-Yellin; S. Brunie; B. S. Green; M. Knossov; G. Tsoucaris. *J. Am. Chem. Soc.* **101**, 7529, (1979).

1.29. T. Iwamoto; M. Kiyoki; N. Matsura. *Bull. Chem. Soc. Jpn.* **51**, 390, (1978).

1.30. R. J. Cross; J. J. McKendrick; D. D. MacNicol. *Nature.* **245**, 146, (1973).

1.31. M. Armand; F. Jeanne. *Chem. Abstr.* **95**, 9378y, (1981).

1.32. D. J. Chleck; C. A. Ziegler. *Nucleonics.* **17**, 130, (1959).

1.33. *The Economist*. p. 94, Jan 12th, 1991.

1.34. R. F. Gamble; F. J. Di Salvo; R. A. Klemm; T. H. Geballe. *Science.* **168**, 568, (1970).

1.35. G. Acosta; N. M. Chapela. *J. Incl. Phenom.* **3**, 9, (1985).

1.36. J. E. D. Davies; W. Kemula; H. M. Powell; N. O. Smith. *J. Incl. Phenom.* **1**, 3, (1983).

1.37. D. D. MacNicol; J. J. McKendrick; D. R. Wilson. *Chem. Soc. Rev.* **7**, 65, (1978).

1.38. E. Weber; H-P. Josel. *J. Incl. Phenom.* **1**, 79, (1983).

1.39. M. I. Hart; N. O. Smith. *J. Am. Chem. Soc.* **84**, 1816, (1962).

1.40. R. M. Barrer in Chapter 6 of Ref. 20, Vol. 1.

1.41. T. Iwamoto in Chapter 2 of Ref 20, Vol. 1.

1.42. J. Lipkowski in Chapter 3 of Ref. 20, Vol. 1.

1.43. K. Takemoto; N. Sonoda in Chapter 2 of Ref. 20, Vol. 2.

1.44. A. E. Smith. *Acta Crystallogr.* **5**, 224, (1952).

1.45. L. C. Fetterly, Chapter 8 in *Non-Stoichiometric Compounds*, (ed. L. Mandelcorn), Academic Press, New York, (1964).

1.46. E. J. Fuller. *Enclyp. Chem. Process. Des.* **8**, 333, (1979).

1.47. D. D. MacNicol; D. R. Wilson. *J. Chem. Soc., Chem. Commun.* 494, (1976).

1.48. D. D. MacNicol in Chapter 5 of Ref. 20, Vol. 2.

1.49. S. A. Puckett; I. C. Paul; D. Y. Curtin. *J. Chem. Soc., Perkin Trans. 2*, 1873, (1976).

1.50. A. Allemand; R. Gerdil. *Acta Crystallogr.* **A31**, S130, (1975).

1.51. A. Rahman; D. van der Helm. *Cryst. Struct. Commun.* **10**, 731, (1981).

1.52. J. F. Norris. *J. Am. Chem. Soc.* **38**, 702, (1916).

1.53. E. Weber; K. Skobridis; I. Goldberg. *J. Chem. Soc., Chem. Commun.* 1195, (1989).

1.54. E. Weber; M. Hecker; E. Koepp; W. Orlia; M. Czugler; I. Csöregh. *J. Chem. Soc., Perkin Trans. II.* 1251, (1988).

1.55. E. Giglio in Chapter 7 of Ref. 20, Vol. 2.

1.56. W. Saenger in Chapter 8 of Ref. 20, Vol. 2.

1.57. I. Goldberg in Chapter 9 of Ref. 20, Vol. 2.

1.58. C. J. Pedersen. *J. Am. Chem. Soc.* **89**, 7017, (1967).

1.59. B. Dietrich; J. M. Lehn; J. P. Sauvage. *Tetrahedron Lett.* 2885, (1969).

1.60. E. Blasius; K. P. Janzen in *Host Guest Complex Chemistry I*, (ed. F. Vögtle), Springer-Verlag, Berlin, 163, (1981).

1.61. G. R. Painter; B. C. Pressman in *Host Guest Complex Chemistry II* (ed. F. Vögtle), Springer-Verlag, Berlin,83,(1982)

1.62. D. J. Cram. *Acc. Chem. Res.* **4**, 204, (1971).

1.63. S. P. Miller; H. W. Whitlock. *J. Am. Chem. Soc.* **106**, 1492, (1984).

1.64. (a) I. Tabushi; K. Yamamura; H. Nonoguchi; K. Hirotsu; T. Higuchi. *J. Am. Chem. Soc.* **106**, 2621, (1984).
(b) K. Saigo; R-J. Lin; M. Kubo; A. Youda, M. Hasegawa. *J. Am. Chem. Soc.* **108**, 1996, (1986).

1.65. C. D. Gutsche. *Acc. Chem. Res.* **16**, 161, (1983).

1.66. E. Weber. 'Clathrate Chemistry Today - Some Problems and Reflections.', in *Topics in Current Chemistry.* **140**, 2, Springer-Verlag, Berlin Heidelberg, (1987)

1.67. E. Weber. *J. Mol. Graph.* **7**, 12, (1989).

1.68. E. Weber. *Chem. Ber.* **123**, 811, (1990).

1.69. E. Weber; I. Csöregh; B. Stensland; M. Czugler. *J. Am. Chem. Soc.* **106**, 3297, (1984).

1.70. M. Czugler; E. Weber; J. Ahrendt. *J. Chem. Soc., Chem. Commun.* 1632, (1984).

1.71. (a) H. R. Alcock in Chapter 8 of Ref. 20, Vol. 1.
(b) H. R. Alcock. *Acc. Chem. Res.* **11**, 81, (1978).

1.72. F. Toda; K. Akagi. *Tetr. lett.* 3695, (1968).

1.73. H. Hart; L-T. W. Lin; D. L. Ward. *J.Am. Chem. Soc.* **106**, 4043, (1984).

1.74. E. Weber; M. Hecker; I. Csöregh; M. Czugler. *Mol. Cryst. Liq. Cryst.* **187**, 165, (1990).

1.75. F. Toda; K. Tanaka; M. C. Wong; T. C. W. Mak. *Chemistry letters.* 2069, (1987).

1.76. F. Toda; A. Kai; R. Toyotaka; W-H. Yip; T. C. W. Mak. *Chemistry letters*. 1921, (1989).

1.77. D. R. Bond; L. Johnson; L. R. Nassimbeni; F. Toda. *J. Sol. State Chem.* **92**, 68, (1991).

1.78. D. R. Bond; F. Toda. *Acta Cryst.* **C47**, 348, (1991))

1.79. F. Toda; K. Tanaka; Y. Wang; G-H. Lee. *Chemistry letters*. 109, (1986).

1.80. I. Goldberg; Z. Stein; A. Kai; F. Toda. *Chemistry letters*. 1617, (1987).

1.81. I. Goldberg; Z. Stein; K. Tanaka; F. Toda. *J. Incl. Phenom.* **6**, 15, (1988).

1.82. E. Weber; M. Czugler. 'Functional Group Assisted Clathrate Formation in Scissor-like and Roof-shaped Molecules.' in *Topics in Current Chemistry*. **149**, 46, Springer-Verlag, Berlin Heidelberg, (1988).

CHAPTER 2 : EXPERIMENTAL.

The twenty crystal structures described can be divided into four classes, based on their host compounds.
Class A : Compounds of 1,1,2,2-Tetraphenylethane-1,2-diol, $C_{26}H_{22}O_2$.
Class B : Compounds of Triphenylmethanol, Ph_3COH.
Class C : Compounds of Triphenylsilanol, Ph_3SiOH.
Class D : Compounds of Tri-1-naphthylsilanol, $(C_{10}H_7)_3SiOH$.

Table 2.1 shows the compounds studied with their code names. The host : guest ratio quoted is that obtained from various analytical methods and used in the crystal structures. This table is repeated on a fold-out sheet in the back cover for easy reference.

Host compounds.

1,1,2,2-Tetraphenylethane-1,2-diol was synthesized by Toda. Various methods have been described.[2.1] The most commonly used involves the addition of 665 g (850 cm^3, 11 moles) of isopropyl alcohol to 150 g (0.82 moles) of benzophenone and one drop of glacial acetic acid. The mixture is exposed to bright sunlight for several days until crystals appear. The solution is chilled in ice, filtered with suction, washed with isopropyl alcohol and air dried. Yields are usually 93 - 94% and the compound melts at 188 - 190°C with decomposition.

A novel synthesis has recently been reported by Tanaka *et al.* [2.2] A mixture of benzophenone (1 g), Zn powder (5 g), $ZnCl_2$ (1 g) and 50% aqueous THF (10 ml) is stirred at room temperature for 1 hour. 3 M HCl (5 ml) is added and the solution filtered to remove the Zn. The filtrate is extracted with toluene; the toluene solution is washed with water, dried over $MgSO_4$ and evaporated to give the host compound in 84% yield. A similar procedure has been used to produce the coupling reaction in the solid state. A mixture of benzophenone, Zn and $ZnCl_2$ in the same proportions as above is kept at room temperature for 6 hours, then combined with 3 M HCl (5 ml) and toluene (10 ml) and filtered to remove Zn. The filtrate is worked up as before to give the product in 86% yield.

Triphenylmethanol and triphenylsilanol are commercially available but were rather obtained from E. Weber, der Universität Bonn, Germany.

Table 2.1. Compounds studied.

Host	Guest	Host:Guest	Code name
Class A.			
$C_{26}H_{22}O_2$	-	-	**PEDIL**
	dmso	1:2	**DEMPE**
	dioxane	1:1	**PEDIOX**
	p-chlorotoluene	2:1	**PECTIL**
	2,6-lutidine	1:1	**DINM**
	3,5-lutidine	1:2	**LUTI**
	3,4-lutidine	1:2	**DINO**
	acetone	1:1	**PEACH**
Class B.			
Ph_3COH	dioxane	1:1	**W1DIOX**
Class C.			
Ph_3SiOH	-	-	**WEB2**
	dmso	2:1	**TRIPSID**
	dioxane	4:1	**BASIL**
	ethanol	4:1	**SETH**
Class D.			
$(C_{10}H_7)_3SiOH$	dmso	1:1	**DUNCAN**
	dioxane	1:1	**NADIO**
	toluene	1:1	**NATOL**
	o-xylene	1:1	**ODIN**
	m-xylene	1:1	**MAXINE**
	p-xylene	1:2	**NAPPY**
	triethylamine	1:1	**NATRET**

Tri-1-naphthylsilanol has been synthesized by Skobridis.[2.3] 131.2 ml (0.21 mol) *n*-BuLi (1.6M in *n*-hexane) was added slowly to a stirred solution of 44.0 g (0.21 mol) 1-bromonaphthalene in 100 ml dry Et_2O under argon. The temperature is kept between 0° and 5°C. After stirring for 20 min, a solution of 10.2 g (60mmol) $SiCl_4$ in 50 ml dry Et_2O is added under the same temperature conditions. Stirring is continued for two hours at this temperature before the mixture is poured on to 100 ml dilute HCl. The precipitate which forms is collected and washed with a few millilitres of cold MeOH. The organic layer is separated, washed with H_2O and dried over Na_2SO_4. Evaporation of the solvent yields a viscous oil which solidifies on addition of a few millilitres of EtOH. The two crops of solid are combined and recrystallized from toluene to give the 1 : 1 clathrate which is decomposed under vacuum (15 Torr) and heating (100°C) to yield the pure host compound in 53% yield and melt point of 209 - 211°C (lit.[2.4] mp. 208-209°C).

Inclusion compound formation.

Inclusion compounds of classes A, B and C were formed by dissolving the host compound in diethyl ether, which had been dried over a molecular sieve and sodium wire. A small amount of the guest liquid, in at least ten times molar excess of the host, was then added. The resulting solution was allowed to evaporate slowly at room temperature until crystals formed. In cases where crystals would not grow, or grew as fine needles, the solutions were filtered before being allowed to evaporate. In extreme cases, the solutions were kept at 10°C, to prevent the guest liquid from evaporating too quickly which allowed only poor quality crystals to grow. Compounds in class D were formed in an identical manner to that described above, except that the solvent used for the host was chloroform.

Physical Analyses.

Deterioration was rapid for most of the inclusion compounds so crystals were removed from their mother liquor and blotted dry on filter paper just before analysis. The time that they were exposed to the atmosphere before analysis was kept to a minimum. The isothermal decay of **SETH** crystals is illustrated in Figure 2.1.

(a)

(b)

(c)

Figure 2.1. Isothermal decay of **SETH** crystals.

(a) t = 0 minutes,

(b) t = 2 minutes,

(c) t = 5 minutes.

Microanalysis.

The four hosts and their inclusion compounds were analyzed for their carbon, hydrogen and nitrogen content using an Heraeus Universal combustion analyser, Model CHN-RAPID.[2.5] The results of the microanalyses of the host compounds are shown in Table 2.2. Microanalysis results of inclusion compounds are reported in Chapter 3. The hosts show close agreement between calculated and observed values but a wider range was accepted for the inclusion compounds because :

(a) inclusion compounds of this type are not necessarily stoichiometric.

(b) the low stability of most of these compounds affects their microanalyses. Once a crystal has been removed from its mother liquor it may begin to decay within minutes. This is particularly true of crystals containing guests with high vapour pressures, or guests which are weakly held within the host lattice.

Table 2.2. C, H, N microanalysis of the host compounds.

	Observed			Calculated		
Compound (Formula)	%C	%H		%C	%H	
1,1,2,2-Tetraphenyl-ethane-1,2-diol ($C_{26}H_{22}O_2$)	85.0	6.1		85.2	6.0	
Triphenylmethanol ($C_{19}H_{16}O$)	87.5	6.2		87.7	6.2	
Triphenylsilanol ($C_{18}H_{16}OSi$)	78.0	5.9		78.2	5.8	
Tri-1-naphthylsilanol ($C_{30}H_{22}OSi$)	84.1	5.2		84.5	5.2	

Density measurements.

Densities were measured by the flotation method. A crystal was blotted dry and immersed in a mixture of saturated potassium iodide solution and water. Further additions of the KI solution or water were made until the density of the solution matched that of the crystal. Once the crystal was suspended in a homogeneous solution, the density of the solution was measured using a Paar Digital Densitymeter DMA35. The density was corrected for variations in temperature, although this factor was never more than 0.005 gcm^{-3}. This method was fairly slow so that decomposition of the crystal may have occurred.

Melting points.

These were measured visually on a Linkam TH600 hot stage mounted on a Nikon microscope equipped with polarizing and overhead light. The temperature was controlled by a Linkam CO600 temperature controller. The hot stage was calibrated using azobenzene (68°C), benzil (95°C), benzanilide (163°C) and dicyandiamide (210°C).

For the inclusion compounds, loss of guest was always the first event seen. This was usually evidenced by a gradual "clouding over" of the crystal surface. Sometimes a rearrangement of the remaining compound could be seen, but generally, the crystal retained its shape until the melting point of the host was reached. These thermal results were corroborated by differential scanning calorimetry (DSC).

Infrared Spectroscopy.

This technique was used to identify the O-H stretching frequency of each sample. Crystals which had been blotted dry were ground with nujol into a mull. This was applied to KBr plates. The percentage transmission was measured from 3000 to 4000 cm^{-1} and recorded using a double-beam Perkin Elmer 983 spectrophotometer.

Nuclear Magnetic Resonance Spectroscopy.

Samples were dissolved in $CDCl_3$ and ^1H NMR spectra were recorded at 200 MHz on a Varian VXR200 spectrometer using sodium 2-dimethyl-2-silapentane (DSS) as reference.

X-Ray Powder Diffraction.

Crystals were crushed to an approximately uniform particle size, then pressed into a sample holder. It was not possible to sieve the crushed crystals or to otherwise ensure a uniform particle size because of the instability of the compounds. Thus preferred orientation effects were possible. Powder diffraction patterns were obtained using a Philips vertical goniometer PW1050/80 with a PW1394 motor control unit, using X-rays generated by a Philips X-ray generator operating at 45kV and 30mA. Nickel filtered copper K_α radiation (λ = 1.5418Å) was used with divergent and receiving slits of ½° each and an anti-scatter slit of 1°. The range scanned was $8° \leq 2\theta \leq 40°$ at a scanning speed of 2° $(2\theta).min^{-1}$.

Thermal Analysis.

Thermogravimetry (TG) and Differential Scanning Calorimetry (DSC) were used to :
(i) establish the stoichiometry of the inclusion compounds,
(ii) determine at what temperature guests were released from the crystal,
(iii) determine whether any phase changes occurred in the crystal structure before or after guest loss and
(iv) evaluate the enthalpy associated with such phase changes or guest losses.

In some systems, TG was also used to evaluate the activation energy of the guest release reaction.

TG and DSC were performed on a Perkin Elmer PC Series 7 system. Sample weights were typically between 3 and 10 mg and the thermal analyses were run over a temperature range of 30 - 250°C at a heating rate of $10°Cmin^{-1}$ unless otherwise stated. A continual stream of dry nitrogen was passed over the samples at a flow rate of $30\ mlmin^{-1}$. An empty aluminium pan was used as the reference material for DSC.

Because the TG and DSC were run on different instruments at different times the curves do not always align perfectly. In particular, TG was performed by placing the crushed sample in an open platinum pan suspended in the furnace, while DSC was carried out using crimped, vented aluminium pans.

Figure 2.2 shows a schematic thermobalance and DSC furnace.

The TG analyser was calibrated using built-in procedures for furnace and weight calibration. In addition, Curie points were determined for alumel (163°C) and perkalloy (596°C) and used to calibrate the furnace.

The DSC was calibrated using the melting points of Indium (156.4°C) and Zinc (419.5°C) as well as the enthalpy of melting of Indium ($28.5\ Jg^{-1}$)

The sample size was kept small and samples were crushed and evenly spread to give the best reproducibility.[2.6]

Competition experiment.

Varying mole fractions of 2,6- and 3,5-lutidine were added to the host, 1,1,2,2-tetraphenylethane-1,2-diol, which had been dissolved in Et_2O. The solutions were left for several weeks until crystals formed. These were dissolved in acetone and analyzed by gas chromatography using a Pye Unicam PU4500 Chromatograph which was equipped with a Flame Ionizer Detector; output was plotted on a pen recorder. The columns used were glass tubing packed with 10% (w/w) Squalane on Chromosorb W (80/100 mesh) at a temperature of 180°C. Nitrogen was used as the carrier gas (30 $mlmin^{-1}$) and the flame of the detector was supported by an air/hydrogen mixture. The injector and detector temperatures were 250°C and the sample aliquot was 5 μl. X-ray powder diffraction studies were performed as described previously, to determine the phase changes in the crystals.

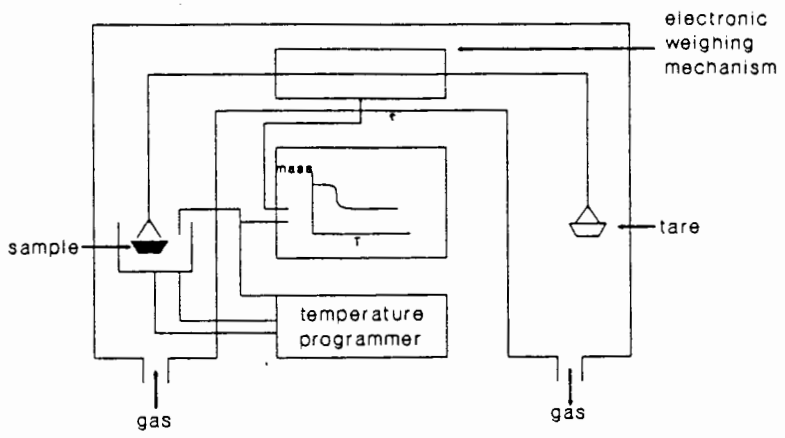

(a)

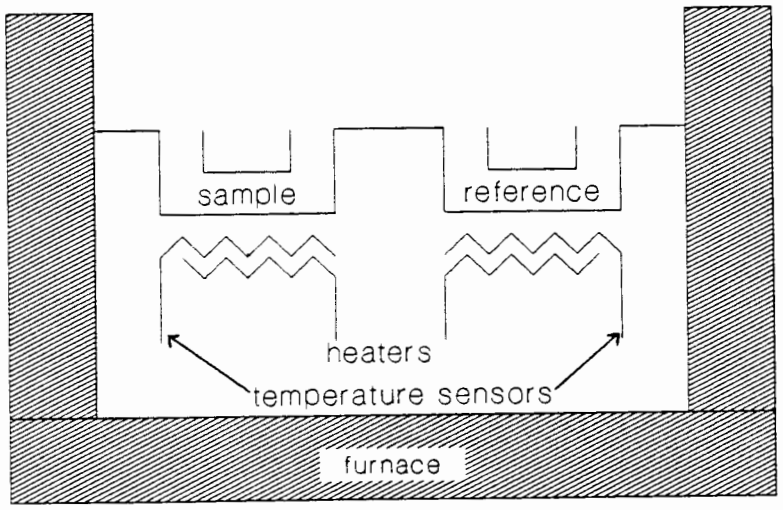

(b)

Figure 2.2. Schematic diagrams of (a) a thermobalance and (b) a Differential Scanning Calorimeter furnace.

Crystal Structure Analysis.

Single crystals were selected on the basis of their ability to extinguish polarized light. If necessary, crystals were cut to suitable size. Once a crystal had been selected or cut, it was mounted in either a 0.3 mm or a 0.5 mm Lindemann capillary tube with a little of its mother liquor. This helped to prevent deterioration of the crystal caused by guest desorption. Both ends of the capillary were sealed in a naked flame; sometimes sealing wax was used on the wider end to give a better seal. The capillary was then mounted in a brass pin suitable for insertion into a goniometer head. A photograph of a crystal of **NADIO** in its Lindemann tube is shown in Figure 2.3.

Approximate cell parameters and space group symmetry were obtained from oscillation and Weissenberg photographs taken on a Stöe camera using nickel filtered Copper K_α radiation (λ = 1.5418Å).

Accurate cell parameters were obtained by least squares analysis on the setting angles of 24 high θ reflections collected and centred on an Enraf Nonius CAD4 diffractometer. For intensity data collection, graphite monochromated Molybdenum K_α radiation (λ = 0.7107Å) and the ω - 2θ method were used, with a final acceptance limit of 20σ at 20°min^{-1} and a maximum recording time of 40 seconds. The vertical aperture length was fixed at 4mm. The aperture width was set at (x + 1.05tan θ) mm and scan width at (y + 0.35 tan θ) $\Delta\omega^{\circ -1}$. The intensities and orientation of reference reflections were monitored periodically to check crystal stability and orientation and instrumental stability. Data reduction included corrections for Lorentz and polarization effects and, in some cases, an empirical absorption correction[2.7] was also applied. Final refinements were based only on those reflections that satisfied the condition I > 2σI. Crystal data, experimental and refinement parameters are given in Tables 2.3 - 2.13.

Refinement of **PEDIL** and **PECTIL**, using data collected at 293K, proved unsatisfactory. The electron density maps indicated that the central ethane carbon atoms were disordered and the final model, in each case, yielded poor standard deviations for bond lengths and angles, very high temperature factors and final R-factors of 0.135 and 0.118 respectively with non-hydrogen atoms treated anisotropically. It was therefore decided to recollect the intensity data at a lower temperature. This was done by blowing cooled dry nitrogen on to a crystal which was enclosed in a Lindemann capillary. An FTS Systems Air Jet XR-85-1 cooling device, which reached a temperature of 228±2K was used. The data, and final structures, reported for **PEDIL** and **PECTIL** are those obtained at this lower temperature.

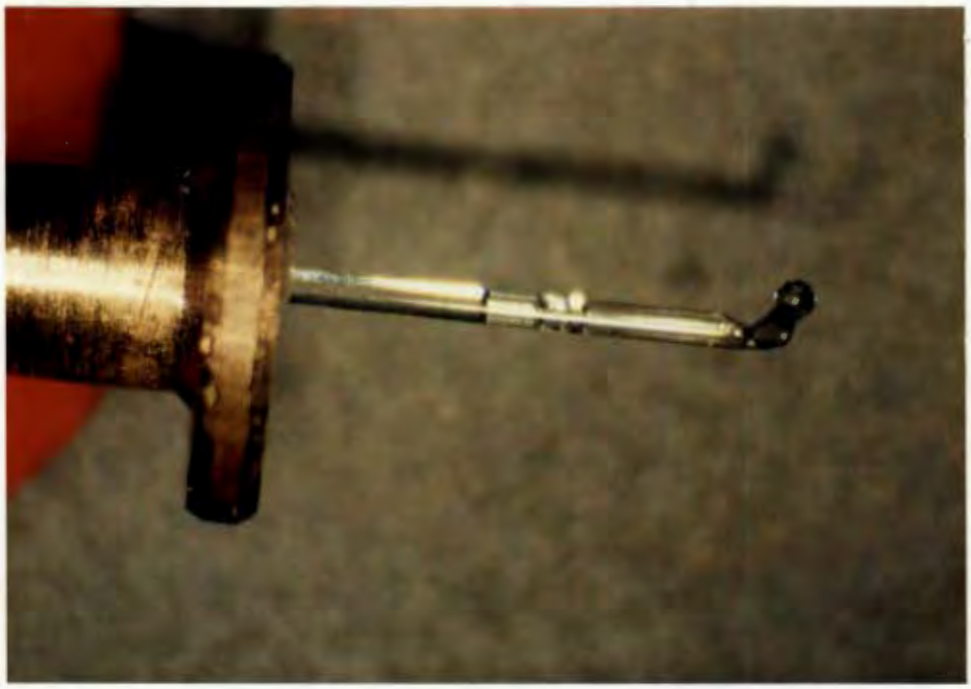

Figure 2.3. A crystal of **NADIO** mounted in a Lindemann capillary to prevent desorption of the guest during data collection.

Computation.

Computations were performed on a VAX/VMS (version 5.4) mainframe computer at the University of Cape Town Computer Centre.

All structures were solved by direct methods using SHELXS-86.[2.8] Refinement was carried out using the SHELX76[2.9] program system which uses the atomic radii calculated by Pauling.[2.10] Complex neutral atom scattering factors for non-hydrogen atoms were those of Cromer and Mann[2.11], that of hydrogen was taken from Stewart *et al.*[2.12] Dispersion corrections were taken from Cromer and Liberman.[2.13]

Agreement between the observed (F_o) and calculated (F_c) structure factors is expressed by the residual index, R, which is defined as

$$R = \Sigma| \, |F_o| - |F_c| \, | \, / \Sigma \, |F_o|$$
$$= \Sigma \, |\Delta| \, / \Sigma \, |F_o|$$

Agreement may also be expressed in terms of the weighted residual, R_w,

$$R_w = \Sigma \, w^{½} \, |\Delta| \, / \Sigma \, w^{½} \, |F_o| \quad \text{where } w = (\sigma^2 F + gF^2)^{-1}$$

The generalised residual used for the application of the Hamilton test is given as

$$R_G = \surd [(\Sigma \, w \, |\Delta|^2) / \Sigma \, |F_o|^2]$$

Molecular geometry calculations were performed using PARST.[2.14] Figures of molecules and packing diagrams were drawn using PLUTO.[2.15]

OPEC [2.16] was used to calculate the shape and size of guest cavities by computing molecular volumes. By sampling a very large number of probe points contained in an envelope space, and counting the number of points inside at least one of the spheres described by the atomic radii of the atoms present, it was possible to calculate the molecular volume. Using this technique it was possible to map the space occupied by the host molecules, and hence to identify the cavities or channels which may be occupied by guest molecules.

EENY[2.17] was employed for energy calculations. It uses atom pair potentials to calculate inter- and intramolecular non-bonded interactions. Van der Waals energy is of the form

$$U(r) = a \exp(-br)/r^d - c/r^6 \qquad (1)$$

where r is the distance between any pair of atoms (in Å) and a,b,c,d are coefficients as calculated by Giglio[2.18] and Pavel *et al.*[2.19] so that U(r) is evaluated in $kcalmol^{-1}$.

Function (**1**) takes no account of hydrogen bonding. In fact, when an O···O or O···N distance of 2.5 - 3.0 Å is encountered (typical of a strong hydrogen bond), the energy evaluated by (**1**) is unrealistically high.

EENY was therefore only useful when no hydrogen bonds were present in the structure.

HEENY[2.20], a modified version of EENY which includes a simple function to recognise angle-dependent hydrogen bonding, was therefore employed. The function chosen was

$$V_{hb} = ((A/R^{16}) - (C/R^{10})) \cos^2 \theta \qquad (2)^{2.21}$$

where R is the distance between the hydrogen and the acceptor, θ is the angle at the hydrogen and the constants A and C are related to the well depth V_{min} and the equilibrium distance R_o by :

$$A = -5R_o^{12} V_{min} \; ; \; C = -6R_o^{10} V_{min}.$$

The main drawback of equation (**2**) is that a hydrogen bond detected at θ = 90° is allowed the same close contact as one at the more plausible θ = 180°. Therefore, a "mixing scheme" (equation (**3**)) was used so that a full non-bonded potential, V_{normal}, is progressively switched on as the angle deviates from ideal hydrogen bonding geometry.

$$V_{total} = V_{hb} + (1-\lambda) V_{normal} \; ; \; \lambda = \cos^2\theta \qquad (3)$$

The Cambridge Structural Database[2.22] was used to retrieve and analyse crystallographic data. Each search in CSD was performed by defining a molecular fragment (using CONNser). The GSTAT program was then used, when necessary, to calculate interatomic distances and geometry. Scatterplots of hydrogen bonded Donor···Acceptor distances versus Donor-hydrogen···Acceptor angles were generated.

ALCHEMY II[2.23] provided a minimization function for individual molecules and was also used to generate colour plots. The potential energy of a molecule was minimized in terms of bond stretching, angle bending, torsion deformation, van der Waals interactions and out of plane bending.

Table 2.3 Crystal data, experimental and refinement parameters.

Host : 1,1,2,2-tetraphenylethane-1,2-diol

Compound	**PEDIL**	**DEMPE**
Guest	none	dmso
H : G ratio	-	1:2
M_r	366.46	522.72
D_m (gcm^{-3})	1.26	1.24
D_c (gcm^{-3})	1.26	1.26
μ (Mo K_α) (cm^{-1})	0.42	1.84
F(000)	776	1112
Space group	$P2_1/n$	$P\bar{1}$
a (Å)	17.669(6)	9.317(5)
b (Å)	6.144(6)	18.384(6)
c (Å)	17.873(6)	18.496(3)
α (°)	90	61.16(2)
β (°)	92.67(3)	83.22(3)
γ (°)	90	88.06(3)
Volume ($Å^3$)	1938(1)	2754(2)
Z	4	4
Data collection temperature (K)	228	293
Crystal dimensions (mm)	0.39 x 0.50 x 0.50	0.50 x 0.44 x 0.47
θ range scanned (°)	1 - 25	1 - 20
Range of indices *h, k, l*	±21, +7, +21	±8, ±17, +17
Total exposure time (hrs)	17	40
Crystal stability (%)	1.0	4.3
Scan width, x (°)	0.90	0.85
Aperture width, y (mm)	1.12	1.12
Vertical aperture length (mm)	4	4
Unique reflections	2115	5334
Observed reflections	1405	3978
Number of variables	252	658
R	0.071	0.103
Rw	0.079	0.120
w	$(\sigma^2F + 0.002F^2)^{-1}$	$(\sigma^2F + 0.02F^2)^{-1}$
Max. shift/e.s.d.	0.088	0.270
Max., min. heights in emap ($eÅ^{-3}$)	0.24, -0.24	0.62, -0.63

Table 2.4 Crystal data, experimental and refinement parameters.

Host : 1,1,2,2-tetraphenylethane-1,2-diol

Compound	**PEDIOX**	**PECTIL**
Guest	dioxane	*p*-chlorotoluene
H : G ratio	1:1	2:1
M_r	454.57	859.51
D_m (gcm^{-3})	1.26	1.27
D_c (gcm^{-3})	1.26	1.25
μ (Mo K_α) (cm^{-1})	0.46	0.97
F(000)	968	454
Space group	*C*2/*c*	$P\bar{1}$
a (Å)	8.648(1)	6.093(1)
b (Å)	16.551(1)	9.103(2)
c (Å)	17.038(4)	20.933(10)
α (°)	90	93.95(3)
β (°)	100.40(2)	93.23(3)
γ (°)	90	103.86(2)
Volume ($Å^3$)	2398(3)	1121.4(6)
Z	4	1
Data collection temperature (K)	293	228
Crystal dimensions (mm)	0.38 x 0.41 x 0.44	0.30 x 0.45 x 0.50
θ range scanned (°)	1 - 25	1 - 20
Range of indices *h, k, l*	±10, ±11, +20	±5, ±8, +20
Total exposure time (hrs)	29.4	16.6
Crystal stability (%)	0.4	2.7
Scan width, x (°)	0.85	0.85
Aperture width, y (mm)	1.12	1.12
Vertical aperture length (mm)	4	4
Unique reflections	4363	2157
Observed reflections	3008	1760
Number of variables	178	249
R	0.077	0.096
Rw	0.087	0.115
w	$(\sigma^2F + 0.001F^2)^{-1}$	$(\sigma^2F + 0.001F^2)^{-1}$
Max. shift/e.s.d.	0.001	0.097
Max., min. heights in emap ($eÅ^{-3}$)	0.60, -0.73	0.42, -0.44

Table 2.5 Crystal data, experimental and refinement parameters.

Host : 1,1,2,2-tetraphenyl-1,2-diol

Compound	**DINM**	**LUTI**
Guest	2,6-lutidine	3,5-lutidine
H : G ratio	1:1	1:2
M_r	473.62	580.77
D_m (gcm^{-3})	1.17	1.12
D_c (gcm^{-3})	1.20	1.15
μ (Mo K_α) (cm^{-1})	0.40	0.64
F(000)	504	1240
Space group	$P\bar{1}$	$P\bar{1}$
a (Å)	9.414(7)	12.099(4)
b (Å)	11.191(4)	17.869(5)
c (Å)	13.328(18)	17.873(10)
α (˚)	82.81(7)	64.65(3)
β (˚)	70.78(12)	87.32(4)
γ (˚)	86.44(4)	75.25(2)
Volume ($Å^3$)	1315(2)	3368(3)
Z	2	4
Data collection temperature (K)	293	293
Crystal dimensions (mm)	0.30 x 0.55 x 0.50	0.40 x 0.40 x 0.30
θ range scanned (˚)	1 - 22	1 - 22
Range of indices *h, k, l*	±9, ±11, +14	±11, ±17, +17
Total exposure time (hrs)	33.7	67.8
Crystal stability (%)	3.9	5.2
Scan width, x (˚)	0.95	0.90
Aperture width, y (mm)	1.20	1.12
Vertical aperture length (mm)	4	4
Unique reflections	3382	8561
Observed reflections	2501	4561
Number of variables	338	700
R	0.043	0.070
Rw	0.048	0.082
w	$(\sigma^2F + 0.002F^2)^{-1}$	$(\sigma^2F + 0.02F^2)^{-1}$
Max. shift/e.s.d.	0.054	0.010
Max., min. heights in emap ($eÅ^{-3}$)	0.30, -0.19	0.33, -0.25
Minimum transmission (%)	91.65	
Maximum transmission (%)	99.97	
Average transmission (%)	95.69	

Table 2.6 Crystal data, experimental and refinement parameters.

Host : 1,1,2,2-tetraphenylethane-1,2-diol

Compound	**DINO**	**PEACH**
Guest	3,4-lutidine	acetone
H : G ratio	1:2	1:1
M_r	580.77	424.54
D_m (gcm^{-3})	1.14	1.19
D_c (gcm^{-3})	1.15	1.19
μ (Mo K_α) (cm^{-1})	0.38	0.71
F(000)	620	904
Space group	$P\bar{1}$	$P2_1/c$
a (Å)	9.163(4)	9.250(3)
b (Å)	11.740(4)	18.183(4)
c (Å)	17.721(7)	14.272(3)
α (°)	69.50(3)	90
β (°)	74.22(4)	99.38(2)
γ (°)	73.09(4)	90
Volume ($Å^3$)	1677(1)	2368(2)
Z	2	4
Data collection temperature (K)	293	293
Crystal dimensions (mm)	0.45 x 0.35 x 0.50	0.37 x 0.37 x 0.50
θ range scanned (°)	1 - 23	1 - 25
Range of indices *h, k, l*	±10, ±12, +19	±11, +21, +17
Total exposure time (hrs)	40.6	30.0
Crystal stability (%)	2.6	5.4
Scan width, x (°)	0.95	0.85
Aperture width, y (mm)	1.20	1.12
Vertical aperture length (mm)	4	4
Unique reflections	4828	4488
Observed reflections	2927	2772
Number of variables	419	298
R	0.067	0.045
Rw	0.071	0.058
w	$(\sigma^2F + 0.001F^2)^{-1}$	$(\sigma^2F + 0.005F^2)^{-1}$
Max. shift/e.s.d.	0.008	0.180
Max., min. heights in emap ($eÅ^{-3}$)	0.28, -0.23	0.15, -0.17
Minimum transmission (%)	82.60	
Maximum transmission (%)	99.71	
Average transmission (%)	92.26	

Table 2.7 Crystal data, experimental and refinement parameters.

Host :	Triphenylmethanol
Compound	**W1DIOX**
Guest	dioxane
H : G ratio	1:1
M_r	348.44
D_m (gcm^{-3})	1.24
D_c (gcm^{-3})	1.22
μ (Mo K_α) (cm^{-1})	0.45
F(000)	372
Space group	$P\bar{1}$
a (Å)	8.441(8)
b (Å)	10.544(2)
c (Å)	11.562(2)
α (°)	67.47(1)
β (°)	83.96(5)
γ (°)	89.08(5)
Volume ($Å^3$)	944.9(2)
Z	2
Data collection temperature (K)	293
Crystal dimensions (mm)	0.38 x 0.44 x 0.44
θ range scanned (°)	1 - 25
Range of indices *h, k, l*	±10, ±12, +13
Total exposure time (hrs)	28.2
Crystal stability (%)	2.6
Scan width, x (°)	0.85
Aperture width, y (mm)	1.12
Vertical aperture length (mm)	4
Unique reflections	4061
Observed reflections	2824
Number of variables	241
R	0.052
Rw	0.047
w	$(\sigma^2F)^{-1}$
Max. shift/e.s.d.	0.001
Max., min. heights in emap ($eÅ^{-3}$)	0.21, -0.35

Table 2.8 Crystal data, experimental and refinement parameters.

Host :	Triphenylsilanol	
Compound	**WEB2**	**TRIPSID**
Guest	none	dmso
H : G ratio	-	2:1
M_r	276.41	602.87
D_m (gcm^{-3})	1.18	1.12
D_c (gcm^{-3})	1.18	1.19
μ (Mo K_α) (cm^{-1})	1.35	2.44
F(000)	2336	640
Space group	$P\bar{1}$	$P\bar{1}$
a (Å)	15.235(5)	8.681(4)
b (Å)	19.983(13)	9.550(2)
c (Å)	23.250(18)	24.104(4)
α (°)	108.76(6)	95.97(2)
β (°)	103.47(5)	90.06(3)
γ (°)	101.17(5)	117.03(2)
Volume ($Å^3$)	6234(8)	1767(2)
Z	16	2
Data collection temperature (K)	293	293
Crystal dimensions (mm)	0.34 x 0.41 x 0.44	0.31 x 0.38 x 0.44
θ range scanned (°)	1 - 23	1 - 25
Range of indices h, k, l	±16, ±22, +25	±9, ±10, +26
Total exposure time (hrs)	106.1	47.0
Crystal stability (%)	0.7	1.5
Scan width, x (°)	0.80	0.85
Aperture width, y (mm)	1.12	1.20
Vertical aperture length (mm)	4	4
Unique reflections	16002	6217
Observed reflections	9420	4170
Number of variables	1444	423
R	0.082	0.049
Rw	0.080	0.057
w	$(\sigma^2F)^{-1}$	$(\sigma^2F + 0.002F^2)^{-1}$
Max. shift/e.s.d.	0.075	0.002
Max., min. heights in emap ($eÅ^{-3}$)	0.37, -0.40	0.22, -0.24
Minimum transmission (%)	97.01	
Maximum transmission (%)	99.88	
Average transmission (%)	98.11	

Table 2.9 Crystal data, experimental and refinement parameters.

Host :	Triphenylsilanol	
Compound	**BASIL**	**SETH**
Guest	dioxane	ethanol
H : G ratio	4:1	4:1
M_r	1193.75	1151.71
D_m (gcm^{-3})	1.14	1.16
D_c (gcm^{-3})	1.21	1.17
μ (Mo K_α) (cm^{-1})	1.06	0.52
F(000)	1264	1220
Space group	$P\bar{1}$	$P\bar{1}$
a (Å)	9.378(7)	13.682(4)
b (Å)	11.851(2)	15.119(6)
c (Å)	14.891(2)	15.990(6)
α (°)	87.85(1)	88.23(3)
β (°)	81.05(1)	81.83(3)
γ (°)	87.65(1)	87.07(3)
Volume ($Å^3$)	1632(1)	3268(6)
Z	1	2
Data collection temperature (K)	293	293
Crystal dimensions (mm)	0.34 x 0.38 x 0.38	0.25 x 0.28 x 0.41
θ range scanned (°)	1 - 25	1 - 20
Range of indices *h, k, l*	±11, ±14, +17	±13, ±14, +15
Total exposure time (hrs)	39.5	49.6
Crystal stability (%)	1.2	9.8
Scan width, x (°)	0.85	0.85
Aperture width, y (mm)	1.12	1.12
Vertical aperture length (mm)	4	4
Unique reflections	5970	6399
Observed reflections	4468	3957
Number of variables	414	620
R	0.041	0.101
Rw	0.053	0.100
w	$(\sigma^2F + 0.005F^2)^{-1}$	$(\sigma^2F)^{-1}$
Max. shift/e.s.d.	0.001	0.316
Max., min. heights in emap ($eÅ^{-3}$)	0.30, -0.24	0.47, -0.43
Minimum transmission (%)	97.23	
Maximum transmission (%)	99.94	
Average transmission (%)	98.50	

Table 2.10 Crystal data, experimental and refinement parameters.

Host : Tri-1-naphthylsilanol

Compound	**DUNCAN**	**NADIO**
Guest	dmso	dioxane
H : G ratio	1:1	1:1
M_r	504.72	514.70
D_m (gcm^{-3})	1.26	1.26
D_c (gcm^{-3})	1.27	1.26
μ (Mo K_α) (cm^{-1})	1.54	1.15
F(000)	532	544
Space group	$P\bar{1}$	$P\bar{1}$
a (Å)	9.122(2)	9.298(4)
b (Å)	12.852(3)	12.577(9)
c (Å)	12.873(2)	12.859(6)
α (°)	61.75(2)	115.63(5)
β (°)	87.79(2)	90.99(3)
γ (°)	83.49(2)	92.34(5)
Volume ($Å^3$)	1320.7(5)	1353(1)
Z	2	2
Data collection temperature (K)	293	293
Crystal dimensions (mm)	0.22 x 0.25 x 0.31	0.41 x 0.41 x 0.50
θ range scanned (°)	1 - 25	1 - 25
Range of indices *h, k, l*	±10, ±15, +15	±11, ±15, +15
Total exposure time (hrs)	34.9	33.1
Crystal stability (%)	1.5	2.9
Scan width, x (°)	0.85	0.85
Aperture width, y (mm)	1.12	1.12
Vertical aperture length (mm)	4	4
Unique reflections	4864	4973
Observed reflections	3066	3883
Number of variables	352	349
R	0.090	0.038
Rw	0.116	0.048
w	$(\sigma^2F + 0.05F^2)^{-1}$	$(\sigma^2F + 0.002F^2)^{-1}$
Max. shift/e.s.d.	0.041	0.002
Max., min. heights in emap ($eÅ^{-3}$)	0.55, -0.40	0.23, -0.17
Minimum transmission (%)	95.44	95.15
Maximum transmission (%)	99.92	99.96
Average transmission (%)	97.86	97.79

Table 2.11 Crystal data, experimental and refinement parameters.

Host :	Tri-1-naphthylsilanol	
Compound	**NATOL**	**ODIN**
Guest	toluene	*o*-xylene
H : G ratio	1:1	1:1
M_r	518.73	532.76
D_m (gcm^{-3})	1.21	1.23
D_c (gcm^{-3})	1.23	1.24
μ (Mo K_α) (cm^{-1})	1.06	0.75
F(000)	548	564
Space group	$P\bar{1}$	$P\bar{1}$
a (Å)	9.465(3)	9.399(5)
b (Å)	12.424(2)	12.475(6)
c (Å)	13.344(4)	13.577(5)
α (°)	116.07(2)	115.96(4)
β (°)	91.67(2)	90.37(4)
γ (°)	92.77(2)	92.71(4)
Volume ($Å^3$)	1405.6(7)	1429(1)
Z	2	2
Data collection temperature (K)	293	293
Crystal dimensions (mm)	0.38 x 0.40 x 0.40	0.25 x 0.22 x 0.31
θ range scanned (°)	1 - 23	1 - 25
Range of indices *h, k, l*	±10, ±13, +14	±11, ±14, +16
Total exposure time (hrs)	28.8	38.1
Crystal stability (%)	1.7	7.8
Scan width, x (°)	0.90	0.85
Aperture width, y (mm)	1.12	1.12
Vertical aperture length (mm)	4	4
Unique reflections	4113	5252
Observed reflections	2958	2735
Number of variables	353	374
R	0.059	0.080
Rw	0.070	0.077
w	$(\sigma^2F + 0.002F^2)^{-1}$	$(\sigma^2F + 0.005F^2)^{-1}$
Max. shift/e.s.d.	0.005	0.006
Max., min. heights in emap ($eÅ^{-3}$)	0.83, -0.22	0.23, -0.36
Minimum transmission (%)	87.19	47.18
Maximum transmission (%)	99.96	99.50
Average transmission (%)	94.56	69.79

Table 2.12 Crystal data, experimental and refinement parameters.

Host :	Tri-1-naphthylsilanol	
Compound	**MAXINE**	**NAPPY**
Guest	*m*-xylene	*p*-xylene
H : G ratio	1:1	1:2
M_r	532.76	638.93
D_m (gcm^{-3})	1.22	1.15
D_c (gcm^{-3})	1.24	1.17
μ (Mo K_α) (cm^{-1})	1.06	0.94
F(000)	564	680
Space group	$P\bar{1}$	$P\bar{1}$
a (Å)	11.974(3)	9.315(6)
b (Å)	12.243(2)	12.462(1)
c (Å)	12.317(2)	15.901(4)
α (°)	65.16(1)	82.51(2)
β (°)	72.50(2)	82.08(4)
γ (°)	61.85(2)	87.25(5)
Volume ($Å^3$)	1432.9(6)	1811(1)
Z	2	2
Data collection temperature (K)	293	293
Crystal dimensions (mm)	0.31 x 0.34 x 0.34	0.28 x 0.31 x 0.31
θ range scanned (°)	1 - 25	1 - 25
Range of indices *h, k, l*	±14, ±14, +14	±10, ±13, +17
Total exposure time (hrs)	35.3	49.1
Crystal stability (%)	3.5	1.2
Scan width, x (°)	0.85	0.85
Aperture width, y (mm)	1.12	1.12
Vertical aperture length (mm)	4	4
Unique reflections	5305	6455
Observed reflections	4086	3856
Number of variables	375	456
R	0.038	0.048
Rw	0.044	0.057
w	$(\sigma^2F + 0.001F^2)^{-1}$	$(\sigma^2F + 0.005F^2)^{-1}$
Max. shift/e.s.d.	0.201	0.042
Max., min. heights in emap ($eÅ^{-3}$)	0.20, -0.25	0.30, -0.20
Minimum transmission (%)	89.82	84.60
Maximum transmission (%)	99.85	99.19
Average transmission (%)	94.34	90.42

Table 2.13 Crystal data, experimental and refinement parameters.

Host :	Tri-1-naphthylsilanol
Compound	**NATRET**
Guest	triethylamine
H : G ratio	1:1
M_r	527.78
D_m (gcm^{-3})	1.19
D_c (gcm^{-3})	1.17
μ (Mo K_α) (cm^{-1})	1.02
F(000)	564
Space group	$P\bar{1}$
a (Å)	12.254(6)
b (Å)	12.472(11)
c (Å)	12.675(7)
α (°)	119.51(5)
β (°)	107.35(5)
γ (°)	99.07(5)
Volume ($Å^3$)	1497(2)
Z	2
Data collection temperature (K)	293
Crystal dimensions (mm)	0.38 x 0.38 x 0.40
θ range scanned (°)	1 - 23
Range of indices h, k, l	±13, ±13, +13
Total exposure time (hrs)	31.8
Crystal stability (%)	3.3
Scan width, x (°)	0.90
Aperture width, y (mm)	1.12
Vertical aperture length (mm)	4
Unique reflections	4378
Observed reflections	3047
Number of variables	368
R	0.050
Rw	0.046
w	$(\sigma^2F)^{-1}$
Max. shift/e.s.d.	0.008
Max., min. heights in emap ($eÅ^{-3}$)	0.21, -0.22
Minimum transmission (%)	86.25
Maximum transmission (%)	99.79
Average transmission (%)	94.94

References.

2.1. A. H. Blatt (Ed.). *Org. Synth. Coll. Vol. II.* John Wiley and Sons, New York. 71, (1943) and references therein.

2.2. K. Tanaka; S. Kishigami; F. Toda. *J. Org. Chem.* **55**, 2981, (1990).

2.3. S. A. Bourne; L. R. Nassimbeni; K. Skobridis; E. Weber. In preparation.

2.4. H. Gilman; C. G. Branneu. *J. Am. Chem. Soc.* **73**, 4640, (1951).

2.5. I. Monar. *Mikrochimica Acta*, **6**, 784, (1972).

2.6. M. E. Brown. *Introduction to Thermal Analysis - techniques and applications.* Chapman & Hall, London, (1988).

2.7. A. C. T. North; D. C. Phillips; F. S. Mathews. *Acta Crystallogr.*, **A24**, 351, (1968).

2.8. G. M. Sheldrick in '*Crystallographic Computing 3.*' G. M. Sheldrick; C. Kruger and R. Goddard (Eds.) Oxford University, 175, (1985).

2.9. G. M. Sheldrick in '*Computing in Crystallography*', H.Schenk; R. Olthof-Hazekamp; J. Von Koningsveld and G. C. Bassi (Eds.) Delft University Press, 34, (1978).

2.10. L. Pauling in '*The Nature of the Chemical Bond.*' Cornell University Press, Ithaca, New York.

2.11. D. T. Cromer and J. B. Mann *Acta Crystallogr.*, **A24**, 321, (1968).

2.12. R. F. Stewart; E. R. Davidson; W. T. Simpson. *J. Chem. Phys.*, **42**, 3175, (1965).

2.13. D. T. Cromer and D. Liberman. *J. Chem. Phys.*, **53**, 1891, (1970).

2.14. M. Nardelli. '*PARST - A system of Computer Routines for Calculating Molecular Parameters from Results of Crystal Structure Analysis.*', University of Parma, Italy, (1982).

2.15. W. D. S. Motherwell in '*PLUTO and PLUTOX - programs for plotting molecular and crystal structures*', Cambridge University, England, unpublished.

2.16. A. Gavezzotti. *J. Am. Chem. Soc.*, **105**(16), 5220, (1983).

2.17. W. D. S. Motherwell in *'EENY - Potential Energy Program'*, Cambridge University, England, unpublished.

2.18. E. Giglio. *Nature*, **222**, 339, (1969).

2.19. N. V. Pavel; C. Quagliata; N. Scarcelli. *Z. Kristallogr.*, **144**, 64, (1976).

2.20. C. F. Marais. *'HEENY - Modification of EENY to allow H-bonding calculations.'* University of Cape Town, (1990).

2.21. J. Dunitz. *J. Am. Chem. Soc.* **107**, 7653, (1985).

2.22. Cambridge Structural Database & Cambridge Structural Database System, January 1991, Version 4.4, Cambridge Crystallographic Data Centre, University Chemical Laboratory, Cambridge, England.

2.23. ALCHEMY II, Tripos Associates Inc., St. Louis, Missouri, 1988.

CHAPTER 3 : PHYSICAL CHARACTERISATION.

Crystal data, data collection parameters and final refinement data were given in Tables 2.3 - 2.13. Tables of bond lengths, bond angles, fractional atomic coordinates of geometrically placed hydrogen atoms, analyses of variance and structure factors are included in Appendices 2 - 5.

Structure solution and refinement were similar for all twenty compounds. A general description is given below. No attempt is made to explain the theory of crystallography since such theory is readily available in several books.[3.1 - 3.4] Further details about direct methods can also be found in more specific literature.[3.5]

Physical methods of characterisation.

Microanalysis.

Microanalysis results are shown in Table 3.1 for the inclusion compounds and their respective hosts in each class.

Although the microanalysis results served to indicate the gross composition of these compounds, it would be inappropriate to attempt to estimate host to guest ratios because of the inherent drawbacks of this method.

Large deviations from expected values were obtained in some cases because the inclusion compounds are very unstable and suffer from severe decay (caused by guest loss) within minutes of being removed from their mother liquor. Repeated measurements gave the same results and these were accepted for the reasons outlined in Chapter 2.

Densities.

Despite the organic nature of the crystals, and their relatively low stabilities, precise density measurements could be made. The results are shown in Table 3.2.

Melting Points.

The melting points of the hosts are listed in Table 3.3. In general, the melt occurred only after some visible deterioration of the crystal and sometimes after an obvious change of phase. These effects however, can most clearly be explained in conjunction with the thermal analysis results of the compounds, which are given in Chapter 7.

Table 3.1. Microanalysis results.

	Observed			Calculated		
Compound (Formula)	%C	%H	%N	%C	%H	%N
Class A.						
PEDIL ($C_{26}H_{22}O_2$)	85.0	6.1	0	85.2	6.0	0
DEMPE ($C_{26}H_{22}O_2 . (C_2H_6OS)_2$)	63.5	5.4	0	68.9	6.6	0
PEDIOX ($C_{26}H_{22}O_2 . C_4H_8O_2$)	75.3	6.5	0	79.3	6.7	0
PECTIL ($C_{26}H_{22}O_2 . (C_7H_7Cl)_{0.5}$)	82.2	6.1	0	82.4	6.0	0
DINM ($C_{26}H_{22}O_2 . C_7H_9N$)	83.3	6.5	3.0	83.7	6.6	3.0
LUTI ($C_{26}H_{22}O_2 . (C_7H_9N)_2$)	83.2	6.8	4.65	82.8	6.9	4.9
DINO ($C_{26}H_{22}O_2 . (C_7H_9N)_2$)	82.2	6.9	4.9	82.8	6.9	4.9
PEACH ($C_{26}H_{22}O_2 . C_3H_6O$)	75.8	5.55	0	82.1	6.7	0
Class B.						
($C_{19}H_{16}O$)	87.5	6.2	0	87.7	6.2	0
W1DIOX ($C_{19}H_{16}O . C_4H_8O_2$)	82.8	7.0	0	83.1	7.3	0
Class C.						
WEB2 ($C_{18}H_{16}OSi$)	78.0	5.9	0	78.2	5.8	0
TRIPSID ($C_{18}H_{16}OSi . (C_2H_6OS)_{0.5}$)	71.5	5.8	0	72.3	6.1	0
BASIL ($C_{18}H_{16}OSi . (C_4H_8O_2)_{0.25}$)	75.4	6.0	0	76.5	6.1	0
SETH ($C_{18}H_{16}OSi . (C_2H_6O)_{0.25}$	76.7	6.3	0	77.2	6.1	0
Class D.						
($C_{30}H_{22}OSi$)	84.1	5.2	0	84.5	5.2	0
DUNCAN ($C_{30}H_{22}OSi . C_2H_6OS$)	74.0	5.5	0	76.2	5.6	0
NADIO ($C_{30}H_{22}OSi . C_4H_8O_2$)	78.1	5.8	0	79.3	5.9	0
NATOL ($C_{30}H_{22}OSi . C_7H_8$)	85.1	6.2	0	85.7	5.8	0
ODIN ($C_{30}H_{22}OSi . C_8H_{10}$)	85.1	6.1	0	85.7	6.1	0
MAXINE ($C_{30}H_{22}OSi . C_8H_{10}$)	85.1	6.1	0	85.7	6.1	0
NAPPY ($C_{30}H_{22}OSi . (C_8H_{10})_2$)	86.9	6.5	0	86.5	6.6	0
NATRET ($C_{30}H_{22}OSi . C_3H_{15}N$)	81.7	7.3	2.7	81.9	7.1	2.7

Table 3.2 . Densities.

Compound	D_C (gcm^{-3})	D_M (gcm^{-3})
Class A.		
PEDIL	1.256	1.255
DEMPE	1.260	1.242
PEDIOX	1.259	1.258
PECTIL	1.254	1.267
DINM	1.196	1.168
LUTI	1.145	1.119
DINO	1.150	1.135
PEACH	1.191	1.188
Class B.		
W1DIOX	1.224	1.240
Class C.		
WEB2	1.178	1.177
TRIPSID	1.185	1.120
BASIL	1.214	1.142
SETH	1.170	1.161
Class D.		
DUNCAN	1.270	1.262
NADIO	1.263	1.264
NATOL	1.225	1.211
ODIN	1.238	1.232
MAXINE	1.235	1.224
NAPPY	1.171	1.154
NATRET	1.171	1.087

PEDIL, the host 1,1,2,2-tetraphenylethane-1,2-diol, was reported[3.6] to have a melting point of 189°C. Toda *et al.*[3.6] also reported the melting point of the dmso complex (**DEMPE**) to be 136-138°C. This value roughly corresponds to a crystal structure rearrangement observed on the hot stage microscope at a rapid heating rate. This is discussed further in Chapter 7.

Table 3.3. Melting points

Compound	Melting Point (°C)
Class A.	
PEDIL	198.5
DEMPE	180
PEDIOX	190.5
PECTIL	198 - 200
DINM	198
LUTI	187
DINO	182
PEACH	198
Class B.	
$C_{19}H_{16}O$	160 - 161
W1DIOX	161
Class C.	
WEB2	155
TRIPSID	decomposes between 65 - 95°C
BASIL	150
SETH	155
Class D.	
$C_{30}H_{22}OSi$	208 - 209
DUNCAN	decomposes between 125 - 220°C
NADIO	207
NATOL	202
ODIN	212
MAXINE	209
NAPPY	212
NATRET	206

Infrared Spectroscopy.

Infrared spectra were measured to establish the presence of hydrogen bonds in the structures. Because the effect of hydrogen bonding on in-plane and out-of-plane bending is small[3.7], only the stretching frequencies of the hydroxyl group were examined. The results are listed in Table 3.4.

The stretching frequency of a non-bonded or "free" hydroxyl group[3.7] is about 3600cm^{-1}. When a hydrogen bond is formed, the O-H bond becomes longer, thus lowering the frequency of the hydroxyl stretch and broadening the band. Intermolecular hydrogen bonding gives rise to bands in the region 3600-3200cm^{-1} while intramolecular "chelate" hydrogen bonds give bands in the range 3200-2700cm^{-1}. Hydrogen bonds of the non-chelate type between identical molecules, such as those found between 1,2-diols, show sharp bands between 3570 and 3450cm^{-1}, the precise position of which depends on the strength of the hydrogen bond.[3.7]

PEDIL, the host compound for Class A, shows a sharp band at 3540cm^{-1} as expected for a 1,2-diol. All the guests used in this class, with the exception of *p*-chlorotoluene (**PECTIL**), participate in hydrogen bonding with the host's hydroxyl groups. **DEMPE**, **PEDIOX**, **DINM**, **LUTI**, **DINO** and **PEACH** showed a decrease in the O-H stretching frequency. **PECTIL** showed no change, which was expected as the hydrogen bonding scheme in **PECTIL** is identical with that of **PEDIL**.

Triphenylmethanol is thought to have a cyclic hydrogen-bonding network in its non-porous α-phase. This is given greater weight by the relatively low band at 3500cm^{-1}. On complexation with dioxane, the wave number of the O-H stretch is reduced, owing to the stronger host-guest hydrogen bond.

Triphenylsilanol, in the non-porous phase, has a peak at 3250cm^{-1}. The structure of this compound has been solved (compound **WEB2**) and shown to contain a very strong cyclic hydrogen-bonding network. The inclusion of oxygen-containing guests does not lead to very much stronger hydrogen bonding which accounts for the low $\Delta\nu$ values observed in this class.

It is clear that the α-phase of the host trinaphthylsilanol contains only a "free" hydroxyl group. **NATOL**, **ODIN**, **MAXINE** and **NAPPY**, where the guests are toluene and *o*-, *m*- and *p*-xylene, give similar spectra to that of the host in this region, since the guests interact weakly with the host's hydroxyl group. **DUNCAN**, **NADIO** and **NATRET** however, exhibit significantly different spectra owing to the host-guest hydrogen bonding.

Table 3.4. Infrared results.

Compound	ν O-H (cm^{-1})
Class A.	
PEDIL	3540 (3550)*
DEMPE	3312 (3250)
PEDIOX	3520, 3450 (3520, 3450)
PECTIL	3540 (3550)
DINM	3260
LUTI	3200
DINO	3300, 3160
PEACH	3551, 3373
Class B.	
$C_{19}H_{16}O$	3500
W1DIOX	3470
Class C.	
WEB2	3250
TRIPSID	3200
BASIL	3190
SETH	3200-3240
Class D.	
$C_{30}H_{22}OSi$	3670
DUNCAN	3520
NADIO	3540
NATOL	3605
ODIN	3610
MAXINE	3620
NAPPY	3620
NATRET	3490

* Numbers in brackets indicate the values obtained by Toda.[3.6]

Other complexes of 1,1,2,2-tetraphenylethane-1,2-diol reported by Toda.[3.6]

Guest	ν O-H (cm^{-1})
acetone (1:2)	3540
cyclopentanone (1:2)	3550
γ-butyrolactone (1:2)	3450
tetrahydrofuran (1:1)	3450
carbon tetrachloride (1:1)	3540
dimethylformamide (1:2)	3280
benzene (1:1)	3540
p-xylene (2:1)	3530
pyridine (1:2)	3220
2-methylquinoline (1:1)	3560, 3170
quinoline (1:2)	3300

NMR Spectroscopy.

^{1}H NMR spectra were used to establish the presence of a guest in an inclusion compound. Integration of the spectra allowed the calculation of the molar ratios of host and guest. These corresponded well with the ratios calculated using density measurements. The results are presented in Table 3.5. The italicised figures are those obtained for the pure guest compound from Pouchet.[3.8]

Thermogravimetry.

The results obtained by thermogravimetry (TG) are given in Table 3.6. These are the total weight losses observed for each of the inclusion compounds.

Stoichiometry of the inclusion compounds.

Density measurements, thermogravimetric and NMR results were all used to determine the stoichiometries of the inclusion compounds. The host to guest ratios obtained are listed in Table 3.7. All of these methods demonstrated again that these compounds do not necessarily have integral stoichiometries. It was deemed unnecessary to use fractional site occupancy factors in the crystal structure refinements however, since, in each case, the stoichiometry calculated was very close to an integral value.

Table 3.5 NMR spectra.

Compound	δ (ppm) (multiplicity)
Class A.	
PEDIL	3.1(s), 7.3(m)
$C_{26}H_{22}O_2$	*3.1(s), 7.3(m)*
DEMPE	2.6(s), 3.2(s), 7.2(m)
dmso	*2.6(s)*
PEDIOX	3.0(s), 3.7(s), 7.2(m)
dioxane	*3.7(s)*
PECTIL	2.4(s), 3.1(s), 7.2(m)
p-chlorotoluene	*2.35(s), 7.2(m)*
DINM	2.6(s), 3.1(s), 7.2(m)
2,6-lutidine	*2.55(s), 7.3(m)*
LUTI	2.3(s), 3.3(s), 7.2(m), 8.3(s)
3,5-lutidine	*2.3(s), 7.3(s), 8.3(s)*
DINO	2.3(s), 3.1(s), 7.2(m), 8.3(s)
3,4-lutidine	*2.3(s), 7.0(d), 8.3(d)*
PEACH	2.2(s), 3.0(s), 7.2(m)
acetone	*2.2(s)*
Class B	
$C_{19}H_{16}O$	2.8(s), 7.3(m)
$C_{19}H_{16}O$	*2.75(s), 7.3(s)*
W1DIOX	2.2(s), 3.7(s), 7.3(s)
dioxane	*3.7(s)*
Class C	
WEB2	2.6(s), 7.4(m) -
$C_{18}H_{16}OSi$	*3.0(s), 7.1-7.7(m)*
TRIPSID	2.5(s), 2.6(s), 7.4(m)
dmso	*2.6(s)*
BASIL	2.2(s), 2.9(s), 3.7(s), 7.4(m)
dioxane	*3.7(s)*
SETH	1.2(t), 2.7(s), 3.7(q), 7.4(m)
ethanol	*1.2(t), 2.3(s), 3.7(q)*

Table 3.5 ctd.

Class D	
$C_{30}H_{22}OSi$	3.2(s), 7.6(m)
DUNCAN	2.6(s), 3.3(s), 7.6(m)
dmso	*2.6(s)*
NADIO	3.2(s), 3.7(s), 7.6(m)
dioxane	*3.7(s)*
NATOL	2.3(s), 3.2(s), 7.4(m)
toluene	*2.35(s), 7.2(s)*
ODIN	2.3(s), 3.1(s), 7.4(m)
o-xylene	*2.25(s), 7.15(s)*
MAXINE	2.3(s), 3.2(s), 7.4(m)
m-xylene	*2.3(s), 6.9-7.0(m)*
NAPPY	2.4(s), 3.3(s), 7.4(m)
p-xylene	*2.3(s), 7.0(m)*
NATRET	1.0(t), 2.4(q), 3.2(s), 7.6(m)
triethylamine	*1.0(t), 2.5(q)*

Table 3.6. Thermogravimetry results.

Compound	Observed weight loss (%)
Class A	
DEMPE	29.51
PEDIOX	19.80
PECTIL	14.38
DINM	22.42
LUTI	36.83
DINO	36.35
PEACH	13.01
Class B	
W1DIOX	23.40
Class C	
TRIPSID	unclear
BASIL	6.78
SETH	3.99
Class D	
DUNCAN	15.08
NADIO	16.81
NATOL	17.55
ODIN	19.50
MAXINE	17.53
NAPPY	32.80
NATRET	17.54

Table 3.7. Stoichiometries of the inclusion compounds, as derived from the physical techniques employed.

Compound	Density	NMR	TG	crystal structure
DEMPE	1:1.90	1:1.95	1:1.97	1:2
PEDIOX	1:1.00	1:1.00	1:1.03	1:1
PECTIL	1:0.49	1:0.48	1:0.49	1:0.5
DINM	1:0.90	1:0.93	1:0.99	1:1
LUTI	1:1.88	1:1.87	1:2.00	1:2
DINO	1:1.93	1:1.91	1:1.95	1:2
PEACH	1:0.98	1:0.98	1:0.94	1:1
W1DIOX	1:1.05	1:1.09	1:0.90	1:1
TRIPSID	1:0.49	1:0.48	unclear	1:0.5
BASIL	1:0.20	1:0.22	1:0.23	1:0.25
SETH	1:0.20	1:0.20	1:0.25	1:0.25
DUNCAN	1:0.96	1:0.85	1:0.97	1:1
NADIO	1:1.01	1:1.00	1:0.98	1:1
NATOL	1:0.93	1:0.96	1:0.99	1:1
ODIN	1:0.98	1:0.97	1:0.97	1:1
MAXINE	1:0.96	1:0.97	1:0.86	1:1
NAPPY	1:1.91	1:1.98	1:1.96	1:2
NATRET	1:1.07	1:0.95	1:0.90	1:1

General description of structure solution and refinement.

For any given structure, the collected reflections are examined for systematically absent or "unobserved" ($4\sigma(F) \geq F$) reflections. These are automatically suppressed. An R_σ value is calculated ($R_\sigma = \Sigma\sigma F^2 / \Sigma F^2$) to determine whether the diffractometer data are of good quality. The number of unique data as a function of resolution in the range 1.1 to 1.2Å is then examined. If a sufficiently high number of the theoretically possible reflections (more than one quarter for centrosymmetric structures) are observed, it is probable that the direct methods will succeed. Mean $|E^2-1|$ values for the projections *0kl*, *h0l*, *hk0* and the remainder are checked for consistency with space group symmetry. For centrosymmetric space groups, all projections are expected to be centric, with $|E^2-1|$ close to 0.968. The program then selects a reflection subset for the initial phase refinement on the basis of α_{est} and the number of negative quartets it generates. The "best" 10% of the subset phase permutations are then subjected to multisolution tangent refinement. The "best" solution is extended by further tangent expansion. After one cycle of E-Fourier recycling, the point atom R-factor based on E-values is evaluated.[3.9] If $R_E < 0.3$, the structure is considered correct, provided that it is also chemically sensible. Most, if not all, of the non-hydrogen atoms in the structure were found this way, and the correctness of the structure was confirmed by a sharp cutoff in the list of peak heights, and by successful subsequent refinement.

The atoms located in the direct methods were input into SHELX76[3.10] for refinement. In most cases, full-matrix least squares refinement was employed but, in cases where the number of variables exceeded 500, large block least squares were used for refinement.

The final model usually consisted of anisotropic refinement of all non-hydrogen atoms. Non-hydroxyl hydrogen atoms were geometrically constrained to 1.00Å from their parent atoms and refined with linked temperature factors. Approximate positions for the hydroxyl hydrogens were found in difference Fourier maps and they were refined with independent isotropic temperature factors but with a bond length constraint. These hydrogens were fixed at set lengths from their parent oxygens according to a function of O···O (or O···N) vs O-H distance.[3.11]

A weighting scheme ($w=(\sigma^2F + gF^2)^{-1}$) was employed in the final stages of refinement to yield satisfactory variation in the intensity of reflections as a function of parity groups, sin θ, $\sqrt{F}/F_{max}$ and the Miller indices. The analyses of variance obtained in this fashion are shown in Appendix 5.

Hydrogen Bonds.

Hydrogen bonds are present in all of the compounds in this study. Twelve examples of O-H•••O and four of O-H•••N hydrogen bonding were found. In order to have comparative values against which the observed parameters could be checked, hydrogen bonding data were retrieved from the Cambridge Structural Database.[3.12] The command lines used are printed out in Appendix 1.

Initially, systems containing only C, H, O, N, Si and S were searched for the combination of one fragment consisting of any atom bonded to both an hydroxyl and a phenyl group and a second fragment which contained a neutral oxygen atom. The structures which were found in this way were then tested for the presence of hydrogen bonds, using the GSTAT subroutine. A similar strategy was used to find O-H•••N hydrogen bonds. Scatterplots (Figures 3.1 and 3.2) were generated for 71 O-H•••O and 51 O-H•••N hydrogen bonds. The information found in the scatterplots was used to check the consistency of the hydroxyl hydrogen constraints for each structure.

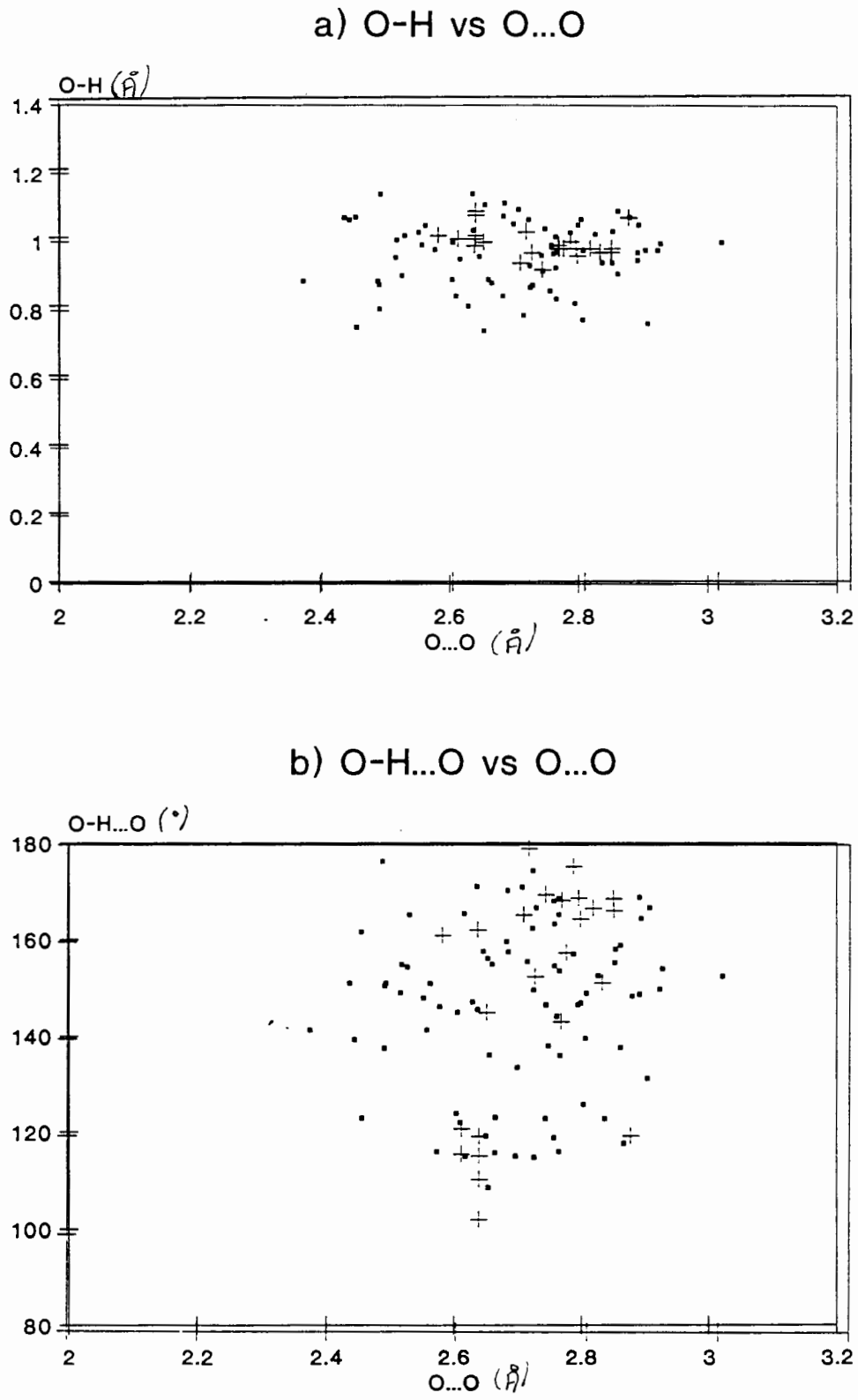

Figure 3.1. Scatterplots relating parameters tor O-H···O hydrogen bonds : (•) values obtained from the Cambridge Structural Database, (+) values obtained in this study.

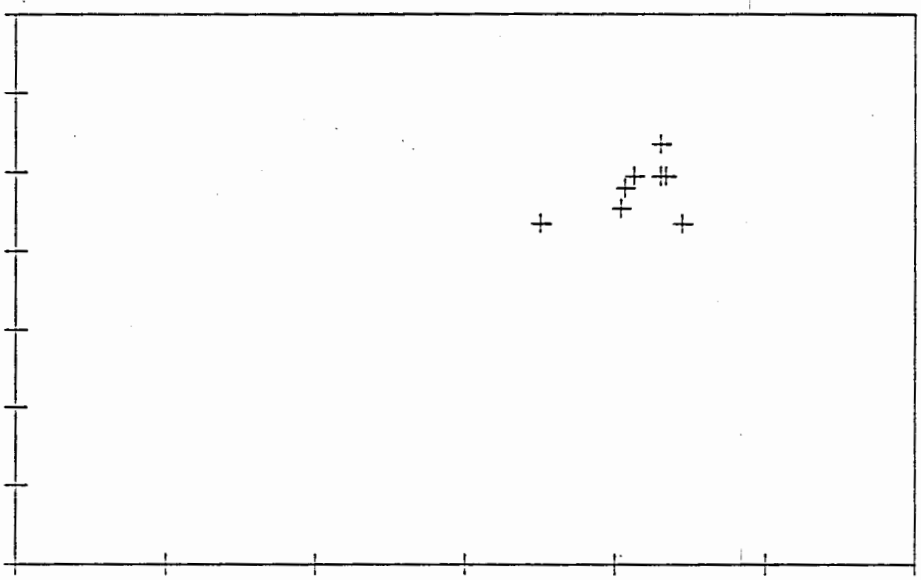

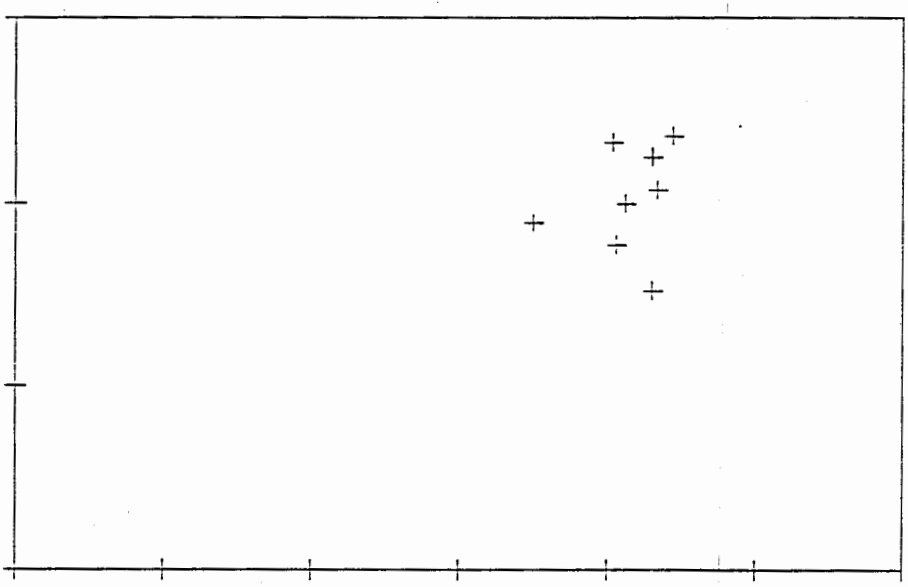

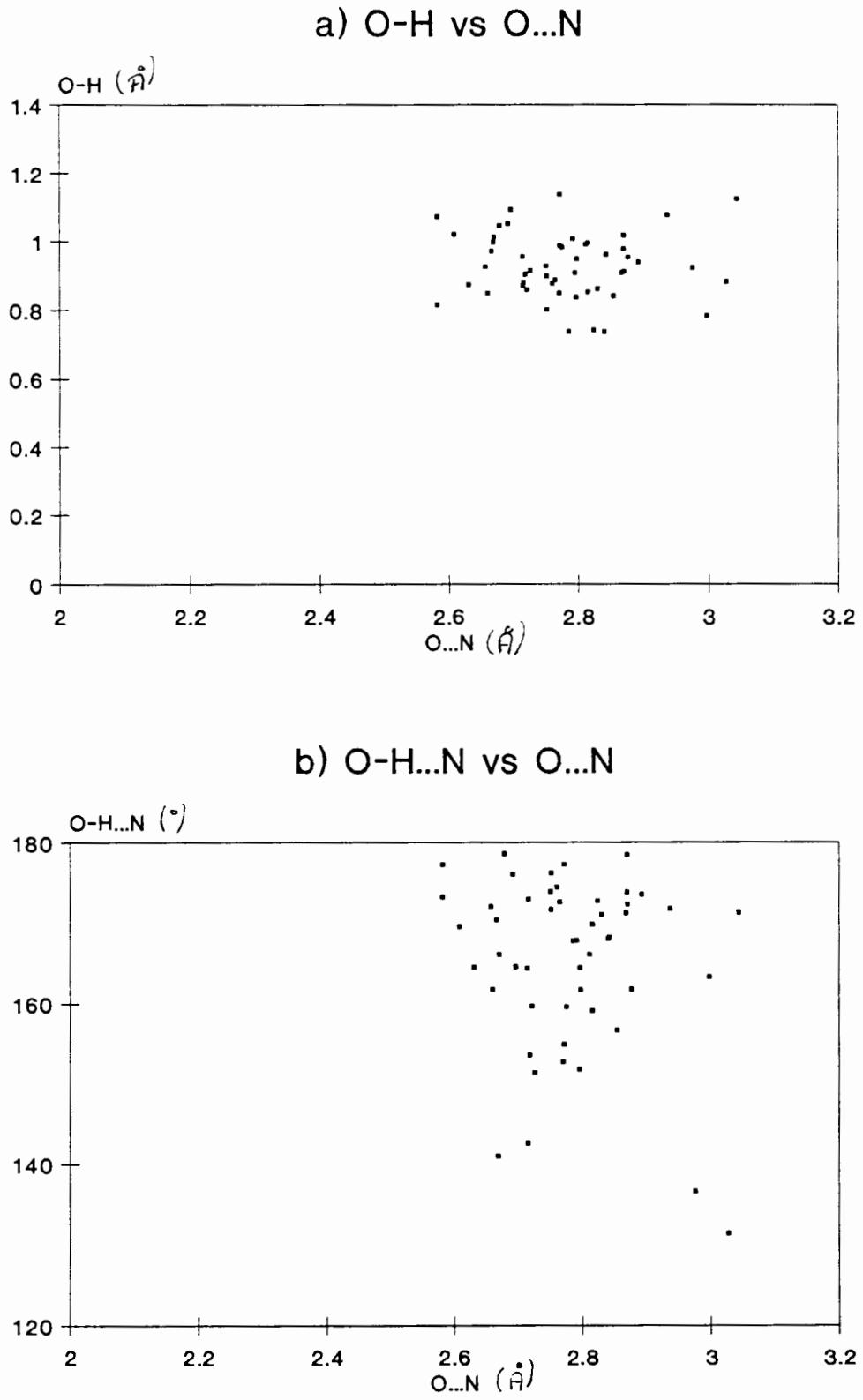

Figure 3.2. Scatterplots relating parameters for O-H···N hydrogen bonds : (•) values obtained from the Cambridge Structural Database, (+) values obtained in this study.

References.

3.1. T. Hahn (Ed.) *'International Tables for Crystallography.'* Volume A. D. Reidel Publishing Co., Holland, (1983).

3.2. G. H. Stout and L. H. Jensen. *'X-Ray Structure Determination. A Practical Guide.'* 2nd edition. John Wiley & Sons, New York. (1989).

3.3. P. Luger. *'Modern X-Ray Analysis in Single Crystals.'* Walter de Cruyter, (1980).

3.4. M. J. Buerger. *'Crystal Structure Analysis.'* John Wiley & Sons, New York. (1967).

3.5. H. Hauptman. *Science*, **323**, 178, (1986).

3.6. F. Toda; K. Tanaka; Y. Wang; G-H. Lee. *Chem. lett.* 109, (1986).

3.7. D. H. Williams; I. Fleming. *'Spectroscopic methods in Organic Chemistry.'* 3rd edition, McGraw-Hill, London. (1980).

3.8. C. J. Pouchet. Vols I & II of *'The Aldrich Library of NMR Spectra.'* 2nd edition, Aldrich Chemical Co. Inc., USA, (1983).

3.9. G. M. Sheldrick, 'SHELXS-86' in *Crystallographic Computing 3.* G. M. Sheldrick; C. Kruger; R. Goddard (Eds.) Oxford University Press, 175, (1985).

3.10. G. M. Sheldrick, 'SHELX76' in *Computing in Crystallography*. H. Schenk; R. Olthof-Hazekamp; H. von Koningsveld; G. C. Bassi. Delft University Press, 34, (1978).

3.11. P. Schuster; G. Zundel; C. Sanderfy (Eds.) *'The Hydrogen Bond II. Structure and Spectroscopy.'* Chapter 8. North-Holland Publishing Co., Amsterdam. (1976).

3.12. Cambridge Structural Database and CSD System, January 1991, Version 4.4. Cambridge Crystallographic Data Centre, University Chemical Laboratory, Cambridge, England.

CHAPTER 4 : CRYSTAL AND MOLECULAR STRUCTURE - CLASS A.

The host to guest ratios, space group and cell parameters are summarised at the beginning of the discussion about each structure. Fractional atomic coordinates, thermal parameters and details of hydrogen bonding are given in Tables 4.4 - 4.12 at the end of this chapter.

The atom labelling scheme used for the host, 1,1,2,2-tetraphenyl-1,2-diol, is shown in Figure 4.1. The labelling used for the guest is shown at the beginning of the discussion about each compound. The geometry of the host is discussed in detail at the end of this chapter.

PEDIL : $C_{26}H_{22}O_2$.

Space group : $P2_1/n$
a = 17.669(6) Å
b = 6.144(6) Å β = 92.67(3)°
c = 17.873(6) Å
Z = 4

Refinement of this structure using intensity data collected at 293K proved unsatisfactory. With all non-hydrogen atoms treated anisotropically, the final model yielded very high temperature factors, poor standard deviations for bond lengths and angles and a final R of 0.135.

An FTS systems Air Jet XR-85-1 cooling device was used to blow cooled dry nitrogen on a crystal in order to recollect the intensity data at 228K. The direct methods solution of these data found 28 atoms. Refinement proceeded as detailed at the beginning of this chapter.

The central ethane carbon atoms were disordered and were therefore modelled as half atoms. The hydroxyl oxygen atoms were located unambiguously nearly midway between the disordered carbons. An electron density map of the region between the oxygen atoms of neighbouring molecules showed a diffuse peak. The hydroxyl hydrogens, therefore, could not be located unambiguously and were instead modelled as follows : two hydrogens (each with a site occupancy of 0.5) were fixed to each oxygen at points on an arc 1.00Å from the oxygen.

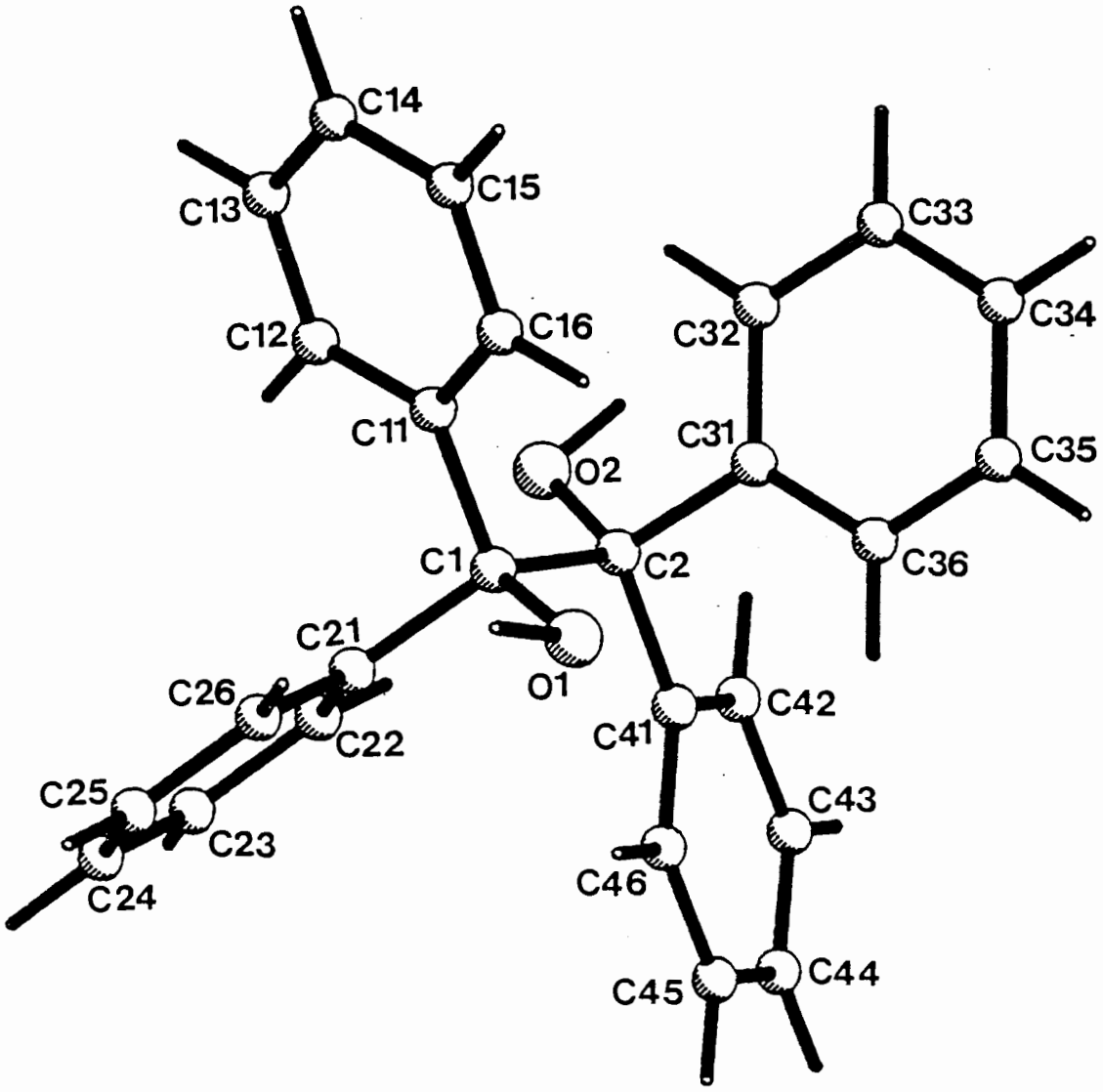

Figure 4.1. Atom labelling scheme for 1,1,2,2-tetraphenylethane-1,2-diol (Class A).

This model of the disordered molecule is shown in Figure 4.2.

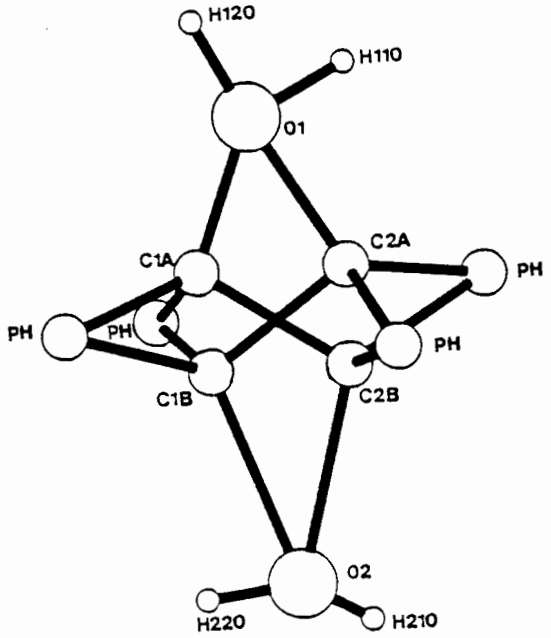

Figure 4.2. Disorder found in **PEDIL**. Individual molecules may be O(1)-C(1A)-C(2B)-O(2) or O(1)-C(2A)-C(1B)-O(2).

The final electron density map showed no feature greater than 0.24 $eÅ^{-3}$ or less than -0.24 $eÅ^{-3}$. Final coordinates and thermal parameters are listed in Table 4.5.

Molecular structure.

The central ethane moiety of this compound is statistically disordered as shown in Figure 4.2. The individual molecules may be O(1) - C(1A) - C(2B) - O(2) or O(1) - C(2A) - C(1B) - O(2). Relevant bond lengths are listed in Table 4.1.

Table 4.1. Bond distances of disordered atoms in **PEDIL**. (Å)

O(1) - C(1A)	1.48(1)
O(1) - C(2A)	1.55(1)
O(2) - C(1B)	1.50(1)
O(2) - C(2B)	1.53(1)
C(1A) - C(2B)	1.57(1)
C(1B) - C(2A)	1.59(1)

A packing diagram of **PEDIL**, viewed along [010] is shown in Figure 4.3(a). To emphasize the highly packed nature of this structure, the same view, with atoms drawn

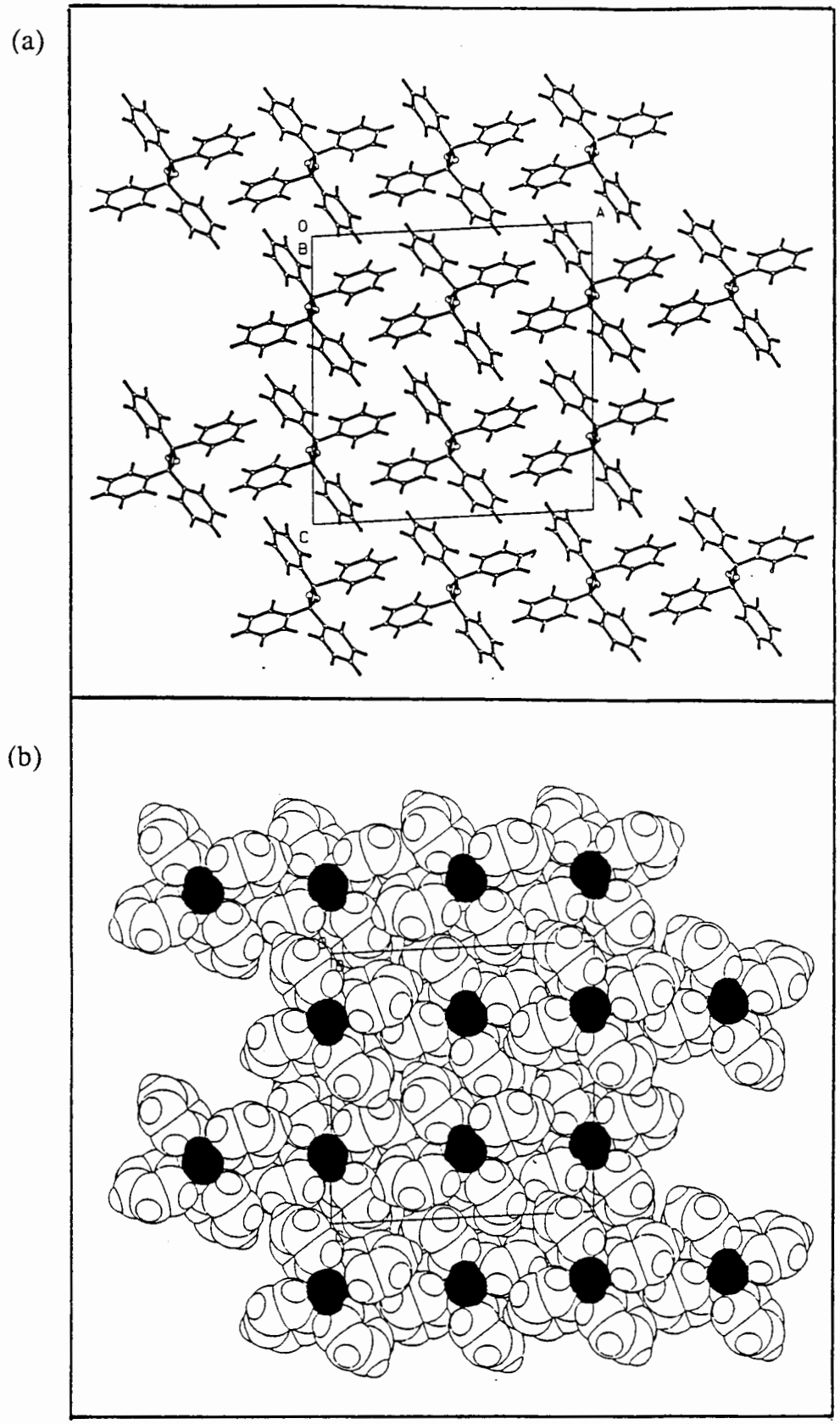

Figure 4.3. (a) Packing diagram of **PEDIL** viewed along [010], (b) Space-filled diagram of **PEDIL** viewed along [010], with hydroxyl groups shaded.

with their van der Waals radii, is shown in Figure 4.3(b). The hydroxyl groups are shaded to highlight the fact that they are exposed on one surface of the crystal. This has important implications for the absorption of vapours onto the α-phase.

The molecules are hydrogen bonded in chains lying parallel to [010]. The O(1)•••O(2) distance is 2.635(5)Å, typical of a strong hydrogen bond. Details are shown in Figure 4.4.

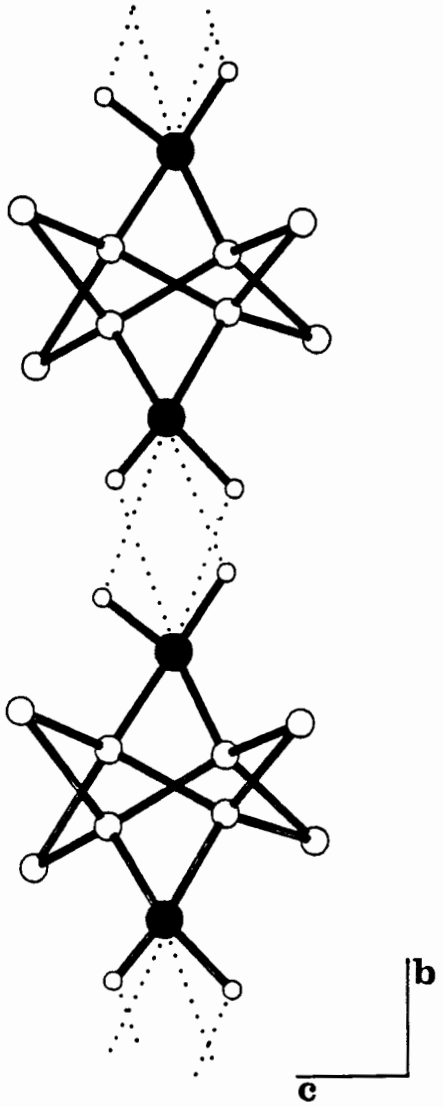

Figure 4.4. Details of hydrogen-bonding in **PEDIL**. The disordered central sections of two molecules are shown, oxygens shaded.

DEMPE : ($C_{26}H_{22}O_2$) . 2 dmso.

Space group : $P\bar{1}$	H : G = 1 :2
a = 9.317(5) Å	α = 61.16(2)°
b = 18.384(6) Å	β = 83.22(3)°
c = 18.496(3) Å	γ = 88.06(3)°
Z = 4	

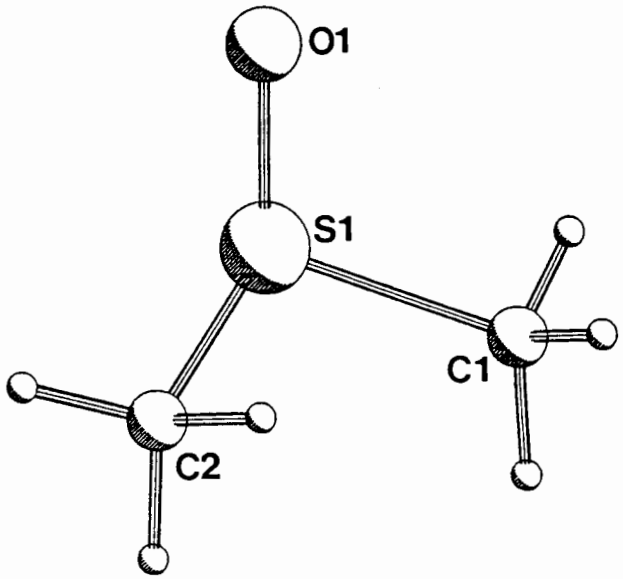

Direct methods for this structure found 69 atoms with an R_E of 0.312. This meant that two crystallographically independent host molecules could be discerned as well as one complete guest molecule and parts of a further two guests.

These atoms were placed in SHELX76 which, on refinement, allowed the remainder of the guest molecules to be found. At this stage, two hosts and four guests were allowed to refine.

The host molecules showed none of the disorder observed in **PEDIL**, but two of the four guest dmso molecules were disordered. They were modelled as each having two sulphur atoms with different site occupancy factors, as shown in Figure 4.5.

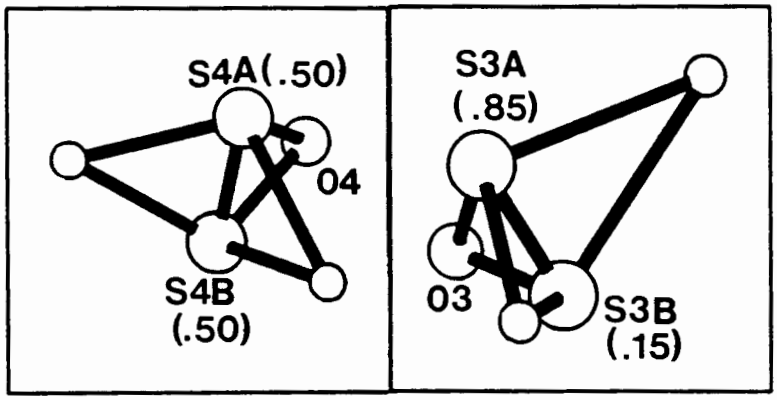

Figure 4.5. The disordered guest molecules in **DEMPE**. Numbers in brackets indicate the s.o.f. for each atom.

All four hydroxyl hydrogens were located in difference electron density maps and refined with appropriate O-H bond length constraints but with individual temperature factors.

S(3A) and S(3B) were assigned fixed isotropic temperature factors of 0.06 and only their positional coordinates were refined. The guests' methyl carbons were refined isotropically because we could not model their anisotropic movement satisfactorily.

All other non-hydrogen atoms were allowed to refine anisotropically. Although the maximum height in the final electron density map was 0.62 $eÅ^{-3}$, this was very close to one of the guest molecules, and was therefore ascribed to an imperfect model.

Final coordinates of thermal parameters are listed in Table 4.6.

Molecular structure.

The asymmetric unit of **DEMPE** is shown in Figure 4.6. Hydrogen bonds are shown by dotted lines.

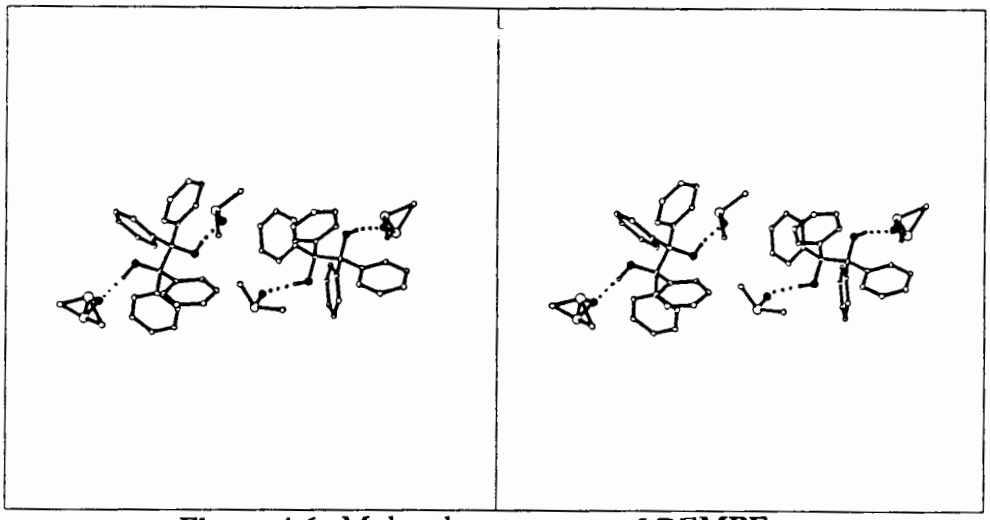

Figure 4.6. Molecular structure of **DEMPE**.

S-O bond lengths for all four guests and S-C lengths in the two well-ordered guests are very close to theoretical values. In guests 3 and 4 however, S-C bond lengths range from 1.697(16) to 1.935(18) Å. Bond angles in the dmso molecules are also close to expected values. C-S-C angles are between 94.5(12) and 98.9(5)° and O-S-C angles are between 103.8(9) and 113.6(1)°.

The host molecules pack to form an infinite cross-network of channels running parallel to [010] and [100] in which the dmso molecules are located, as shown in Figure 4.7.

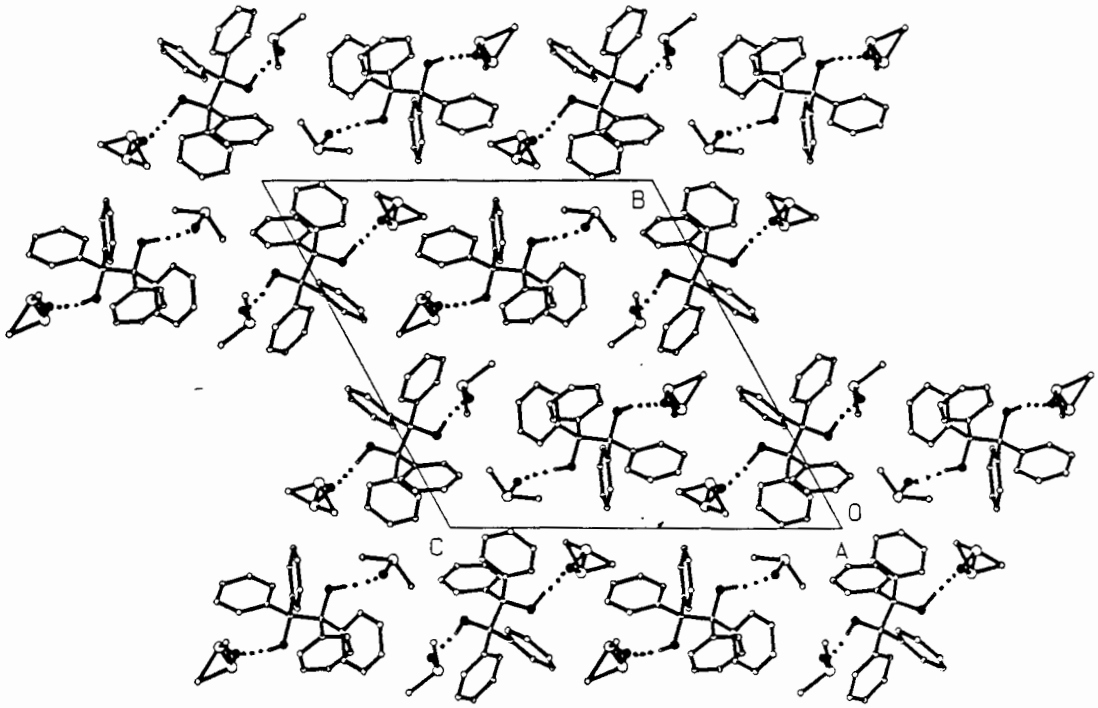

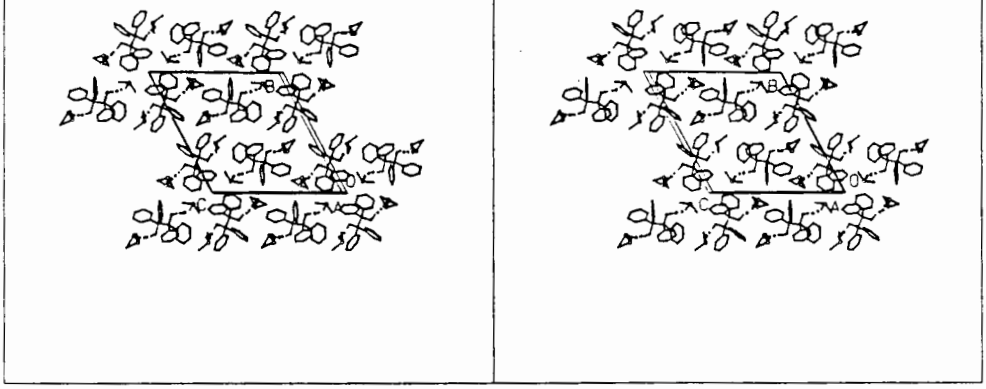

Figure 4.7. Packing diagram of **DEMPE** viewed along [100]. The two alternative orientations for each of the disordered guests are shown and H-bonds indicated by dotted lines.

PEDIOX : $(C_{26}H_{22}O_2)$. dioxane

Space group : C2/c H : G = 1 : 1

a = 8.648(1) Å

b = 16.551(1) Å β = 100.40(2)°

c = 17.038(4) Å

Z = 4

The conditions obtained for non-extinction were :

hkl : $h+k$ = 2n	*0k0* : k = 2n
0kl : k = 2n	*h00* : h = 2n
hk0 : $h+k$ = 2n	*00l* : l = 2n
h0l : h,l = 2n	

These indicate two possible space groups - C2/c or Cc. Parallel refinements were carried out in both space groups until all non-hydrogen atoms had been placed and refined for several least squares cycles. At that stage the Hamilton test [4.1,4.2] was applied to the R_G values for each space group. The hypothesis that C2/c was the correct space group could be accepted at the 99% confidence level. This choice was vindicated by the subsequent successful refinement in C2/c.

In order to satisfy the symmetry requirements, both host and guest molecules must be located at special positions. The host molecule is place on the diad while the guest lies about a centre of inversion at (¼, ¼, 0) which is Wyckoff position *c*.

In the early stages of refinement, it became apparent that both host and guest were disordered. Difference Fourier maps revealed a peak of approximately 1.7 eÅ^{-3} near the central host carbon (C(1)) and another of about 1.5 eÅ^{-3} in the region of the guest.

It was found that the best model for the host was a system of disorder similar to that in **PEDIL**, but with site occupancy factors of 0.70 and 0.30 for C(1A) and C(1B) respectively. The extra guest peak was assigned to an oxygen (O(2G)) with site occupancy 0.20. This model of the guest has the two carbon atoms in the asymmetric unit lying in a plane with the centre of inversion at (¼, ¼, 0), with an oxygen atom both above and below the plane. This leads to two superimposed guest molecules, each in the "chair" conformation, as shown in Figure 4.8. (The same disorder had been observed in the refinement in Cc.)

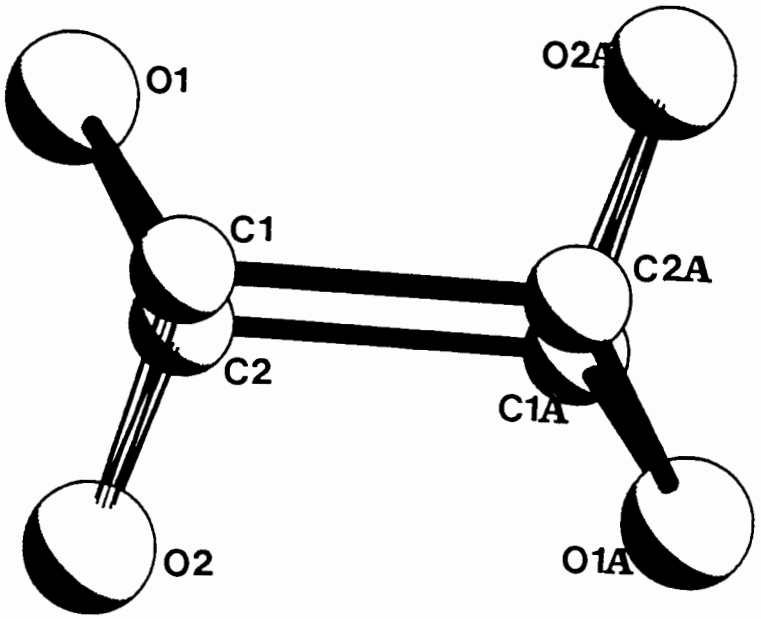

Figure 4.8. The dioxane is disordered as shown. Individual molecules have the backbones -O(1)-C(1)-C(2A)-O(1A)-C(1A)-C(2)- and -O(2)-C(1)-C(2A)-O(2A)-C(1A)-C(2)-.

This model proved to be satisfactory and was expanded to include anisotropic refinement of all non-hydrogen atoms. Aromatic host hydrogens and guest hydrogens were geometrically constrained to their parent carbons and linked via common temperature factors.

O···O distances of 2.868 Å (O(1)···O(1G)) and 2.948 Å (O(1)···O(2G)) suggested the presence of hydrogen bonding. An attempt was made to model the host's hydroxyl hydrogen over two positions, to reflect each hydrogen bond, but this proved unsatisfactory, probably owing to the extremely low site occupancy of the second guest oxygen. The hydroxyl hydrogen was therefore tied to its parent O(1) and to O(1G), and allowed to refine isotropically. Final coordinates and thermal parameters are listed in Table 4.7.

Molecular structure.

The molecular structure is shown in Figure 4.9. The hydrogen bond is indicated by the dotted line. The disorder in both host and guest has been omitted, for clarity.

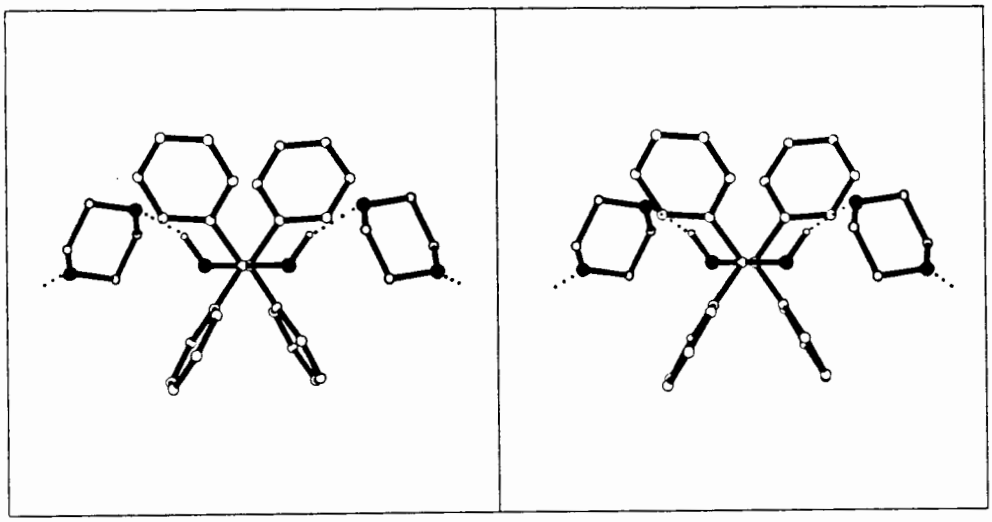

Figure 4.9. The molecular structure of **PEDIOX.**

The guest's conformation was determined using the method described in Duax and Norton [4.3]. This defines "asymmetry parameters" for mirror planes and two-fold axes which a ring may possess. Using these parameters, a ring may be described as planar, a chair, boat, twist, sofa or half-chair. Both of the guest rings in this compound had asymmetry parameters corresponding to the chair conformation. Bond lengths and angles were within acceptable limits.

Dioxane contains two oxygens which are able to act as proton acceptors in a hydrogen bond. The host molecule in **PEDIOX** sits on a 2-fold axis and its hydroxyl group is hydrogen bonded to one of the dioxane oxygens. This gives rise to an infinite ribbon of hydrogen bonded host and guest molecules in the direction [-101]. Figure 4.10(a) and (b) show packing diagrams viewed down [100] and [010]. The phenyl rings of the host have been omitted from the same views on the overlay so that the ribbon-like structure may more easily be seen.

The dioxane molecules lie in undulating channels (direction [1 0 1]) with centres at y = 0.25 and y = 0.75. These channels are drawn in Figure 4.11. Guest molecules drawn with van der Waals radii are included to show the close fit of the guest into the channels.

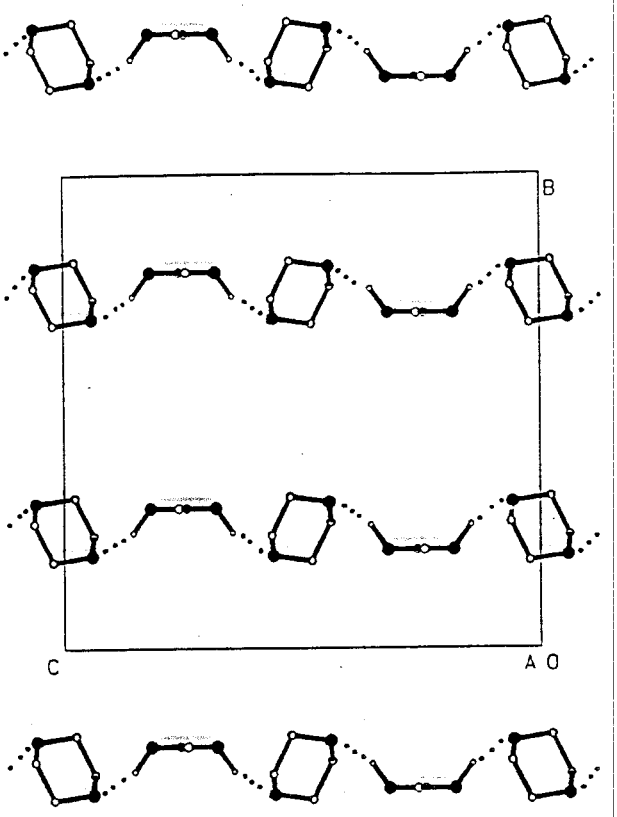
B
C
A 0

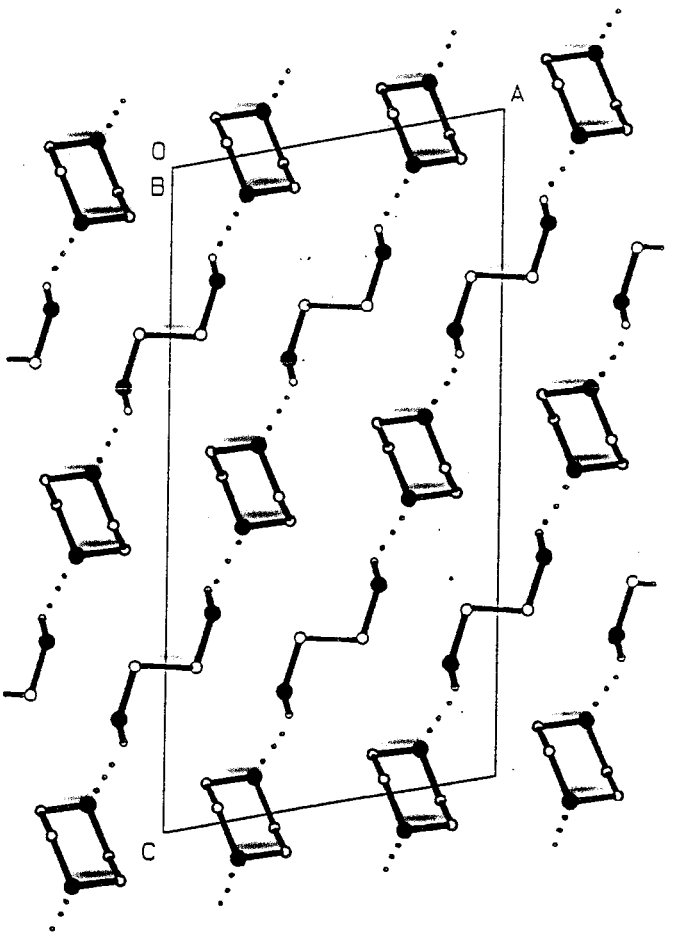
A
0
B
C

(a)

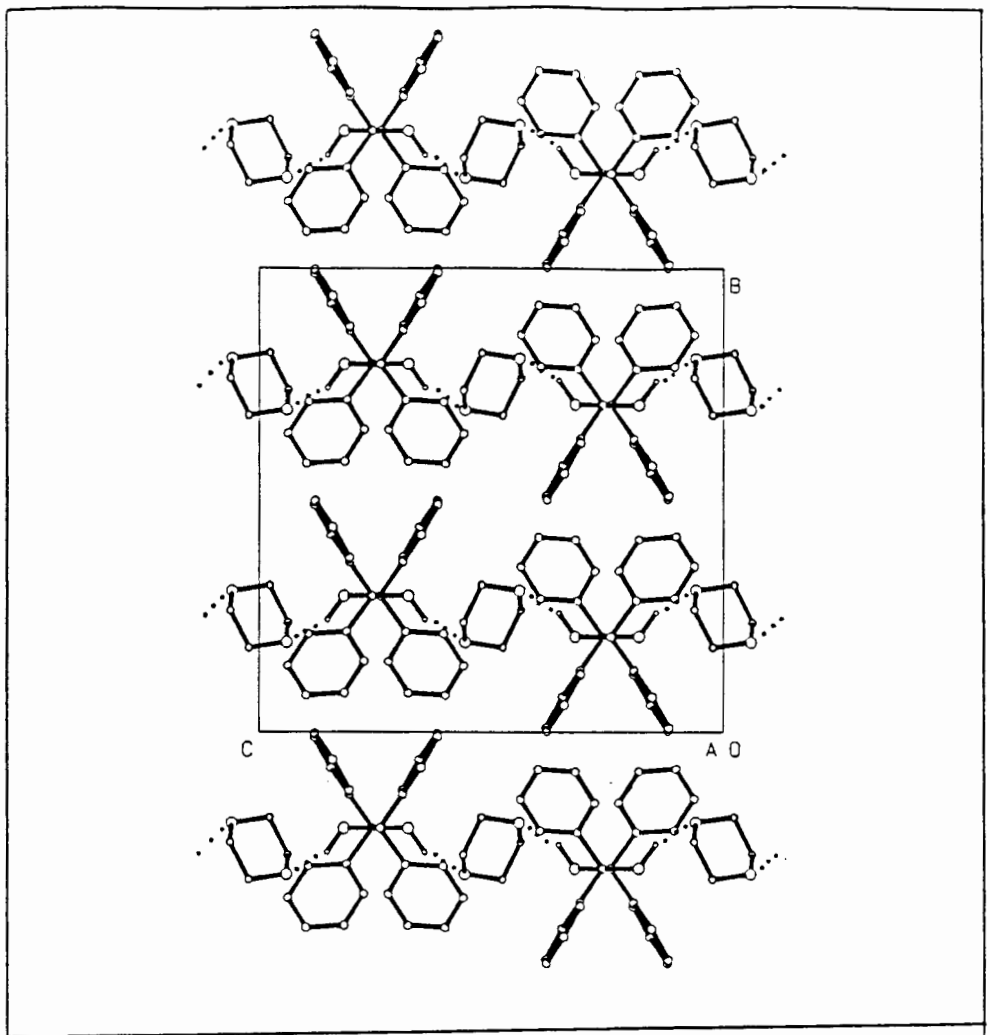

(b)

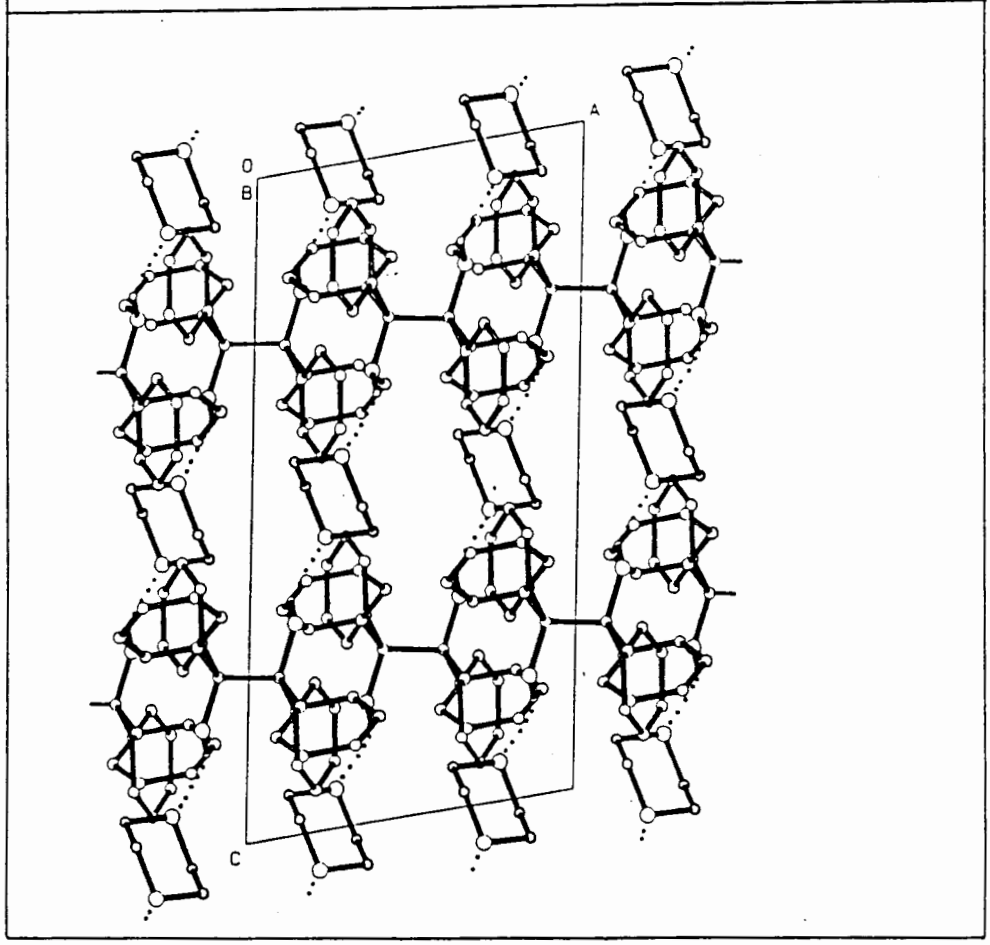

Figure 4.10. Packing diagrams of **PEDIOX** (a) viewed along [100] and (b) viewed along [010].

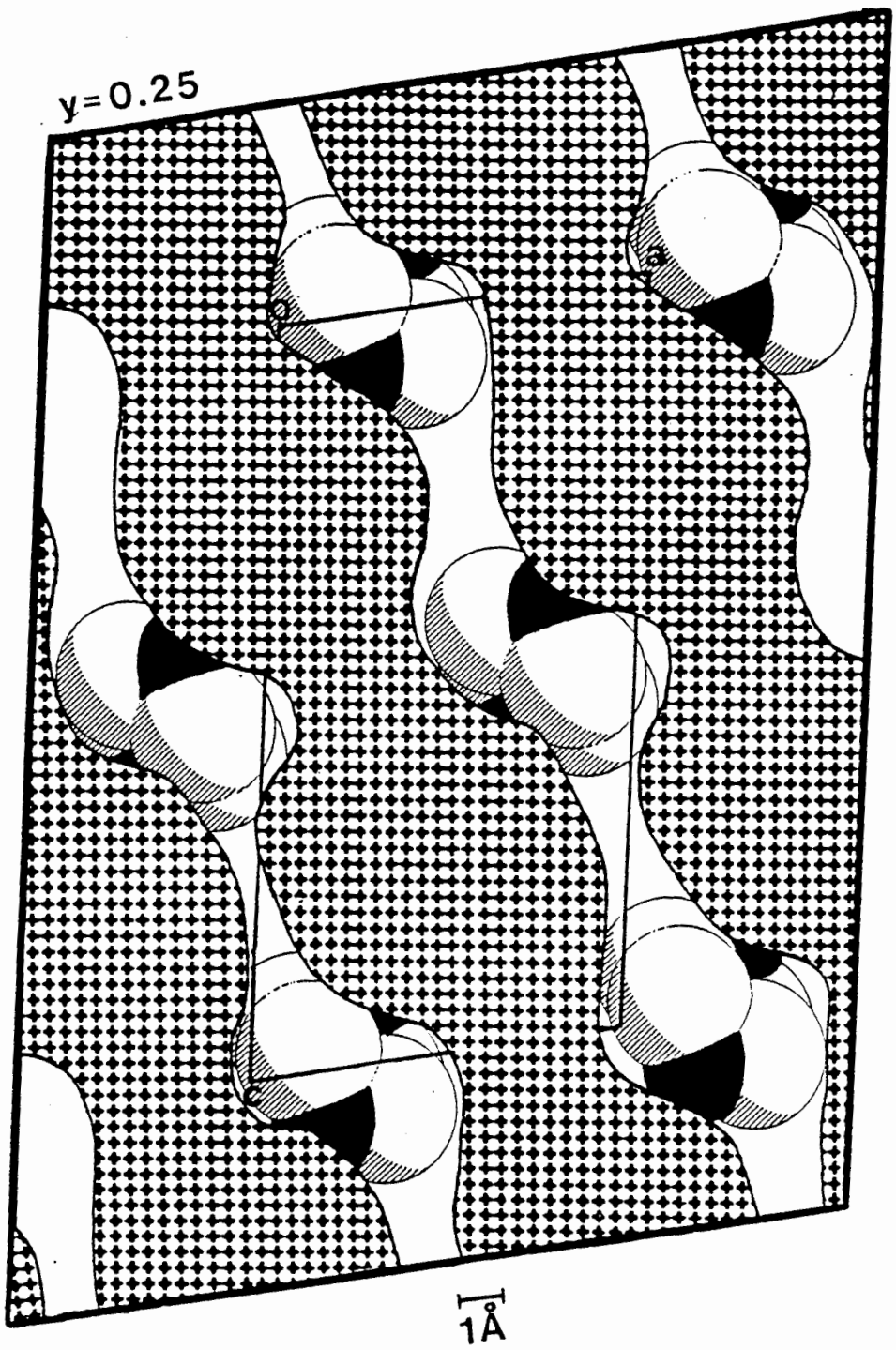

Figure 4.11. PEDIOX - a cross-section of the cell at y = ¼. Shaded areas are those occupied by host molecules. Guest molecules drawn with van der Waals radii are shown in their positions in the channels.

PECTIL : $(C_{26}H_{22}O_2)_2$. p-chlorotoluene

Space group : $P\bar{1}$	H : G = 2 : 1
a = 6.093(1) Å	α = 93.95(3)°
b = 9.103(2) Å	β = 93.23(3)°
c = 20.933(10) Å	γ = 103.86(2)°
Z = 1	

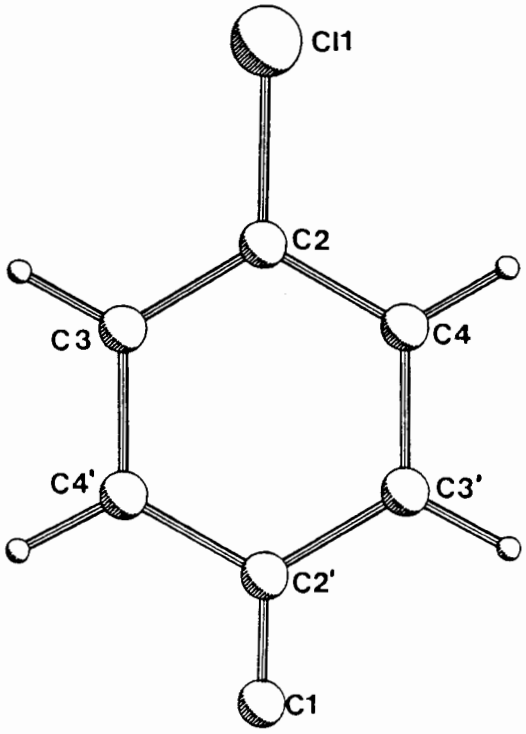

Density measurements, NMR and TG showed that the host : guest ratio was 2 : 1 for Z = 1. Intensity data for this structure were initially collected at 293K. Refinement using these data was unsatisfactory : temperature factors averaged 0.20 $Å^2$, even with anisotropic refinement and the final R was 0.123.

A fresh crystal was selected and new data were collected at 228K using the method detailed for **PEDIL**. The structure solution using the new data set was greatly improved. One host molecule and half a guest molecule were found in the asymmetric unit. The host molecule showed the same disorder of the central ethane carbons as has been described for **PEDIL** and **PEDIOX**.

The guest molecule was found to lie about the centre of inversion at Wyckoff position *h*. In order to do so, it has to adopt a pseudo-centre of inversion itself. Thus Cl(1G) and C(1G) appear as peaks on a broad smear of electron density. Both of these atoms could be picked out in a difference Fourier map (Figure 4.12). Each was assigned a site

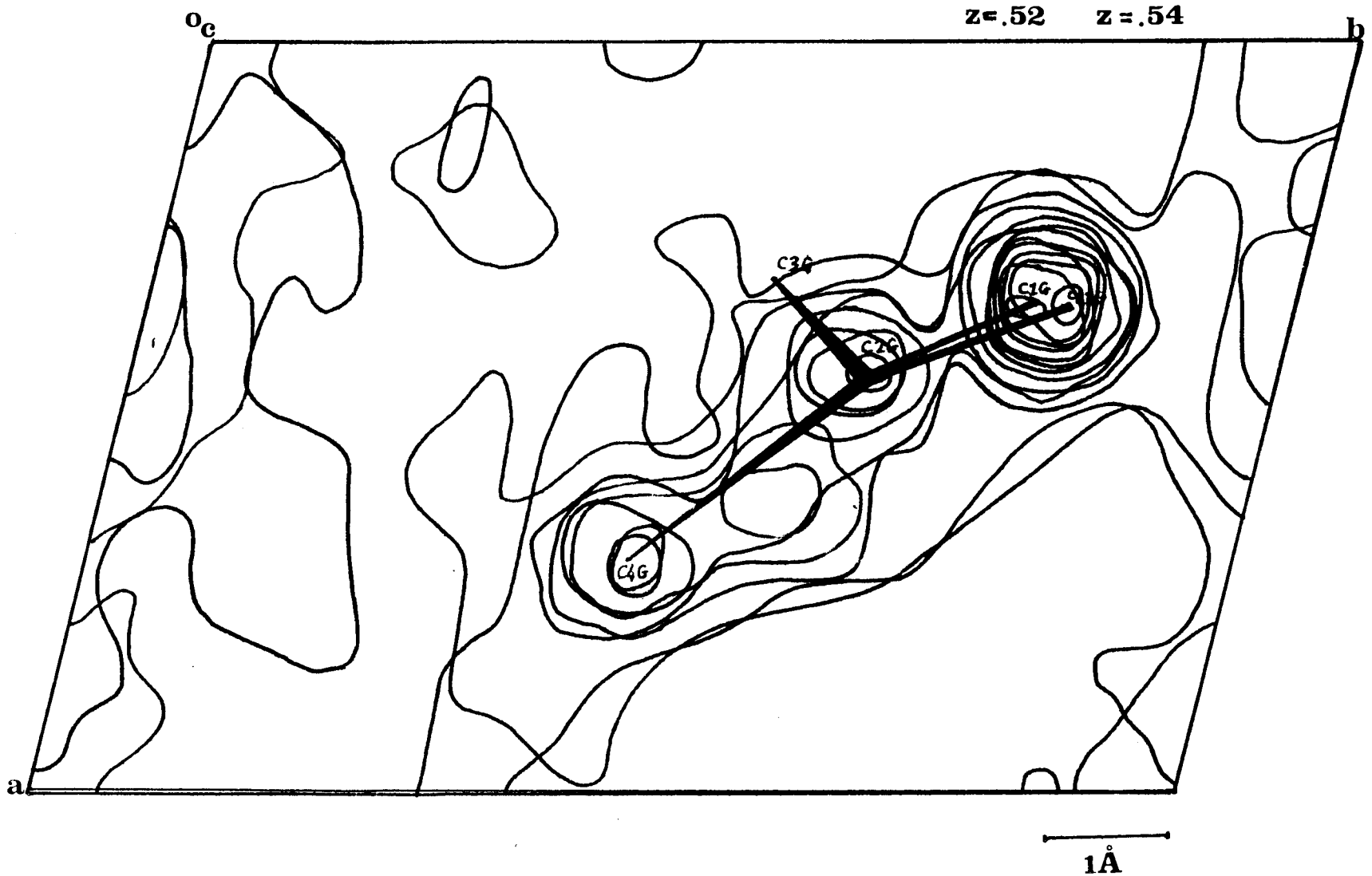

Figure 4.12. Difference electron density map in the region of the guest. Contours are drawn in steps of 0.8 eÅ^{-3}. A centre of inversion is present at z = 0.50, generating the remainder of the *p*-chlorotoluene molecule.

occupancy factor of 0.50, but on refinement, the carbon atom was simply incorporated into the chlorine peak. Therefore the position of the carbon C(1G) was fixed at the coordinates found in Figure 4.12. The chlorine was allowed to refine independently, but was linked to C(1G) by common anisotropic temperature factors.

The final model involved anisotropic refinement of all non-hydrogen atoms except the central carbon atoms of the host. The aromatic hydrogens of the host and guest were geometrically placed and constrained to their parent carbons. The hydroxyl hydrogens of the host were located in a difference Fourier map, fixed at a distance of 0.99Å from their parent atoms and allowed to refine isotropically. No attempt was made to model the hydrogens of the guest's methyl group. The final R was 0.096. Final coordinates and thermal parameters are listed in Table 4.8.

Molecular structure.
This structure was nearly isomorphous to that of the *p*-xylene structure reported by Toda *et al.*[4.4]

Host molecules hydrogen bond in chains parallel to [100] as shown in Figure 4.13. The O···O distance in **PECTIL** is 2.608(6) Å, slightly shorter than that in **PEDIL**.

The a-axis of **PECTIL** is 6.093 Å, very close in value to the b-axis of **PEDIL** (6.144 Å). These are the "stacking" axes of the two structures, *i.e.* the axes parallel to the hydrogen bonding. The inclusion of *p*-chlorotoluene does not disrupt the hydrogen bonding of the α-phase, but appears to simply push the columns of hydrogen-bonded hosts further apart. This is illustrated in Figure 4.14 where (a) is a view of four molecules in **PEDIL**, viewed down [010] and (b) is a packing diagram of **PECTIL** viewed down [100].

The guest is placed in the centre of the cell, in channels which run parallel to [100] and [010]. There are almost circular restrictions in the [100] channel at (0 ½ ½) and in the [010] channel at (½ 0 ½), which cause this compound to be classified an aediculate. The channels occupied by the guest can more readily be seen if depicted as in Figure 4.15 where the shaded zones represent the portions of the cell occupied by host molecules. A *p*-chlorotoluene molecule has been drawn with van der Waals radii to show the way in which the guest fits into the channel. The dimensions of the channel in the z direction are approx. 7 Å at its widest (x = 0.5) and about 2Å at its narrowest (x = 0).

The potential energy of the *p*-chlorotoluene in this lattice was studied. EENY was used to establish the shape of the channel by calculating the potential energy environment of a "probe" hydrogen atom which was systematically moved throughout the cell. The

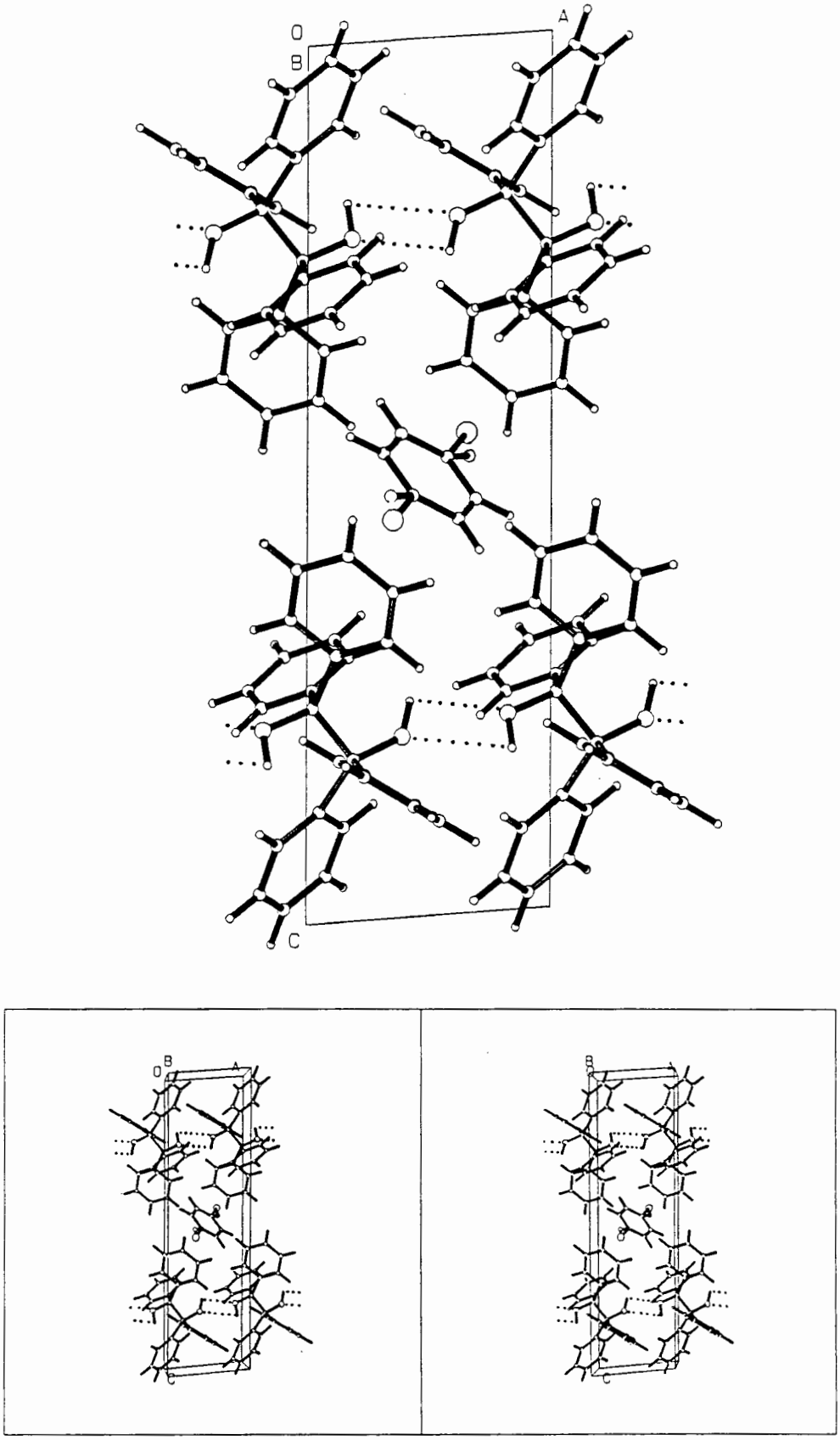

Figure 4.13. Packing diagram of **PECTIL** viewed along [010]. H-bonds are shown as dotted lines. The alternative orientations of the guest molecule are shown.

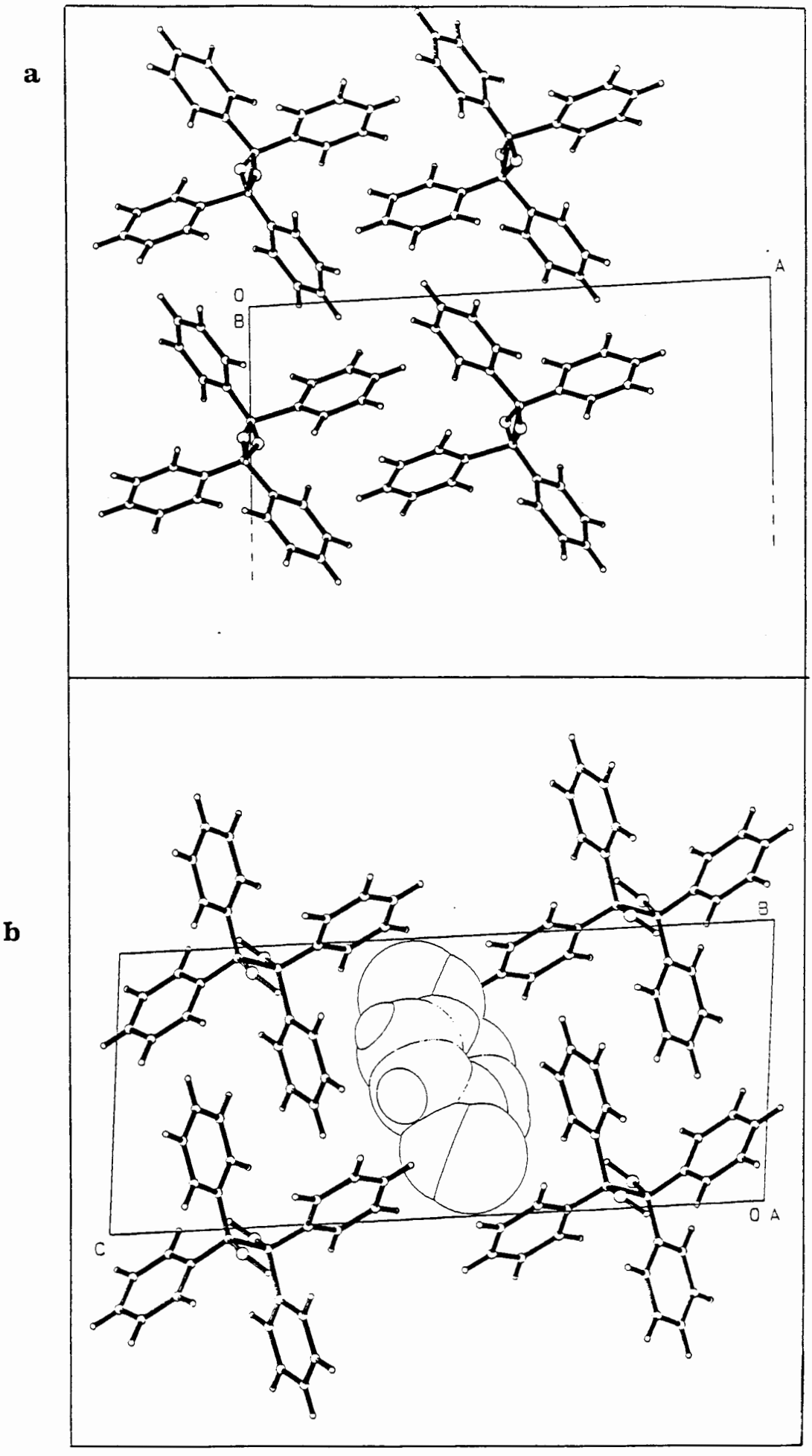

Figure 4.14. The relationship between the host's packing in (a) **PEDIL** and (b) **PECTIL**, each viewed along its "stacking" axis.

maximum width and height of the channel was found to be at y = 0.5 and this region was contoured at the zero energy level.

Movement within EENY is along the orthogonal axes. Thus for a triclinic structure, movement in the *xz* plane is parallel to $\underline{c}$ for a z-translation but the x-translation is in the direction of a^*. Therefore movement in the true x-direction requires translations both in the direction of $\underline{a}$ and of $\underline{c}$, both of which involve a trigonometric function of β.

A model of a *p*-chlorotoluene molecule was positioned at the coordinates found in the crystal structure. This molecule was then translated through the channel in steps of 1 Å and the energy calculated

(a) on the assumption that both host and guest remain rigid as input, and

(b) by allowing the guest small variations in its rotational parameters so that it could twist about its centre, in order to find a local minimum in the energy after each 1Å translation. No account was taken of partial atomic charges or dipole interactions and the energy values obtained are meaningless in an absolute sense. The energy profiles obtained are shown in Figure 4.16. There is a large, shallow minimum which has its midpoint at x = 0.5. At its maximum (x = 1), the energy is still low and, if the guest is allowed to twist about its centre, the energy drops still further. The wide minimum indicates that the *p*-chlorotoluene is weakly held within the host lattice and that the channel may be the means of escape for the guest to diffuse out of the crystal.

Bond lengths and angles of the *p*-chlorotoluene are well within accepted limits for similar molecules. The ring is planar and the chlorine and methyl carbon atoms also lie in the plane of the ring.

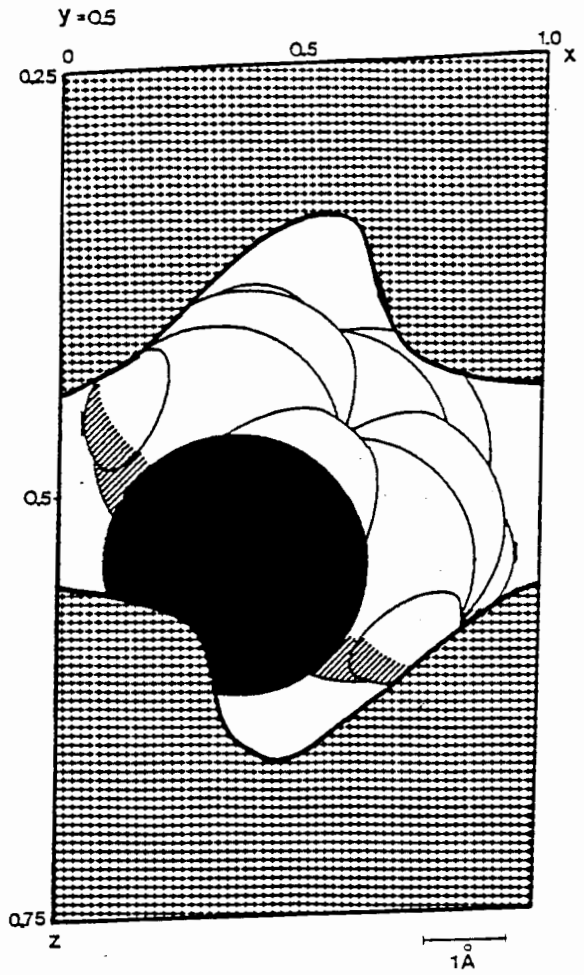

Figure 4.15. Cross-section through **PECTIL** at y = ½. A single guest is shown in one of its two possible orientations. The constrictions in the channel are clear.

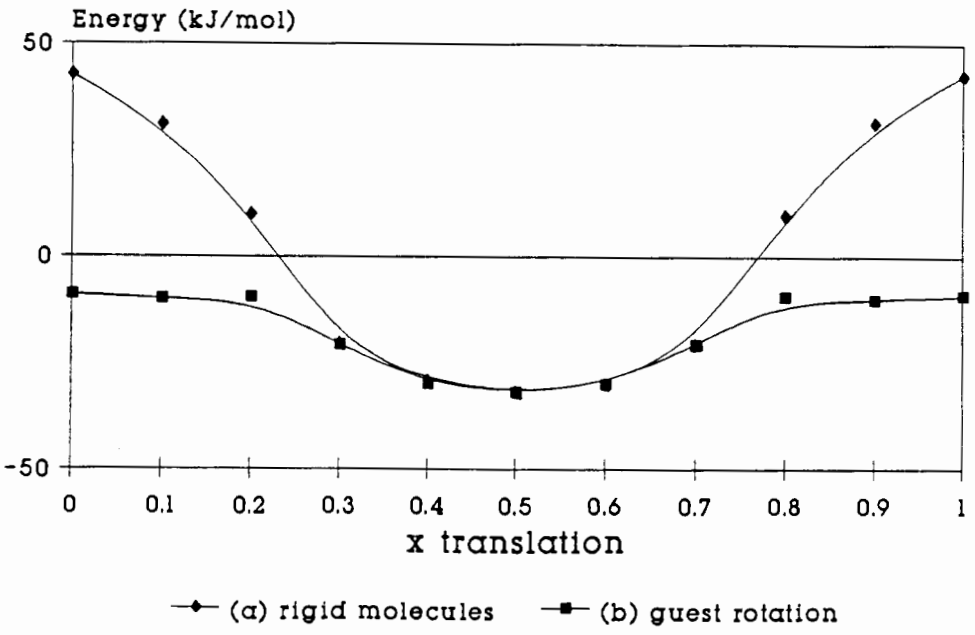

Figure 4.16. Energy profiles obtained for the movement of a *p*-chlorotoluene molecule across the cell.

DINM : ($C_{26}H_{22}O_2$) . 2,6-lutidine

Space group : $P\bar{1}$ H : G = 1 : 1

a = 9.414(7) Å α = 82.81(7)°

b = 11.191(4) Å β = 70.78(12)°

c = 13.328(18) Å γ = 86.44(4)°

Z = 2

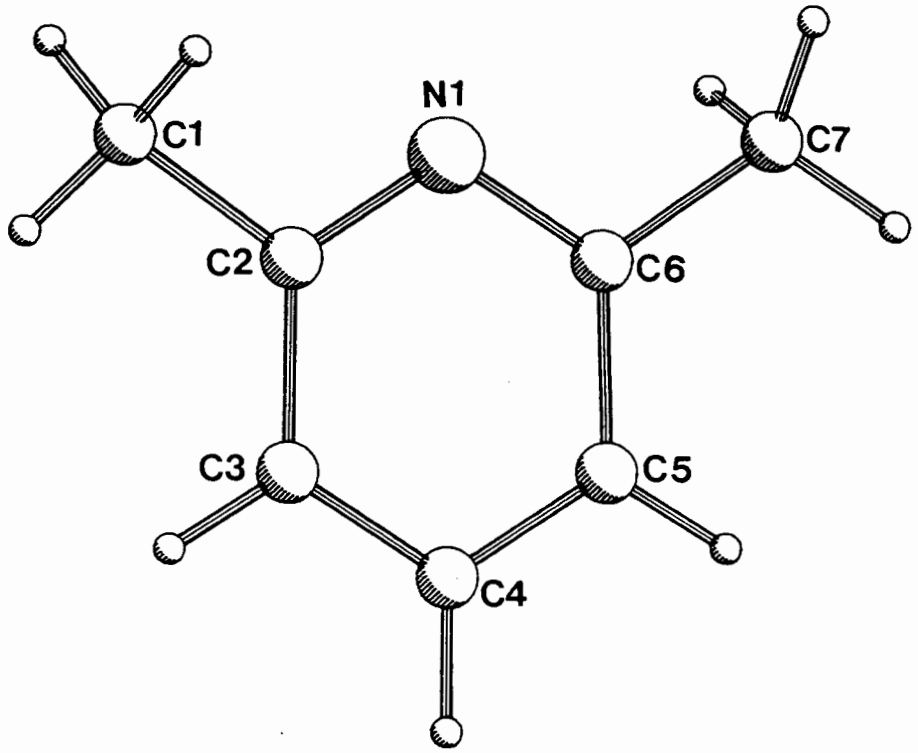

The direct methods solution of this compound revealed 36 atoms with an R_E of 0.21. These correspond to the non-hydrogen atoms of one host and one guest molecule in the asymmetric unit, thus confirming the host to guest ratio established by density, TG and NMR measurements.

The E-statistics of the projections *0kl h0l, hk0* and the remainder were checked and all found to be close to 0.968. This confirmed that DINM was centrosymmetric and it was solved in the space group $P\bar{1}$.

The host and guest molecules refined uneventfully but even with all non-hydrogen atoms refined anisotropically and calculated hydrogens treated as before, only one of the host's two hydroxyl hydrogens was located. This was the one involved in the hydrogen bond between host and guest (O(2)···N(1)); the hydrogen was constrained between its parent oxygen and, more loosely, to the acceptor nitrogen and allowed to refine isotropically. In addition, the host molecule is hydrogen bonded to a symmetry

related molecule across the centre of inversion at Wyckoff position *e*. This hydrogen bond could only be inferred by the short O•••O distance (2.644(4) Å) as the hydrogen could not be found and was omitted from the final refinement. The maximum and minimum heights in the final electron density map were 0.30 eÅ^{-3} and -0.19 eÅ^{-3}. Final coordinates and thermal parameters are listed in Table 4.9.

Molecular structure.

The molecular structure of **DINM** is shown in Figure 4.17.

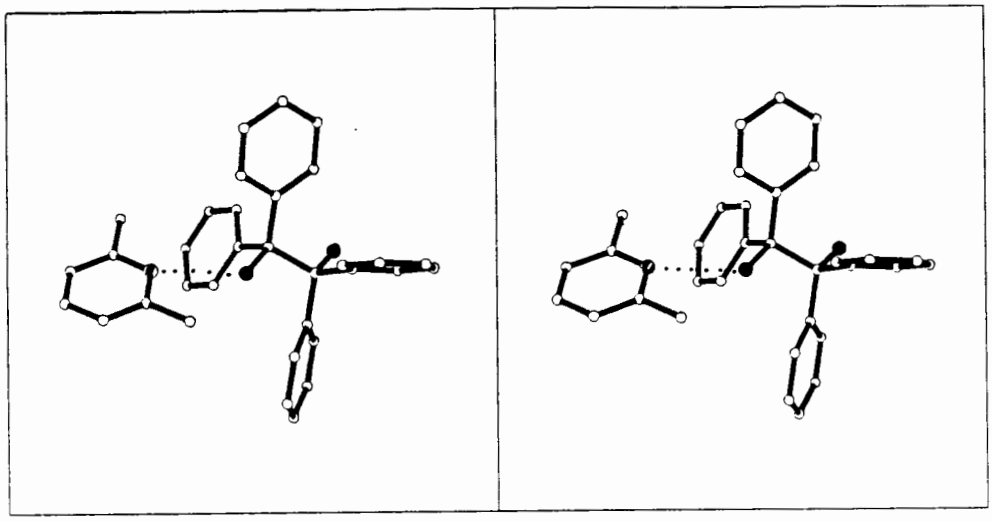

Figure 4.17. Molecular structure of **DINM**.

The host : guest ratio of 1:1 arises from the hydrogen bonding pattern. There is a host-host hydrogen bond across the centre of symmetry at Wyckoff position *e*, and each host is in turn hydrogen bonded to a 2,6-lutidine molecule. Pairs of guest molecules lie in centrosymmetric cavities as may be seen in Figure 4.18, which is a packing diagram viewed down [010]. Hydrogen bonds are drawn with dotted lines. The hydrogen bonding gives rise to chains following the path : N(1)•••O(2) - C(2) - C(1) - O(1)•••O(1) - C(1) - C(2) - O(2)•••N(1). These chains run parallel to [1-1-1].

A better view of the cavity is obtained by shading the areas occupied by host molecules. These areas were calculated using OPEC. The cavity was found to be centred at x = y = 0 and z = 0.5. Figure 4.19 shows the unit cell viewed down [010] with guest molecules drawn with van der Waals radii. The regions occupied by the host are shaded.

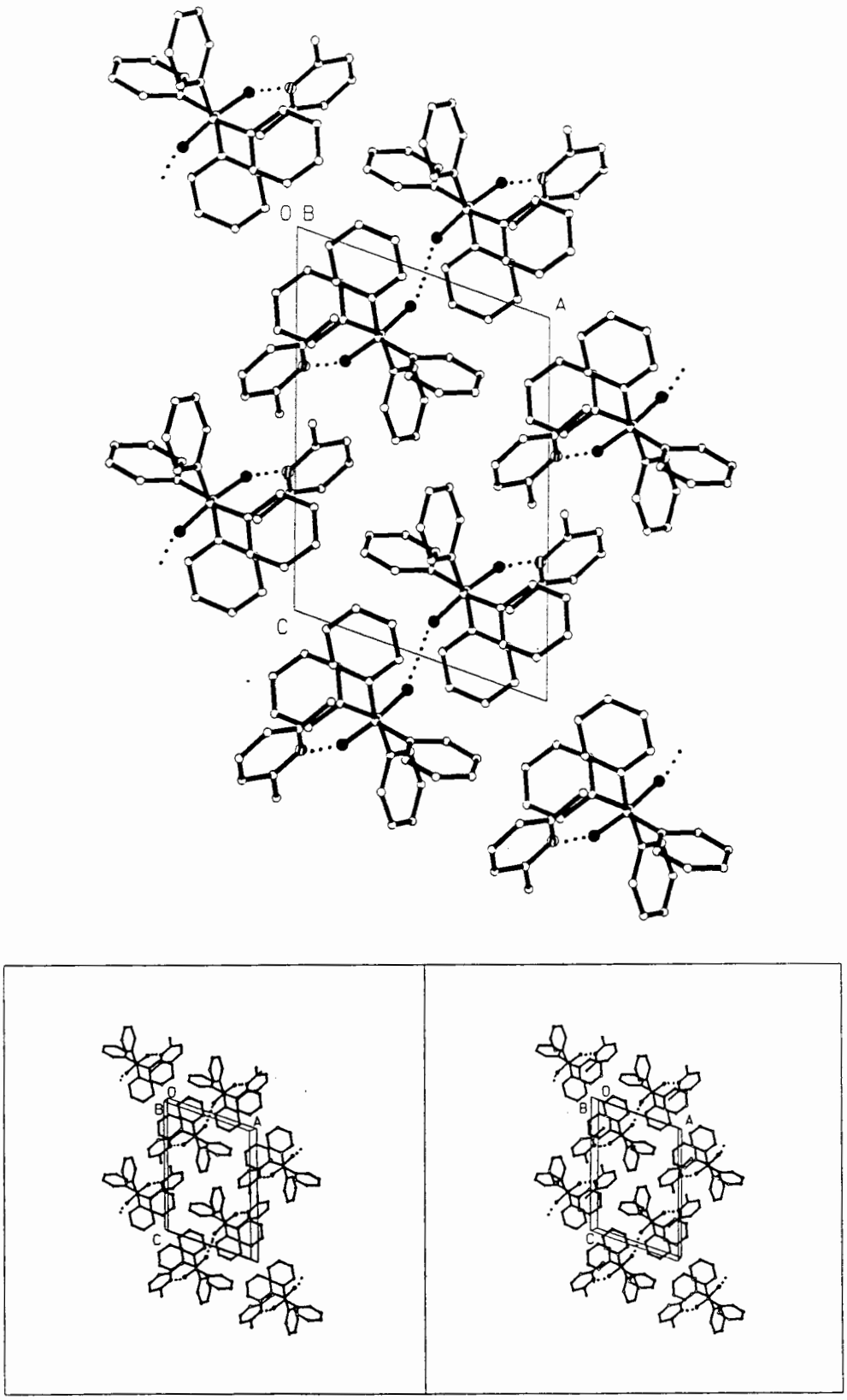

Figure 4.18. Packing diagram of **DINM** viewed along [010]. H-bonds are drawn as dotted lines.

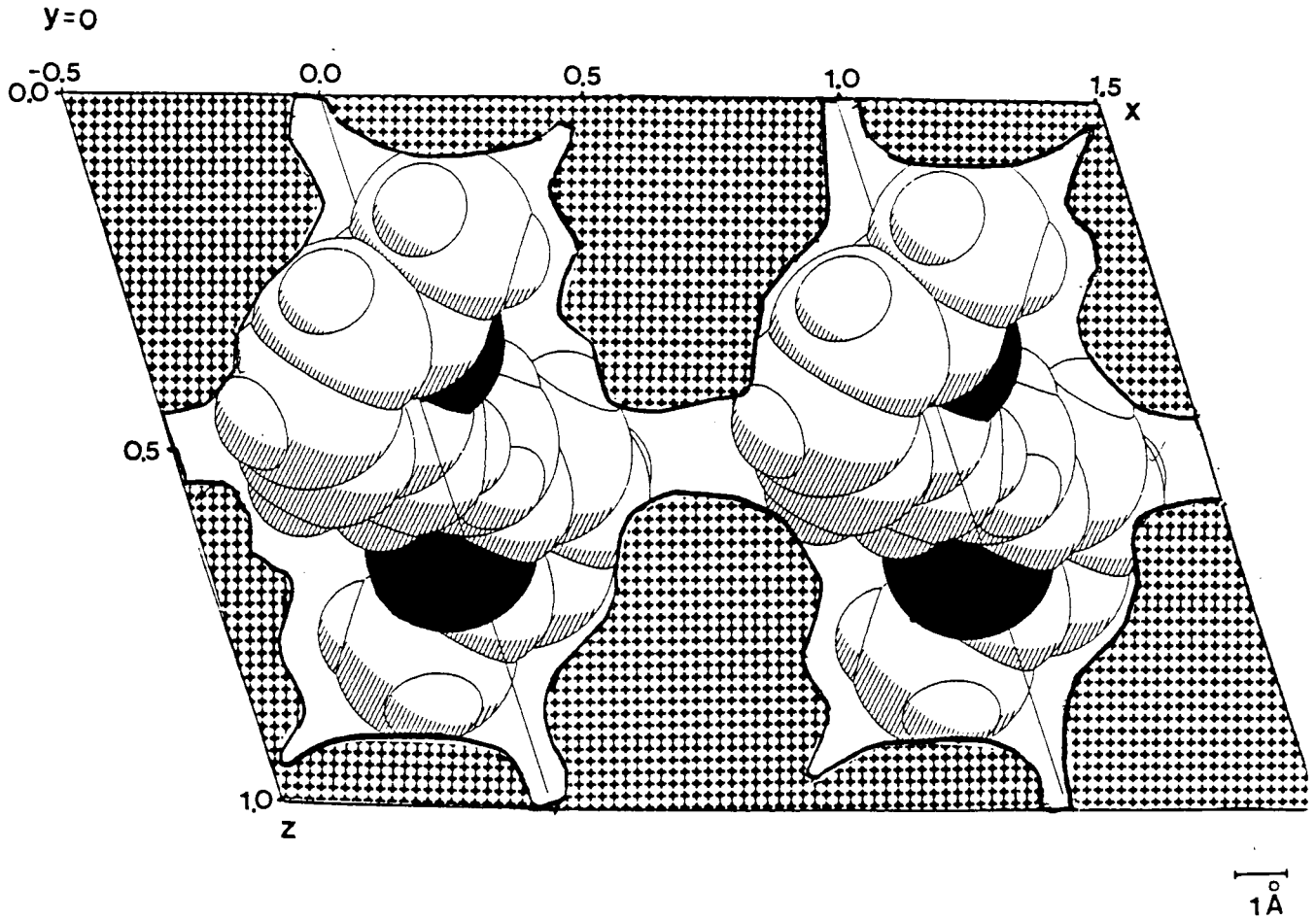

Figure 4.19. DINM : cross-section through the cell showing the cavities in which guests are trapped.

LUTI : ($C_{26}H_{22}O_2$) . 2 (3,5-lutidine)

Space group : $P\bar{1}$	H : G = 1 : 2
a = 12.099(4) Å	α = 64.65(3)°
b = 17.869(5) Å	β = 87.32(4)°
c = 17.873(10) Å	γ = 75.25(2)°
Z = 4	

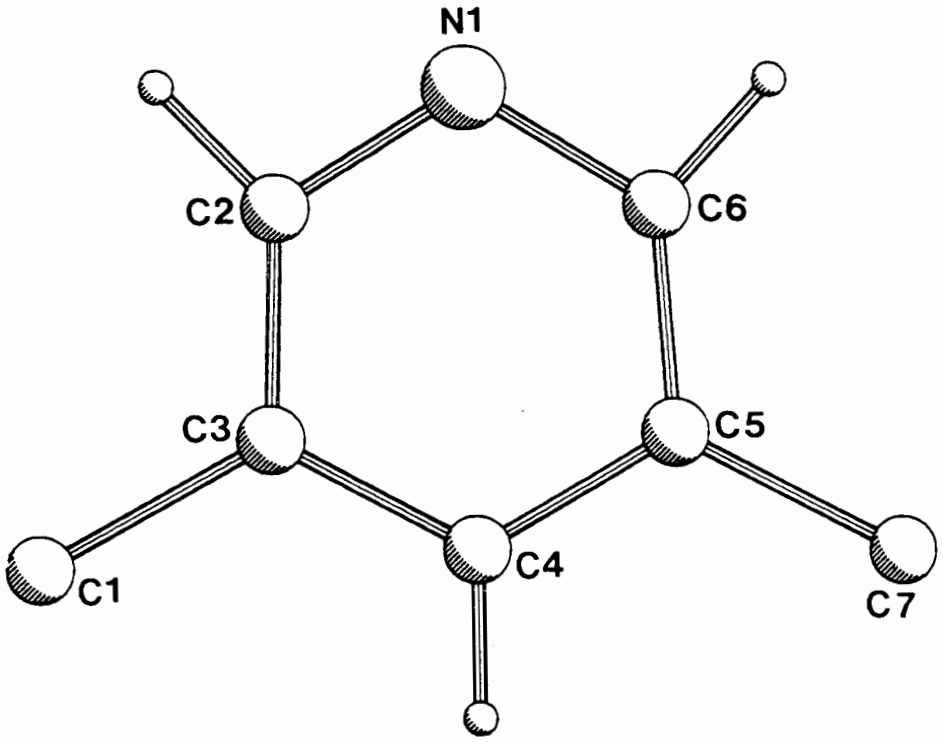

There were two host and four guest molecules in the asymmetric unit of the unit cell. Each of the hosts' hydroxyl groups is hydrogen bonded to the nitrogen atom of a guest molecule.

The large number of parameters made it necessary to refine this structure by means of large-block least squares. In addition, the phenyl rings of the hosts were refined as regular hexagons to avoid too low a reflection-to-parameter ratio.

Even when modelled anisotropically, the guests' methyl carbons had temperature factors significantly higher than those of the phenyl carbons. The methyl groups can be expected to have higher vibrational energy, hence greater thermal motion. The methyl hydrogens were not modelled. The final electron density map gave maxima and minima of 0.33 $eÅ^{-3}$ and -0.25 $eÅ^{-3}$ respectively. Final coordinates and thermal parameters are listed in Table 4.10.

Molecular structure.

The two hosts and their associated four guests in the asymmetric unit are shown in Figure 4.20.

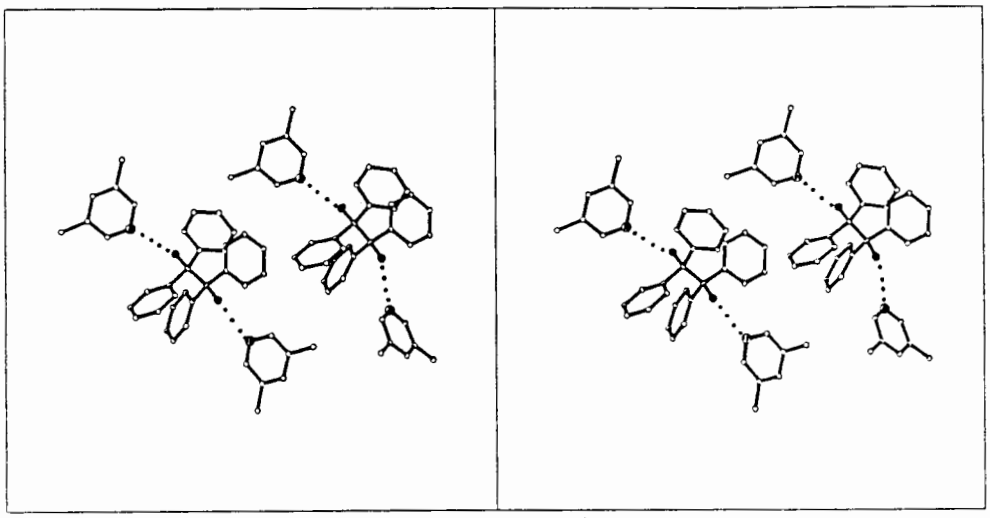

Figure 4.20. The asymmetric unit of **LUTI.**

3,5-Lutidine has the same fundamental shape as 2,6-lutidine but the nitrogen atom is more accessible to the host's hydroxyl groups. The formation of two host-guest hydrogen bonds per host molecule dictates the structural packing as illustrated in Figure 4.21.

The 3,5-lutidine molecules lie in channels which run parallel to [0-11] (centred at x = 0 and x = 0.5) and [10-1] (centred at y = 0 and y = 0.5).

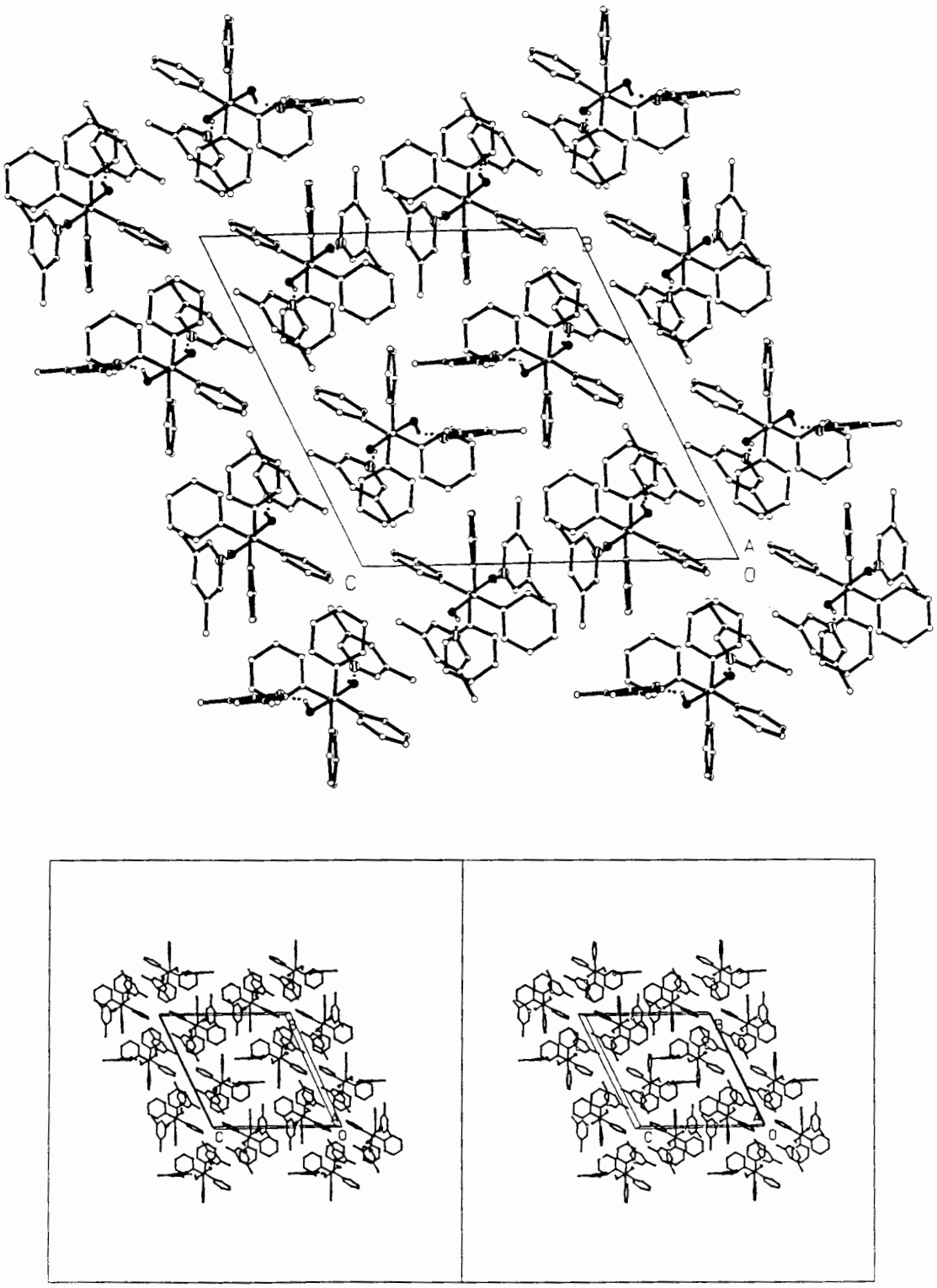

Figure 4.21. Packing diagram of **LUTI** viewed along [100].

DINO : ($C_{26}H_{22}O_2$) . 2 (3,4-lutidine)

Space group : $P\bar{1}$	H : G = 1 : 2
a = 9.163(4) Å	α = 69.50(3)°
b = 11.740(4) Å	β = 74.22(4)°
c = 17.721(7) Å	γ = 73.09(4)°
Z = 2	

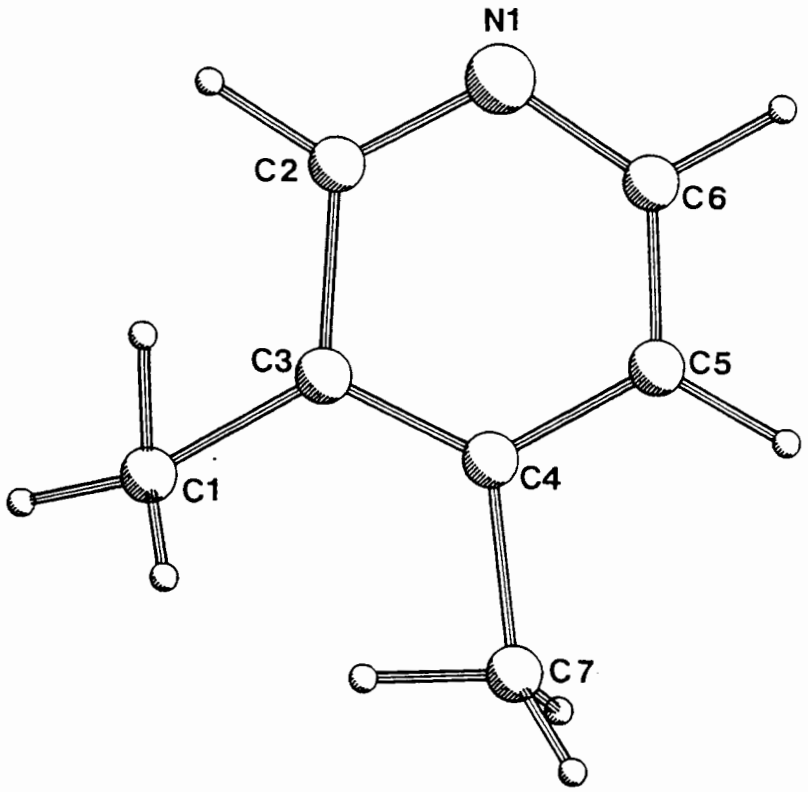

One host and two guests were found in the asymmetric unit, as predicted by density, TG and NMR.

Refinement proceeded in the usual manner and the final model included anisotropic modelling of all non-hydrogen atoms. All hydrogens, except the hydroxyls, were placed at calculated positions and refined with linked temperature factors. O···N distances of 2.889 Å and 2.808 Å suggested the presence of hydrogen bonding. The hydroxyl hydrogens were located in difference Fourier maps and fixed at set distances from their parent oxygens and the acceptor nitrogens and allowed to refine isotropically.

The final maximum shift/e.s.d. was 0.008 and the final heights in the difference Fourier map were 0.28 $eÅ^{-3}$ and -0.23 $eÅ^{-3}$. Final coordinates and thermal parameters are listed in Table 4.11.

Molecular structure.

DINO is structurally similar to **LUTI** in that each host is hydrogen bonded to two guests, as shown in Figure 4.22.

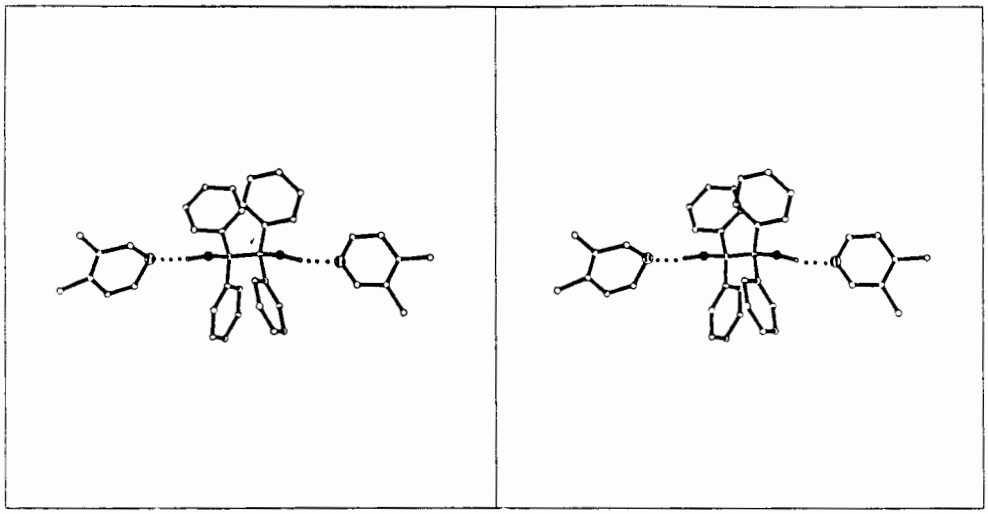

Figure 4.22. Molecular structure of **DINO**.

A packing diagram, viewed down [100], is given in Figure 4.23. The guest molecules again lie in channels which run parallel to [0-11] and [100].

Since they are isomers, the conformation of the guests in **DINM**, **LUTI** and **DINO** are discussed together. N-C bonds range between 1.306(10) and 1.347(9) Å, C_{ring} - C_{methyl} between 1.490(3) and 1.565(13) Å and C_{ring} - C_{ring} between 1.343(9) and 1.396(11) Å. Angles inside the rings range between 116.7(5) and 120.9(4)°. These are all close to the values expected for such structures. In each case, the pyridine ring is planar (the maximum deviation from the plane never exceeds 0.03 Å).

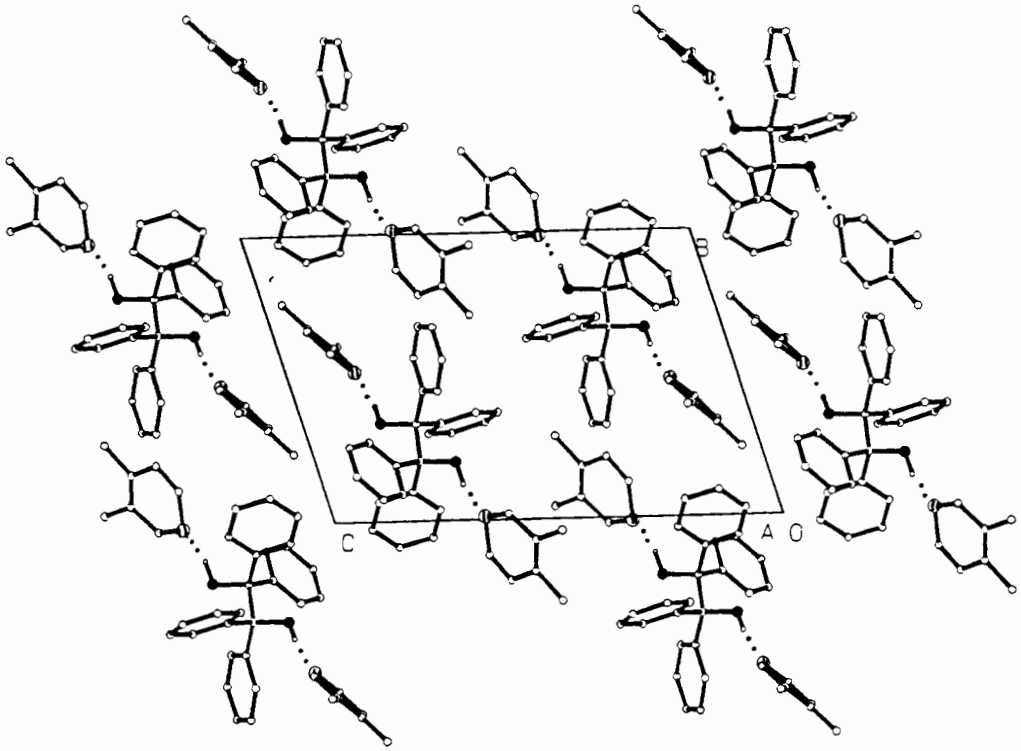

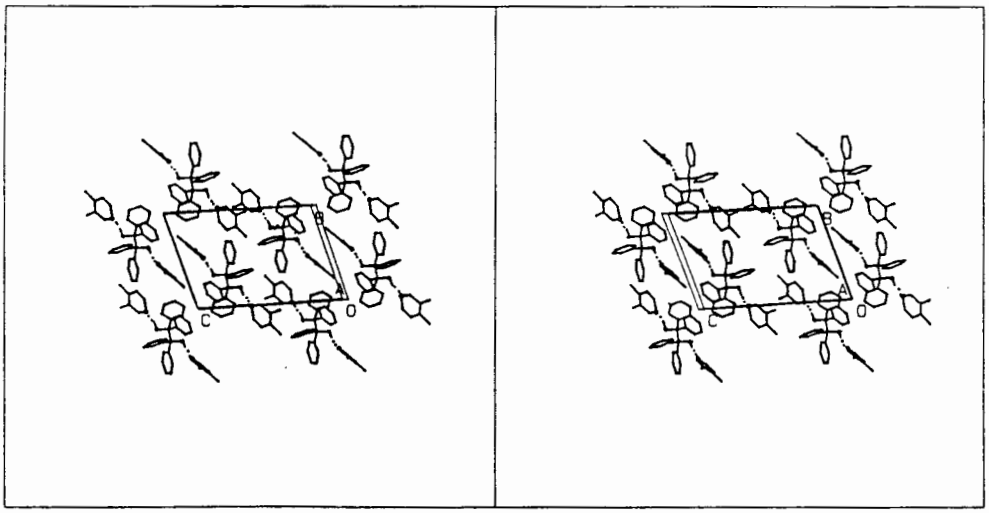

Figure 4.23. Packing diagram of **DINO** viewed down [100]. H-bonds are indicated by dotted lines.

PEACH : $(C_{26}H_{22}O_2)$. acetone

Space group : $P2_1/c$ H : G = 1 : 1

a = 9.250(3) Å

b = 18.183(4) Å β = 99.38(2)°

c = 14.272(3) Å

Z = 4

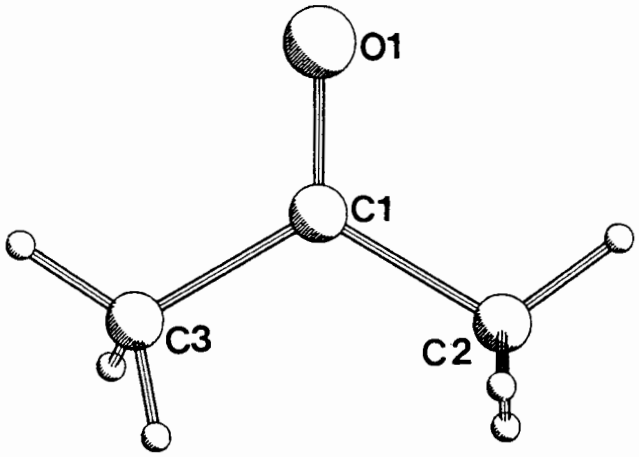

Oscillation, zero- and first-level Weissenberg photographs revealed the following non-extinction reflection conditions :

h0l	l = 2n
0k0	k = 2n
00l	l = 2n

These identified the structure as monoclinic, $P2_1/c$.

The structure refined uneventfully to a final R factor of 0.045, with one host and one guest molecule treated as described previously.

The final electron density map showed no feature greater than 0.15 $eÅ^{-3}$ or less than -0.17 $eÅ^{-3}$, indicating that there were no missing nor incorrectly placed atoms. Final coordinates and thermal parameters are listed in Table 4.12.

Molecular structure.

Only one of the host's hydroxyl groups is involved in a hydrogen bond, as shown in Figure 4.24. The other hydroxyl is free. This explains the appearance of two peaks in the infrared spectrum of **PEACH**. One has ν = 3373 cm^{-1} (a hydrogen bonded hydroxyl group); the other is at 3551 cm^{-1}.

No unusual features were seen in the conformation of the acetone molecule. All parameters are within acceptable limits.

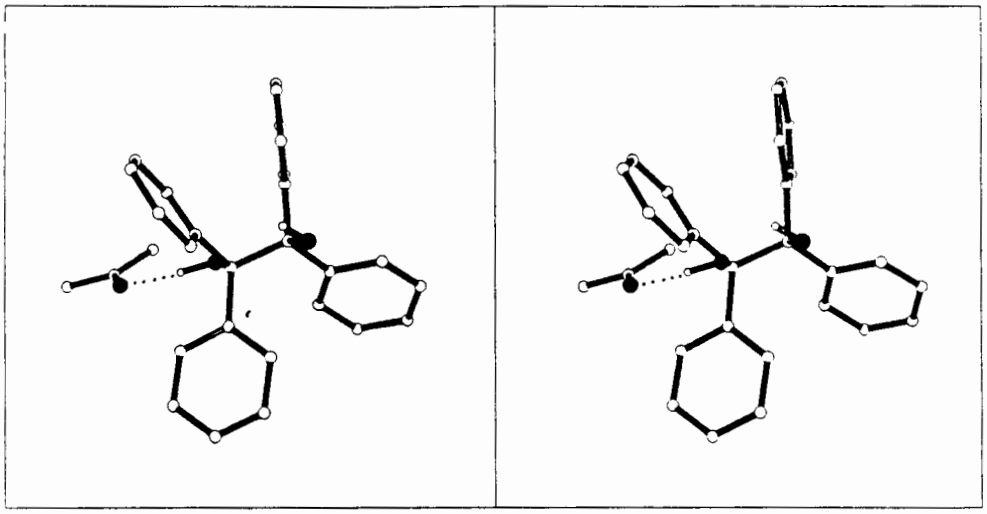

Figure 4.24 Molecular structure of **PEACH.**

Acetone molecules lie in a channel parallel to [100] whose walls are composed of phenyl and hydroxyl groups. The channel is shown in Figure 4.25, in which the guest has been removed and the host plotted with van der Waals radii. Hydroxyl groups are shaded.

The inverse diagram showing the channel along [100] is given in Figure 4.26. In this case, acetone molecules are drawn with van der Waals radii and their oxygen atoms are shaded. The space in the cell occupied by host atoms (calculated by OPEC) is shaded.

Figure 4.27 is a packing diagram viewed down [100]. This shows the hydrogen bonding present as well as the presence of two acetone molecules, related by an inversion centre, in each channel. The host's second hydroxyl group can also be seen and is clearly not involved in any intermolecular interaction. This is unusual; all structures previously reported have involved both of the host's hydroxyl groups in hydrogen bonds.

In order to understand the shape of the channel more clearly, HEENY was used to model the energy of the guest. A model of acetone, in one of the two orientations shown in Figure 4.26, was positioned in the channel. This molecule was then translated through the channel in steps of 1 Å and the intermolecular energy calculated at each point. Again, no account was taken of partial atomic charges or dipole interactions. However, the hydrogen bond found in the crystal structure was modelled, as described in Chapter 2. The energy profile thus obtained is shown in Figure 4.28(a). There is a narrow, steep-sided valley at x = 0.25. This is approximately the position of the guest in the crystal structure.

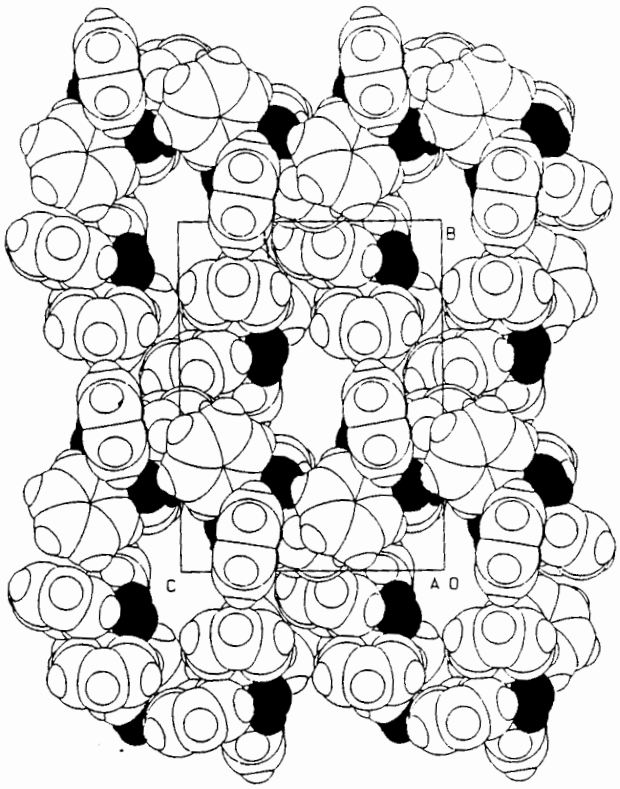

Figure 4.25. Packing diagram of **PEACH** viewed along [100]. The guest has been omitted and the host drawn with van der Waals radii so that the channels can be clearly seen.

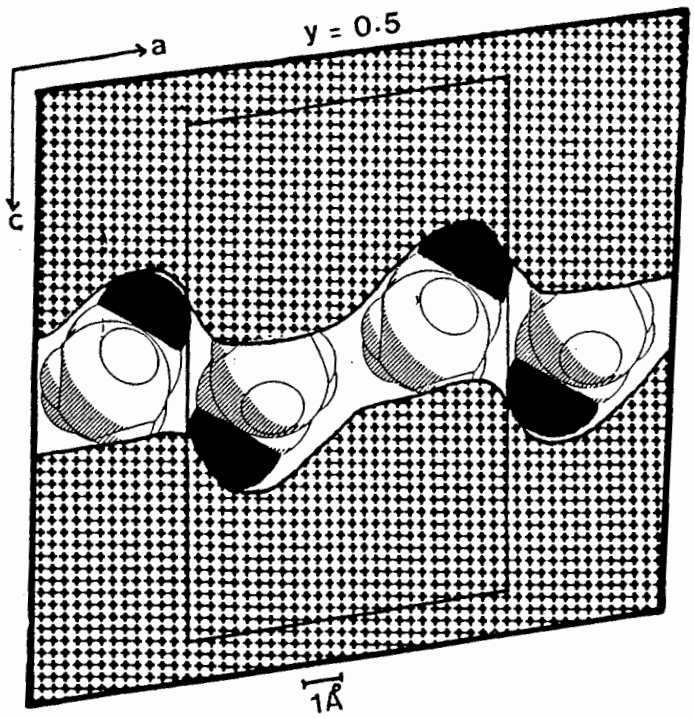

Figure 4.26. Cross-section of the cell at y = ½. The channel in which the acetone is accommodated is clear.

Allowing the acetone to twist about its centre after each translation resulted in the energy profile shown in Figure 4.28(b). This is probably a more realistic view since it allows the acetone molecule to adapt its orientation according to the space available. There is a much wider valley, between x = 0.75 and x = 1.25. Figure 4.26 shows that this is the region where the channel is widest and where the acetone molecules are found. At $x \approx 0.5$, the channel becomes much narrower; this corresponds to the sharp rise in energy at this point in Figure 4.28(b).

Crystals of the α-phase were exposed to actone vapours and their mass monitored. The exposure of the hydroxyl groups on one face of the α-phase (Figure 4.3) probably aids the reaction at this surface. After 10 hours, the mass increase indicated that a 1:2 complex had formed. This complex was extremely unstable and decomposed within two minutes after being removed from the acetone atmosphere. It is reasonable to postulate that in this complex, both of the host's hydroxyl groups are involved in hydrogen bonding to acetone molecules. The structural packing seems likely to be quite different from that of the 1:1 complex, **PEACH**. This remains postulation however, since no method of analysis was fast enough to provide supporting evidence.

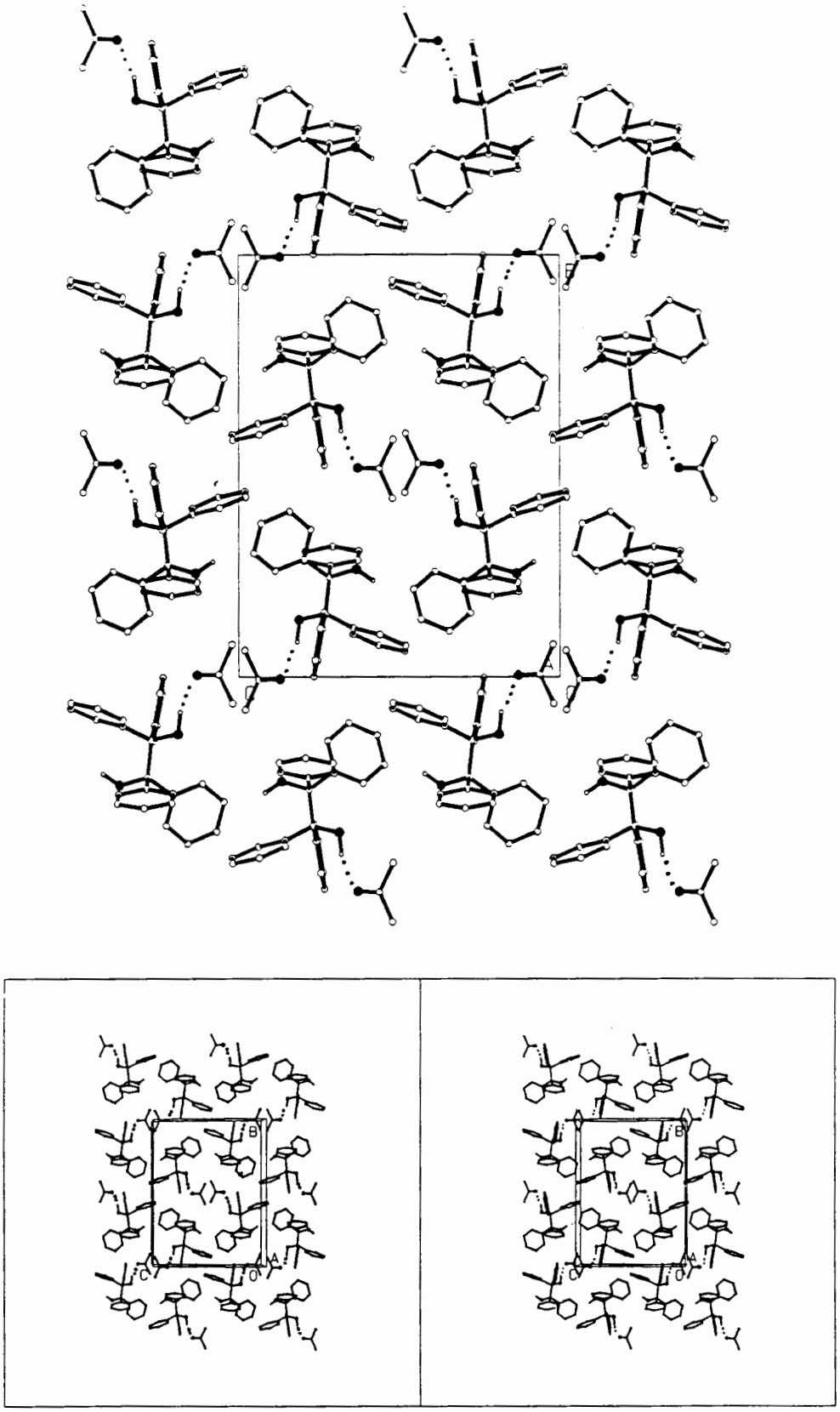

Figure 4.27. Packing diagram of **PEACH** viewed along [100]. H-bonds are indicated by dotted lines.

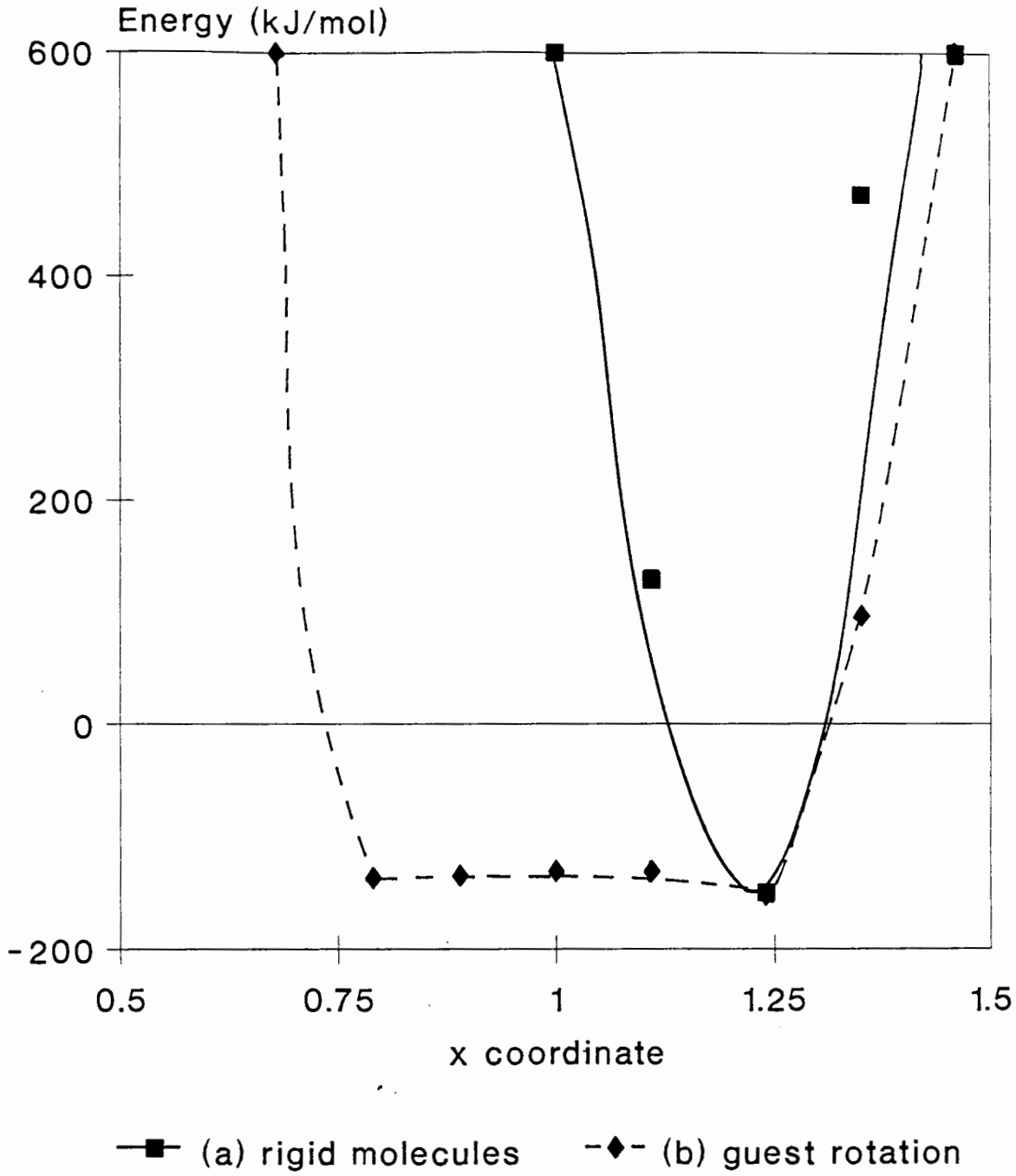

Figure 4.28. Energy profiles obtained by moving an acetone molecule across the cell.

Host conformation in Class A structures.

The design of this host was based on the idea of a "wheel-and-axle".[4.5] Compounds with a long molecular axis ("axle") and large groups at each end ("wheels") form inclusion compounds because the large groups act as spacers to prevent efficient packing.

1,1,2,2-Tetraphenylethane-1,2-diol is a rather flexible molecule where each moiety is able to rotate to a greater or lesser degree.

A study of the conformation of this molecule should include:

(i) Bond lengths and angles.
(ii) The geometry of the sp^3 carbons.
(iii) The planarity of the phenyl rings.
(iv) The orientation of the hydroxyl groups.
(v) The orientation of the phenyl rings.

Bond lengths and angles.

Since the molecule is not expected to be under great strain, no major deviations from theoretical values for bond lengths and angles are expected. Any variations in these parameters for the structures in this class are caused by vibrational effects. Table 4.2 is an indication of the ranges into which these parameters fall. Complete lists are given in the Appendix.

Table 4.2. Bond lengths and angles - Class A.

O-C	1.409(6) - 1.574(17) Å
C_{ethane} - C_{ethane}	1.572(7) - 1.594(8) Å
C_{ethane} - C_{ring}	1.511(9) - 1.561(6) Å
C_{ring} - C_{ring}	1.341(14) - 1.396(4) Å
Angles inside rings	117.6(3) - 122.4(9)°

The "ethane" carbons are sp^3 hybridized and are hence almost tetrahedral. Most of the angles around these atoms are close to the ideal 109.5° but in some cases they are distorted to as low as 103.6° and as high as 116.2°. Figure 4.29 shows the distribution of these angles.

As expected, the aromatic rings are planar. The maximum deviation of any atom from the mean least squares plane through the ring never exceeds 0.02 Å.

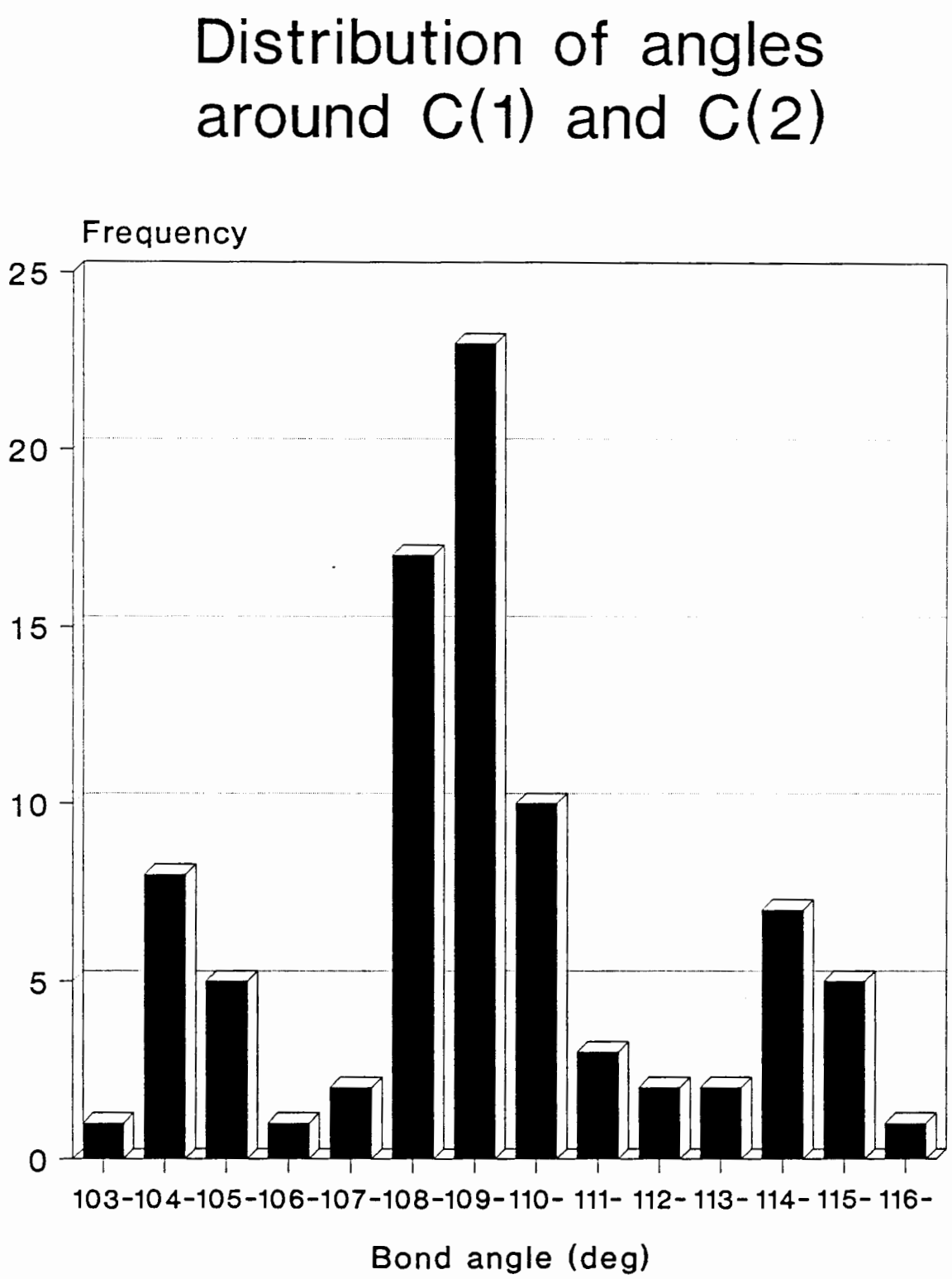
Distribution of angles around C(1) and C(2)
Frequency
25
20
15
10
5
0
103-104-105-106-107-108-109-110- 111- 112- 113- 114- 115- 116-
Bond angle (deg)

Figure 4.29.

The orientation of the hydroxyl groups relative to each other can be seen by the torsion angle O(1) - C(1) - C(2) - O(2). These are listed in Table 4.3. This angle falls between 171.7° and 180°, thus the hydroxyl groups are always anti.

Table 4.3.	O(1) - C(1) - C(2) - O(2)
PEDIL	172.0(5)
	172.1(5)
DEMPE	175.9(6)
	172.4(6)
PEDIOX	180.0(0)*
PECTIL	174.5(8)
	174.8(8)
DINM	171.7(3)
LUTI	177.2(4)
	174.4(4)
DINO	179.1(3)
PEACH	176.4(2)

* Forced to be 180° by symmetry

The torsion angles H(1) - O(1) - C(1) - C(2) and H(2) - O(2) - C(2) - C(1) define the orientation of the hydroxyl moiety to the central portion of the molecule. This angle varies a great deal, which is to be expected since the hydroxyl group is free to rotate to any degree in order to align the hydrogen atom with the hydrogen bond acceptor atom.

The orientation of the phenyl rings.

"Adjacent" phenyl rings, *i.e.* those attached to a common carbon atom are always approximately perpendicular to each other, with dihedral angles ranging from 78.65(13)° to 98.28(27)°.

A more useful parameter to describe the orientation of these rings is the torsion angle between them, highlighted below :

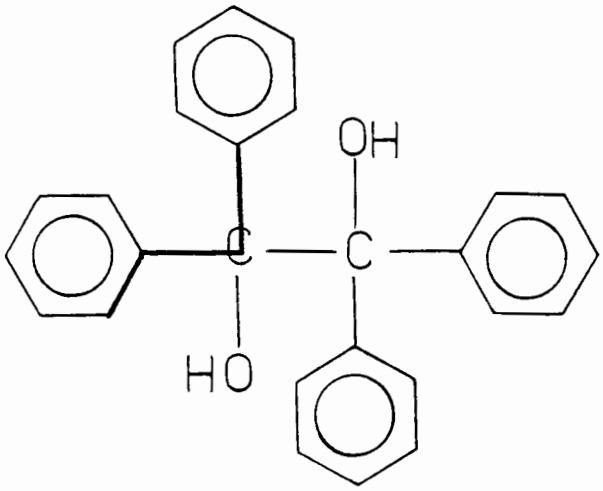

The initial labelling of the ring atoms had been carried out arbitrarily so it was necessary to examine both torsion angles for each ring. The angle < 90° was selected for each ring.

The values of this torsion angle are displayed as a bar graph in Figure 4.30. The angles for two adjacent rings are shaded with the same pattern to distinguish them from those of the rings attached to a neighbouring carbon atom. Also included in Figure 4.30 are the values obtained from an ALCHEMY II minimized molecule. This molecule is shown in space-filled form as Figure 4.31.

Average values for adjacent rings are approximately 70° and 40°. There is little deviation from these values in the host molecules examined. This indicates that the phenyl rings, while they act as spacers to form voids in the host lattice, are not directly involved in determining the placing of the guest within the voids.

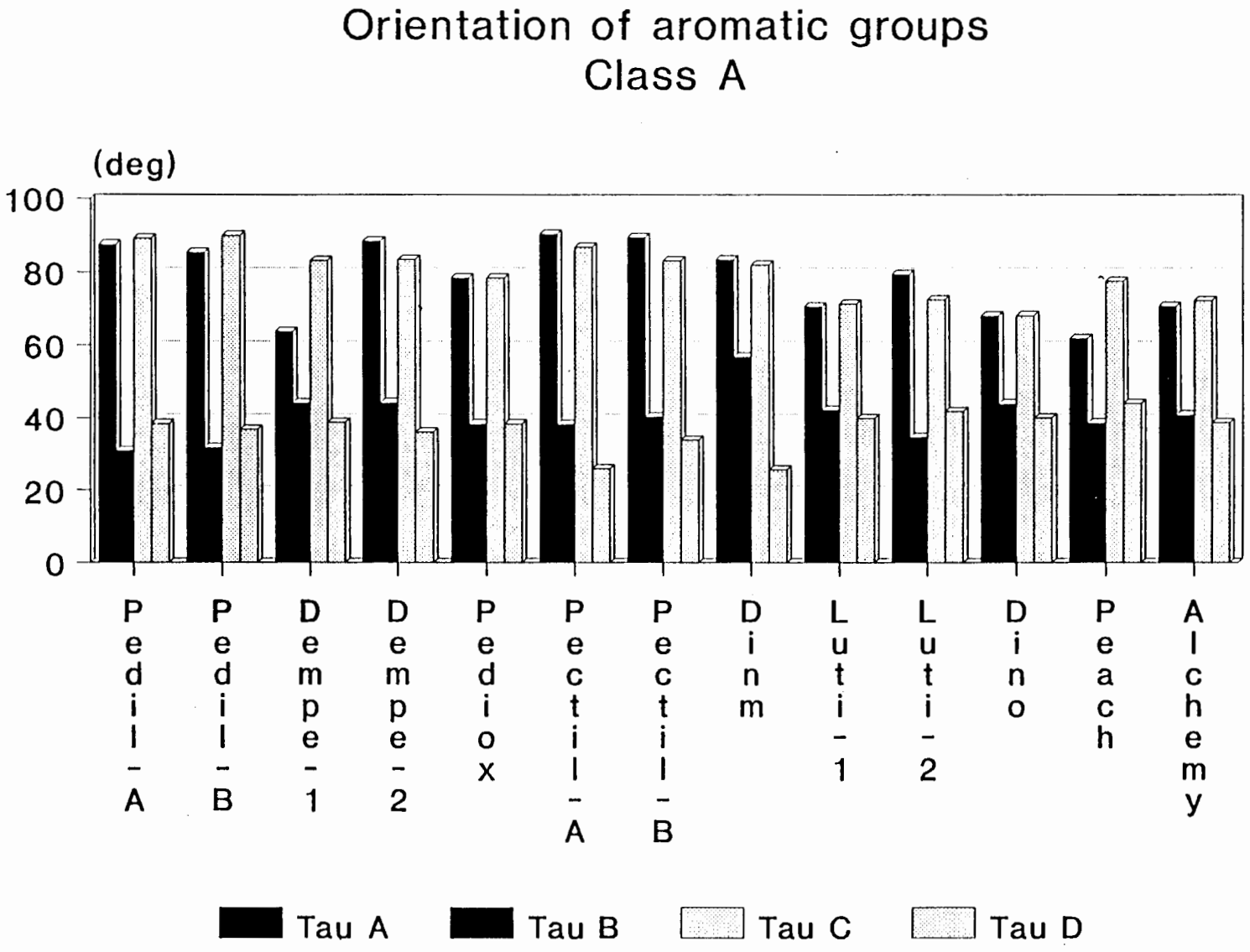

Figure 4.30. Values of torsion angles between phenyl rings.

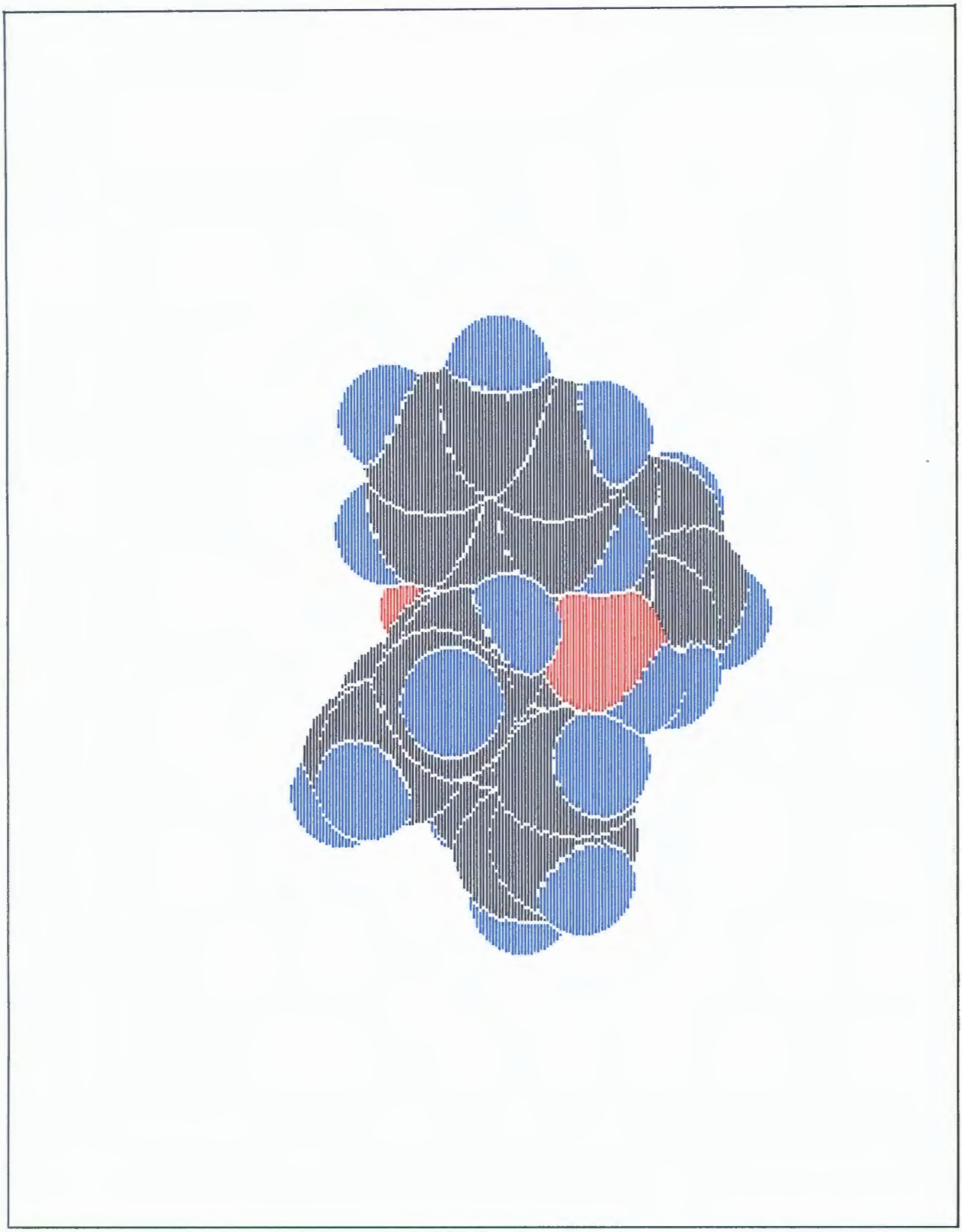

Figure 4.31. Space-filled diagram of the host molecule (Class A).

Table 4.4. Details of Hydrogen bonding in Class A.

Compound	Donor-H	Donor ··· Acceptor	D-H···Acceptor
PEDIL			
O(1)-H(110)···O(2)	0.99(3)	2.635(5)	103.1(67)
O(1)-H(12)···O(2)	1.00(4)	2.635(5)	116.0(45)
O(2)-H(210)···O(1)	1.06(3)	2.635(5)	120.0(58)
O(2)-H(220)···O(1)	1.07(3)	2.635(5)	111.2(66)
DEMPE			
O(1)-H(1)···O(2G)	0.97(8)	2.760(8)	143.6(66)
O(2)-H(2)···O(3G)	0.96(6)	2.840(10)	166.4(62)
O(1H)-H(1H)···O(4G)	0.96(4)	2.786(8)	169.0(50)
O(2H)-H(2H)···O(1G)	0.96(5)	2.808(7)	166.9(49)
PEDIOX			
O(1)-H(1)···O(1G)	1.05(4)	2.865(4)	120.1(28)
PECTIL			
O(1)-H(1)···O(2)	0.99(10)	2.608(6)	121.5(75)
O(2)-H(2)···O(1)	0.99(6)	2.608(6)	116.4(64)
DINM			
O(1)···O(1')	-	2.644(4)	-
O(2)-H(2)···N(1)	0.99(1)	2.825(3)	159.9(17)
LUTI			
O(1)-H(1)···N(1B)	0.99(3)	2.861(6)	165.0(40)
O(2)-H(2)···N(1C)	0.99(2)	2.868(5)	161.4(52)
O(1H)-H(1H)···N(1A)	0.96(7)	2.813(8)	155.4(55)
O(2H)-H(2H)···N(1D)	1.07(2)	2.861(5)	150.4(34)
DINO			
O(1)-H(1)···N(1A)	0.87(4)	2.889(6)	167.2(38)
O(2)-H(2)···N(1B)	0.91(5)	2.808(4)	166.5(49)
PEACH			
O(1)-H(1)···O(1G)	0.96(2)	2.768(3)	157.8(24)

TABLE 4.5 Fractional atomic coordinates (x 10^4) and Thermal Parameters ($Å^2$ + 10^3) with e.s.d. s in parentheses for PEDIL

Atom	x/a	y/b	z/c	U_{iso}/U_{equiv}(*)
C(11)	4083(3)	3389(10)	3073(2)	59(2) *
C(12)	3598(2)	5059(8)	2883(2)	48(2) *
C(13)	2856(3)	5041(9)	3123(3)	55(2) *
C(14)	2603(3)	3349(9)	3536(3)	59(2) *
C(15)	3085(4)	1691(9)	3719(3)	70(2) *
C(16)	3829(4)	1719(10)	3495(3)	76(3) *
C(21)	5449(3)	3274(9)	3525(2)	55(2) *
C(22)	5466(4)	4979(10)	4032(4)	85(3) *
C(23)	5937(4)	4880(12)	4670(4)	85(3) *
C(24)	6377(3)	3141(14)	4817(3)	79(3) *
C(25)	6363(3)	1463(11)	4333(3)	71(2) *
C(26)	5904(3)	1509(8)	3691(3)	55(2) *
C(31)	5911(2)	2859(9)	1896(2)	54(2) *
C(32)	6510(2)	4196(8)	2096(2)	46(2) *
C(33)	7219(3)	3775(10)	1868(3)	63(2) *
C(34)	7360(3)	2002(13)	1452(3)	76(3) *
C(35)	6776(6)	630(10)	1244(3)	99(4) *
C(36)	6050(4)	1073(11)	1474(3)	96(3) *
C(41)	4583(3)	3815(9)	1460(2)	51(2) *
C(42)	4705(5)	5655(11)	1048(4)	105(3) *
C(43)	4262(6)	6154(11)	447(5)	111(4) *
C(44)	3680(4)	4806(18)	215(3)	98(4) *
C(45)	3559(3)	2944(12)	607(3)	77(3) *
C(46)	4010(3)	2466(8)	1243(2)	49(2) *
C(1A)	4998(4)	4041(15)	2855(4)	28(2)
C(1B)	4823(5)	2615(15)	2815(5)	36(2)
C(2A)	5078(5)	4052(16)	2129(5)	37(2)
C(2B)	5140(4)	2629(15)	2142(4)	29(2)
O(1)	5152(2)	6237(5)	2561(2)	65(1) *
O(2)	4863(2)	447(5)	2433(2)	71(2) *

Anisotropic atoms have thermal parameters ($Å^2$ x 10^3) of the form :
$\exp[-2\pi^2(U_{11}h^2a^{*2} + U_{22}k^2b^{*2} + U_{33}l^2c^{*2} + 2U_{23}klb^*c^* + 2U_{13}hla^*c^* + 2U_{12}hka^*b^*)]$

Atom	U_{11}	U_{22}	U_{33}	U_{23}	U_{13}	U_{12}
C(11)	56(3)	104(5)	16(3)	7(3)	8(2)	45(3)
C(12)	47(3)	63(3)	36(3)	-1(2)	8(2)	10(3)
C(13)	46(3)	69(4)	51(3)	2(3)	8(3)	18(3)
C(14)	50(3)	75(4)	49(3)	10(3)	-2(3)	-2(3)
C(15)	112(5)	59(4)	38(3)	8(3)	1(3)	-10(4)
C(16)	101(5)	91(5)	38(3)	14(3)	12(3)	55(4)
C(21)	48(3)	92(4)	27(3)	15(3)	13(2)	29(3)
C(22)	127(5)	87(5)	44(4)	11(4)	46(4)	48(4)
C(23)	123(6)	85(5)	51(5)	-18(4)	45(4)	-27(5)
C(24)	52(4)	133(6)	50(4)	-2(5)	0(3)	-9(4)
C(25)	63(4)	103(5)	47(4)	7(4)	-12(3)	25(3)
C(26)	56(3)	66(4)	43(3)	4(3)	-1(3)	14(3)
C(31)	51(3)	91(4)	21(3)	-6(3)	9(2)	-23(3)
C(32)	46(3)	57(3)	35(3)	-2(2)	5(2)	-2(3)
C(33)	39(3)	102(5)	48(3)	-2(3)	6(3)	5(3)
C(34)	80(5)	102(5)	49(4)	11(4)	14(3)	44(4)
C(35)	212(9)	50(4)	39(4)	-4(3)	46(5)	10(5)
C(36)	141(6)	107(5)	44(4)	-30(4)	42(4)	-71(5)
C(41)	50(3)	83(4)	22(3)	-4(3)	3(2)	-17(3)
C(42)	178(7)	100(5)	38(4)	-7(4)	34(5)	-75(5)
C(43)	209(10)	73(5)	53(5)	15(4)	45(6)	15(6)
C(44)	91(5)	172(8)	32(4)	25(5)	11(4)	73(5)
C(45)	51(4)	141(6)	38(4)	2(4)	-7(3)	-9(4)
C(46)	44(3)	62(3)	40(3)	-3(3)	0(3)	-6(3)
O(1)	65(2)	26(2)	101(3)	4(2)	-13(2)	-1(2)
O(2)	64(2)	23(2)	124(3)	-7(2)	-9(2)	0(2)

TABLE 4.6 Fractional atomic coordinates (x 10^4) and Thermal Parameters ($Å^2$ x 10^3) with e.s.d. s in parentheses for DEMPE

Atom	x/a	y/b	z/c	U_{iso}/U_{equiv}(*)
O(1)	1038(5)	1767(3)	6042(3)	33(2) *
O(2)	-89(5)	3352(3)	4115(3)	37(2) *
C(1)	787(7)	2606(4)	5440(4)	31(3) *
C(2)	265(7)	2527(3)	4694(4)	29(3) *
C(11)	-416(7)	2970(4)	5807(4)	33(4) *
C(12)	-608(8)	3809(5)	5452(5)	49(4) *
C(13)	-1714(9)	4116(6)	5804(7)	64(6) *
C(14)	-2569(10)	3622(7)	6498(7)	71(6) *
C(15)	-2399(9)	2780(7)	6863(5)	73(6) *
C(16)	-1295(7)	2443(5)	6528(4)	48(4) *
C(21)	2165(6)	3116(4)	5225(4)	27(3) *
C(22)	2867(7)	3606(4)	4420(5)	43(4) *
C(23)	4138(8)	4064(5)	4285(5)	56(5) *
C(24)	4736(8)	4039(5)	4938(6)	56(5) *
C(25)	4036(9)	3567(5)	5733(5)	57(5) *
C(26)	2781(8)	3125(5)	5860(5)	46(4) *
C(31)	-1074(7)	1967(4)	5014(4)	30(3) *
C(32)	-2430(8)	2301(5)	4984(4)	48(4) *
C(33)	-3667(9)	1776(7)	5302(6)	67(5) *
C(34)	-3567(10)	928(7)	5644(6)	70(6) *
C(35)	-2270(11)	585(5)	5704(5)	66(4) *
C(36)	-981(8)	1110(5)	5362(4)	53(4) *
C(41)	1426(7)	2201(4)	4256(4)	30(3) *
C(42)	1333(8)	2418(4)	3429(4)	48(4) *
C(43)	2345(9)	2117(5)	3009(5)	59(4) *
C(44)	3401(9)	1609(5)	3397(5)	53(5) *
C(45)	3511(8)	1389(5)	4207(5)	52(4) *
C(46)	2509(8)	1679(5)	4638(5)	46(4) *
O(1H)	6200(5)	2343(3)	10920(3)	40(2) *
O(2H)	4814(5)	2663(3)	9068(3)	37(2) *
C(1H)	5886(7)	2097(4)	10328(4)	26(3) *
C(2H)	5310(6)	2922(4)	9604(4)	29(3) *
C(11H)	4734(7)	1399(4)	10731(4)	33(4) *
C(12H)	4482(7)	895(4)	10377(5)	40(4) *
C(13H)	3422(8)	277(5)	10757(5)	46(4) *
C(14H)	2672(8)	114(5)	11482(6)	53(5) *
C(15H)	2902(9)	601(7)	11829(5)	67(5) *
C(16H)	3917(7)	1238(5)	11466(5)	44(4) *
C(21H)	7275(8)	1784(4)	10046(4)	35(4) *
C(22H)	7567(8)	1845(5)	9265(5)	46(4) *
C(23H)	8811(8)	1499(5)	9058(6)	48(4) *
C(24H)	9757(9)	1108(5)	9625(6)	66(5) *
C(25H)	9490(11)	1072(7)	10378(7)	97(7) *
C(26H)	8293(9)	1406(6)	10567(6)	71(5) *
C(31H)	4008(8)	3224(4)	9984(4)	38(3) *
C(32H)	2642(9)	2940(5)	10053(5)	50(4) *
C(33H)	1462(9)	3193(6)	10419(6)	73(5) *
C(34H)	1728(10)	3728(6)	10737(6)	64(5) *
C(35H)	3071(11)	4009(5)	10676(5)	65(5) *
C(36H)	4239(8)	3777(5)	10295(5)	47(4) *
C(41H)	6469(8)	3617(4)	9126(4)	36(4) *
C(42H)	6319(9)	4205(5)	8314(5)	55(5) *
C(43H)	7315(11)	4850(5)	7868(5)	68(4) *
C(44H)	8461(9)	4933(5)	8206(6)	53(5) *
C(45H)	8629(10)	4356(5)	8993(6)	57(5) *
C(46H)	7665(8)	3708(4)	9459(5)	43(4) *
S(1)	8108(2)	5906(1)	2280(1)	50(1) *
O(1G)	3325(6)	3728(4)	7722(3)	65(3) *
C(1G)	9395(10)	6703(6)	2011(6)	77(3)
C(2G)	8384(11)	5276(6)	3331(6)	77(3)
S(2)	7218(3)	9084(1)	1905(1)	68(1) *
O(2G)	1512(6)	1333(4)	7644(3)	66(3) *
C(3G)	6256(12)	8332(7)	1810(8)	98(4)
C(4G)	5935(15)	9150(9)	2654(9)	123(4)
S(3A)	7009(3)	3996(2)	2489(2)	60(0)
S(3B)	7428(17)	3415(10)	2437(10)	60(0)

Table 4.6 ctd.

O(3G)	-1643(7)	3604(4)	2784(4)	79(4) *
C(5G)	7282(16)	4415(9)	1394(9)	125(5)
C(6G)	5720(14)	3273(9)	2685(10)	127(5)
S(4A)	8133(7)	1287(4)	12737(4)	96(3) *
S(4B)	7589(7)	634(5)	13171(4)	96(4) *
O(4G)	6740(7)	1156(5)	12512(4)	86(4) *
C(7G)	9231(15)	423(10)	12763(11)	144(5)
C(8G)	8052(24)	1048(14)	13645(14)	217(9)

Anisotropic atoms have thermal parameters ($Å^2 \times 10^3$) of the form :
$\exp[-2\pi^2(U_{11}h^2a^{*2} + U_{22}k^2b^{*2} + U_{33}l^2c^{*2} + 2U_{23}klb^*c^* + 2U_{13}hla^*c^* + 2U_{12}hka^*b^*)]$

Atom	U_{11}	U_{22}	U_{33}	U_{23}	U_{13}	U_{12}
O(1)	45(3)	29(3)	25(3)	-8(2)	-12(2)	3(2)
O(2)	50(3)	29(3)	34(3)	-13(2)	-13(2)	2(2)
C(1)	43(4)	33(4)	17(4)	-10(3)	-4(3)	5(3)
C(2)	43(4)	14(4)	28(4)	-6(3)	-9(3)	3(3)
C(11)	38(4)	44(5)	26(4)	-20(4)	-13(4)	3(4)
C(12)	46(5)	56(6)	63(5)	-41(5)	-14(4)	8(4)
C(13)	52(5)	72(6)	101(8)	-65(7)	-19(6)	20(5)
C(14)	55(6)	108(9)	76(7)	-64(7)	-10(6)	24(6)
C(15)	51(6)	131(10)	39(5)	-43(6)	-4(4)	-3(6)
C(16)	37(4)	76(6)	31(5)	-25(5)	-7(4)	10(4)
C(21)	23(4)	29(4)	30(4)	-13(3)	-6(3)	0(3)
C(22)	44(5)	45(5)	44(5)	-23(4)	-6(4)	-5(4)
C(23)	49(5)	73(6)	57(6)	-40(5)	1(4)	-3(5)
C(24)	41(5)	67(6)	74(7)	-43(5)	-15(5)	-4(4)
C(25)	62(6)	71(6)	50(6)	-34(5)	-16(5)	-2(5)
C(26)	46(5)	56(5)	39(5)	-23(4)	-6(4)	-8(4)
C(31)	30(4)	35(5)	26(4)	-12(4)	-7(3)	-7(3)
C(32)	60(6)	51(5)	39(5)	-24(4)	-5(4)	-1(5)
C(33)	43(5)	94(8)	72(6)	-44(6)	-7(5)	-13(5)
C(34)	52(6)	88(8)	66(6)	-31(6)	-2(5)	-35(6)
C(35)	85(7)	44(5)	54(6)	-10(4)	1(5)	-32(6)
C(36)	62(5)	57(6)	34(5)	-13(4)	-22(4)	3(5)
C(41)	36(4)	27(4)	29(5)	-11(3)	-12(3)	3(3)
C(42)	59(5)	52(5)	36(5)	-21(4)	-16(4)	23(4)
C(43)	74(6)	74(6)	36(5)	-33(5)	-2(5)	-2(5)
C(44)	60(6)	55(5)	50(6)	-29(5)	0(4)	8(4)
C(45)	64(5)	50(5)	49(6)	-25(4)	-24(4)	7(4)
C(46)	54(5)	57(5)	40(5)	-30(4)	-14(4)	18(4)
O(1H)	63(3)	38(3)	25(3)	-17(2)	-18(2)	19(2)
O(2H)	52(3)	36(3)	33(3)	-21(3)	-22(2)	14(2)
C(1H)	33(4)	24(4)	26(4)	-14(3)	-6(3)	1(3)
C(2H)	28(4)	33(4)	28(4)	-13(4)	-14(3)	7(3)
C(11H)	34(4)	34(4)	26(4)	-10(4)	-4(4)	17(3)
C(12H)	30(4)	44(5)	47(5)	-22(4)	-2(4)	6(4)
C(13H)	42(5)	35(5)	57(6)	-18(4)	-1(5)	1(4)
C(14H)	38(5)	45(5)	54(6)	-5(5)	-5(5)	0(4)
C(15H)	57(6)	91(7)	34(5)	-17(6)	7(4)	6(6)
C(16H)	30(4)	56(5)	40(5)	-18(4)	-4(4)	4(4)
C(21H)	51(5)	25(4)	25(5)	-7(3)	-4(4)	5(4)
C(22H)	55(5)	41(5)	47(6)	-25(4)	-6(4)	8(4)
C(23H)	41(5)	47(5)	61(6)	-31(5)	4(5)	2(4)
C(24H)	52(6)	52(5)	68(7)	-16(5)	26(6)	15(5)
C(25H)	77(7)	122(10)	56(7)	-15(7)	-15(6)	72(7)
C(26H)	64(6)	100(7)	44(6)	-29(5)	-23(5)	56(6)
C(31H)	49(5)	37(4)	20(4)	-6(4)	-5(3)	14(4)
C(32H)	47(6)	47(5)	58(6)	-23(5)	-16(4)	14(4)
C(33H)	41(6)	77(7)	78(7)	-19(6)	-5(5)	21(5)
C(34H)	48(6)	63(6)	77(7)	-32(6)	1(5)	13(5)
C(35H)	84(8)	60(6)	53(6)	-32(5)	-3(5)	25(6)
C(36H)	55(5)	41(5)	55(5)	-30(4)	-9(4)	11(4)
C(41H)	54(5)	34(4)	27(5)	-20(4)	-7(4)	15(4)
C(42H)	56(5)	56(6)	37(6)	-8(5)	-12(4)	-10(5)
C(43H)	99(7)	49(6)	21(5)	11(4)	-3(5)	-15(6)
C(44H)	60(6)	40(5)	55(7)	-23(5)	6(5)	1(4)
C(45H)	69(6)	50(6)	57(7)	-26(6)	-18(5)	7(5)

Table 4.6 ctd.

C(46H)	54(5)	38(5)	37(5)	-15(4)	-8(4)	0(4)
S(1)	63(1)	42(1)	49(1)	-21(1)	-17(1)	6(1)
O(1G)	71(4)	69(4)	46(4)	-17(3)	-24(3)	19(3)
S(2)	78(2)	66(2)	54(2)	-22(1)	-21(1)	9(1)
O(2G)	58(4)	101(5)	41(3)	-32(3)	-21(3)	18(3)
O(3G)	73(4)	92(5)	65(4)	-22(4)	-46(4)	3(4)
S(4A)	106(5)	82(4)	68(4)	0(4)	-50(4)	-17(4)
S(4B)	94(4)	118(6)	78(4)	-44(4)	-29(4)	19(4)
O(4G)	95(5)	123(6)	38(4)	-32(4)	-36(3)	48(4)

TABLE 4.7 Fractional atomic coordinates (x 10^4)
and Thermal Parameters ($Å^2$ x 10^3)
with e.s.d. s in parentheses for PEDIOX

Atom	x/a	y/b	z/c	U_{iso}/U_{equiv}(*)
O(1)	1399(3)	2060(1)	1816(1)	51(1) *
C(1A)	933(4)	2061(2)	2583(2)	30(1) *
C(1B)	-319(11)	2141(5)	2048(7)	36(3) *
C(11)	1460(3)	2838(2)	3128(2)	52(1) *
C(12)	1523(4)	2887(2)	3946(2)	60(1) *
C(13)	2106(3)	3568(2)	4377(2)	57(1) *
C(14)	2667(4)	4210(2)	3983(2)	57(1) *
C(15)	2633(4)	4158(2)	3183(2)	59(1) *
C(16)	2019(4)	3481(2)	2761(2)	54(1) *
C(21)	1602(3)	1331(2)	3077(2)	50(1) *
C(22)	3191(4)	1237(2)	3067(2)	64(1) *
C(23)	4017(4)	590(2)	3421(2)	63(1) *
C(24)	3292(4)	21(2)	3804(2)	59(1) *
C(25)	1709(4)	98(2)	3824(2)	54(1) *
C(26)	875(4)	753(2)	3473(2)	48(1) *
O(1G)	2276(3)	3057(2)	591(2)	59(1) *
O(2G)	1562(18)	1832(10)	118(10)	98(7) *
C(1G)	1624(5)	3168(3)	-231(3)	86(2) *
C(2G)	3712(4)	2625(3)	627(2)	83(2) *

Anisotropic atoms have thermal parameters ($Å^2$ x 10^3) of the form :
$\exp[-2\pi^2(U_{11}h^2a^{*2} + U_{22}k^2b^{*2} + U_{33}l^2c^{*2} + 2U_{23}klb^*c^* + 2U_{13}hla^*c^* + 2U_{12}hka^*b^*)]$

Atom	U_{11}	U_{22}	U_{33}	U_{23}	U_{13}	U_{12}
O(1)	59(1)	47(1)	55(1)	0(1)	32(1)	0(1)
C(1A)	22(2)	34(2)	34(2)	-1(2)	5(2)	2(2)
C(1B)	28(5)	27(5)	50(6)	-3(4)	4(5)	0(4)
C(11)	40(2)	39(2)	66(2)	12(1)	-22(1)	-5(1)
C(12)	40(2)	59(2)	75(2)	23(2)	-6(2)	-12(2)
C(13)	43(2)	69(2)	57(2)	4(2)	5(1)	7(2)
C(14)	54(2)	44(2)	66(2)	-6(2)	-3(2)	0(1)
C(15)	65(2)	46(2)	63(2)	6(2)	2(2)	-16(2)
C(16)	58(2)	43(2)	54(2)	2(1)	-2(1)	-10(2)
C(21)	49(2)	35(2)	55(2)	6(1)	-19(1)	-6(1)
C(22)	51(2)	65(2)	68(2)	16(2)	-7(2)	-16(2)
C(23)	47(2)	68(2)	69(2)	-3(2)	0(2)	2(2)
C(24)	63(2)	42(2)	66(2)	1(2)	-4(2)	12(2)
C(25)	59(2)	40(2)	60(2)	12(1)	4(2)	0(1)
C(26)	45(2)	39(2)	55(2)	3(1)	-3(1)	0(1)
O(1G)	74(2)	54(2)	55(2)	0(1)	24(1)	9(1)
O(2G)	82(10)	107(12)	107(12)	10(10)	21(9)	-10(9)
C(1G)	83(3)	78(3)	99(3)	23(3)	21(2)	28(2)
C(2G)	55(2)	127(4)	65(2)	-3(3)	4(2)	-2(2)

TABLE 4.8 Fractional atomic coordinates (x 10^4) and Thermal Parameters ($Å^2$ x 10^3) with e.s.d. s in parentheses for PECTIL

Atom	x/a	y/b	z/c	U_{iso}/U_{equiv}(*)
O(1)	-3899(6)	919(5)	2053(3)	72(2) *
O(2)	1790(7)	416(5)	2229(3)	58(2) *
C(1A)	-1960(25)	333(13)	1820(6)	39(3)
C(1B)	-522(28)	388(15)	1847(7)	50(4)
C(2A)	-1561(26)	1120(15)	2432(6)	50(4)
C(2B)	-218(21)	806(12)	2436(5)	30(3)
C(12)	1189(9)	797(6)	914(3)	89(4) *
C(13)	1914(9)	1556(6)	378(3)	89(5) *
C(14)	933(9)	2705(6)	185(3)	80(4) *
C(15)	-774(9)	3094(6)	527(3)	75(4) *
C(16)	-1500(9)	2335(6)	1063(3)	52(3) *
C(11)	-518(9)	1186(6)	1256(3)	53(3) *
C(22)	-1333(6)	-2427(5)	1815(2)	47(3) *
C(23)	-2338(6)	-3949(5)	1623(2)	64(4) *
C(24)	-4390(6)	-4345(5)	1248(2)	69(3) *
C(25)	-5438(6)	-3219(5)	1064(2)	84(5) *
C(26)	-4433(6)	-1697(5)	1256(2)	86(4) *
C(21)	-2380(6)	-1301(5)	1632(2)	52(3) *
C(32)	1852(7)	3597(5)	2490(2)	53(3) *
C(33)	2397(7)	5140(5)	2696(2)	59(3) *
C(34)	907(7)	5741(5)	3055(2)	63(4) *
C(35)	-1128(7)	4800(5)	3207(2)	71(4) *
C(36)	-1674(7)	3258(5)	3000(2)	79(4) *
C(31)	-184(7)	2656(5)	2640(2)	55(3) *
C(42)	671(6)	254(6)	3473(2)	71(3) *
C(43)	425(6)	-480(6)	4038(2)	71(4) *
C(44)	-1665(6)	-1411(6)	4153(2)	70(4) *
C(45)	-3513(6)	-1609(6)	3703(2)	65(3) *
C(46)	-3269(6)	-875(6)	3138(2)	54(3) *
C(41)	-1177(6)	55(6)	3023(2)	56(3) *
CL(1G)	3481(8)	7883(4)	5472(2)	69(2) *
C(1G)	3400(0)	7600(0)	5200(0)	69(2) *
C(2G)	4286(13)	6275(8)	5202(4)	56(3) *
C(3G)	3121(13)	5299(9)	4701(4)	61(3) *
C(4G)	6161(14)	5957(9)	5506(4)	66(4) *

Anisotropic atoms have thermal parameters ($Å^2$ x 10^3) of the form :
$\exp[-2\pi^2(U_{11}h^2a^{*2} + U_{22}k^2b^{*2} + U_{33}l^2c^{*2} + 2U_{23}klb^*c^* + 2U_{13}hla^*c^* + 2U_{12}hka^*b^*)]$

Atom	U_{11}	U_{22}	U_{33}	U_{23}	U_{13}	U_{12}
O(1)	7(2)	59(3)	157(5)	25(3)	4(3)	19(2)
O(2)	22(3)	77(4)	87(4)	36(3)	15(2)	24(2)
C(12)	122(8)	128(8)	47(5)	-6(6)	0(5)	95(7)
C(13)	54(5)	149(9)	60(7)	-16(6)	8(4)	20(6)
C(14)	93(7)	70(6)	51(5)	9(5)	15(5)	-30(5)
C(15)	111(7)	54(5)	60(6)	21(4)	0(5)	19(5)
C(16)	45(4)	51(4)	57(5)	15(4)	0(4)	9(4)
C(11)	83(5)	41(4)	38(4)	10(3)	-8(4)	22(4)
C(22)	43(4)	46(5)	61(5)	18(4)	7(3)	21(4)
C(23)	94(6)	46(5)	57(5)	13(4)	5(5)	24(4)
C(24)	54(5)	84(6)	50(5)	0(4)	5(4)	-18(5)
C(25)	34(4)	160(10)	63(6)	-16(6)	-8(4)	43(6)
C(26)	129(8)	97(7)	49(5)	-17(5)	-31(5)	78(6)
C(21)	80(5)	39(4)	44(4)	7(3)	8(4)	28(4)
C(32)	46(4)	53(5)	54(5)	16(4)	-3(3)	0(4)
C(33)	63(5)	39(5)	64(5)	7(4)	-7(4)	-6(4)
C(34)	93(6)	48(5)	50(5)	12(4)	-9(4)	24(5)
C(35)	62(6)	101(7)	50(5)	9(5)	2(4)	18(5)
C(36)	49(5)	112(8)	54(5)	4(5)	9(4)	-22(5)
C(31)	63(5)	49(4)	36(4)	12(3)	0(4)	-20(4)
C(42)	51(5)	93(6)	51(5)	-1(5)	9(4)	-14(4)
C(43)	61(6)	88(6)	63(6)	-2(5)	-2(4)	20(5)
C(44)	99(7)	54(5)	57(5)	17(4)	0(5)	19(5)
C(45)	73(5)	55(5)	57(5)	20(4)	18(5)	-9(4)

Table 4.8 ctd.

C(46)	47(4)	52(4)	56(5)	12(4)	10(4)	-5(4)
C(41)	70(5)	49(4)	38(4)	7(3)	10(4)	-6(4)
CL(1G)	102(3)	72(3)	42(3)	0(2)	16(2)	36(2)
C(1G)	102(3)	72(3)	42(3)	0(2)	16(2)	36(2)
C(2G)	54(5)	66(5)	47(5)	28(4)	7(4)	5(4)
C(3G)	56(5)	68(6)	56(5)	16(4)	-8(4)	9(5)
C(4G)	74(6)	71(6)	42(5)	4(4)	-2(5)	-2(5)

TABLE 4.9 Fractional atomic coordinates ($x\cdot10^4$) and Thermal Parameters ($Å^2 \times 10^3$) with e.s.d. s in parentheses for DINM

Atom	x/a	y/b	z/c	U_{iso}/U_{equiv}(*)
O(1)	4491(2)	5262(1)	1007(1)	49(1) *
O(2)	1937(2)	6958(1)	3035(1)	47(1) *
C(1)	3336(2)	5410(2)	2005(2)	40(1) *
C(2)	3222(2)	6810(2)	2131(2)	40(1) *
C(11)	1850(3)	4932(2)	1988(2)	44(1) *
C(12)	1742(3)	4563(2)	1060(2)	62(1) *
C(13)	421(4)	4133(3)	1036(3)	79(2) *
C(14)	-820(4)	4060(3)	1912(3)	82(2) *
C(15)	-741(3)	4392(2)	2859(3)	70(1) *
C(16)	588(3)	4817(2)	2898(2)	53(1) *
C(21)	3834(2)	4618(2)	2850(2)	41(1) *
C(22)	3490(3)	4878(2)	3897(2)	51(1) *
C(23)	3932(3)	4105(3)	4635(2)	63(1) *
C(24)	4721(3)	3063(3)	4352(2)	68(1) *
C(25)	5060(3)	2791(2)	3326(2)	69(1) *
C(26)	4619(3)	3553(2)	2577(2)	56(1) *
C(31)	4614(2)	7270(2)	2319(2)	42(1) *
C(32)	6045(3)	6754(2)	1975(2)	58(1) *
C(33)	7242(3)	7248(3)	2146(2)	68(1) *
C(34)	7056(3)	8265(3)	2646(2)	66(1) *
C(35)	5644(3)	8790(2)	2991(2)	64(1) *
C(36)	4439(3)	8294(2)	2840(2)	52(1) *
C(41)	2984(2)	7524(2)	1135(2)	43(1) *
C(42)	4142(3)	8083(2)	306(2)	56(1) *
C(43)	3859(4)	8750(3)	-557(2)	70(1) *
C(44)	2435(4)	8850(3)	-623(2)	76(2) *
C(45)	1274(4)	8286(3)	187(3)	74(1) *
C(46)	1546(3)	7631(2)	1052(2)	57(1) *
N(1)	306(2)	9128(2)	3544(2)	52(1) *
C(1G)	1482(4)	10578(3)	2028(3)	96(2) *
C(2G)	210(3)	10216(2)	3025(2)	62(1) *
C(3G)	-1018(4)	10980(3)	3409(3)	81(2) *
C(4G)	-2116(4)	10621(3)	4341(3)	91(2) *
C(5G)	-2004(3)	9529(3)	4880(2)	70(1) *
C(6G)	-787(3)	8788(2)	4459(2)	51(1) *
C(7G)	-649(3)	7569(2)	5017(2)	71(1) *

Anisotropic atoms have thermal parameters ($Å^2 \times 10^3$) of the form :
$\exp[-2\pi^2(U_{11}h^2a^{*2} + U_{22}k^2b^{*2} + U_{33}l^2c^{*2} + 2U_{23}klb^*c^* + 2U_{13}hla^*c^* + 2U_{12}hka^*b^*)]$

Atom	U_{11}	U_{22}	U_{33}	U_{23}	U_{13}	U_{12}
O(1)	48(1)	55(1)	36(1)	-12(1)	0(1)	5(1)
O(2)	41(1)	45(1)	44(1)	-5(1)	1(1)	3(1)
C(1)	39(1)	43(1)	34(1)	-6(1)	-3(1)	2(1)
C(2)	34(1)	44(1)	37(1)	-4(1)	-3(1)	2(1)
C(11)	48(1)	35(1)	49(2)	-1(1)	-17(1)	2(1)
C(12)	74(2)	61(2)	58(2)	-1(1)	-30(2)	-12(1)
C(13)	96(3)	73(2)	83(2)	4(2)	-51(2)	-19(2)
C(14)	76(2)	61(2)	128(3)	10(2)	-64(2)	-13(2)
C(15)	49(2)	50(2)	101(3)	11(2)	-15(2)	-3(1)
C(16)	47(2)	44(1)	63(2)	-1(1)	-11(1)	-1(1)
C(21)	37(1)	42(1)	40(1)	-1(1)	-7(1)	1(1)
C(22)	59(2)	52(1)	40(2)	-4(1)	-13(1)	5(1)
C(23)	72(2)	72(2)	45(2)	0(1)	-22(1)	0(2)

Table 4.9 ctd.

C(24)	65(2)	74(2)	63(2)	10(2)	-24(2)	9(2)
C(25)	64(2)	59(2)	74(2)	0(2)	-14(2)	20(1)
C(26)	59(2)	54(2)	50(2)	-7(1)	-11(1)	14(1)
C(31)	46(1)	44(1)	36(1)	0(1)	-12(1)	-2(1)
C(32)	45(2)	60(2)	69(2)	-10(1)	-15(1)	0(1)
C(33)	48(2)	73(2)	85(2)	-4(2)	-24(2)	-6(1)
C(34)	67(2)	73(2)	68(2)	8(2)	-33(2)	-21(2)
C(35)	79(2)	60(2)	61(2)	-6(1)	-29(2)	-13(2)
C(36)	56(2)	52(2)	51(2)	-7(1)	-18(1)	-3(1)
C(41)	46(1)	40(1)	43(1)	-1(1)	-13(1)	0(1)
C(42)	52(2)	61(2)	50(2)	2(1)	-10(1)	-5(1)
C(43)	79(2)	72(2)	51(2)	17(2)	-15(2)	-10(2)
C(44)	99(3)	69(2)	68(2)	14(2)	-42(2)	-2(2)
C(45)	76(2)	70(2)	87(2)	14(2)	-48(2)	-6(2)
C(46)	52(2)	54(2)	67(2)	9(1)	-24(1)	-5(1)
N(1)	54(1)	42(1)	59(1)	-4(1)	-19(1)	2(1)
C(1G)	124(3)	57(2)	93(3)	16(2)	-21(2)	-6(2)
C(2G)	78(2)	43(2)	70(2)	-5(1)	-31(2)	3(1)
C(3G)	109(3)	49(2)	95(3)	-11(2)	-48(2)	23(2)
C(4G)	86(3)	85(3)	104(3)	-33(2)	-33(2)	37(2)
C(5G)	63(2)	74(2)	74(2)	-26(2)	-17(2)	15(2)
C(6G)	47(2)	53(2)	54(2)	-16(1)	-16(1)	2(1)
C(7G)	70(2)	62(2)	64(2)	1(2)	-1(2)	1(1)

TABLE 4.10 Fractional atomic coordinates (x 10^4)
and Thermal Parameters ($Å^2$ x 10^3)
with e.s.d. s in parentheses for LUTI

Atom	x/a	y/b	z/c	U_{iso}/U_{equiv}(*)
O(1)	2506(3)	9559(2)	6728(2)	54(2) *
O(2)	4917(3)	8576(2)	8222(2)	51(2) *
C(1)	3046(4)	9103(3)	7536(3)	46(1)
C(2)	4350(4)	9071(3)	7415(3)	39(1)
C(12)	1283(3)	9721(2)	8070(2)	72(3) *
C(13)	680(3)	10151(2)	8517(2)	93(3) *
C(14)	1269(3)	10398(2)	8986(2)	95(4) *
C(15)	2462(3)	10218(2)	9009(2)	90(4) *
C(16)	3066(3)	9788(2)	8562(2)	66(3) *
C(11)	2476(3)	9539(2)	8093(2)	53(2) *
C(22)	2629(3)	7829(2)	7422(2)	69(4) *
C(23)	2523(3)	6990(2)	7770(2)	92(4) *
C(24)	2696(3)	6496(2)	8626(2)	96(4) *
C(25)	2975(3)	6842(2)	9137(2)	81(4) *
C(26)	3082(3)	7681(2)	8790(2)	61(3) *
C(21)	2909(3)	8175(2)	7934(2)	54(3) *
C(32)	3770(2)	10748(2)	6705(2)	55(3) *
C(33)	4083(2)	11518(2)	6421(2)	67(3) *
C(34)	5234(2)	11510(2)	6467(2)	69(3) *
C(35)	6072(2)	10732(2)	6797(2)	67(3) *
C(36)	5759(2)	9961(2)	7081(2)	56(3) *
C(31)	4608(2)	9969(2)	7034(2)	47(2) *
C(42)	4644(2)	9092(1)	5987(2)	47(2) *
C(43)	5022(2)	8679(1)	5478(2)	55(3) *
C(44)	5541(2)	7799(1)	5830(2)	62(3) *
C(45)	5682(2)	7332(1)	6691(2)	61(3) *
C(46)	5304(2)	7747(1)	7200(2)	51(2) *
C(41)	4785(2)	8626(1)	6848(2)	41(2) *
N(1A)	4231(4)	6202(3)	3794(3)	77(3) *
C(1A)	4048(7)	6032(5)	5982(5)	110(5) *
C(2A)	3840(5)	6163(3)	4530(5)	75(3) *
C(3A)	4532(5)	6067(3)	5184(4)	72(3) *
C(4A)	5679(6)	6003(3)	5026(5)	79(4) *
C(5A)	6091(5)	6043(4)	4277(5)	79(4) *
C(6A)	5333(5)	6154(4)	3682(4)	77(4) *
C(7A)	7389(6)	5956(5)	5884(6)	131(6) *
N(1B)	-156(4)	10278(4)	3626(4)	92(4) *
C(1B)	1820(7)	8095(5)	4954(6)	149(6) *
C(2B)	330(5)	9428(5)	4014(4)	88(4) *
C(38)	1316(5)	9075(4)	4523(4)	81(4) *

Table 4.10 ctd.

C(4B)	1830(5)	9645(5)	4597(4)	87(4) *
C(5B)	1377(5)	10496(4)	4202(5)	85(4) *
C(6B)	402(5)	10790(4)	3714(5)	89(4) *
C(7B)	1982(7)	11102(5)	4310(7)	149(7) *
O(1H)	-2557(3)	14315(2)	6773(2)	52(2) *
O(2H)	-175(2)	13501(2)	8285(2)	47(2) *
C(1H)	-2022(4)	13921(3)	7593(3)	42(1)
C(2H)	-732(4)	13969(3)	7472(3)	41(1)
C(12H)	-3871(2)	14646(2)	7955(2)	68(3) *
C(13H)	-4544(2)	15105(2)	8353(2)	83(4) *
C(14H)	-4027(2)	15332(2)	8878(2)	74(3) *
C(15H)	-2836(2)	15099(2)	9005(2)	74(3) *
C(16H)	-2162(2)	14640(2)	8608(2)	59(3) *
C(11H)	-2680(2)	14413(2)	8083(2)	46(2) *
C(22H)	-2119(3)	12522(2)	7593(2)	57(2) *
C(23H)	-2148(3)	11665(2)	8002(2)	66(3) *
C(24H)	-2114(3)	11267(2)	8867(2)	70(3) *
C(25H)	-2051(3)	11725(2)	9322(2)	63(3) *
C(26H)	-2023(3)	12582(2)	8913(2)	56(3) *
C(21H)	-2057(3)	12980(2)	8047(2)	44(2) *
C(32H)	-1467(2)	15635(2)	6714(2)	50(2) *
C(33H)	-1244(2)	16440(2)	6402(2)	66(3) *
C(34H)	-129(2)	16503(2)	6463(2)	71(3) *
C(35H)	763(2)	15762(2)	6833(2)	71(3) *
C(36H)	540(2)	14958(2)	7146(2)	54(3) *
C(31H)	-575(2)	14894(2)	7086(2)	43(2) *
C(42H)	-386(3)	13997(1)	6043(2)	55(2) *
C(43H)	44(3)	13594(1)	5533(2)	67(3) *
C(44H)	653(3)	12732(1)	5885(2)	70(3) *
C(45H)	829(3)	12273(1)	6745(2)	63(3) *
C(46H)	400(3)	12676(1)	7255(2)	52(3) *
C(41H)	-209(3)	13538(1)	6903(2)	44(2) *
N(1C)	2647(4)	2114(4)	1560(3)	85(3) *
C(1C)	206(6)	4029(5)	1254(5)	110(5) *
C(2C)	1992(5)	2816(4)	1595(4)	77(4) *
C(3C)	899(5)	3210(4)	1210(4)	77(3) *
C(4C)	501(5)	2836(5)	776(4)	84(4) *
C(5C)	1152(6)	2109(5)	740(4)	82(4) *
C(6C)	2233(5)	1771(4)	1136(4)	83(4) *
C(7C)	729(8)	1680(5)	267(5)	134(6) *
N(1D)	2264(4)	2992(3)	8508(3)	79(3) *
C(1D)	4918(6)	1253(6)	8636(6)	139(6) *
C(2D)	3003(5)	2358(4)	8411(4)	76(3) *
C(3D)	4110(5)	2022(5)	8757(4)	87(4) *
C(4D)	4449(5)	2373(5)	9229(4)	90(4) *
C(5D)	3719(5)	3034(4)	9345(4)	76(4) *
C(6D)	2648(5)	3301(4)	8979(4)	82(4) *
C(7D)	4070(7)	3427(5)	9874(4)	113(5) *

Anisotropic atoms have thermal parameters ($Å^2 \times 10^3$) of the form :
$\exp[-2\pi^2(U_{11}h^2a^{*2} + U_{22}k^2b^{*2} + U_{33}l^2c^{*2} + 2U_{23}klb^*c^* + 2U_{13}hla^*c^* + 2U_{12}hka^*b^*)]$

Atom	U_{11}	U_{22}	U_{33}	U_{23}	U_{13}	U_{12}
O(1)	37(2)	62(2)	54(2)	-19(2)	-5(2)	-5(2)
O(2)	52(2)	57(2)	42(2)	-16(2)	-4(2)	-12(2)
C(12)	52(4)	74(4)	70(4)	-25(3)	10(3)	8(3)
C(13)	76(4)	81(5)	76(5)	-15(4)	29(4)	18(4)
C(14)	128(7)	62(4)	80(5)	-29(4)	40(5)	-7(4)
C(15)	153(7)	74(4)	65(4)	-42(4)	41(4)	-48(4)
C(16)	88(4)	57(3)	66(4)	-35(3)	26(3)	-23(3)
C(11)	70(4)	37(3)	45(3)	-13(2)	10(3)	-10(2)
C(22)	53(3)	78(4)	94(5)	-47(4)	9(3)	-25(3)
C(23)	76(4)	79(5)	149(7)	-66(5)	20(5)	-37(4)
C(24)	64(4)	58(4)	172(8)	-51(5)	42(5)	-27(3)
C(25)	62(4)	55(4)	99(5)	-10(4)	23(4)	-12(3)
C(26)	56(3)	48(3)	71(4)	-18(3)	12(3)	-13(3)
C(21)	40(3)	52(3)	72(4)	-30(3)	14(3)	-10(2)
C(32)	70(3)	44(3)	51(3)	-21(3)	14(3)	-13(3)

Table 4.10 ctd.

C(33)	93(5)	44(3)	64(4)	-24(3)	17(3)	-17(3)
C(34)	105(5)	57(4)	61(4)	-29(3)	24(3)	-39(4)
C(35)	76(4)	72(4)	71(4)	-35(3)	10(3)	-41(3)
C(36)	55(3)	64(3)	60(3)	-33(3)	4(3)	-19(3)
C(31)	60(3)	46(3)	43(3)	-25(2)	6(2)	-15(2)
C(42)	52(3)	45(3)	49(3)	-21(3)	8(2)	-18(2)
C(43)	62(3)	60(3)	51(3)	-27(3)	8(3)	-23(3)
C(44)	67(4)	64(4)	73(4)	-43(3)	14(3)	-21(3)
C(45)	59(3)	48(3)	82(4)	-35(3)	8(3)	-9(3)
C(46)	46(3)	43(3)	63(3)	-22(3)	0(3)	-9(2)
C(41)	31(2)	42(3)	52(3)	-21(3)	2(2)	-8(2)
N(1A)	84(4)	72(3)	69(4)	-15(3)	-17(3)	-29(3)
C(1A)	154(7)	95(5)	75(5)	-37(4)	13(5)	-20(5)
C(2A)	64(4)	51(3)	96(5)	-15(3)	-14(4)	-19(3)
C(3A)	71(4)	46(3)	90(5)	-20(3)	-26(4)	-7(3)
C(4A)	78(5)	54(4)	98(6)	-23(4)	-40(4)	-12(3)
C(5A)	72(4)	60(4)	108(6)	-32(4)	-7(4)	-21(3)
C(6A)	72(4)	71(4)	91(5)	-31(4)	-4(4)	-27(3)
C(7A)	66(5)	121(7)	211(10)	-76(7)	19(5)	-25(4)
N(1B)	60(3)	95(4)	118(5)	-46(4)	-18(3)	-6(3)
C(1B)	127(7)	77(5)	180(9)	-1(5)	-20(6)	-11(5)
C(2B)	58(4)	107(6)	106(6)	-46(5)	4(4)	-28(4)
C(3B)	58(4)	73(4)	94(5)	-24(4)	-4(4)	-3(3)
C(4B)	59(4)	95(5)	105(5)	-39(4)	-19(4)	-17(4)
C(5B)	54(4)	77(5)	130(6)	-51(4)	-3(4)	-10(3)
C(6B)	62(4)	73(4)	126(6)	-41(4)	-18(4)	-4(3)
C(7B)	109(6)	117(7)	251(12)	-99(7)	-28(7)	-37(5)
O(1H)	47(2)	54(2)	47(2)	-13(2)	-10(2)	-13(2)
O(2H)	40(2)	59(2)	39(2)	-18(2)	-2(2)	-10(2)
C(12H)	47(3)	71(4)	76(4)	-29(3)	3(3)	-2(3)
C(13H)	53(4)	86(4)	92(5)	-33(4)	10(3)	5(3)
C(14H)	73(4)	66(4)	73(4)	-28(3)	28(3)	-4(3)
C(15H)	87(5)	70(4)	80(4)	-43(3)	28(4)	-25(3)
C(16H)	55(3)	60(3)	69(4)	-33(3)	10(3)	-13(3)
C(11H)	36(3)	45(3)	51(3)	-14(2)	6(2)	-6(2)
C(22H)	47(3)	51(3)	71(4)	-21(3)	-5(3)	-12(2)
C(23H)	63(4)	55(3)	88(5)	-34(3)	-5(3)	-16(3)
C(24H)	56(3)	52(3)	89(5)	-18(4)	10(3)	-14(3)
C(25H)	59(3)	51(3)	61(4)	-11(3)	11(3)	-8(3)
C(26H)	53(3)	51(3)	58(4)	-17(3)	9(3)	-15(2)
C(21H)	34(3)	46(3)	56(3)	-23(3)	2(2)	-13(2)
C(32H)	52(3)	44(3)	58(3)	-22(3)	7(3)	-16(2)
C(33H)	65(4)	53(3)	72(4)	-21(3)	14(3)	-13(3)
C(34H)	79(4)	55(3)	84(4)	-28(3)	26(3)	-28(3)
C(35H)	60(4)	77(4)	97(5)	-47(4)	19(3)	-36(3)
C(36H)	42(3)	59(3)	69(4)	-30(3)	7(3)	-17(3)
C(31H)	46(3)	47(3)	41(3)	-21(2)	9(2)	-14(2)
C(42H)	61(3)	56(3)	52(4)	-24(3)	4(3)	-18(3)
C(43H)	80(4)	79(4)	57(4)	-38(3)	15(3)	-25(3)
C(44H)	83(4)	75(4)	80(5)	-55(4)	26(3)	-27(3)
C(45H)	59(3)	55(3)	86(5)	-43(3)	12(3)	-9(3)
C(46H)	46(3)	51(3)	58(3)	-24(3)	9(3)	-11(2)
C(41H)	41(3)	49(3)	49(3)	-24(3)	10(2)	-16(2)
N(1C)	72(4)	92(4)	89(4)	-33(3)	-22(3)	-19(3)
C(1C)	85(5)	115(6)	140(7)	-74(5)	14(5)	-8(4)
C(2C)	57(4)	84(4)	83(5)	-28(4)	-10(3)	-15(3)
C(3C)	53(4)	101(5)	76(4)	-31(4)	7(3)	-28(3)
C(4C)	59(4)	106(5)	79(5)	-28(4)	-10(3)	-24(4)
C(5C)	83(5)	93(5)	73(5)	-28(4)	-13(4)	-31(4)
C(6C)	75(4)	86(5)	73(5)	-25(4)	-16(4)	-3(4)
C(7C)	176(8)	122(6)	126(7)	-58(6)	-46(6)	-49(6)
N(1D)	54(3)	91(4)	91(4)	-40(3)	-15(3)	-7(3)
C(1D)	63(4)	182(9)	205(10)	140(8)	-3(5)	15(5)
C(2D)	46(4)	107(5)	79(4)	-43(4)	-2(3)	-18(3)
C(3D)	46(4)	131(6)	99(5)	-61(5)	5(3)	-22(4)
C(4D)	48(4)	134(6)	94(5)	-51(5)	-7(3)	-24(4)
C(5D)	65(4)	85(4)	74(4)	-26(4)	-4(3)	-24(4)
C(6D)	74(5)	81(4)	81(5)	-27(4)	-5(4)	-10(4)
C(7D)	143(7)	131(6)	85(5)	-50(5)	-13(5)	-57(5)

TABLE 4.11 Fractional atomic coordinates (x 10^4) and Thermal Parameters ($Å^2$ x 10^3) with e.s.d. s in parentheses for DINO

Atom	x/a	y/b	z/c	U_{iso}/U_{equiv}(*)
O(1)	1982(3)	2020(3)	6855(2)	50(1) *
O(2)	-1003(3)	3396(2)	8259(2)	48(1) *
C(1)	1100(4)	2071(3)	7643(2)	39(2) *
C(2)	-106(4)	3357(3)	7472(2)	41(2) *
C(11)	231(4)	1011(3)	8026(2)	44(2) *
C(12)	-399(4)	658(3)	8863(2)	47(2) *
C(13)	-1213(5)	-266(4)	9207(3)	61(2) *
C(14)	-1408(5)	-894(4)	8731(4)	71(3) *
C(15)	-798(5)	-578(4)	7907(4)	74(3) *
C(16)	11(5)	373(4)	7554(3)	58(2) *
C(21)	2205(4)	1932(3)	8205(2)	45(2) *
C(22)	2051(5)	2742(4)	8647(2)	55(2) *
C(23)	3155(6)	2557(5)	9111(3)	70(3) *
C(24)	4389(5)	1577(5)	9149(3)	74(3) *
C(25)	4535(5)	759(5)	8730(3)	77(3) *
C(26)	3448(5)	930(4)	8265(3)	61(2) *
C(31)	-1149(4)	3371(3)	6917(2)	40(2) *
C(32)	-2555(4)	3019(4)	7264(3)	54(2) *
C(33)	-3500(5)	3030(4)	6763(3)	70(3) *
C(34)	-3044(6)	3385(4)	5926(3)	70(3) *
C(35)	-1658(5)	3727(4)	5578(3)	60(2) *
C(36)	-696(4)	3723(3)	6065(2)	48(2) *
C(41)	630(4)	4508(3)	7076(2)	44(2) *
C(42)	2191(5)	4496(4)	6748(2)	53(2) *
C(43)	2721(6)	5580(5)	6427(3)	68(3) *
C(44)	1736(7)	6720(5)	6409(3)	74(3) *
C(45)	177(6)	6758(4)	6718(3)	70(3) *
C(46)	-370(5)	5666(4)	7046(3)	58(2) *
N(1A)	5633(6)	111(5)	3412(3)	88(3) *
C(1A)	2015(11)	435(11)	5030(6)	213(8) *
C(2A)	4403(9)	-176(7)	3957(4)	113(4) *
C(3A)	3310(7)	736(6)	4388(4)	89(3) *
C(4A)	3722(6)	1824(6)	4145(3)	77(3) *
C(5A)	4949(8)	2124(6)	3538(5)	108(4) *
C(6A)	5838(8)	1241(7)	3222(5)	121(5) *
C(7A)	2870(10)	2873(8)	4526(5)	152(5) *
N(1B)	6249(4)	5193(4)	8473(3)	74(2) *
C(1B)	1921(6)	6107(6)	8683(4)	99(3) *
C(2B)	4791(5)	5296(4)	8434(3)	67(2) *
C(3B)	3527(5)	6057(4)	8779(3)	60(2) *
C(4B)	3797(5)	6761(4)	9195(3)	64(2) *
C(5B)	5303(6)	6664(5)	9227(3)	86(3) *
C(6B)	6481(6)	5876(5)	8874(4)	86(3) *
C(7B)	2487(7)	7615(6)	9591(4)	102(3) *

Anisotropic atoms have thermal parameters ($Å^2$ x 10^3) of the form :
$\exp[-2\pi^2(U_{11}h^2a^{*2} + U_{22}k^2b^{*2} + U_{33}l^2c^{*2} + 2U_{23}klb^*c^* + 2U_{13}hla^*c^* + 2U_{12}hka^*b^*)]$

Atom	U_{11}	U_{22}	U_{33}	U_{23}	U_{13}	U_{12}
O(1)	44(2)	56(2)	45(2)	-19(1)	-7(1)	3(1)
O(2)	43(2)	53(2)	41(2)	-17(1)	-8(1)	5(1)
C(1)	34(2)	47(2)	36(2)	-15(2)	-9(2)	0(2)
C(2)	38(2)	48(2)	36(2)	-15(2)	-11(2)	0(2)
C(11)	34(2)	42(2)	52(3)	-14(2)	-14(2)	4(2)
C(12)	35(2)	44(2)	56(3)	-8(2)	-12(2)	-3(2)
C(13)	40(2)	60(3)	70(3)	-5(2)	-11(2)	-5(2)
C(14)	47(3)	57(3)	104(5)	-12(3)	-17(3)	-12(2)
C(15)	66(3)	64(3)	111(5)	-45(3)	-25(3)	-9(3)
C(16)	56(3)	59(3)	66(3)	-28(2)	-14(2)	-5(2)
C(21)	39(2)	51(2)	42(2)	-5(2)	-13(2)	-6(2)
C(22)	59(3)	59(3)	54(3)	-10(2)	-27(2)	-10(2)
C(23)	84(3)	74(3)	66(3)	-8(2)	-39(3)	-28(3)
C(24)	56(3)	101(4)	66(3)	-4(3)	-33(3)	-21(3)

Table 4.11 ctd.

C(25)	44(3)	98(4)	73(4)	-10(3)	-24(3)	6(3)
C(26)	44(2)	69(3)	61(3)	-16(2)	-21(2)	7(2)
C(31)	34(2)	43(2)	44(2)	-12(2)	-11(2)	-3(2)
C(32)	41(2)	68(3)	49(3)	-14(2)	-10(2)	-5(2)
C(33)	48(3)	86(4)	79(4)	-12(3)	-22(3)	-18(2)
C(34)	70(3)	82(3)	74(4)	-19(3)	-39(3)	-17(3)
C(35)	72(3)	69(3)	49(3)	-13(2)	-26(2)	-17(2)
C(36)	47(2)	54(2)	45(3)	-15(2)	-11(2)	-10(2)
C(41)	50(2)	47(2)	39(2)	-11(2)	-19(2)	-7(2)
C(42)	50(3)	58(3)	54(3)	-9(2)	-17(2)	-14(2)
C(43)	66(3)	79(4)	65(3)	-7(3)	-23(3)	-29(3)
C(44)	97(4)	68(3)	72(3)	-5(3)	-35(3)	-39(3)
C(45)	99(4)	45(3)	75(3)	-16(2)	-36(3)	-11(3)
C(46)	66(3)	50(3)	61(3)	-19(2)	-22(2)	-3(2)
N(1A)	90(3)	77(3)	99(4)	-43(3)	-14(3)	0(3)
C(1A)	155(9)	290(13)	119(7)	75(8)	-39(7)	-90(8)
C(2A)	110(5)	109(5)	106(5)	-11(4)	-33(5)	-13(4)
C(3A)	95(4)	84(4)	77(4)	-2(3)	-37(4)	-10(4)
C(4A)	51(3)	115(5)	62(3)	-34(3)	-16(3)	4(3)
C(5A)	103(5)	97(5)	138(6)	-47(4)	-46(5)	-3(4)
C(6A)	118(5)	91(5)	166(7)	-52(5)	-52(5)	5(4)
C(7A)	175(8)	131(6)	174(8)	-97(6)	-87(7)	47(5)
N(1B)	59(3)	82(3)	73(3)	-34(2)	-8(2)	9(2)
C(1B)	66(3)	104(4)	136(5)	-45(4)	-31(4)	-8(3)
C(2B)	61(3)	63(3)	70(3)	-20(2)	-13(3)	2(2)
C(3B)	51(3)	59(3)	60(3)	-13(2)	-16(2)	2(2)
C(4B)	63(3)	70(3)	56(3)	-26(2)	-19(2)	9(2)
C(5B)	66(3)	112(4)	95(4)	-58(4)	-29(3)	6(3)
C(6B)	60(3)	109(4)	97(4)	-53(4)	-25(3)	8(3)
C(7B)	84(4)	115(5)	105(5)	-68(4)	-16(3)	26(3)

TABLE 4.12 Fractional atomic coordinates (x 10^4)
and Thermal Parameters ($Å^2$ x 10^3)
with e.s.d. s in parentheses for PEACH

Atom	x/a	y/b	z/c	U_{iso}/U_{equiv}(*)
O(1)	817(2)	8653(1)	1870(1)	47(1) *
O(2)	-267(2)	7455(1)	3674(1)	53(1) *
C(1)	201(2)	8514(1)	2705(1)	39(1) *
C(2)	251(2)	7641(1)	2812(2)	43(1) *
C(11)	1162(2)	8848(1)	3577(2)	41(1) *
C(12)	2631(3)	8992(1)	3571(2)	50(1) *
C(13)	3520(3)	9262(1)	4365(2)	62(1) *
C(14)	2966(3)	9390(2)	5187(2)	67(1) *
C(15)	1500(3)	9264(1)	5205(2)	63(1) *
C(16)	600(3)	9002(1)	4405(2)	50(1) *
C(21)	-1333(2)	8861(1)	2597(1)	41(1) *
C(22)	-1421(3)	9617(1)	2444(2)	52(1) *
C(23)	-2741(3)	9987(1)	2340(2)	60(1) *
C(24)	-4013(3)	9604(2)	2376(2)	69(1) *
C(25)	-3948(3)	8856(2)	2529(2)	73(1) *
C(26)	-2619(3)	8486(1)	2647(2)	56(1) *
C(31)	-751(2)	7218(1)	2026(2)	44(1) *
C(32)	-1259(3)	7490(1)	1123(2)	54(1) *
C(33)	-2165(3)	7068(2)	464(2)	66(1) *
C(34)	-2544(3)	6366(2)	691(2)	72(1) *
C(35)	-2008(3)	6082(2)	1574(2)	73(1) *
C(36)	-1127(3)	6506(1)	2238(2)	58(1) *
C(41)	1832(3)	7368(1)	2848(2)	49(1) *
C(42)	2429(3)	7259(1)	2030(2)	60(1) *
C(43)	3865(3)	7030(2)	2069(3)	76(1) *
C(44)	4732(3)	6910(2)	2930(3)	83(2) *
C(45)	4173(3)	7014(2)	3746(3)	82(1) *

Table 4.12 ctd.

C(46)	2726(3)	7239(1)	3714(2)	65(1) *
O(1G)	1465(4)	10046(1)	1275(2)	126(1) *
C(1G)	2090(4)	10060(2)	613(2)	68(1) *
C(2G)	2500(7)	9377(2)	184(3)	126(2) *
C(3G)	2433(6)	10771(2)	208(3)	112(2) *

Anisotropic atoms have thermal parameters ($Å^2 \times 10^3$) of the form :
$\exp[-2\pi^2(U_{11}h^2a^{*2} + U_{22}k^2b^{*2} + U_{33}l^2c^{*2} + 2U_{23}klb^*c^* + 2U_{13}hla^*c^* + 2U_{12}hka^*b^*)]$

Atom	U_{11}	U_{22}	U_{33}	U_{23}	U_{13}	U_{12}
O(1)	59(1)	39(1)	49(1)	0(1)	24(1)	-1(1)
O(2)	70(1)	45(1)	47(1)	5(1)	17(1)	-7(1)
C(1)	42(1)	36(1)	42(1)	0(1)	14(1)	-1(1)
C(2)	47(1)	37(1)	45(1)	1(1)	11(1)	-1(1)
C(11)	41(1)	32(1)	51(1)	0(1)	9(1)	0(1)
C(12)	45(1)	41(1)	66(2)	0(1)	10(1)	0(1)
C(13)	47(1)	54(2)	81(2)	6(1)	-4(1)	-6(1)
C(14)	72(2)	56(2)	66(2)	0(1)	-12(2)	-6(1)
C(15)	80(2)	58(2)	49(1)	-4(1)	7(1)	-1(1)
C(16)	50(1)	49(1)	51(1)	-5(1)	12(1)	-2(1)
C(21)	45(1)	42(1)	38(1)	-3(1)	9(1)	1(1)
C(22)	59(2)	45(1)	52(1)	0(1)	11(1)	4(1)
C(23)	69(2)	55(2)	56(2)	-1(1)	8(1)	21(1)
C(24)	52(2)	81(2)	73(2)	-10(2)	8(1)	19(2)
C(25)	45(2)	78(2)	101(2)	-15(2)	23(1)	0(1)
C(26)	49(1)	50(1)	74(2)	-5(1)	24(1)	0(1)
C(31)	42(1)	38(1)	54(1)	-4(1)	12(1)	2(1)
C(32)	58(2)	51(1)	54(1)	-5(1)	6(1)	0(1)
C(33)	65(2)	72(2)	57(2)	-12(1)	1(1)	6(1)
C(34)	57(2)	69(2)	86(2)	-27(2)	5(2)	-11(1)
C(35)	73(2)	50(2)	97(2)	-12(2)	14(2)	-17(1)
C(36)	62(2)	41(1)	72(2)	-2(1)	14(1)	-5(1)
C(41)	48(1)	29(1)	68(2)	-2(1)	8(1)	-1(1)
C(42)	55(2)	49(1)	78(2)	-8(1)	16(1)	0(1)
C(43)	58(2)	60(2)	116(3)	-13(2)	33(2)	0(1)
C(44)	45(2)	56(2)	147(3)	1(2)	10(2)	6(1)
C(45)	64(2)	56(2)	116(3)	12(2)	-10(2)	7(1)
C(46)	64(2)	49(2)	78(2)	8(1)	-2(1)	5(1)
O(1G)	228(3)	53(1)	125(2)	-2(1)	115(2)	-12(2)
C(1G)	91(2)	62(2)	54(2)	5(1)	23(2)	-8(2)
C(2G)	201(5)	86(3)	116(3)	2(2)	98(4)	15(3)
C(3G)	172(4)	82(3)	86(2)	12(2)	32(3)	-48(3)

References.

4.1. W. C. Hamilton. *Acta Crystallogr.*, **18**, 502, (1965).

4.2. J. A. Ibers; W. C. Hamilton (Eds.) *International Tables for Crystallography. Volume IV*, The Knyoch Press, Birmingham. 285, (1974).

4.3. W. L. Duax; D. A. Norton (Eds.) *Atlas of Steroid Structure, Volume I*, Plenum Press, London, Chapter 2, (1975).

4.4. F. Toda; K. Tanaka; Y. Wang; G-H. Lee. *Chem lett.* 109, (1986).

4.5. H. Hart; L-T. Lin; D. L. Ward. *J. Am. Chem. Soc.* **106**, 4043, (1984).

CHAPTER 5 : CRYSTAL AND MOLECULAR STRUCTURE - CLASSES B AND C.

The host to guest ratios, space group and cell parameters are summarised at the beginning of the discussion about each structure. Fractional atomic coordinates, thermal parameters and details of hydrogen bonding are given in Tables 5.1 - 5.6 at the end of this chapter.

Class B.

The atom labelling scheme used for the host, triphenylmethanol, is given in Figure 5.1. The labelling used for the guest is shown at the beginning of the discussion about the structure. The geometry of the host is discussed in detail at the end of this chapter.

W1DIOX : $(C_{19}H_{16}O)$. dioxane

Space group : $P\bar{1}$	H : G = 1 :1
a = 8.441(8)Å	α = 67.47(1)°
b = 10.544(2)Å	β = 83.96(5)°
c = 11.562(2)Å	γ = 89.08(5)°
Z = 2	

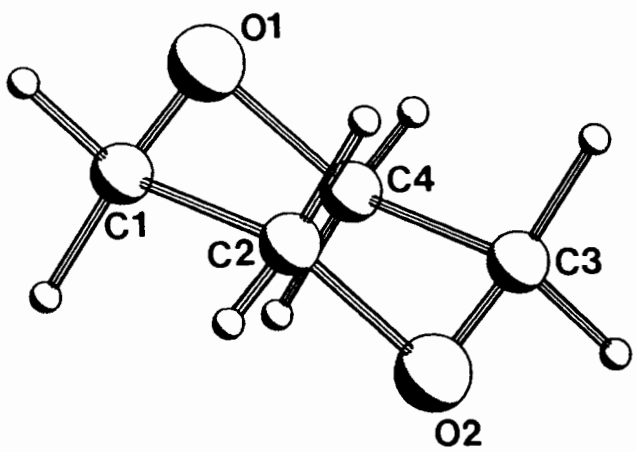

Solution and refinement of this structure were routine. The guest was well-ordered; hydrogens were fixed at 1.00Å from their parent carbons. The hydroxyl hydrogen was located in the difference electron density map. It was fixed at appropriate distances[5.1] from O(1) and O(1G) and assigned its own isotropic temperature factor. The maximum shift/e.s.d. in the final cycle was 0.001 and the highest and lowest features on the final difference electron density map were 0.21 and -0.35 eÅ^{-3} which were deemed satisfactory. Final coordinates and thermal parameters are listed in Table 5.2.

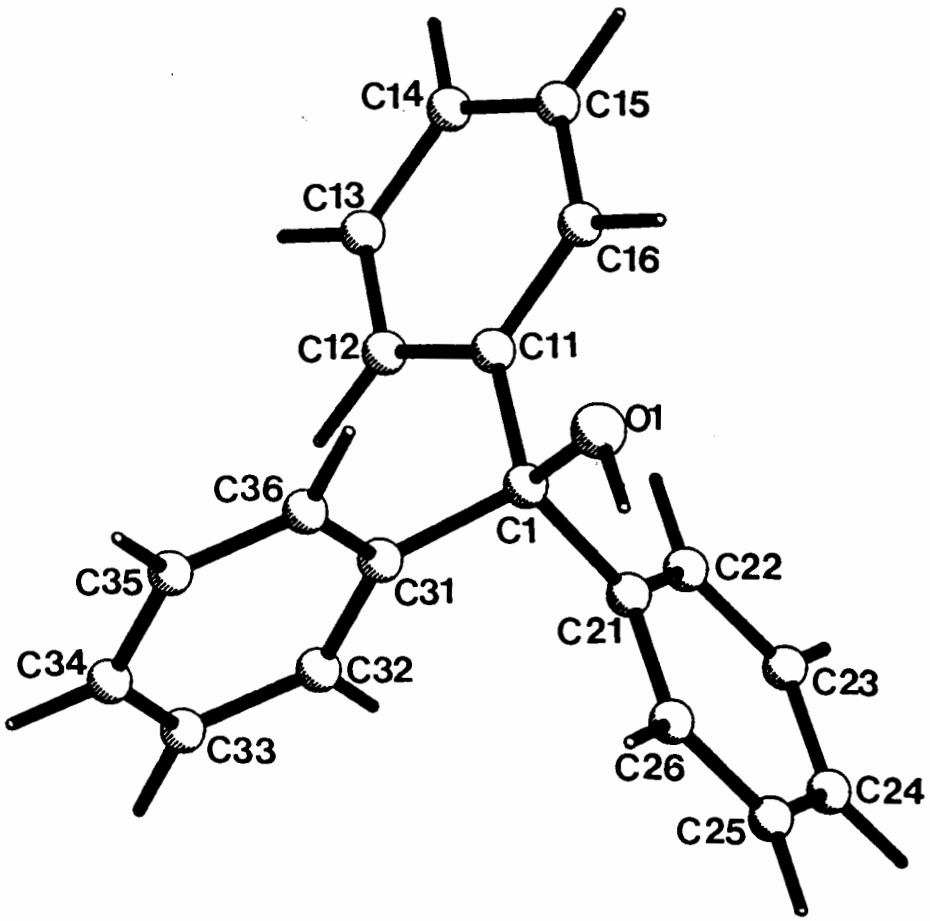

Figure 5.1. Atom labelling scheme for triphenylmethanol (Class B).

Molecular structure.

The molecular packing for this structure is illustrated in Figure 5.2. Two dioxane molecules are located in a centrosymmetric cavity, centred at (½ ½ 0), Wyckoff position *e*. Only one of the oxygens of each dioxane acts as an acceptor in a hydrogen bond with the host. The oxygen at the other end of the molecule is sited in a pocket created by the phenyl substituents of neighbouring host molecules. The asymmetry parameters for the guest ring confirmed the presence of three mirror planes and three 2-fold axes, thus identifying the conformation as a chair.

Inclusion compounds of triphenylmethanol with methanol(1:1), dmso(2:1) and acetone(2:1) have been reported.[5.2] In each case the mode of hydrogen bonding is different, testifying to the versatility of this host's packing.

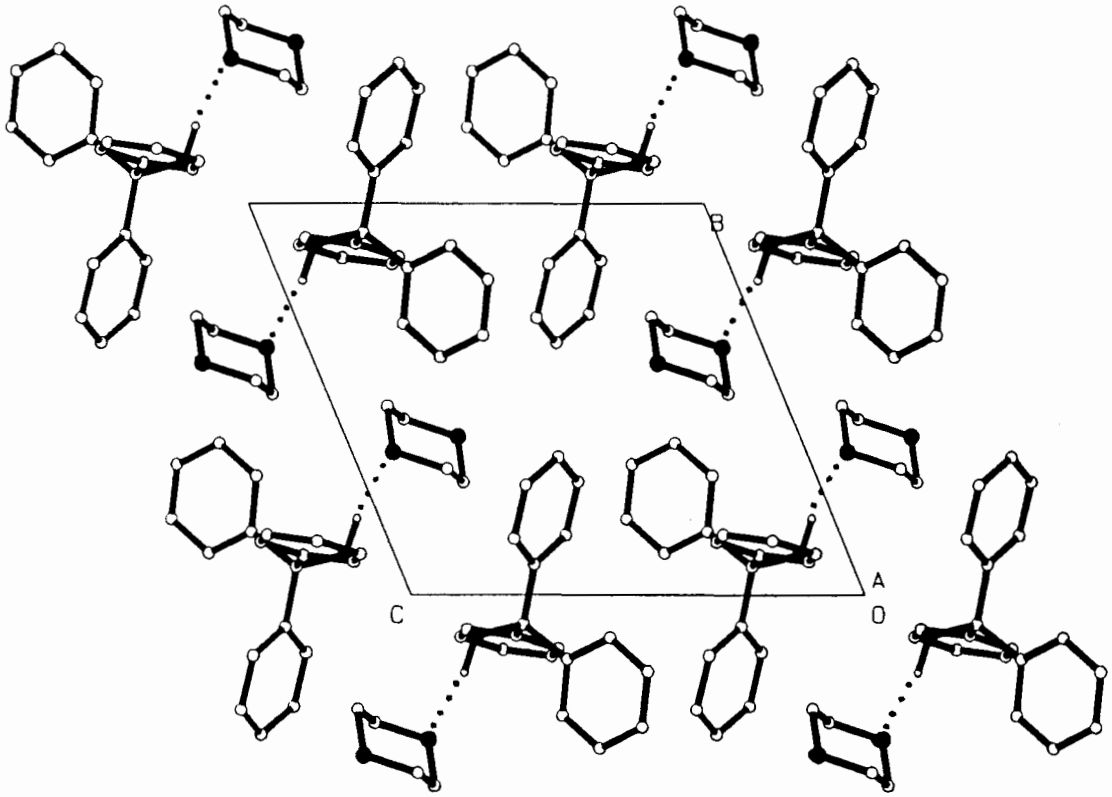

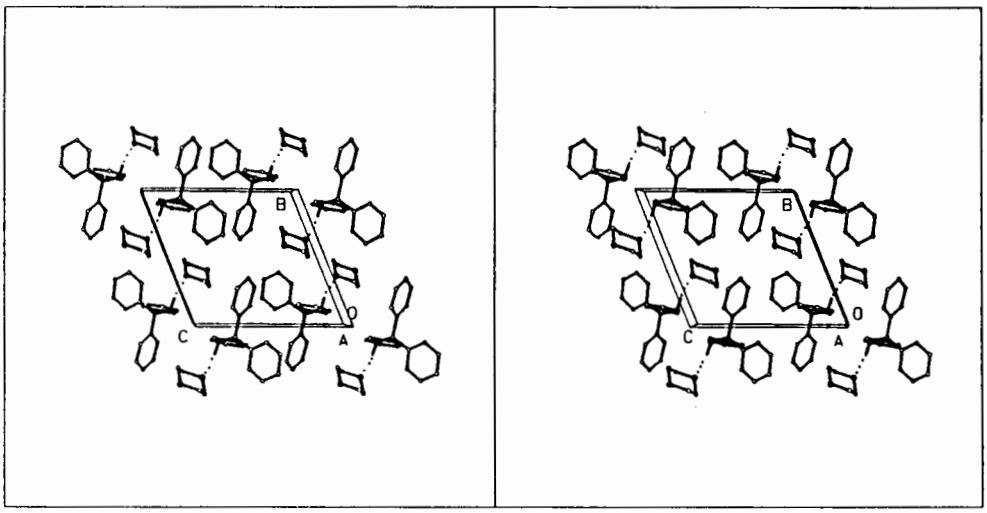

Figure 5.2. Packing diagram of **W1DIOX** viewd along [100].

Class C.

The atom labelling scheme used for the host, triphenylsilanol, is shown in Figure 5.3. The labelling used for the guest is shown at the beginning of the discussion about each compound. The geometry of the host is discussed in detail at the end of this chapter.

WEB2: $C_{18}H_{16}OSi$

Space group : $P\bar{1}$

a = 15.235(5)Å	α = 108.76(6)°
b = 19.983(13)Å	β = 103.47(5)°
c = 23.250(18)Å	γ = 101.17(5)°

Z = 16

Crystals of triphenylsilanol were grown from 1-propanol in an attempt to make a 1-propanol complex. Density measurements however, showed that no propanol had been included. This was confirmed by NMR which showed that the crystals were those of the non-porous α-phase.

There were eight molecules in the asymmetric unit, *i.e.* 160 non-hydrogen atoms. This made the refinement difficult - the computer files were large and any refinement of the model took a relatively large amount of CPU time.

Large-block least-squares refinement was necessary as the number of parameters exceeded the maximum that SHELX76 could refine in a single cycle. All 160 non-hydrogen atoms were refined anisotropically (final R = 0.082) but no hydrogens could be included as SHELX76 includes a constraint that

$$N(\text{anisotropic atoms}) + 2N(\text{isotropic atoms}) < 400.$$

The alternative, to place hydrogens appropriately and refine all carbons isotropically, and silicon and oxygen atoms anisotropically, yielded an R-factor of 0.15 and several peaks of high (> 1eÅ^{-3}) electron density.

A Hamilton test[5.3] on these two models (at equivalent stages of refinement) confirmed, at the 95% confidence level, that the first model was significantly better. The final model adopted therefore was that which involved anisotropic treatment of all atoms, and the omission of hydrogens.

Hydrogen bonds were inferred from the short O···O distances (Table 5.1) although the hydroxyl hydrogens could not be located. Even a close examination of the electron density in the region of the oxygens did not reveal any peaks attributable to hydrogens.

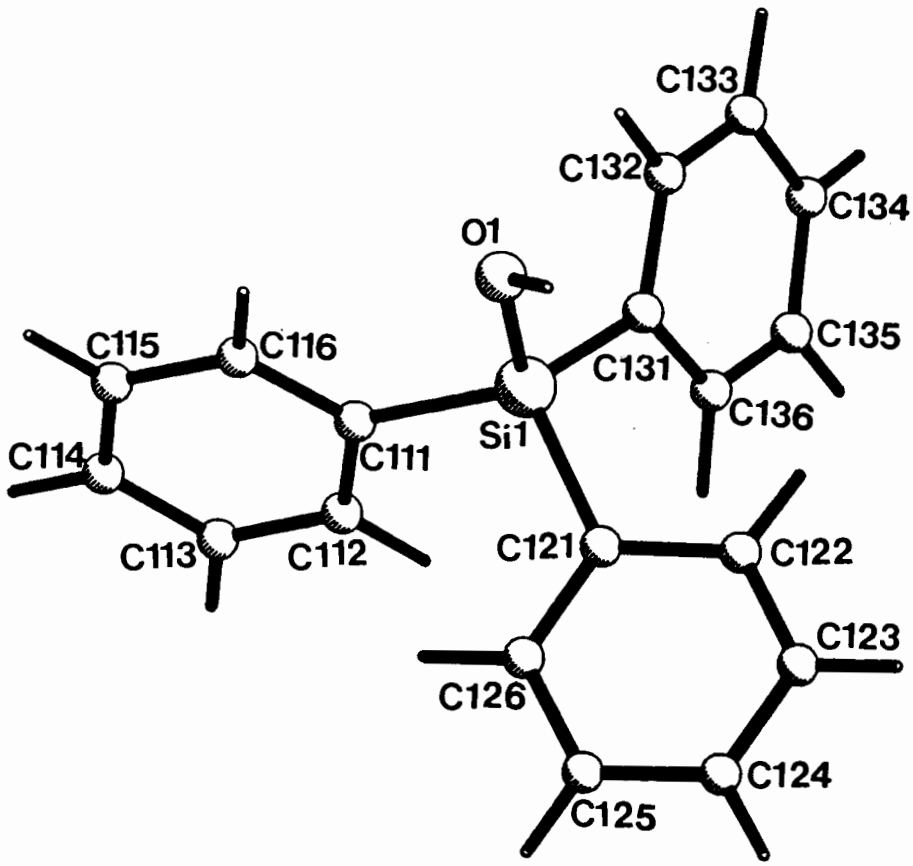

Figure 5.3. Atom labelling scheme for triphenylsilanol (Class C).

The maximum shift/e.s.d. in the final cycle of refinement was 0.075 and the electron density map showed no feature greater than 0.37 eÅ^{-3} or less than -0.40 eÅ^{-3}. Final coordinates and thermal parameters are listed in Table 5.3.

This structure had been solved previously.[5.4] All atoms were refined isotropically and no hydrogens were located. The parameters were refined to R = 0.122. Consistently higher standard deviations were reported for fractional atomic coordinates, bond lengths and bond angles, and it was therefore deemed worthwhile to report this improved structure.

Molecular structure.

The asymmetric unit contains two tetrameric clusters in which the four oxygen atoms lie at the apices of a tetrahedron while the phenyl rings point outwards. One unit is drawn in Figure 5.4. The molecules are held in these units by strong hydrogen bonds, indicated by dotted lines.

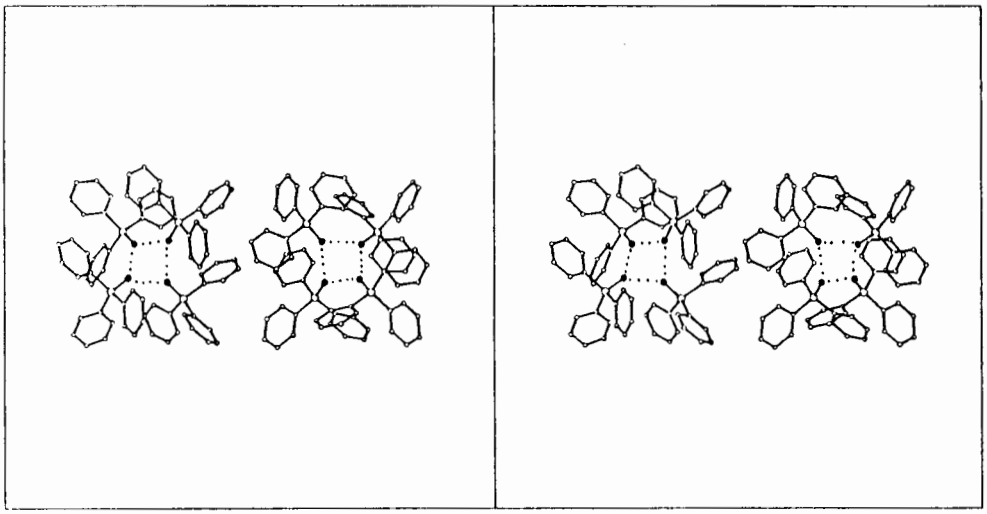

Figure 5.4. Asymmetric unit of **WEB2**. Oxygens are shaded and H-bonds shown as dotted lines.

Table 5.1 lists the eight intermolecular O···O contacts which vary between 2.639(6) and 2.684(6) Å. The existence of a hydrogen bond can only be confirmed if the hydrogen involved is located.[5.1] However, if the van der Waals radius of oxygen is taken as 1.4 Å [5.5], hydrogen as 1.0 Å [5.6] and a covalent O-H distance as approximately 1.0 Å, any O···O distance less than 3.4Å may be considered to be a hydrogen bond, provided that the presence of a hydrogen atom is known.

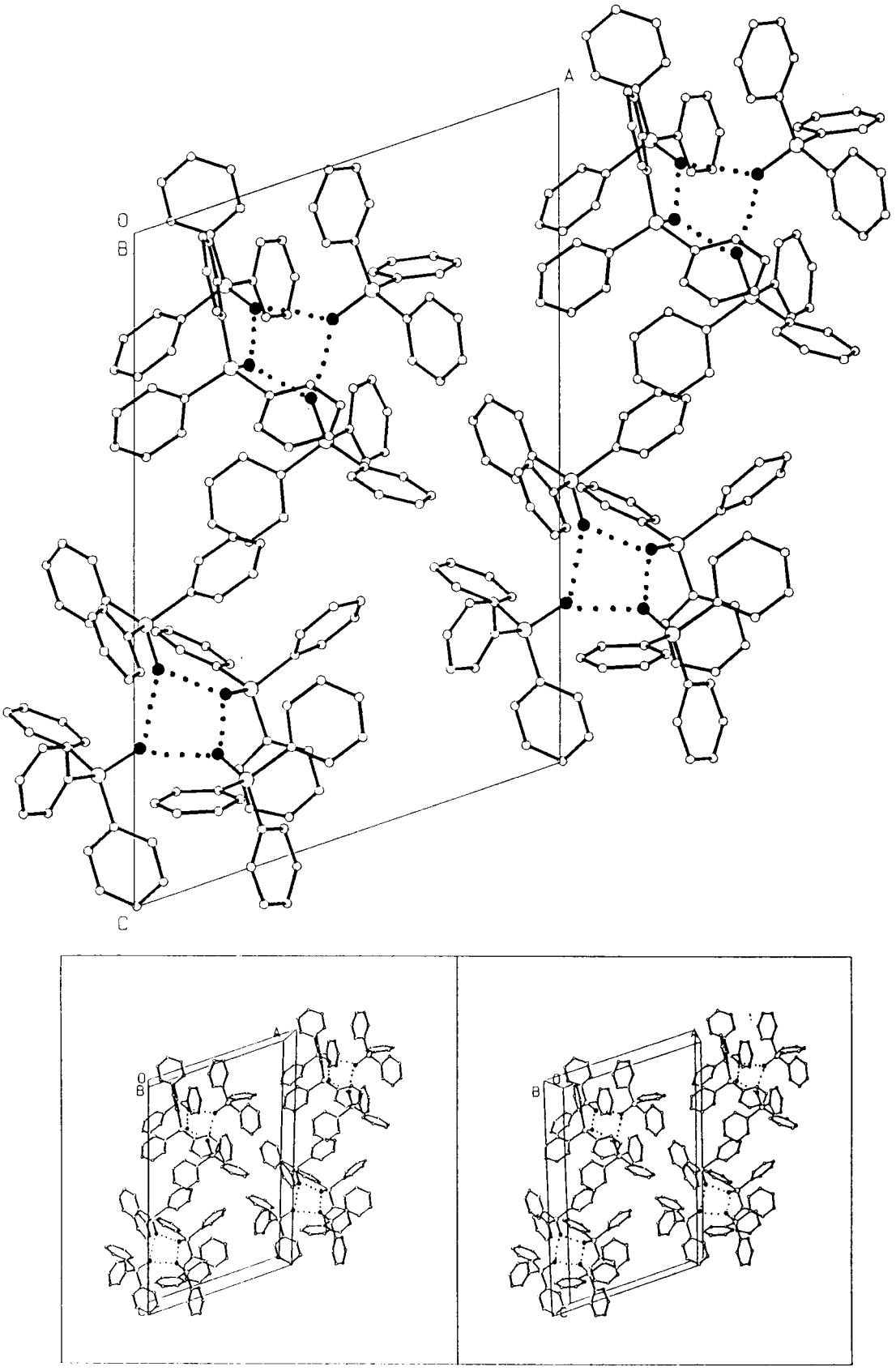

Figure 5.5. Packing diagram of **WEB2** viewed along [010]. H-bonds are indicated by dotted lines and oxygen atoms are shaded.

The occurrence of hydrogen bonding in this structure, in the absence of definite hydrogen atom positions, was confirmed by infrared spectroscopy. The appearance of a broad band at 3250 cm^{-1} indicates strong hydrogen bonding between hydroxyl groups.[5.7]

The crystal packing is shown in Figure 5.5. The tetramer of oxygens is apparently the dominating force in the packing; no phenyl-phenyl interactions are observed.

TRIPSID: $(C_{18}H_{16}OSi)_2$. dmso

Space group : $P\bar{1}$	H : G = 2 : 1
a = 8.681(4)Å	α = 95.97(2)°
b = 9.550(2)Å	β = 90.06(3)°
c = 24.104(4)Å	γ = 117.03(2)°
Z = 2	

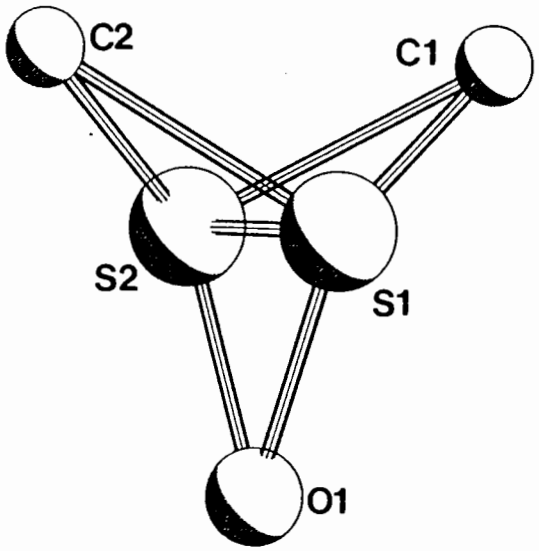

The density measured for this compound indicated a 2:1 ratio of host to guest. This was observed on solving the structure. The guest lies at approximately the same distance from two host molecules and its oxygen acts as a hydrogen bond acceptor to both.

The two hosts were placed in general positions and were well-ordered. Silicon, oxygen and carbon atoms were refined anisotropically and the hydroxyl hydrogens were found and refined as described previously. The aromatic hydrogens of each host were linked by a common temperature factor.

The guest dmso molecule was readily located and refined. Its sulphur atom was disordered over two positions; each was modelled with a site occupancy factor of 0.50. All non-hydrogen atoms were treated anisotropically and hydrogens were geometrically

placed on the methyl carbons. These carbons had high temperature factors (U_{equiv} approx. 0.12 Å^2) owing to the high degree of vibration. Methyl hydrogens are particularly prone to a large amount of thermal motion, resulting in very high temperature factors. U_{iso} for the methyl hydrogens was therefore fixed at a value slightly higher than that of the parent carbons. The final maximum shift/e.s.d. was 0.002 and the maximum and minimum heights in the electron density map were 0.22 and -0.24 eÅ^{-3}. Final coordinates and thermal parameters are listed in Table 5.4.

Molecular structure.

The asymmetric unit of **TRIPSID** is given in Figure 5.6, showing the dmso oxygen acting as a hydrogen bond acceptor to both host hydroxyls. Figure 5.6 also illustrates the disorder observed in the dmso. This is of a similar form to that displayed by two of the guest molecules in **DEMPE**. Bond lengths and angles (apart from the disorder) fell within normal ranges for a dmso molecule.

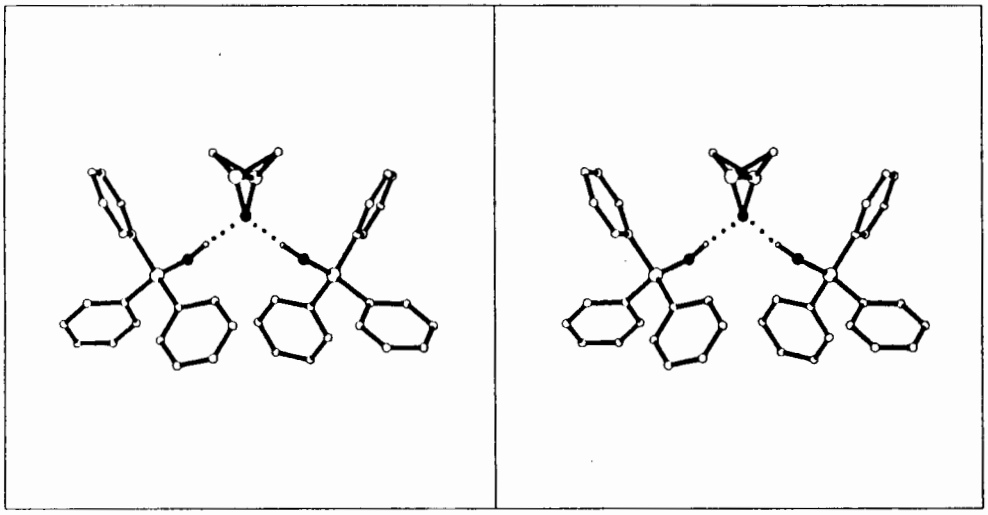

Figure 5.6. Molecular structure of **TRIPSID.**

The dmso lies in a cavity centred at approximately (¾ ½ ¼) as can be seen in Figure 5.7. The guest's oxygen is rigidly held in place by the hydrogen bonding scheme, but the remainder of the molecule has far greater freedom of motion reflected by the higher temperature factors observed for these atoms.

Figure 5.8 shows more clearly the cavity-like nature of the structure as well as the close fit of the guest into the available space.

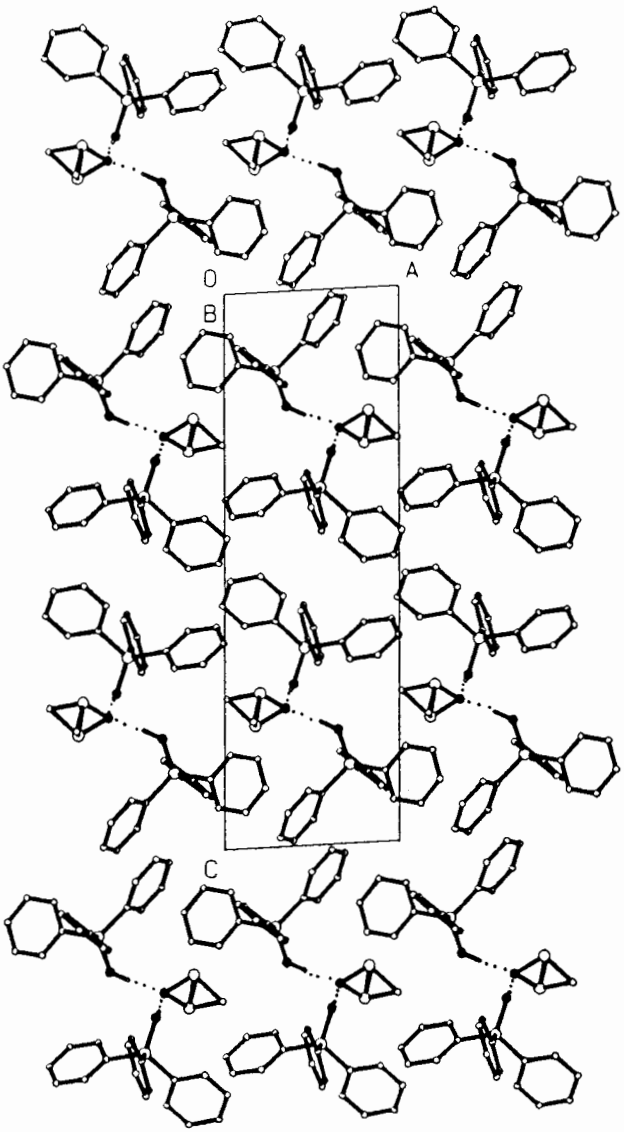

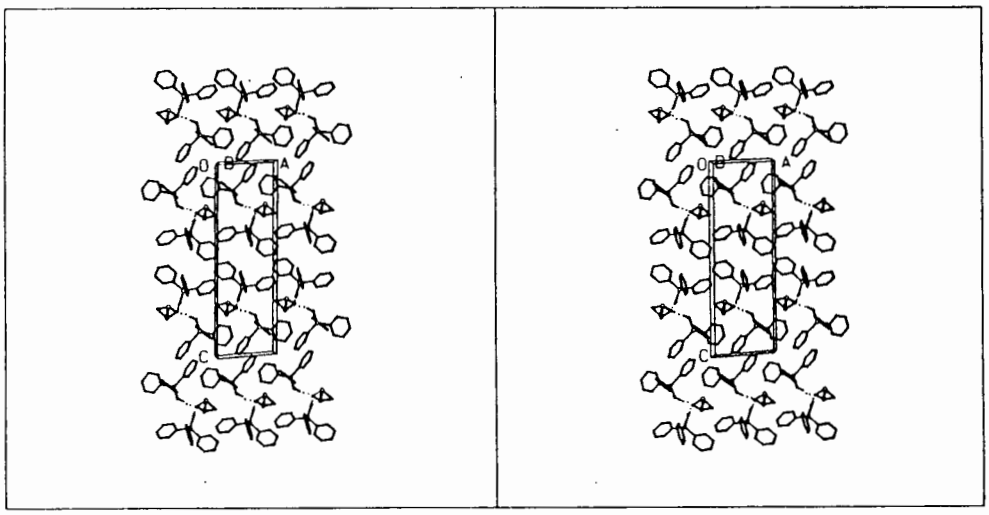

Figure 5.7. Packing diagram of **TRIPSID** viewed along [010].

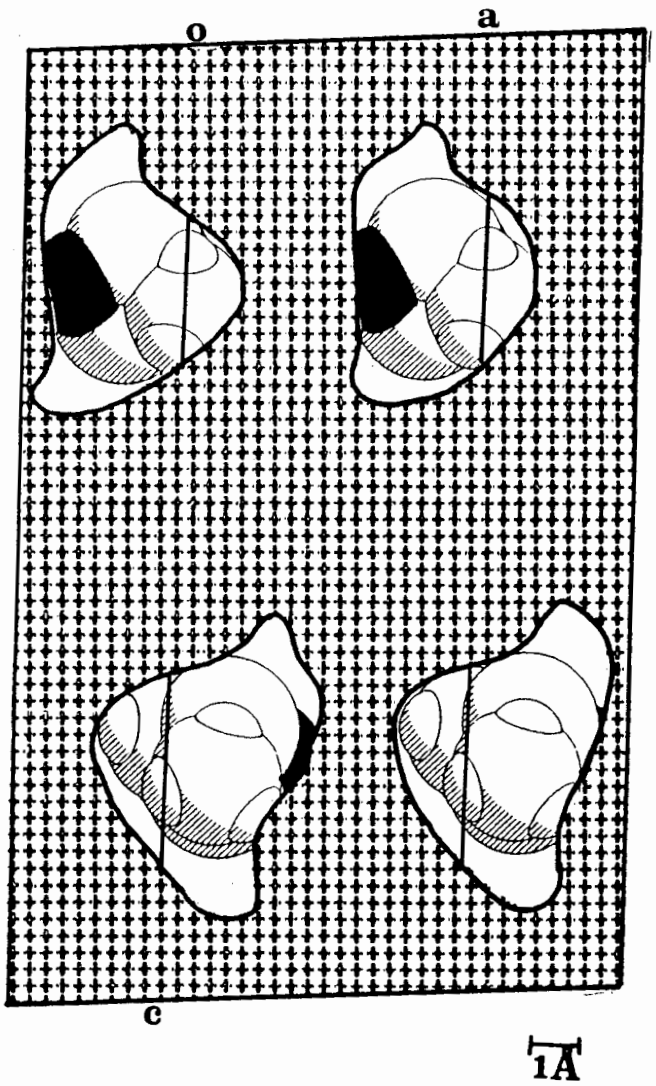

Figure 5.8. TRIPSID : cross-section of unit cell at y = ½. The cavity-like nature of the compound is clear.

BASIL : $(C_{18}H_{16}OSi)_4$. (dioxane)

Space group : $P\bar{1}$	H : G = 4 : 1
a = 9.378(7)Å	α = 87.85(1)°
b = 11.851(2)Å	β = 81.05(1)°
c = 14.891(2)Å	γ = 87.65(1)°
Z = 1	

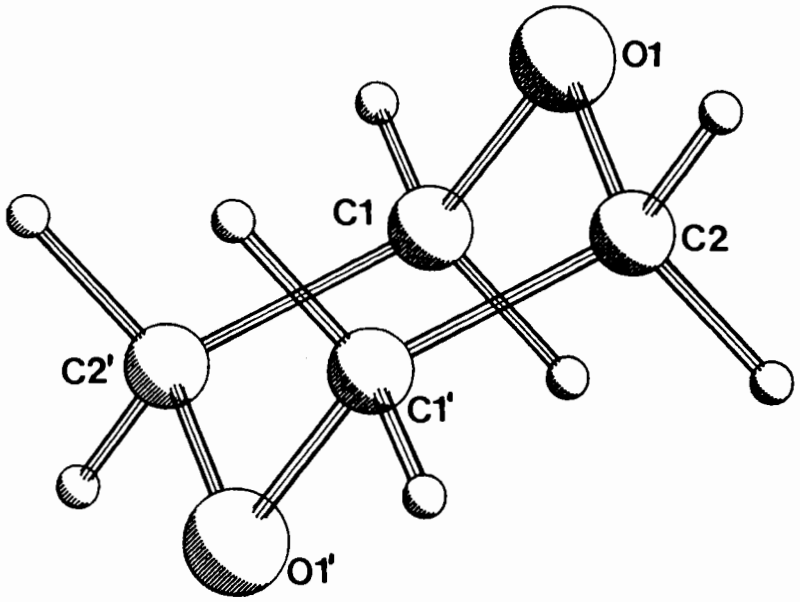

There are four hosts and one guest in the cell, and the guest was located at a centre of inversion.

The structure solution and refinement were quite routine; the guest was found to adopt a chair conformation about the centre of inversion at (½ 0 ½), (Wyckoff position *f*). The guest oxygen atom, in each asymmetric unit, acts as a hydrogen bond acceptor to the hydroxyl of one host molecule which, in turn, is an acceptor to the hydroxyl of the other host.

With all non-hydrogens refined anisotropically, and hydrogens treated in the usual manner, the structure converged to an R-factor of 0.041, with maximum and minimum residual electron densities of 0.30 and -0.24 $eÅ^{-3}$. Final coordinates and thermal parameters are listed in Table 5.5.

Molecular structure.

Dioxane disrupts the cyclic hydrogen bonding found in the α-phase (**WEB2**) although not in the same manner as does dmso (**TRIPSID**). This may be because the oxygen of dmso is more exposed (hence more accessible) than those of dioxane, allowing it to accept two hydrogen bonds. The molecular structure found in **BASIL** is shown in Figure 5.9 which shows a dioxane molecule surrounded by four host molecules.

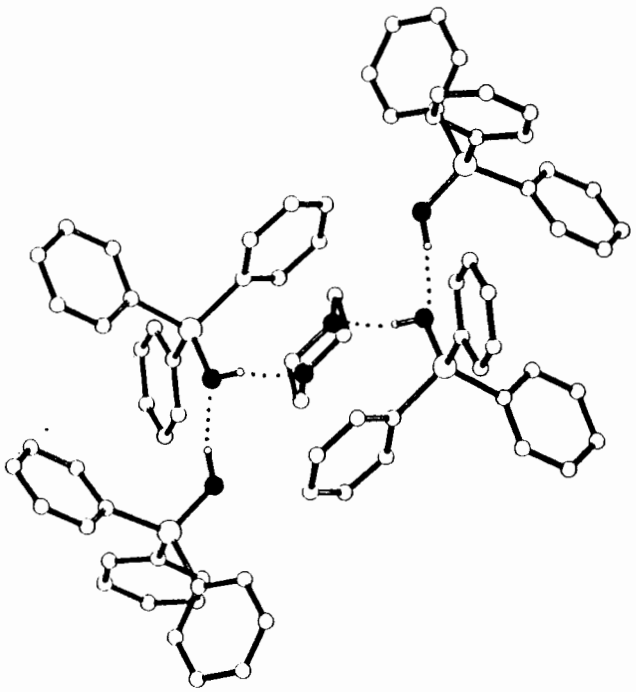

Figure 5.9. Molecular structure of **BASIL**. The dioxane molecule is located on a centre of inversion.

Figure 5.10, a packing diagram down [1 0 0], shows how the hydrogen bonding dictates the packing as there do not appear to be any π - π interactions between the hosts' phenyl groups.

OPEC analysis of the unit cell established that the guest is held within a hydrophilic cavity formed by the hosts' hydroxy moieties. The approximate dimensions of the cavity are 7.5Å (in the x-direction), 4.7Å (in y) and 7.4Å (in z). The manner in which dioxane fits into the cavity is illustrated in Figure 5.11.

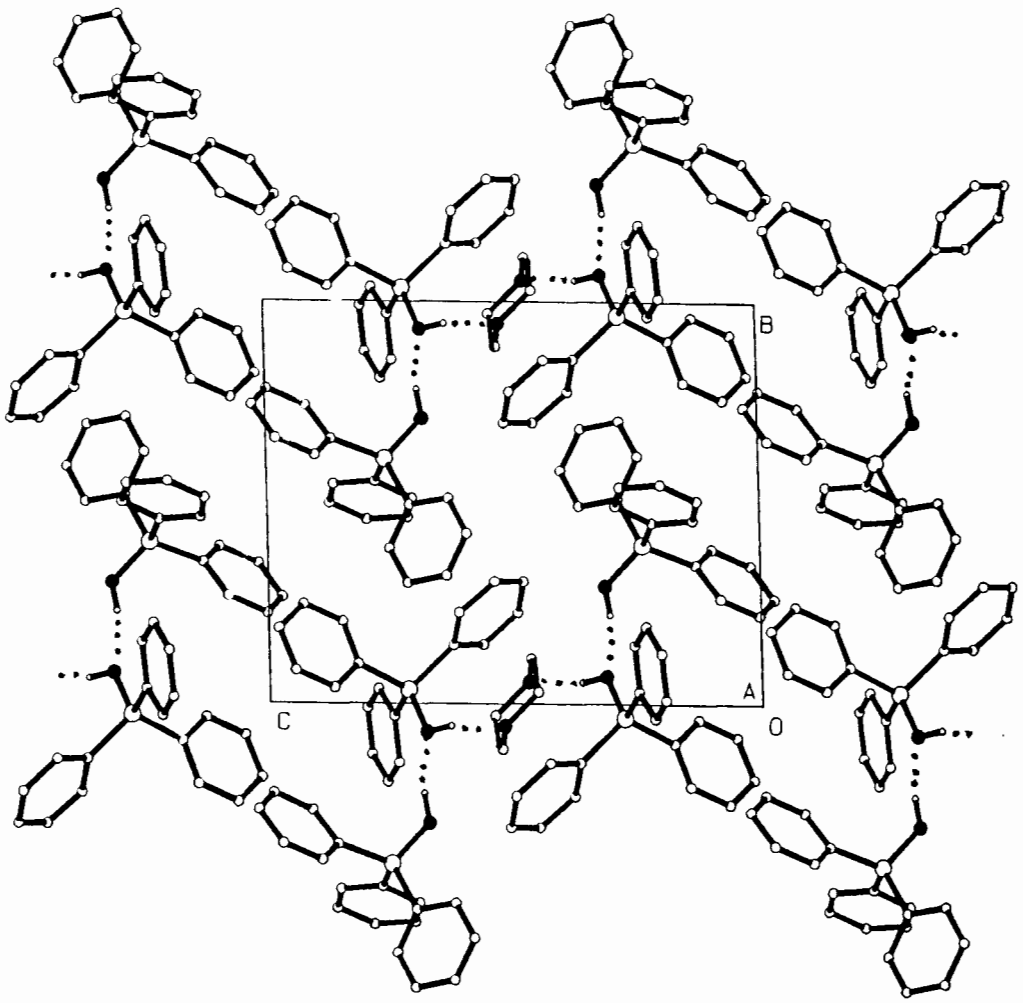

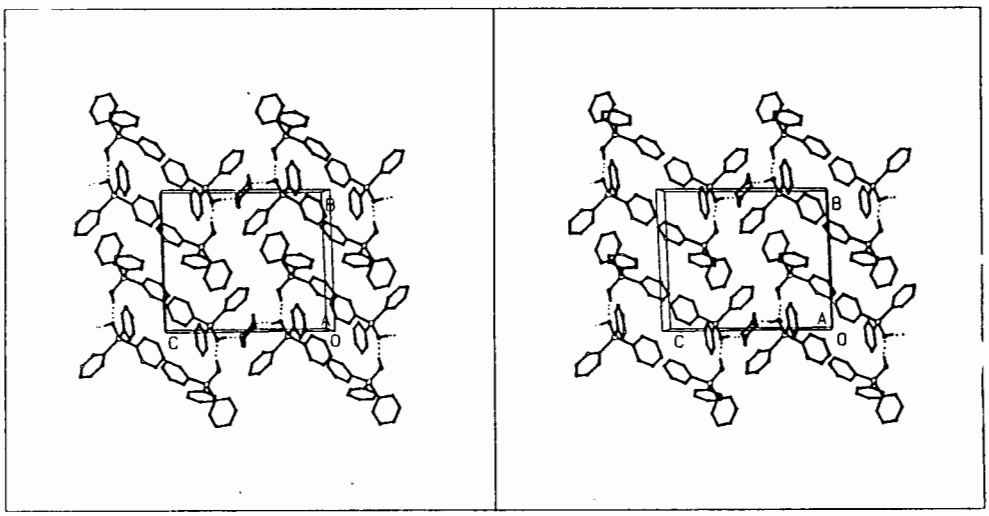

Figure 5.10. Packing diagram of **BASIL** viewed down [100].

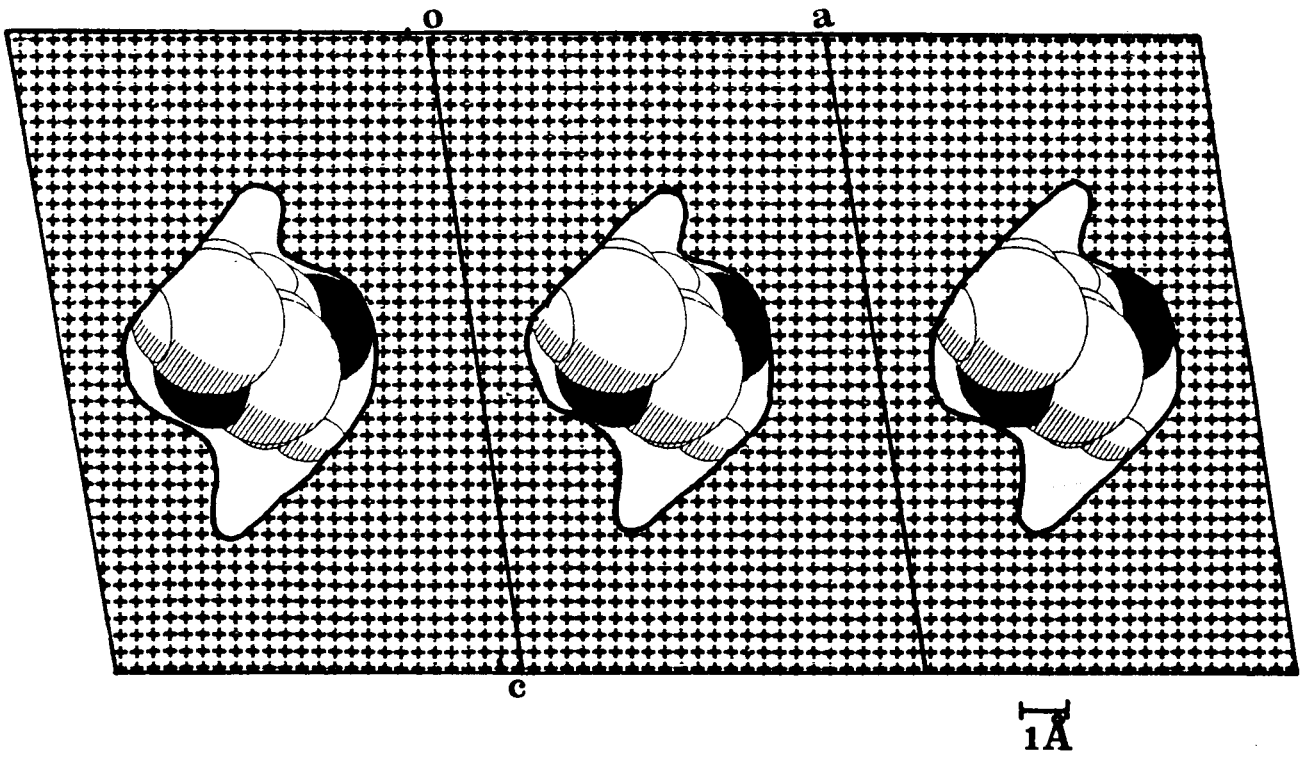

Figure 5.11. Cross-section of **BASIL** at y = 0, showing the cavities in which the dioxane molecules are trapped.

SETH : $(C_{18}H_{16}OSi)_4$. ethanol

Space group : $P\bar{1}$	H : G = 4 : 1
a = 13.682(4)Å	α = 88.23(3)°
b = 15.119(6)Å	β = 81.83(3)°
c = 15.990(6)Å	γ = 87.07(3)°
Z = 2	

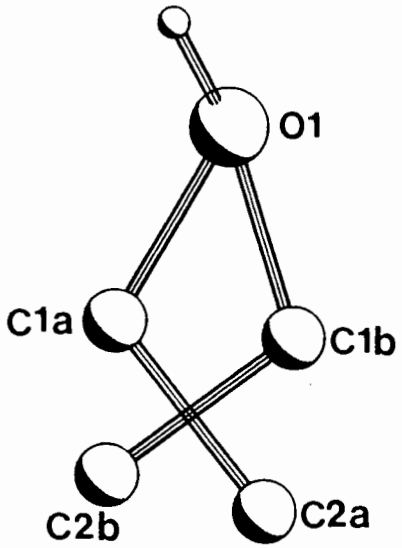

The four host molecules in the asymmetric unit had to be well-refined before sensible peaks for the guest atoms could be found. The phenyl rings of triphenylsilanol were refined as rigid hexagons and all non-hydrogen atoms were treated anisotropically.

The difference electron density map at this stage yielded the position of the ethanol oxygen unambiguously but the ethanol carbons were poorly defined. This can be seen in Figure 5.12 which also shows the model finally chosen for the disordered ethanol. The ethanol molecule can lie in either of two positions, following the backbone O(1G) - C(1GA) - C(2GA) or O(1G) - C(1GB) - C(2GB). Each of the carbons was assigned a site occupancy factor of 0.50 and an isotropic temperature factor. It was necessary to fix the positions of C(1GB) and C(2GB).

The guest hydrogens were omitted, with the exception of the hydroxyl hydrogen which, along with three of the hosts' hydroxyl hydrogens, was located in a difference Fourier map. The hydroxyl hydrogen, H(2), was not located but its position was calculated 1.00Å from O(2) and it was fixed there. The final maximum shift/e.s.d. was 0.316 (for H(1G)); the next highest was 0.112 and the maximum and minimum heights in the final electron density map were 0.47 and -0.43 $eÅ^{-3}$. Final coordinates and thermal parameters are listed in Table 5.6.

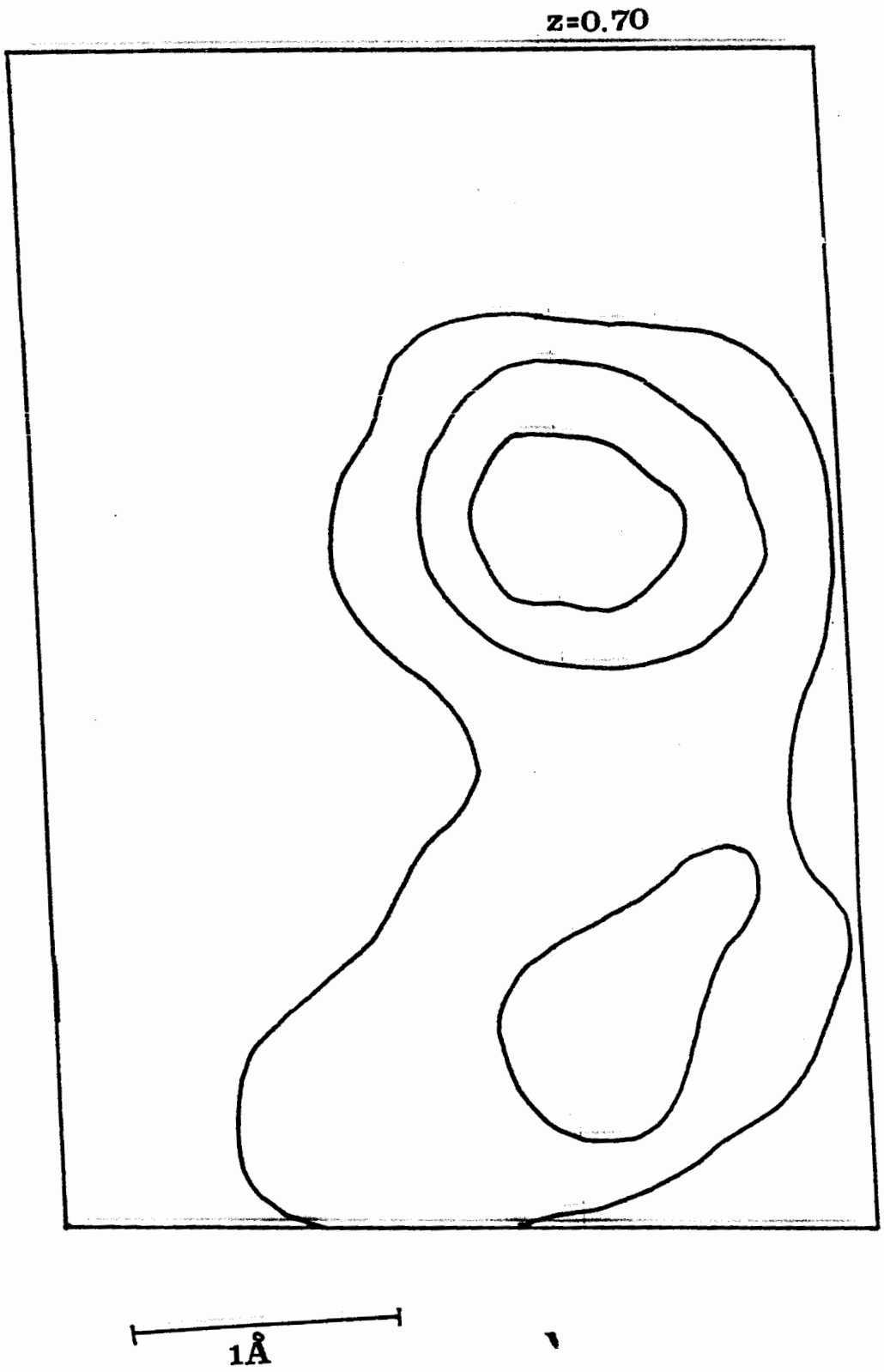
z=0.70
1Å

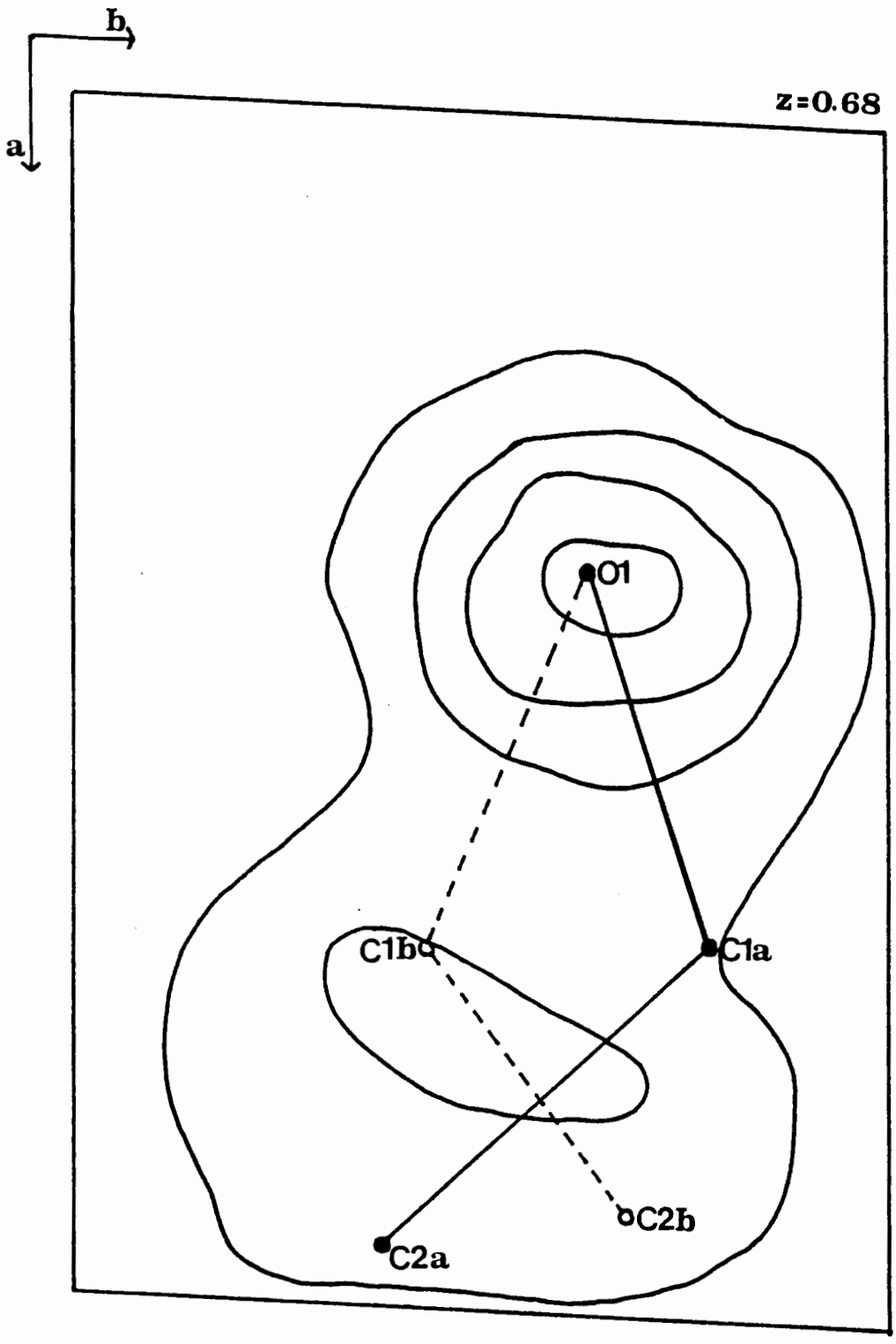

Figure 5.12. Difference electron density map in the region of the guest. Contours are drawn at intervals of 0.7 Å. Individual molecules are O(1G)-C(1GA)-C(2GA) or O(1G)-C(1GB)-C(2GB).

Molecular structure.

This β-phase compound results from the opening of the α-phase's tetrahedral clusters (see **WEB2**) to accommodate the guest's hydroxy moiety in the hydrogen bonding scheme. This is illustrated in Figure 5.13 which shows four triphenylsilanol molecules and ethanol in a cyclic network of hydrogen bonds.

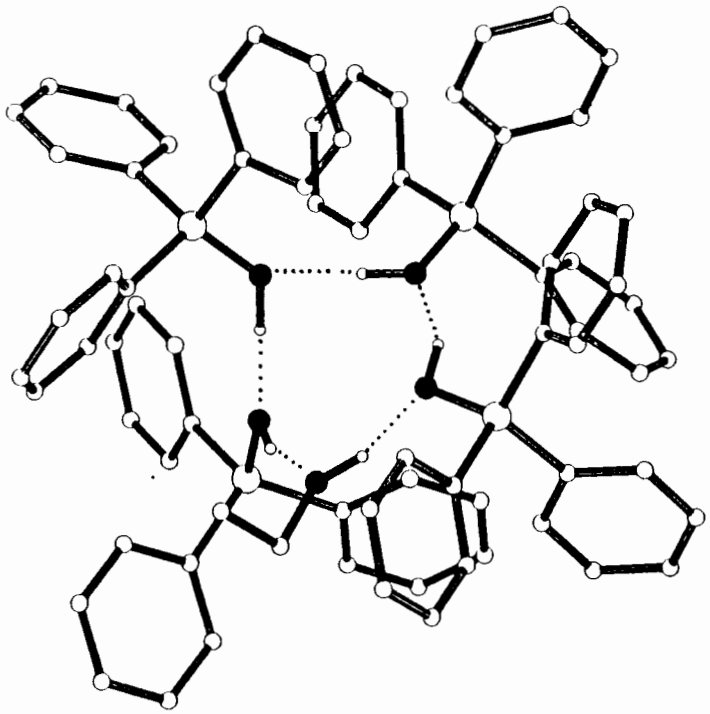

Figure 5.13. Molecular structure of **SETH**.

As was the case in **WEB2**, it is these hydrogen bonded clusters which dominate the crystal packing. This is illustrated in Figure 5.14, which is a packing diagram of **SETH**, viewed along [1 0 0].

Ethanol is able to participate in the hydrogen bonding scheme in this way because it has a hydroxyl group which may act as both donor and acceptor. An attempt was made to find other hydroxy-containing guests for comparison.

Solutions of triphenylsilanol with the following potential guests were made : methanol, 1-propanol, 2-propanol, 1-butanol, cyclohexanol and phenol. Methanol appeared to be included but the crystals decayed immediately on being removed from their mother liquor, too fast for analysis to reveal in what proportion the methanol had been included. None of the other solvents was included.

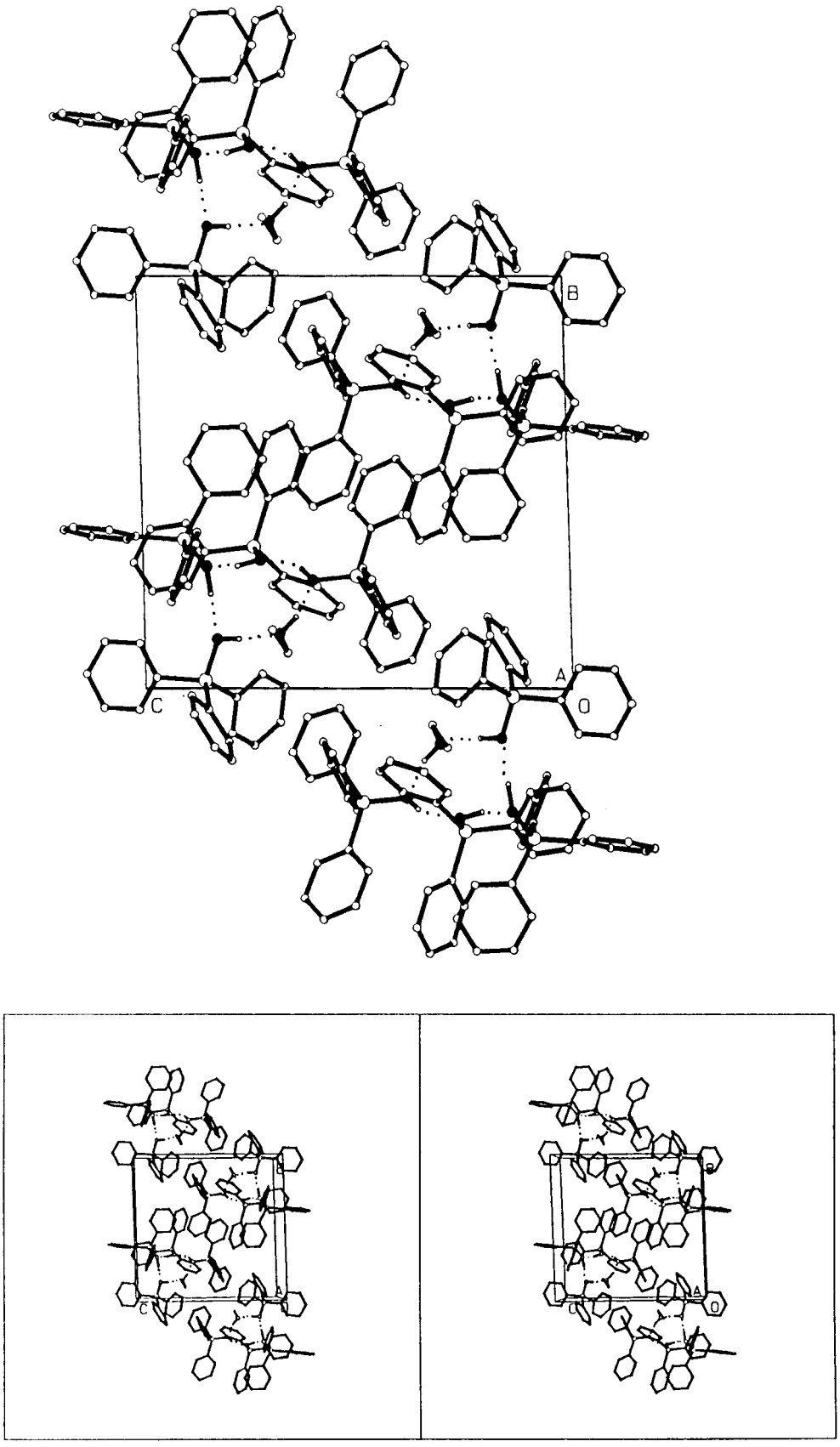

Figure 5.14. Packing diagram of **SETH** viewed along [100]. Only one of the possible orientations of the guest is shown.

It is interesting to speculate on this apparent selectivity for ethanol among the simple alcohols. An examination was made of the space available to the guest. An OPEC analysis of the empty space within the structure revealed a cavity, a section of which (at z = 0.70) is shown in Figure 5.15. Space-filled molecules of methanol, ethanol, 1-propanol and 2-propanol are shown with the cavity superimposed on them. The orientation of the molecules within the cavity is that of the ethanol in **SETH**, with methyl groups added or removed as necessary.

It is clear, from Figure 5.15 that ethanol is the only alcohol that is easily accommodated in the cavity. Methanol is much smaller than the cavity and would probably be able to diffuse out of the crystal very quickly. This was borne out by experimental observations which found that very small crystals of poor quality were formed with methanol. Solutions of triphenylsilanol with higher alcohols yielded only crystals of the α-phase. Neither of the propanols can occupy the cavity in the orientations shown in Figure 5.15. The possibility of different orientations was considered, with the condition that the oxygen remain in approximately the same position as found in **SETH** so as to maintain the hydrogen bonding. 1-Propanol could alter its orientation so that the γ-carbon was directly above or below the β-carbon in the z-direction in order to fit into the space available. That would require that it be found approximately 2Å from C(2), *i.e.* at z = 0.83 or z = 0.57. No empty space is found at either of these two positions, so the inclusion of 1-propanol in this cavity seems impossible. 2-Propanol could orient itself so that its methyl groups project into and out of the plane of the paper. Again, however, this orientation is made impossible by the shallowness of the cavity in z.

All of the above analysis assumes that the host lattice would be unaltered when the guest is changed. This is not necessarily true, but, since this type of packing involves very little disruption of the packing of the α-phase, it could be considered a valid option.

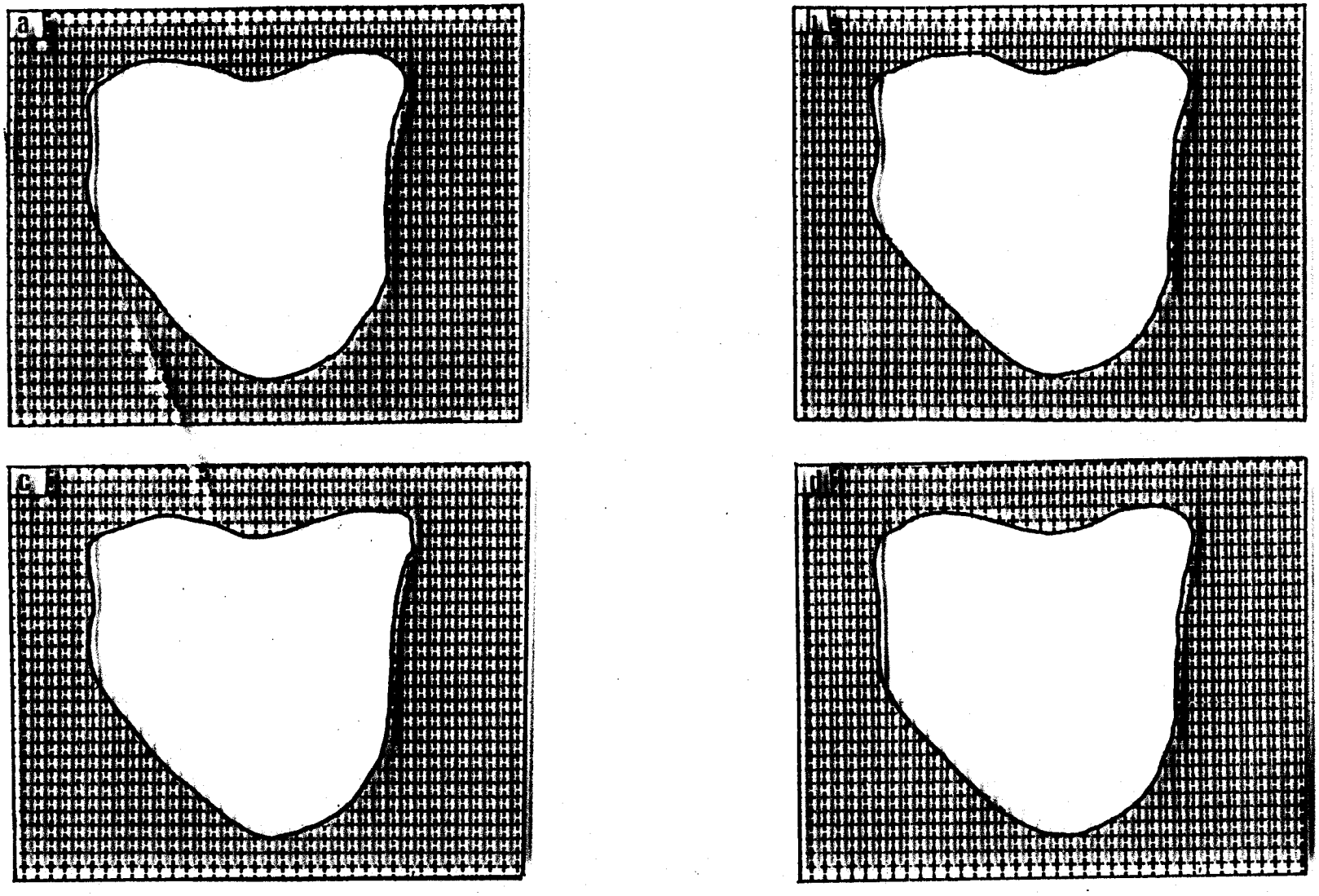
a
b
c
d
y
x

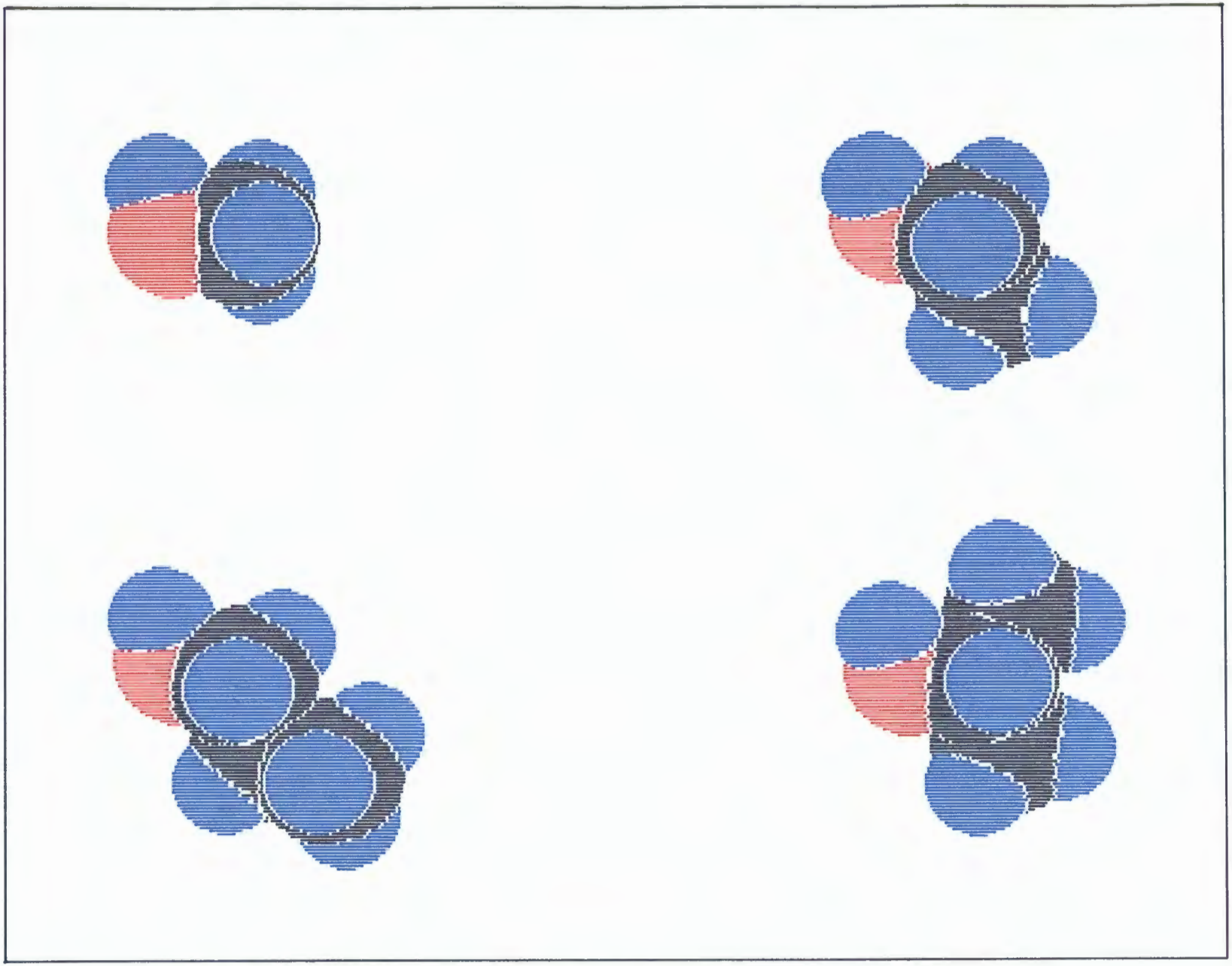

Figure 5.15. Cross-section through **SETH** at z = 0.70 superimposed on molecules of (a) methanol, (b) ethanol, (c) 1-propanol and (d) 2-propanol.

Host conformation in Class B and C structures.

The conformation of triphenylalcohols can be compared to that of triphenylphosphine oxide which has been extensively studied. Bye *et al.* [5.8] mapped the reaction path for the stereoisomerization of Ph_3PO using crystal structure analyses extracted from the Cambridge Structural Database. They found that the equilibrium structure of an isolated Ph_3PO is close to that of a C_3-symmetric propeller with all three phenyl rings rotated from their respective C-P-O planes in the same direction and by approximately the same amount. Starting with a molecule with positive torsion angles the stereoisomerization path involves rotation of all three rings. They identified a transition state as the mirror-symmetric molecule with torsion angles 90°, 10°, -10°. Further rotation of the phenyl rings leads to a propeller of opposite chirality. These structures are shown in the stereo drawings below.

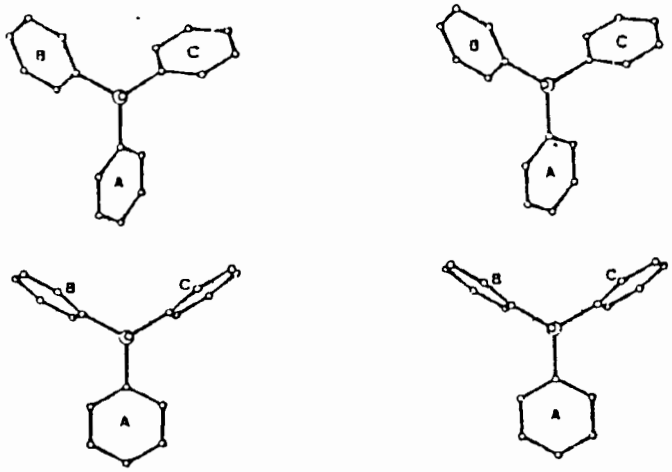

There is no reason to assume that the stereoisomerization paths of Ph_3PO and the triphenylalcohols would be identical but one might expect that their equilibrium conformations would be similar.

A study of the conformation of these hosts should include :

(i) bond lengths and angles.
(ii) the tetrahedral nature of the sp^3 atom.
(iii) the planarity of the aromatic rings.
(iv) the orientation of the hydroxyl moiety.
(v) the orientation of the phenyl rings.

Bond lengths and angles.

Vibrational effects are the only expected causes for deviations from theoretical values in these parameters. The ranges within which these values fall are shown below.

Bond lengths and angles.

Class B.	
O-C	1.433(4) Å
C(1) - C_{ring}	1.532(4) - 1.542(4) Å
C_{ring} - C_{ring}	1.370(5) - 1.392(4) Å
C(1) - C_{ring} - C_{ring}	118.5(3) - 122.9(3)°
Angles inside rings	118.3(3) - 121.2(4)°
Class C.	
O - Si	1.621(12) - 1.666(5) Å
Si - C_{ring}	1.844(18) - 1.902(16) Å
C_{ring} - C_{ring}	1.314(20) - 1.450(26) Å
Si - C_{ring} - C_{ring}	117.9(7) - 123.8(8)°
Angles inside rings	116.3(10) - 122.7(10)°

The central atom, C(1) or Si(1), is sp^3 hybridized. Most of the angles around the central atoms are close to the ideal 109.5°. However, they may be distorted to as low as 104.9° or as high as 113.5°. Figure 5.16 shows the distribution of these angles.

The planarity of the aromatic rings.

The maximum deviation from the mean plane in any of the rings never exceeds 0.04 Å.

The orientation of the hydroxyl group did not appear to follow any trend. This is to be expected since this group is able to rotate about the O-C(1) or O-Si(1) bond until the hydrogen is aligned with the nearest hydrogen-bond acceptor atom.

The orientation of the aromatic rings.

The conformation of a triphenylalcohol molecule is defined by the three torsion angles τ_A, τ_B, τ_C. The torsion angles are defined as τ_i = O(1)-C/Si(1)-C(X1)-C(XY) where i = A, B or C, X = 1 - 3 and Y = 2 or 6. Since the labelling of the rings had been done arbitrarily, it was initially necessary to examine all six possible torsion angles.

The sum of the absolute values of the two torsion angles for one ring is 180°, so the torsion angle with absolute value less than 90° was selected for each ring. Different

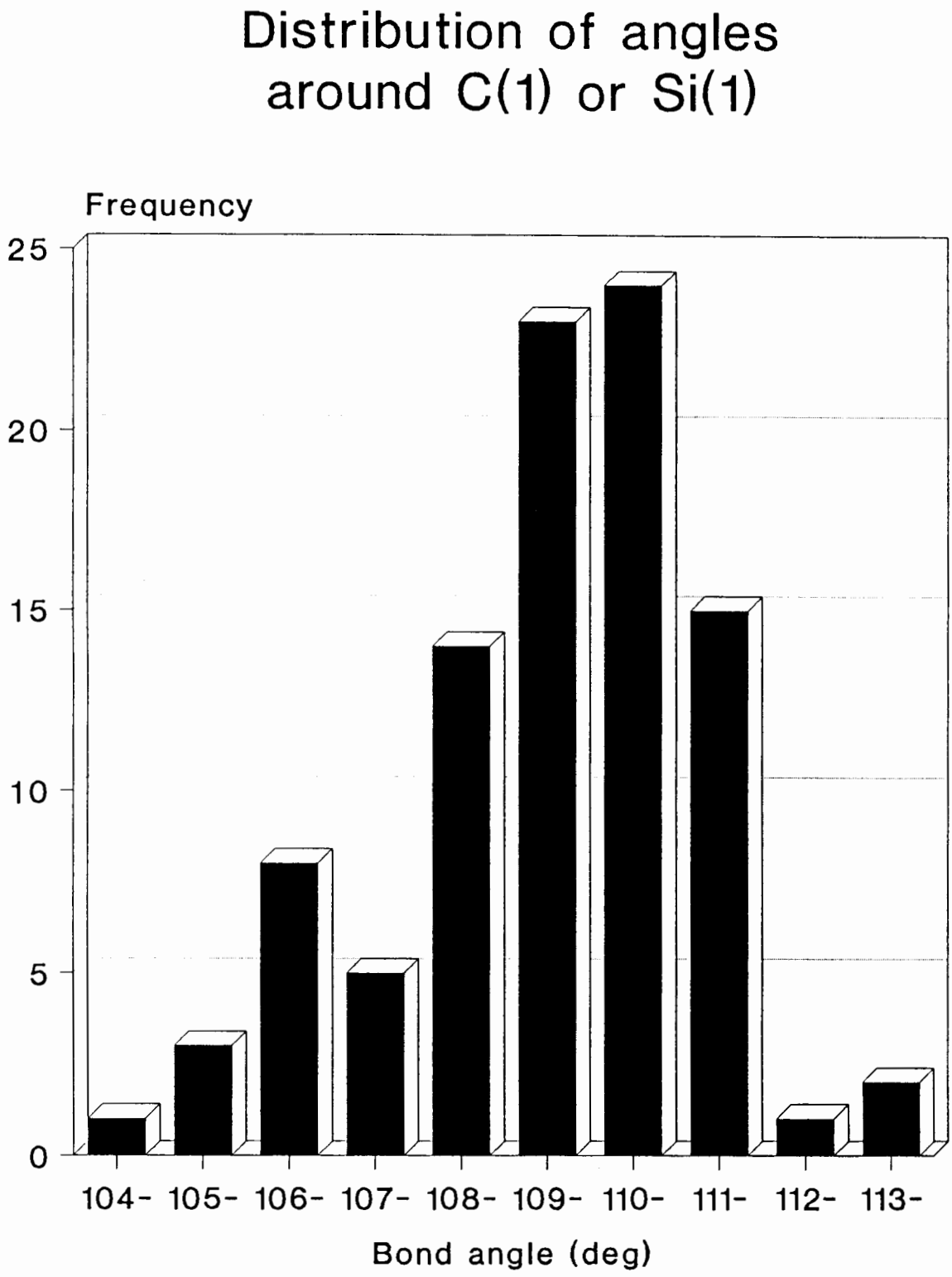
Distribution of angles
around C(1) or Si(1)
Frequency
25
20
15
10
5
0
104-
105-
106-
107-
108-
109-
110-
111-
112-
113-
Bond angle (deg)

Figure 5.16.

enantiomers of molecules crystallizing in a centrosymmetric space group will have opposite signs for the same torsion angle. Thus, although some molecules give negative torsion angles if the supplied coordinates are used, the angles quoted are such that the majority within a structure are positive.

The phenyl ring associated with the largest value of τ was taken as ring A. Rings B and C were then chosen so that the sequence of labels was clockwise when viewed down the O-C/Si direction. The values of τ_A, τ_B and τ_C obtained for the 17 molecules in these classes are displayed as a bar graph in Figure 5.17. Also included in Figure 5.17 are the values obtained from an ALCHEMY II minimized molecule of triphenylsilanol. This molecule is shown in space-filled form as Figure 5.18.

Bye *et al.* [5.8] found that most Ph_3PO molecules adopted the propeller conformation with $\tau_A \approx \tau_B \approx \tau_C \approx 40°$. Similar values are obtained using ALCHEMY II (having set $\tau_i = 40°$ before minimization). Figure 5.17 shows that most triphenylmethanol and triphenylsilanol molecules adopt an approximate propeller conformation. The exceptions are molecule 1 of **BASIL**, molecule 3 of **SETH** and molecules 3 and 4 of **WEB2**. In each of these cases, one ring is rotated in the opposite sense to the other two. An examination was made of the crystal environments of these molecules in an attempt to explain this observation.

BASIL molecule 1 has $\tau_A = 82.1°$. This ring and one on an adjacent host molecule have several C···C contacts of ≈ 3.5 - 3.7 Å. Although this is greater than the sum of the van der Waal radii of C, it is a rather tight fit and could explain the high value of τ_A. Both of the other two τ values for this molecule are low and one ring's plane is almost parallel to the Si-O bond. This angle can also be explained by several close contacts to an adjacent phenyl ring (C···C distances of 3.7 - 3.8 Å).

The rotation of a phenyl ring in **SETH** (molecule 3) in the opposite direction to the other two can likewise be explained by C···C contacts of 3.7 - 3.8 Å. Similar contacts occur in the two molecules of **WEB2** with one negative and two positive torsion angles. These contacts seem quite remote but it is possible that if the ring were rotated in a positive sense, the contacts would be closer, giving rise to a molecule of higher potential energy.

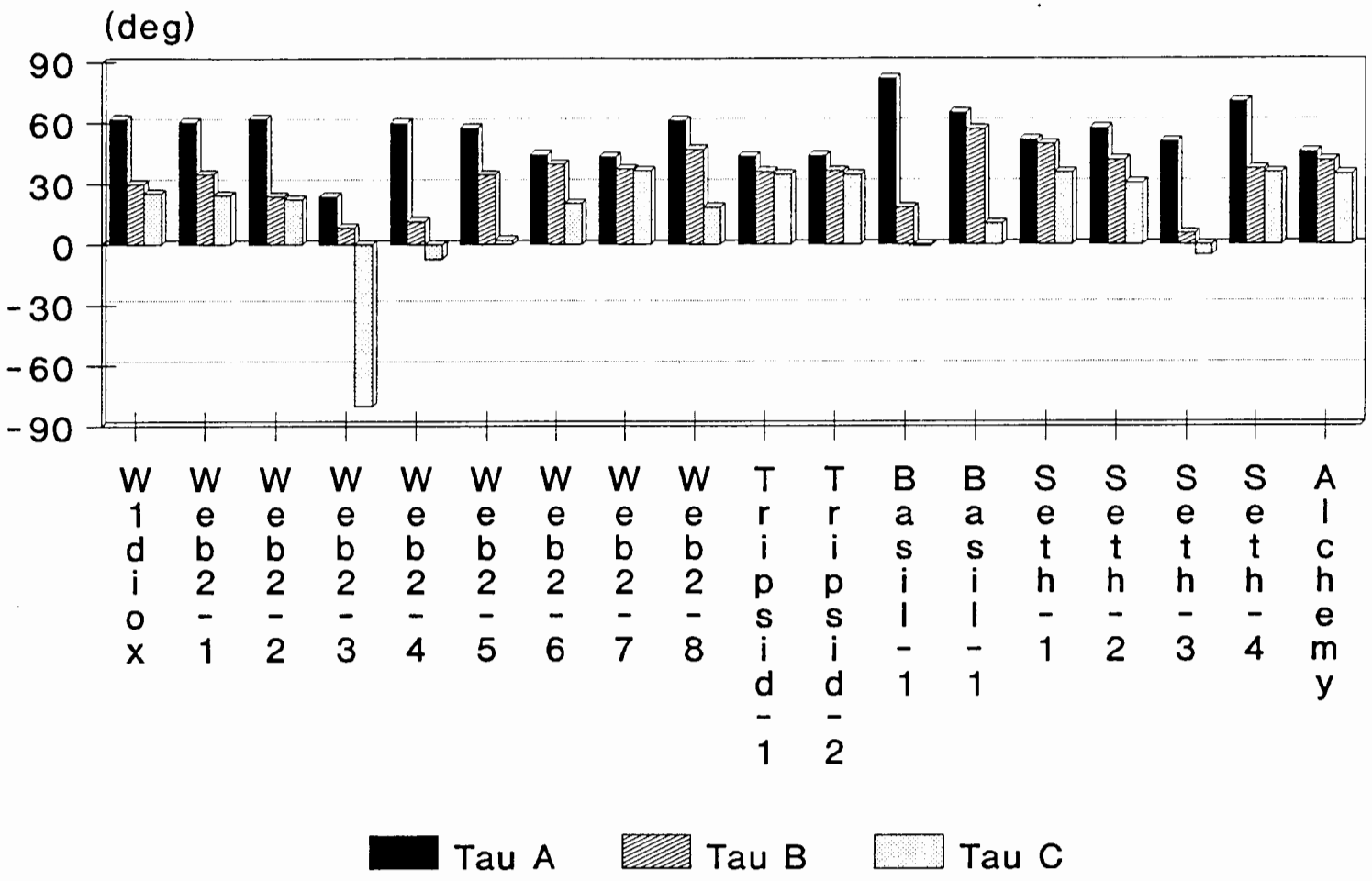

Figure 5.17. Orientation of the phenyl rings.

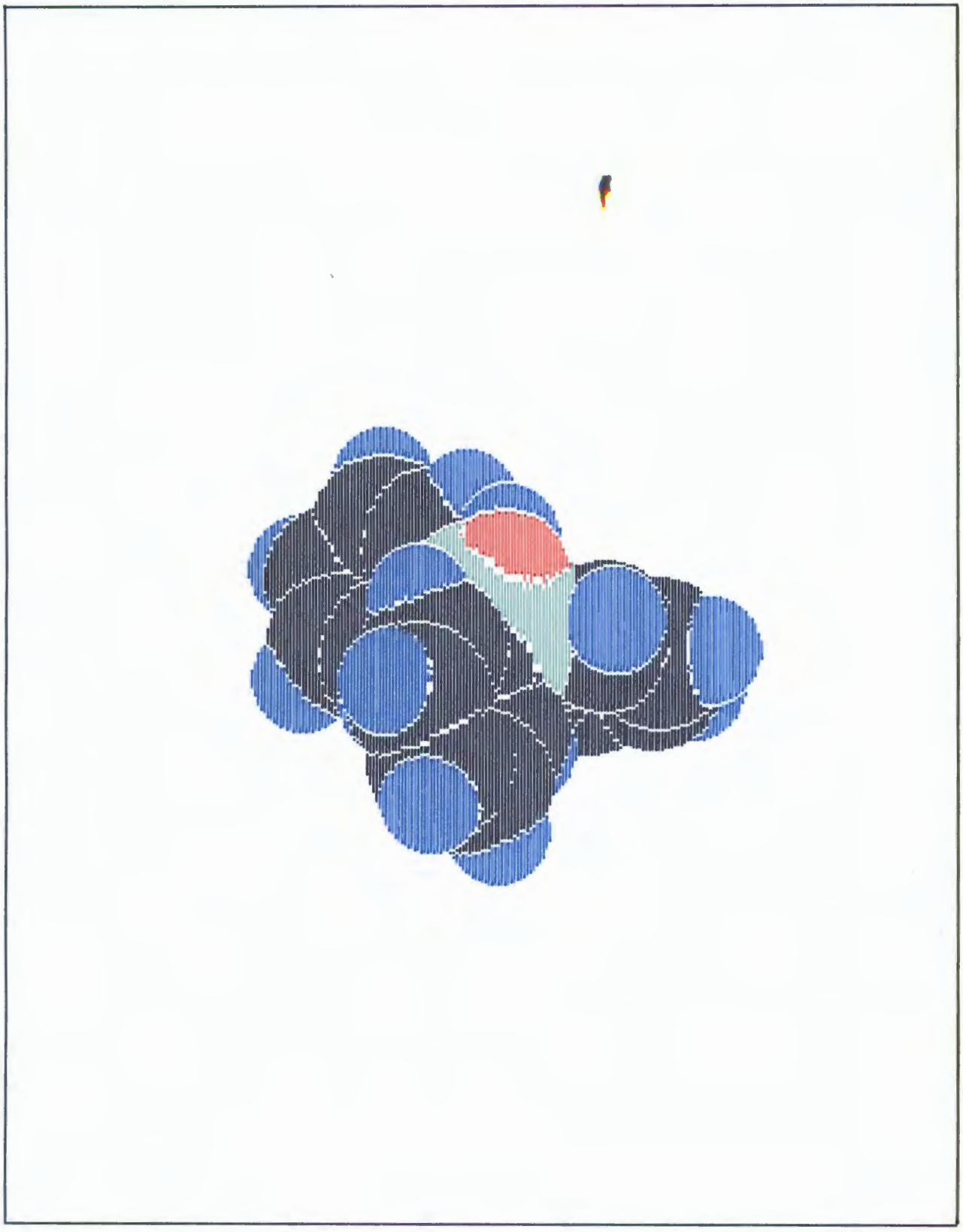

Figure 5.18. Space-filled diagram of the host molecule (Class C).

Table 5.1. Details of Hydrogen bonding in Classes B and C.

Compound	Donor-H	Donor···Acceptor	D-H···Acceptor
W1DIOX			
O(1)-H(1)···O(1G)	0.95(2)	2.839(3)	168.9(23)
WEB2			
O(1)···O(2)		2.683(6)	
O(2)···O(3)		2.648(7)	
O(3)···O(4)		2.655(7)	
O(4)···O(1)		2.684(6)	
O(5)···O(6)		2.666(7)	
O(6)···O(7)		2.648(6)	
O(7)···O(8)		2.639(6)	
O(8)···O(5)		2.678(7)	
TRIPSID			
O(1)-H(1)···O(1G)	0.96(3)	2.761(4)	168.6(5)
O(2)-H(2)···O(1G)	0.98(4)	2.778(4)	175.5(4)
BASIL			
O(1)-H(1)···O(1G)	0.92(2)	2.703(2)	165.6(3)
O(2)-H(2)···O(1)	0.94(3)	2.789(2)	164.7(4)
SETH			
O(1)-H(1)···O(2)	0.95(11)	2.720(17)	152.8(10)
O(2)-H(2)···O(3)	1.01(1)	2.711(16)	179.2(8)
O(3)-H(3)···O(1G)	1.00(10)	2.578(20)	161.3(91)
O(1G)-H(1G)···O(4)	0.97(10)	2.633(24)	162.5(90)m
O(4)-H(4)···O(1)	0.95(11)	2.822(15)	151.5(41)

TABLE 5.2 Fractional atomic coordinates (x 10^4) and Thermal Parameters ($Å^2$ x $10A^3$) with e.s.d. s in parentheses for W1DIOX

Atom	x/a	y/b	z/c	U_{iso}/U_{equiv}(*)
O(1)	1666(2)	8970(2)	8936(2)	43(1) *
C(1)	999(3)	9267(3)	7773(3)	36(1) *
C(11)	1819(3)	8372(3)	7113(3)	37(1) *
C(12)	1656(4)	6949(3)	7715(3)	48(1) *
C(13)	2445(4)	6103(3)	7196(3)	60(2) *
C(14)	3409(4)	6656(4)	6064(4)	61(2) *
C(15)	3553(4)	8061(3)	5454(3)	54(2) *
C(16)	2768(3)	8917(3)	5977(3)	44(1) *
C(21)	-815(3)	8977(3)	8034(3)	37(1) *
C(22)	-1636(3)	8640(3)	7219(3)	46(1) *
C(23)	-3286(4)	8459(3)	7428(3)	56(1) *
C(24)	-4104(4)	8614(3)	8456(4)	64(2) *
C(25)	-3290(4)	8940(4)	9274(3)	65(2) *
C(26)	-1645(4)	9128(3)	9066(3)	49(1) *
C(31)	1345(3)	10798(3)	6996(3)	36(1) *
C(32)	462(4)	11540(3)	6032(3)	46(1) *
C(33)	853(4)	12898(3)	5281(3)	55(1) *
C(34)	2125(4)	13541(3)	5493(3)	56(1) *
C(35)	3014(4)	12819(3)	6468(3)	56(2) *
C(36)	2637(3)	11457(3)	7210(3)	46(1) *
O(1G)	1283(3)	6330(2)	10905(2)	66(1) *
C(1G)	1149(5)	6770(4)	11926(3)	72(2) *
C(2G)	2763(5)	7109(4)	12173(4)	84(2) *
O(2G)	3741(3)	5937(3)	12458(3)	86(2) *
C(3G)	3880(4)	5493(4)	11438(4)	79(2) *
C(4G)	2274(4)	5159(4)	11190(4)	74(2) *

Anisotropic atoms have thermal parameters ($Å^2$ x 10^3) of the form : $\exp[-2\pi^2(U_{11}h^2a^{*2} + U_{22}k^2b^{*2} + U_{33}l^2c^{*2} + 2U_{23}klb^*c^* + 2U_{13}hla^*c^* + 2U_{12}hka^*b^*)]$

Atom	U_{11}	U_{22}	U_{33}	U_{23}	U_{13}	U_{12}
O(1)	39(1)	48(1)	42(1)	-14(1)	-11(1)	-1(1)
C(1)	31(2)	39(2)	38(2)	-14(1)	-5(1)	0(1)
C(11)	26(2)	42(2)	47(2)	-19(1)	-9(1)	6(1)
C(12)	40(2)	41(2)	63(2)	-18(2)	-6(2)	3(1)
C(13)	57(2)	44(2)	84(3)	-28(2)	-14(2)	6(2)
C(14)	44(2)	67(3)	89(3)	-48(2)	-8(2)	12(2)
C(15)	44(2)	64(2)	62(2)	-33(2)	0(2)	3(2)
C(16)	40(2)	47(2)	51(2)	-22(2)	-3(2)	2(1)
C(21)	32(2)	32(2)	44(2)	-10(1)	-4(1)	1(1)
C(22)	39(2)	47(2)	52(2)	-17(2)	-8(2)	-1(1)
C(23)	40(2)	51(2)	72(3)	-13(2)	-18(2)	-5(2)
C(24)	31(2)	59(2)	83(3)	-6(2)	-1(2)	-1(2)
C(25)	41(2)	79(3)	70(3)	-27(2)	10(2)	2(2)
C(26)	37(2)	57(2)	55(2)	-23(2)	-1(2)	2(2)
C(31)	30(2)	37(2)	42(2)	-18(1)	0(1)	1(1)
C(32)	47(2)	43(2)	47(2)	-15(2)	-7(2)	-3(2)
C(33)	63(2)	44(2)	50(2)	-10(2)	-9(2)	3(2)
C(34)	63(2)	40(2)	60(2)	-14(2)	4(2)	-7(2)
C(35)	45(2)	47(2)	77(2)	-27(2)	0(2)	-11(2)
C(36)	39(2)	44(2)	57(2)	-21(2)	-4(1)	0(1)
O(1G)	68(2)	61(2)	65(2)	-18(1)	-17(1)	18(1)
C(1G)	68(3)	81(3)	62(3)	-22(2)	-3(2)	22(2)
C(2G)	90(3)	80(3)	93(3)	-42(3)	-17(3)	12(3)
O(2G)	72(2)	81(2)	106(2)	-29(2)	-35(2)	10(2)
C(3G)	60(3)	66(3)	104(3)	-25(3)	-10(2)	15(2)
C(4G)	77(3)	51(2)	94(3)	-22(2)	-23(2)	14(2)

TABLE 5.3 Fractional atomic coordinates (x 10^4) and Thermal Parameters ($Å^2$ x 10^3) with e.s.d. s in parentheses for WEB2

Atom	x/a	y/b	z/c	U_{iso}/U_{equiv}(*)
SI(1)	2649(1)	10410(1)	8672(1)	59(1) *
O(1)	1969(3)	9589(2)	8141(2)	71(2) *
C(112)	2764(6)	10820(5)	9990(4)	90(5) *
C(113)	3061(8)	10779(6)	10608(5)	116(7) *
C(114)	3599(8)	10310(6)	10705(5)	115(6) *
C(115)	3832(7)	9879(6)	10209(5)	116(7) *
C(116)	3529(6)	9901(5)	9589(4)	94(5) *
C(111)	3014(5)	10376(4)	9487(3)	62(4) *
C(122)	2499(6)	11873(5)	8932(4)	87(5) *
C(123)	1992(8)	12403(5)	8997(4)	108(7) *
C(124)	1004(9)	12184(7)	8819(4)	109(7) *
C(125)	486(7)	11418(6)	8557(5)	109(7) *
C(126)	983(6)	10878(5)	8491(4)	85(5) *
C(121)	1991(5)	11117(4)	8693(3)	63(4) *
C(132)	4585(6)	11010(6)	8834(4)	120(6) *
C(133)	5371(6)	11191(6)	8630(5)	126(7) *
C(134)	5284(8)	10984(7)	8016(6)	128(8) *
C(135)	4402(10)	10604(10)	7583(6)	243(13) *
C(136)	3601(7)	10397(8)	7779(5)	182(9) *
C(131)	3705(5)	10628(4)	8419(4)	66(4) *
SI(2)	-837(1)	8584(1)	7857(1)	62(1) *
O(2)	135(3)	8818(3)	7667(2)	75(3) *
C(212)	-1068(5)	8251(4)	8927(4)	78(5) *
C(213)	-798(7)	8324(5)	9570(5)	90(6) *
C(214)	62(8)	8792(6)	9991(5)	123(7) *
C(215)	684(8)	9157(8)	9764(5)	196(10) *
C(216)	427(7)	9092(7)	9124(5)	155(8) *
C(211)	-469(5)	8648(4)	8701(3)	70(4) *
C(222)	-2451(5)	7472(5)	6875(4)	91(5) *
C(223)	-2961(6)	6725(6)	6470(5)	108(6) *
C(224)	-2578(8)	6157(5)	6487(4)	105(6) *
C(225)	-1654(9)	6312(5)	6892(5)	126(7) *
C(226)	-1135(6)	7055(5)	7301(4)	95(5) *
C(221)	-1532(5)	7625(4)	7301(3)	59(4) *
C(232)	-1568(6)	9501(6)	7281(4)	107(6) *
C(233)	-2132(7)	9958(5)	7178(5)	109(7) *
C(234)	-2663(9)	10145(6)	7537(7)	149(9) *
C(235)	-2591(13)	9940(9)	8054(9)	270(18) *
C(236)	-2013(10)	9470(7)	8169(7)	201(12) *
C(231)	-1537(5)	9231(4)	7762(4)	70(4) *
SI(3)	274(1)	8504(1)	5873(1)	54(1) *
O(3)	569(3)	8469(2)	6591(2)	68(2) *
C(312)	1993(5)	9309(4)	5845(4)	85(5) *
C(313)	2815(6)	9409(5)	5658(5)	110(7) *
C(314)	2987(6)	8823(6)	5242(5)	101(6) *
C(315)	2346(6)	8124(6)	5008(4)	108(6) *
C(316)	1522(6)	8014(5)	5189(4)	94(5) *
C(311)	1348(4)	8609(4)	5611(3)	56(4) *
C(322)	-1034(5)	7128(4)	5565(4)	72(4) *
C(323)	-1743(5)	6449(4)	5146(5)	84(5) *
C(324)	-2044(6)	6275(5)	4483(5)	89(5) *
C(325)	-1668(6)	6772(5)	4240(4)	94(5) *
C(326)	-964(5)	7447(5)	4641(4)	83(4) *
C(321)	-651(4)	7614(4)	5309(3)	57(3) *
C(332)	150(6)	9924(5)	6544(4)	92(5) *
C(333)	-121(8)	10576(5)	6596(5)	116(6) *
C(334)	-697(7)	10628(6)	6053(6)	109(7) *
C(335)	-969(8)	10062(7)	5483(6)	134(7) *
C(336)	-725(6)	9396(5)	5414(4)	107(6) *
C(331)	-144(5)	9337(4)	5953(4)	65(4) *
SI(4)	2752(1)	7792(1)	7352(1)	56(1) *
O(4)	2155(3)	8385(2)	7297(2)	63(2) *
C(412)	4410(6)	7544(5)	7055(4)	101(6) *
C(413)	5188(7)	7683(7)	6819(6)	135(7) *
C(414)	5327(8)	8237(8)	6603(6)	142(10) *
C(415)	4689(9)	8596(8)	6551(7)	180(12) *

Table 5.3 ctd.

C(416)	3914(7)	8489(6)	6797(6)	154(10) *
C(411)	3787(5)	7983(4)	7072(4)	70(4) *
C(422)	2260(6)	6230(4)	6879(4)	87(5) *
C(423)	1687(7)	5508(5)	6488(5)	103(6) *
C(424)	810(7)	5386(5)	6068(4)	99(6) *
C(425)	510(6)	5976(6)	6023(5)	133(7) *
C(426)	1074(6)	6715(5)	6413(4)	106(5) *
C(421)	1945(4)	6839(4)	6843(3)	56(3) *
C(432)	4102(6)	8092(5)	8559(4)	108(6) *
C(433)	4350(8)	8112(6)	9198(5)	126(7) *
C(434)	3646(9)	7903(5)	9441(5)	117(7) *
C(435)	2721(9)	7769(7)	9116(5)	189(9) *
C(436)	2475(7)	7738(7)	8478(5)	149(7) *
C(431)	3134(6)	7870(4)	8199(3)	68(3) *
SI(5)	4523(1)	6407(1)	4054(1)	52(1) *
O(5)	4168(3)	6431(2)	3338(2)	60(2) *
C(512)	5444(5)	5503(4)	4551(3)	64(4) *
C(513)	5889(5)	4937(4)	4513(4)	69(4) *
C(514)	5954(5)	4510(4)	3924(4)	74(4) *
C(515)	5589(6)	4639(4)	3368(4)	84(5) *
C(516)	5156(5)	5206(4)	3404(3)	73(4) *
C(511)	5066(4)	5639(3)	3985(3)	52(3) *
C(522)	2578(5)	5800(4)	3863(4)	77(5) *
C(523)	1769(6)	5665(5)	4061(5)	94(6) *
C(524)	1847(7)	5957(5)	4702(5)	97(6) *
C(525)	2716(7)	6415(5)	5161(4)	96(6) *
C(526)	3529(5)	6565(4)	4970(3)	77(4) *
C(521)	3459(5)	6249(4)	4317(3)	55(4) *
C(532)	5115(6)	7953(4)	4702(4)	94(5) *
C(533)	5755(7)	8644(5)	5109(5)	121(6) *
C(534)	6694(6)	8711(5)	5450(4)	98(5) *
C(535)	6966(5)	8069(5)	5384(4)	83(5) *
C(536)	6326(5)	7366(4)	4969(4)	73(4) *
C(531)	5407(5)	7303(4)	4625(3)	57(3) *
SI(6)	2296(1)	7256(1)	2488(1)	53(1) *
O(6)	2720(3)	6567(2)	2529(2)	66(3) *
C(612)	429(5)	7342(4)	2383(4)	85(5) *
C(613)	-410(6)	7305(5)	2570(5)	108(6) *
C(614)	-449(6)	7073(5)	3070(5)	99(5) *
C(615)	284(7)	6870(6)	3380(4)	110(6) *
C(616)	1116(6)	6926(5)	3197(4)	96(6) *
C(611)	1181(4)	7161(3)	2698(3)	55(3) *
C(622)	1952(6)	7893(5)	1567(4)	99(6) *
C(623)	1719(7)	7875(7)	930(6)	132(9) *
C(624)	1629(7)	7228(8)	403(5)	121(8) *
C(625)	1772(7)	6608(7)	511(5)	132(8) *
C(626)	1973(6)	6600(5)	1136(4)	106(5) *
C(621)	2074(4)	7246(4)	1661(3)	59(4) *
C(632)	4160(5)	8220(4)	3137(4)	82(5) *
C(633)	4849(6)	8870(5)	3590(5)	101(5) *
C(634)	4592(7)	9422(5)	3992(4)	97(5) *
C(635)	3644(7)	9334(4)	3955(4)	94(5) *
C(636)	2940(5)	8678(4)	3508(4)	76(4) *
C(631)	3201(5)	8126(3)	3092(3)	53(3) *
SI(7)	5603(1)	6286(1)	2043(1)	60(1) *
O(7)	4671(3)	6092(3)	2274(2)	72(2) *
C(712)	5630(6)	4796(5)	1780(4)	79(5) *
C(713)	6051(7)	4224(5)	1714(4)	93(5) *
C(714)	7033(8)	4382(6)	1852(5)	111(7) *
C(715)	7583(7)	5110(7)	2063(5)	113(6) *
C(716)	7178(5)	5712(5)	2145(4)	88(5) *
C(711)	6186(5)	5541(4)	1996(3)	62(4) *
C(722)	5547(6)	5999(5)	749(4)	110(6) *
C(723)	5235(8)	6072(6)	145(4)	124(7) *
C(724)	4595(8)	6451(6)	43(5)	107(6) *
C(725)	4236(8)	6771(7)	526(6)	140(8) *
C(726)	4529(7)	6700(5)	1116(5)	112(7) *
C(721)	5199(5)	6334(4)	1234(3)	65(4) *
C(732)	6542(6)	7390(5)	3287(4)	94(5) *
C(733)	7182(7)	8080(6)	3732(4)	104(5) *

Table 5.3 ctd.

C(734)	7706(7)	8539(5)	3529(5)	104(6) *
C(735)	7605(8)	8336(6)	2884(5)	135(7) *
C(736)	6937(7)	7668(5)	2432(4)	120(6) *
C(731)	6418(5)	7190(4)	2639(3)	61(4) *
SI(8)	2153(1)	4519(1)	1234(1)	60(1) *
O(8)	2868(3)	5342(2)	1724(2)	70(2) *
C(812)	549(5)	3603(4)	1300(4)	82(4) *
C(813)	-245(6)	3441(5)	1505(5)	101(6) *
C(814)	-460(6)	4007(7)	1923(5)	111(7) *
C(815)	87(7)	4746(6)	2139(5)	117(7) *
C(816)	873(5)	4920(5)	1927(4)	93(5) *
C(811)	1106(4)	4339(4)	1508(3)	64(4) *
C(822)	3115(5)	3779(5)	1904(4)	82(5) *
C(823)	3614(6)	3276(5)	1980(5)	100(5) *
C(824)	3798(6)	2813(5)	1465(6)	106(6) *
C(825)	3503(7)	2863(5)	859(5)	106(6) *
C(826)	2992(5)	3371(4)	778(4)	84(5) *
C(821)	2808(4)	3841(4)	1306(4)	62(3) *
C(832)	2524(6)	4776(5)	171(4)	91(5) *
C(833)	2307(8)	4774(5)	-453(5)	111(6) *
C(834)	1358(9)	4486(6)	-851(5)	116(7) *
C(835)	657(7)	4198(6)	-619(5)	134(7) *
C(836)	869(6)	4211(5)	6(4)	104(5) *
C(831)	1812(5)	4499(4)	403(3)	68(4) *

Anisotropic atoms have thermal parameters ($Å^2 \times 10^3$) of the form :
$\exp[-2\pi^2(U_{11}h^2a^{*2} + U_{22}k^2b^{*2} + U_{33}l^2c^{*2} + 2U_{23}klb^*c^* + 2U_{13}hla^*c^* + 2U_{12}hka^*b^*)]$

Atom	U_{11}	U_{22}	U_{33}	U_{23}	U_{13}	U_{12}
SI(1)	52(1)	60(1)	54(1)	11(1)	15(1)	15(1)
O(1)	62(3)	61(3)	65(3)	5(3)	11(3)	10(3)
C(112)	114(7)	92(7)	68(6)	27(5)	41(5)	31(6)
C(113)	159(10)	112(9)	83(8)	39(6)	53(7)	34(7)
C(114)	131(9)	125(10)	90(8)	48(7)	32(7)	32(7)
C(115)	131(9)	134(9)	97(8)	55(7)	30(7)	58(7)
C(116)	98(7)	106(7)	85(7)	42(6)	19(5)	50(6)
C(111)	58(5)	55(5)	56(5)	12(4)	12(4)	4(4)
C(122)	122(7)	63(6)	68(6)	18(5)	26(5)	24(6)
C(123)	164(10)	79(7)	70(6)	22(5)	14(7)	52(8)
C(124)	159(11)	130(10)	66(7)	48(7)	35(7)	85(9)
C(125)	128(9)	142(9)	103(8)	65(8)	51(7)	93(8)
C(126)	79(6)	113(7)	81(6)	48(5)	29(5)	48(6)
C(121)	74(5)	73(6)	43(4)	21(4)	18(4)	29(5)
C(132)	54(6)	177(10)	85(7)	29(7)	11(5)	-11(6)
C(133)	68(7)	180(11)	115(9)	58(9)	29(7)	4(7)
C(134)	96(8)	166(11)	125(10)	53(9)	50(8)	30(8)
C(135)	155(13)	388(23)	124(11)	56(13)	89(10)	-36(14)
C(136)	111(9)	303(16)	80(8)	56(9)	39(7)	-28(9)
C(131)	66(5)	67(5)	62(5)	21(4)	27(4)	14(4)
SI(2)	53(1)	70(2)	57(1)	19(1)	22(1)	11(1)
O(2)	52(3)	91(4)	76(3)	26(3)	28(3)	10(3)
C(212)	85(6)	91(6)	76(6)	45(5)	40(5)	26(5)
C(213)	108(8)	102(7)	86(7)	49(6)	49(6)	40(6)
C(214)	117(9)	168(11)	81(7)	61(8)	27(7)	22(8)
C(215)	141(11)	285(17)	84(9)	74(10)	-6(8)	-61(10)
C(216)	102(8)	229(13)	82(8)	66(8)	2(6)	-42(8)
C(211)	62(5)	85(6)	56(5)	26(5)	19(4)	14(4)
C(222)	61(5)	92(7)	83(6)	9(5)	5(5)	6(5)
C(223)	94(7)	95(8)	103(8)	17(7)	23(6)	3(6)

Table 5.3 ctd.

C(224)	132(9)	81(7)	80(7)	29(6)	25(7)	1(7)
C(225)	176(11)	80(8)	106(9)	34(7)	26(8)	32(8)
C(226)	112(7)	69(6)	92(7)	28(5)	10(6)	31(6)
C(221)	58(5)	66(5)	56(5)	25(4)	23(4)	13(4)
C(232)	118(8)	143(9)	81(7)	66(7)	25(6)	56(7)
C(233)	115(8)	111(8)	103(8)	43(7)	24(7)	48(7)
C(234)	177(12)	132(10)	207(15)	96(10)	114(11)	78(9)
C(235)	402(24)	339(21)	423(26)	309(21)	360(23)	319(20)
C(236)	307(17)	242(15)	289(17)	203(14)	257(15)	220(14)
C(231)	54(5)	66(5)	84(6)	20(5)	28(4)	14(4)
SI(3)	48(1)	63(1)	49(1)	20(1)	14(1)	17(1)
O(3)	65(3)	87(4)	50(3)	28(3)	15(2)	24(3)
C(312)	60(5)	80(6)	109(7)	34(5)	30(5)	9(5)
C(313)	75(7)	102(8)	162(10)	49(7)	57(7)	25(6)
C(314)	79(7)	129(9)	119(9)	68(8)	44(6)	32(7)
C(315)	82(7)	127(9)	110(8)	25(7)	53(6)	31(6)
C(316)	80(6)	98(7)	102(7)	19(6)	51(6)	27(5)
C(311)	42(4)	67(5)	53(5)	22(4)	8(4)	13(4)
C(322)	58(5)	75(6)	99(6)	47(5)	32(5)	25(5)
C(323)	64(5)	70(6)	108(7)	26(6)	30(5)	9(5)
C(324)	68(6)	79(6)	105(8)	10(6)	42(6)	15(5)
C(325)	73(6)	105(7)	73(6)	6(6)	30(5)	-1(5)
C(326)	69(5)	101(7)	53(5)	8(5)	22(4)	5(5)
C(321)	40(4)	63(5)	60(5)	16(4)	12(4)	12(4)
C(332)	108(7)	73(6)	92(7)	18(6)	36(6)	36(6)
C(333)	132(9)	84(8)	136(10)	30(7)	55(8)	42(7)
C(334)	96(8)	98(8)	152(11)	50(8)	59(8)	41(7)
C(335)	152(10)	127(10)	146(11)	73(9)	34(9)	75(9)
C(336)	115(8)	109(8)	93(7)	48(6)	-3(6)	50(6)
C(331)	55(5)	74(6)	80(6)	38(5)	28(4)	23(4)
SI(4)	46(1)	57(1)	61(1)	19(1)	12(1)	19(1)
O(4)	56(3)	61(3)	68(3)	21(3)	14(2)	26(2)
C(412)	80(6)	105(7)	127(8)	37(6)	49(6)	35(6)
C(413)	76(7)	170(12)	175(11)	62(9)	71(7)	40(7)
C(414)	97(8)	206(13)	207(13)	151(11)	79(8)	68(9)
C(415)	139(11)	279(17)	266(16)	204(14)	133(11)	118(11)
C(416)	113(8)	202(12)	270(15)	181(12)	118(10)	91(8)
C(411)	46(4)	78(6)	100(6)	47(5)	24(4)	26(4)
C(422)	88(6)	57(6)	112(7)	24(5)	29(5)	30(5)
C(423)	105(8)	67(7)	130(9)	21(6)	48(7)	23(6)
C(424)	80(7)	89(7)	101(8)	17(6)	26(6)	8(6)
C(425)	88(7)	89(8)	162(10)	15(8)	-12(7)	18(7)
C(426)	70(6)	77(7)	123(8)	16(6)	-14(6)	11(5)
C(421)	48(4)	60(5)	54(5)	13(4)	19(4)	16(4)
C(432)	97(7)	142(9)	67(6)	21(6)	-3(5)	64(6)
C(433)	140(10)	146(10)	83(8)	30(7)	7(7)	77(9)
C(434)	154(11)	93(8)	83(8)	45(6)	8(8)	4(8)
C(435)	152(11)	249(15)	94(9)	90(10)	1(8)	-91(10)
C(436)	94(8)	240(13)	77(7)	79(8)	5(6)	-36(8)
C(431)	80(6)	53(5)	54(5)	14(4)	5(5)	10(4)
SI(5)	59(1)	51(1)	46(1)	17(1)	16(1)	21(1)
O(5)	67(3)	65(3)	49(3)	25(2)	14(2)	23(3)
C(512)	64(5)	64(5)	77(6)	39(4)	26(4)	24(4)
C(513)	74(5)	59(5)	82(6)	34(5)	27(5)	23(4)
C(514)	78(6)	56(5)	92(7)	28(5)	31(5)	23(4)
C(515)	103(7)	71(6)	74(6)	17(5)	21(5)	47(5)
C(516)	77(5)	68(5)	64(5)	7(4)	20(4)	31(5)
C(511)	47(4)	41(4)	61(5)	14(4)	16(4)	11(3)
C(522)	67(5)	65(5)	92(6)	25(5)	27(5)	12(4)
C(523)	87(7)	92(7)	106(8)	36(6)	45(6)	18(5)
C(524)	106(8)	82(7)	124(9)	51(7)	57(7)	31(6)
C(525)	108(7)	115(8)	101(8)	52(6)	60(7)	57(7)
C(526)	91(6)	106(7)	61(5)	41(5)	41(5)	50(5)
C(521)	66(5)	56(5)	62(5)	30(4)	29(4)	34(4)
C(532)	104(7)	59(6)	94(7)	10(5)	4(5)	37(5)
C(533)	124(8)	61(6)	123(8)	1(6)	-7(7)	24(6)
C(534)	102(7)	72(6)	84(7)	13(5)	0(6)	12(6)
C(535)	71(6)	74(6)	79(6)	15(5)	12(5)	9(5)
C(536)	51(5)	79(6)	76(6)	22(5)	15(4)	14(4)
C(531)	66(5)	50(5)	50(4)	13(4)	19(4)	15(4)

Table 5.3 ctd.

SI(6)	51(1)	52(1)	54(1)	18(1)	13(1)	21(1)
O(6)	70(3)	53(3)	75(3)	20(3)	19(3)	31(3)
C(612)	58(5)	111(7)	93(6)	45(6)	27(5)	26(5)
C(613)	58(6)	157(9)	104(8)	39(7)	34(6)	27(6)
C(614)	80(7)	112(8)	80(7)	17(6)	27(6)	4(6)
C(615)	101(8)	160(10)	80(7)	51(7)	47(6)	31(7)
C(616)	101(7)	124(8)	94(7)	64(6)	50(6)	39(6)
C(611)	56(5)	53(5)	51(5)	16(4)	13(4)	18(4)
C(622)	106(7)	124(8)	101(7)	78(7)	35(6)	45(6)
C(623)	124(9)	194(13)	140(11)	124(10)	54(9)	66(9)
C(624)	81(7)	201(15)	97(9)	77(10)	31(7)	38(8)
C(625)	135(9)	204(13)	70(7)	57(8)	35(6)	67(9)
C(626)	124(8)	134(9)	55(6)	23(6)	25(6)	56(7)
C(621)	45(4)	79(6)	61(5)	35(5)	17(4)	22(4)
C(632)	61(5)	74(6)	97(7)	30(5)	24(5)	0(5)
C(633)	71(6)	80(7)	125(8)	27(6)	22(6)	-3(6)
C(634)	101(8)	72(7)	95(7)	27(6)	17(6)	-1(6)
C(635)	99(7)	52(6)	107(7)	13(5)	23(6)	11(5)
C(636)	93(6)	44(5)	77(6)	9(4)	20(5)	21(5)
C(631)	61(5)	45(4)	54(4)	24(4)	14(4)	13(4)
SI(7)	48(1)	77(2)	55(1)	24(1)	21(1)	15(1)
O(7)	56(3)	95(4)	69(3)	31(3)	30(3)	18(3)
C(712)	88(6)	69(6)	76(6)	22(5)	31(5)	18(5)
C(713)	114(8)	86(7)	85(7)	32(5)	39(6)	32(6)
C(714)	121(9)	128(9)	109(8)	63(8)	42(7)	58(8)
C(715)	90(7)	148(10)	141(9)	76(9)	44(7)	76(8)
C(716)	54(5)	118(8)	99(7)	51(6)	19(5)	31(5)
C(711)	60(5)	87(6)	45(4)	29(4)	20(4)	24(4)
C(722)	130(8)	169(10)	68(6)	52(6)	58(6)	83(7)
C(723)	150(10)	175(11)	70(7)	50(7)	48(7)	75(8)
C(724)	135(9)	109(8)	78(7)	43(6)	29(7)	36(7)
C(725)	170(11)	187(12)	111(9)	97(9)	42(8)	92(9)
C(726)	136(9)	152(9)	109(8)	82(7)	65(7)	91(8)
C(721)	59(5)	69(5)	56(5)	20(4)	17(4)	5(4)
C(732)	87(6)	111(7)	56(6)	21(5)	14(5)	0(6)
C(733)	102(7)	107(8)	70(6)	27(6)	5(6)	2(6)
C(734)	112(8)	72(7)	112(9)	39(6)	9(7)	18(6)
C(735)	156(10)	106(9)	97(8)	36(7)	13(8)	-23(7)
C(736)	126(8)	102(8)	97(8)	37(7)	23(7)	-24(6)
C(731)	51(4)	66(5)	56(5)	17(4)	15(4)	11(4)
SI(8)	51(1)	52(1)	60(1)	8(1)	14(1)	9(1)
O(8)	65(3)	49(3)	68(3)	2(3)	13(3)	2(2)
C(812)	63(5)	72(6)	98(7)	31(5)	17(5)	1(5)
C(813)	72(6)	122(9)	118(8)	58(7)	33(6)	25(6)
C(814)	71(7)	141(10)	136(10)	71(9)	36(7)	30(7)
C(815)	75(7)	146(10)	141(9)	47(8)	59(7)	43(7)
C(816)	71(6)	97(7)	117(8)	29(6)	47(6)	39(5)
C(811)	44(4)	68(5)	69(5)	23(4)	9(4)	8(4)
C(822)	69(6)	95(7)	79(6)	39(5)	17(5)	18(5)
C(823)	77(6)	101(8)	125(9)	55(7)	17(6)	29(6)
C(824)	91(7)	86(8)	134(10)	42(7)	24(7)	28(6)
C(825)	106(8)	79(7)	126(9)	21(6)	34(7)	45(6)
C(826)	85(6)	74(6)	78(6)	8(5)	24(5)	29(5)
C(821)	49(4)	51(5)	66(5)	4(4)	14(4)	8(4)
C(832)	101(7)	102(7)	70(6)	33(5)	35(5)	22(6)
C(833)	131(9)	113(8)	98(8)	44(7)	41(7)	42(7)
C(834)	137(10)	122(9)	88(8)	38(7)	37(8)	40(8)
C(835)	117(9)	171(11)	85(8)	51(8)	-1(7)	14(8)
C(836)	88(7)	123(8)	77(7)	37(6)	-1(6)	13(6)
C(831)	71(5)	58(5)	61(5)	14(4)	15(5)	15(4)

TABLE 5.4 Fractional atomic coordinates (x 10^4) and Thermal Parameters ($Å^2$ x 10^3) with e.s.d. s in parentheses for TRIPSID

Atom	x/a	y/b	z/c	U_{iso}/U_{equiv}(*)
SI(1)	5460(1)	7596(1)	3565(0)	45(0) *
O(1)	6082(3)	7560(3)	2931(1)	59(1) *
C(111)	7119(3)	7629(3)	4072(1)	47(1) *
C(112)	6689(4)	6739(4)	4520(1)	57(2) *
C(113)	7945(5)	6831(5)	4893(2)	72(2) *
C(114)	9660(5)	7821(5)	4831(2)	72(2) *
C(115)	10125(4)	8708(4)	4396(2)	73(2) *
C(116)	8860(4)	8610(4)	4019(2)	63(2) *
C(121)	3299(4)	5872(3)	3634(1)	46(1) *
C(122)	2068(4)	5977(4)	3977(1)	58(2) *
C(123)	458(4)	4697(5)	4014(2)	68(2) *
C(124)	59(4)	3283(4)	3716(2)	66(2) *
C(125)	1244(5)	3123(4)	3369(2)	73(2) *
C(126)	2851(4)	4409(4)	3326(1)	59(1) *
C(131)	5278(4)	9471(3)	3709(1)	48(1) *
C(132)	5679(4)	10345(4)	4233(1)	57(2) *
C(133)	5514(5)	11722(4)	4338(2)	72(2) *
C(134)	4941(6)	12246(5)	3919(2)	83(2) *
C(135)	4527(6)	11411(5)	3398(2)	88(2) *
C(136)	4697(5)	10044(4)	3294(2)	72(2) *
SI(2)	2860(1)	2402(1)	1434(0)	45(0) *
O(2)	3529(3)	2447(3)	2070(1)	60(1) *
C(211)	4483(3)	2375(3)	930(1)	47(1) *
C(212)	4953(4)	3254(4)	479(1)	57(1) *
C(213)	6100(4)	3157(5)	104(2)	72(2) *
C(214)	6833(4)	2177(5)	168(2)	72(2) *
C(215)	6416(5)	1286(5)	604(2)	74(2) *
C(216)	5248(4)	1386(4)	985(2)	63(2) *
C(221)	2427(3)	4128(3)	1367(1)	45(1) *
C(222)	3438(4)	5594(4)	1671(1)	59(1) *
C(223)	3129(5)	6873(4)	1632(2)	70(2) *
C(224)	1779(5)	6723(4)	1286(2)	68(2) *
C(225)	766(5)	5299(5)	982(2)	68(2) *
C(226)	1082(4)	4014(4)	1020(1)	56(1) *
C(231)	805(4)	522(3)	1289(1)	47(1) *
C(232)	344(4)	-337(4)	765(1)	57(2) *
C(233)	-1201(5)	-1705(4)	661(2)	75(2) *
C(234)	-2308(5)	-2248(5)	1078(2)	83(2) *
C(235)	-1885(5)	-1418(5)	1604(2)	89(2) *
C(236)	-343(4)	-39(4)	1705(2)	70(2) *
S(1G)	7986(2)	4738(3)	2791(1)	70(1) *
S(2G)	8246(2)	5255(3)	2208(1)	70(1) *
O(1G)	6555(3)	4998(3)	2499(1)	72(1) *
C(1G)	9877(6)	6505(7)	2717(2)	121(3) *
C(2G)	8346(7)	3468(7)	2281(2)	117(3) *

Anisotropic atoms have thermal parameters ($Å^2$ x 10^3) of the form :

$$\exp[-2\pi^2(U_{11}h^2a^{*2} + U_{22}k^2b^{*2} + U_{33}l^2c^{*2} + 2U_{23}klb^*c^* + 2U_{13}hla^*c^* + 2U_{12}hka^*b^*)]$$

Atom	U_{11}	U_{22}	U_{33}	U_{23}	U_{13}	U_{12}
SI(1)	48(0)	44(0)	47(1)	6(0)	2(0)	24(0)
O(1)	69(1)	62(1)	51(1)	9(1)	9(1)	34(1)
C(111)	46(2)	43(2)	55(2)	0(1)	1(1)	25(1)
C(112)	53(2)	63(2)	60(2)	10(2)	0(1)	31(2)
C(113)	73(2)	85(3)	69(2)	15(2)	-4(2)	44(2)
C(114)	65(2)	78(3)	79(3)	-3(2)	-17(2)	41(2)
C(115)	45(2)	66(2)	103(3)	-5(2)	-9(2)	23(2)
C(116)	52(2)	56(2)	79(2)	5(2)	1(2)	23(2)
C(121)	46(2)	47(2)	50(2)	7(1)	-2(1)	26(1)
C(122)	54(2)	58(2)	62(2)	0(2)	2(2)	25(2)
C(123)	53(2)	78(3)	74(2)	16(2)	10(2)	29(2)
C(124)	50(2)	63(2)	75(2)	19(2)	0(2)	16(2)
C(125)	78(2)	47(2)	83(3)	0(2)	-6(2)	22(2)
C(126)	59(2)	49(2)	68(2)	3(2)	5(2)	24(2)

Table 5.4 ctd.

C(131)	46(2)	44(2)	54(2)	10(1)	4(1)	21(1)
C(132)	62(2)	56(2)	58(2)	2(2)	0(2)	32(2)
C(133)	87(3)	64(2)	69(2)	-5(2)	5(2)	43(2)
C(134)	110(3)	61(2)	99(3)	9(2)	10(3)	56(2)
C(135)	129(4)	80(3)	84(3)	21(2)	0(3)	70(3)
C(136)	102(3)	64(2)	64(2)	8(2)	-6(2)	51(2)
SI(2)	41(0)	44(0)	46(1)	6(0)	-1(0)	16(0)
O(2)	60(1)	65(2)	51(1)	10(1)	-7(1)	23(1)
C(211)	36(1)	47(2)	54(2)	-1(1)	-5(1)	16(1)
C(212)	49(2)	63(2)	58(2)	11(2)	6(1)	25(2)
C(213)	62(2)	86(3)	68(2)	13(2)	12(2)	34(2)
C(214)	55(2)	82(3)	79(3)	-2(2)	10(2)	33(2)
C(215)	60(2)	70(2)	102(3)	-5(2)	-2(2)	41(2)
C(216)	54(2)	61(2)	77(2)	9(2)	1(2)	28(2)
C(221)	38(1)	48(2)	50(2)	9(1)	7(1)	19(1)
C(222)	55(2)	49(2)	67(2)	1(2)	-7(2)	19(2)
C(223)	72(2)	48(2)	82(3)	1(2)	2(2)	21(2)
C(224)	76(2)	66(2)	80(3)	21(2)	17(2)	44(2)
C(225)	63(2)	76(2)	74(2)	13(2)	-1(2)	40(2)
C(226)	53(2)	56(2)	62(2)	2(2)	-4(1)	27(2)
C(231)	45(2)	43(2)	53(2)	8(1)	0(1)	19(1)
C(232)	51(2)	55(2)	57(2)	9(2)	0(1)	17(1)
C(233)	64(2)	62(2)	77(3)	-3(2)	-12(2)	13(2)
C(234)	58(2)	63(2)	96(3)	12(2)	-8(2)	0(2)
C(235)	69(2)	88(3)	77(3)	26(2)	13(2)	2(2)
C(236)	59(2)	69(2)	61(2)	10(2)	8(2)	10(2)
S(1G)	58(1)	102(2)	61(1)	8(1)	0(1)	47(1)
S(2G)	57(1)	103(2)	60(1)	9(1)	3(1)	46(1)
O(1G)	50(1)	78(2)	89(2)	-13(1)	-9(1)	35(1)
C(1G)	59(3)	162(5)	119(4)	-13(4)	-11(3)	38(3)
C(2G)	126(4)	150(5)	114(4)	-16(3)	-5(3)	103(4)

TABLE 5.5 Fractional atomic coordinates (x 10^4) and Thermal Parameters ($Å^2$ x 10^3) with e.s.d. s in parentheses for BASIL

Atom	x/a	y/b	z/c	U_{iso}/U_{equiv}(*)
SI(1)	693(1)	337(0)	7194(0)	42(0) *
O(1)	1860(2)	-688(1)	6842(1)	60(1) *
C(111)	662(2)	1444(2)	6269(1)	41(1) *
C(112)	1717(3)	2258(2)	6143(2)	53(1) *
C(113)	1802(3)	3031(2)	5419(2)	69(1) *
C(114)	826(4)	3036(3)	4830(2)	80(1) *
C(115)	-248(3)	2260(3)	4951(2)	79(1) *
C(116)	-319(3)	1463(2)	5661(2)	59(1) *
C(121)	-1111(2)	-307(2)	7495(1)	46(1) *
C(122)	-2336(2)	355(2)	7810(2)	56(1) *
C(123)	-3674(3)	-106(2)	8043(2)	66(1) *
C(124)	-3823(3)	-1250(3)	7966(2)	70(1) *
C(125)	-2643(3)	-1922(2)	7659(2)	77(1) *
C(126)	-1296(3)	-1455(2)	7420(2)	62(1) *
C(131)	1250(2)	968(2)	8208(1)	46(1) *
C(132)	2207(3)	379(3)	8700(2)	76(1) *
C(133)	2574(4)	804(3)	9478(3)	97(2) *
C(134)	1955(3)	1839(3)	9798(2)	80(1) *
C(135)	1090(3)	2444(3)	9302(2)	72(1) *
C(136)	736(3)	2019(2)	8512(2)	60(1) *
SI(2)	2775(1)	-3939(0)	7609(0)	41(0) *
O(2)	2897(2)	-2929(1)	6833(1)	57(1) *
C(211)	917(2)	-4502(2)	7810(1)	43(1) *
C(212)	389(3)	-4918(2)	7065(2)	57(1) *
C(213)	-951(3)	-5384(2)	7155(2)	69(1) *
C(214)	-1804(3)	-5443(2)	7990(2)	68(1) *
C(215)	-1326(3)	-5047(3)	8738(2)	73(1) *
C(216)	30(3)	-4575(2)	8651(2)	59(1) *
C(221)	4057(2)	-5083(2)	7120(1)	42(1) *
C(222)	4039(3)	-6159(2)	7535(2)	56(1) *
C(223)	4971(3)	-7022(2)	7174(2)	69(1) *
C(224)	5932(3)	-6827(3)	6384(2)	72(1) *
C(225)	5960(3)	-5784(3)	5967(2)	75(1) *
C(226)	5043(3)	-4915(2)	6327(2)	59(1) *
C(231)	3270(2)	-3458(2)	8693(1)	44(1) *
C(232)	4508(3)	-3856(2)	9023(2)	54(1) *
C(233)	4891(3)	-3450(2)	9808(2)	67(1) *
C(234)	4035(3)	-2622(2)	10276(2)	70(1) *
C(235)	2803(3)	-2214(2)	9973(2)	68(1) *
C(236)	2420(3)	-2626(2)	9192(2)	58(1) *
O(1G)	3697(2)	-547(2)	5255(1)	66(1) *
C(1G)	3838(3)	296(3)	4556(2)	64(1) *
C(2G)	5062(3)	-1119(2)	5309(2)	68(1) *

Anisotropic atoms have thermal parameters ($Å^2$ x 10^3) of the form :
$\exp[-2\pi^2(U_{11}h^2a^{*2} + U_{22}k^2b^{*2} + U_{33}l^2c^{*2} + 2U_{23}klb^*c^* + 2U_{13}hla^*c^* + 2U_{12}hka^*b^*)]$

Atom	U_{11}	U_{22}	U_{33}	U_{23}	U_{13}	U_{12}
SI(1)	44(0)	37(0)	44(0)	1(0)	0(0)	1(0)
O(1)	67(1)	44(1)	60(1)	5(1)	10(1)	12(1)
C(111)	43(1)	37(1)	40(1)	-2(1)	0(1)	3(1)
C(112)	58(1)	47(1)	54(1)	0(1)	-2(1)	-8(1)
C(113)	86(2)	51(1)	64(2)	8(1)	3(1)	-11(1)
C(114)	106(2)	71(2)	58(2)	22(1)	-4(2)	8(2)
C(115)	87(2)	98(2)	54(2)	10(2)	-24(1)	2(2)
C(116)	59(1)	65(2)	53(1)	0(1)	-12(1)	-5(1)
C(121)	54(1)	44(1)	39(1)	0(1)	-1(1)	-6(1)
C(122)	51(1)	52(1)	63(1)	-4(1)	0(1)	-5(1)
C(123)	51(1)	70(2)	73(2)	5(1)	0(1)	-7(1)
C(124)	60(2)	79(2)	71(2)	14(1)	-5(1)	-25(1)
C(125)	90(2)	53(2)	86(2)	3(1)	-4(2)	-24(1)
C(126)	69(2)	48(1)	65(2)	-1(1)	4(1)	-8(1)
C(131)	45(1)	48(1)	46(1)	8(1)	-7(1)	-2(1)

Table 5.5 ctd.

C(132)	82(2)	69(2)	84(2)	2(2)	-33(2)	4(2)
C(133)	109(3)	102(3)	93(2)	13(2)	-57(2)	-11(2)
C(134)	90(2)	100(2)	56(2)	-1(2)	-21(2)	-28(2)
C(135)	77(2)	79(2)	58(2)	-15(1)	-3(1)	-6(1)
C(136)	69(2)	61(2)	51(1)	-9(1)	-10(1)	11(1)
SI(2)	40(0)	36(0)	44(0)	2(0)	-2(0)	0(0)
O(2)	67(1)	45(1)	54(1)	8(1)	3(1)	4(1)
C(211)	38(1)	39(1)	51(1)	2(1)	-7(1)	1(1)
C(212)	52(1)	67(2)	55(1)	0(1)	-12(1)	-6(1)
C(213)	56(2)	77(2)	81(2)	-3(2)	-27(1)	-8(1)
C(214)	40(1)	67(2)	100(2)	-2(2)	-18(1)	-4(1)
C(215)	51(1)	80(2)	83(2)	-2(2)	11(1)	-7(1)
C(216)	53(1)	64(2)	56(1)	-7(1)	3(1)	-9(1)
C(221)	38(1)	44(1)	46(1)	-1(1)	-9(1)	-1(1)
C(222)	55(1)	44(1)	69(2)	-3(1)	-12(1)	-1(1)
C(223)	69(2)	44(1)	101(2)	-8(1)	-33(2)	8(1)
C(224)	56(2)	74(2)	91(2)	-35(2)	-21(2)	16(1)
C(225)	55(2)	91(2)	74(2)	-20(2)	4(1)	8(1)
C(226)	53(1)	62(2)	60(1)	-3(1)	0(1)	0(1)
C(231)	46(1)	38(1)	48(1)	0(1)	-2(1)	-8(1)
C(232)	56(1)	46(1)	64(2)	0(1)	-15(1)	-4(1)
C(233)	75(2)	58(2)	77(2)	4(1)	-31(1)	-12(1)
C(234)	91(2)	67(2)	58(2)	-2(1)	-18(1)	-24(2)
C(235)	76(2)	63(2)	64(2)	-15(1)	0(1)	-9(1)
C(236)	57(1)	54(1)	62(2)	-10(1)	-4(1)	-3(1)
O(1G)	48(1)	68(1)	78(1)	5(1)	10(1)	-6(1)
C(1G)	56(1)	74(2)	61(2)	0(1)	-5(1)	-1(1)
C(2G)	56(1)	61(2)	80(2)	7(1)	10(1)	0(1)

TABLE 5.6 Fractional atomic coordinates (x 10^4) and Thermal Parameters ($Å^2$ x 10^3) with e.s.d. s in parentheses for SETH

Atom	x/a	y/b	z/c	U_{iso}/U_{equiv}(*)
SI(1)	650(4)	3457(3)	7399(3)	46(2) *
O(1)	1808(8)	3134(8)	7263(7)	50(5) *
C(112)	258(9)	2512(8)	8950(10)	71(9) *
C(113)	-165(9)	2385(8)	9790(10)	96(13) *
C(114)	-718(9)	3074(8)	10219(10)	89(12) *
C(115)	-850(9)	3890(8)	9809(10)	104(13) *
C(116)	-427(9)	4017(8)	8970(10)	75(10) *
C(111)	126(9)	3328(8)	8541(10)	51(8) *
C(122)	1110(9)	5267(11)	7320(7)	70(10) *
C(123)	1036(9)	6150(11)	7045(7)	89(13) *
C(124)	374(9)	6409(11)	6487(7)	85(11) *
C(125)	-215(9)	5788(11)	6203(7)	80(11) *
C(126)	-141(9)	4906(11)	6479(7)	69(10) *
C(121)	521(9)	4645(11)	7037(7)	62(9) *
C(132)	-946(12)	2526(11)	6982(9)	96(12) *
C(133)	-1420(12)	2030(11)	6452(9)	144(17) *
C(134)	-923(12)	1771(11)	5669(9)	128(18) *
C(135)	49(12)	2007(11)	5416(9)	111(14) *
C(136)	523(12)	2503(11)	5946(9)	74(10) *
C(131)	26(12)	2763(11)	6729(9)	54(9) *
SI(2)	3604(4)	3623(3)	9020(3)	47(2) *
O(2)	2969(8)	2971(7)	8512(7)	57(5) *
C(212)	3665(9)	4746(9)	7580(9)	64(10) *
C(213)	3661(9)	5559(9)	7144(9)	78(10) *
C(214)	3542(9)	6346(9)	7589(9)	81(11) *
C(215)	3428(9)	6320(9)	8470(9)	82(12) *
C(216)	3431(9)	5507(9)	8907(9)	62(9) *
C(211)	3550(9)	4720(9)	8462(9)	46(8) *
C(222)	2001(12)	3629(8)	10371(11)	74(10) *
C(223)	1568(12)	3708(8)	11210(11)	97(12) *
C(224)	2154(12)	3856(8)	11835(11)	116(16) *
C(225)	3171(12)	3926(8)	11619(11)	115(16) *
C(226)	3604(12)	3849(8)	10778(11)	92(13) *
C(221)	3018(12)	3700(8)	10154(11)	52(8) *
C(232)	5679(13)	3794(8)	8710(8)	80(10) *
C(233)	6657(13)	3501(8)	8743(8)	95(13) *
C(234)	6867(13)	2655(8)	9063(8)	91(12) *
C(235)	6099(13)	2100(8)	9349(8)	106(13) *
C(236)	5121(13)	2392(8)	9315(8)	97(12) *
C(231)	4911(13)	3239(8)	8996(8)	48(8) *
SI(3)	2850(4)	203(3)	8604(3)	46(2) *
O(3)	3168(9)	1196(8)	8297(7)	62(5) *
C(312)	2039(11)	1094(8)	10111(10)	75(10) *
C(313)	1544(11)	1138(8)	10935(10)	101(13) *
C(314)	1240(11)	365(8)	11373(10)	88(11) *
C(315)	1430(11)	-452(8)	10986(10)	143(17) *
C(316)	1925(11)	-497(8)	10161(10)	123(14) *
C(311)	2229(11)	276(8)	9724(10)	51(8) *
C(322)	4764(13)	-177(8)	8932(8)	86(10) *
C(323)	5683(13)	-632(8)	8881(8)	105(14) *
C(324)	5856(13)	-1414(8)	8432(8)	93(12) *
C(325)	5111(13)	-1742(8)	8034(8)	105(13) *
C(326)	4192(13)	-1287(8)	8086(8)	85(11) *
C(321)	4018(13)	-505(8)	8535(8)	53(8) *
C(332)	1646(11)	-1068(9)	8002(8)	72(9) *
C(333)	987(11)	-1362(9)	7493(8)	81(10) *
C(334)	658(11)	-797(9)	6874(8)	83(11) *
C(335)	988(11)	62(9)	6765(8)	89(12) *
C(336)	1647(11)	357(9)	7274(8)	71(10) *
C(331)	1976(11)	-208(9)	7892(8)	47(7) *
SI(4)	3606(4)	2742(4)	5008(3)	48(2) *
O(4)	3427(9)	2639(9)	6043(7)	67(6) *
C(412)	5672(13)	2919(8)	4866(8)	67(9) *
C(413)	6662(13)	2640(8)	4662(8)	89(12) *
C(414)	6910(13)	1825(8)	4283(8)	86(12) *
C(415)	6168(13)	1289(8)	4107(8)	112(14) *

Table 5.6 ctd.

C(416)	5177(13)	1569(8)	4311(8)	90(12) *
C(411)	4929(13)	2384(8)	4690(8)	57(8) *
C(422)	2739(11)	1104(11)	4890(8)	94(13) *
C(423)	2245(11)	480(11)	4505(8)	111(14) *
C(424)	1867(11)	701(11)	3757(8)	85(12) *
C(425)	1983(11)	1547(11)	3393(8)	83(11) *
C(426)	2477(11)	2171(11)	3778(8)	62(9) *
C(421)	2855(11)	1949(11)	4527(8)	51(8) *
C(432)	3837(9)	4227(11)	3899(9)	79(11) *
C(433)	3585(9)	5065(11)	3585(9)	101(14) *
C(434)	2812(9)	5579(11)	4021(9)	90(11) *
C(435)	2291(9)	5254(11)	4771(9)	105(13) *
C(436)	2543(9)	4415(11)	5086(9)	72(10) *
C(431)	3316(9)	3902(11)	4651(9)	49(7) *
O(1G)	4259(13)	1324(15)	6849(11)	156(11) *
C(1G8)	5215(0)	864(0)	6670(0)	75(14)
C(1GA)	5348(35)	1542(35)	6935(35)	99(19)
C(2GB)	5922(0)	1412(0)	7009(0)	155(24)
C(2GA)	5992(50)	668(42)	6753(46)	192(30)

Anisotropic atoms have thermal parameters ($Å^2 \times 10^3$) of the form :
$\exp[-2\pi^2(U_{11}h^2a^{*2} + U_{22}k^2b^{*2} + U_{33}l^2c^{*2} + 2U_{23}klb^*c^* + 2U_{13}hla^*c^* + 2U_{12}hka^*b^*)]$

Atom	U_{11}	U_{22}	U_{33}	U_{23}	U_{13}	U_{12}
SI(1)	39(3)	50(4)	49(3)	-2(3)	-4(3)	3(3)
O(1)	57(9)	53(8)	39(9)	-2(7)	-3(7)	5(7)
C(112)	67(15)	92(19)	51(15)	7(13)	4(12)	-22(13)
C(113)	92(20)	124(24)	72(21)	11(17)	2(15)	-41(18)
C(114)	92(19)	124(23)	49(16)	22(18)	2(14)	-38(18)
C(115)	94(20)	144(28)	64(19)	-27(18)	30(16)	-5(18)
C(116)	66(15)	76(17)	74(18)	2(14)	8(13)	15(13)
C(111)	51(13)	51(14)	49(13)	15(12)	-6(10)	-4(11)
C(122)	78(16)	39(14)	95(17)	-5(13)	-14(13)	-13(12)
C(123)	111(21)	73(21)	92(19)	-16(15)	-41(16)	-1(15)
C(124)	99(19)	51(16)	95(20)	-5(15)	16(16)	4(15)
C(125)	100(19)	55(16)	84(17)	23(15)	-18(14)	16(14)
C(126)	63(15)	80(19)	63(15)	4(13)	-7(12)	5(12)
C(121)	56(14)	90(17)	37(13)	-3(12)	10(11)	-4(13)
C(132)	84(20)	119(22)	87(18)	-20(16)	-8(16)	-21(16)
C(133)	134(26)	156(30)	160(31)	4(25)	-44(26)	103(24)
C(134)	224(39)	61(18)	129(28)	1(19)	113(26)	-46(22)
C(135)	145(26)	113(23)	83(20)	1(17)	-22(20)	-50(20)
C(136)	69(15)	99(18)	64(16)	-31(14)	-24(14)	-22(14)
C(131)	48(14)	34(12)	81(17)	5(11)	-11(12)	-14(10)
SI(2)	53(4)	46(4)	43(3)	-6(3)	-4(3)	-6(3)
O(2)	65(9)	44(8)	64(9)	-16(7)	-15(7)	-4(7)
C(212)	87(16)	44(15)	61(17)	15(12)	-7(12)	-22(11)
C(213)	84(17)	87(18)	63(16)	-3(17)	-1(12)	-27(14)
C(214)	62(15)	80(20)	98(21)	29(17)	-3(14)	-12(13)
C(215)	91(18)	69(19)	84(19)	-10(15)	3(15)	-12(13)
C(216)	71(15)	31(13)	83(16)	0(14)	-10(12)	-2(10)
C(211)	55(13)	35(13)	48(14)	3(10)	-9(10)	-3(9)
C(222)	88(19)	55(15)	69(18)	-9(12)	22(14)	-14(13)
C(223)	100(20)	83(19)	95(21)	-8(17)	27(19)	1(15)
C(224)	205(36)	64(18)	61(20)	9(14)	25(22)	34(22)
C(225)	205(34)	89(20)	50(20)	-21(15)	-22(19)	23(21)
C(226)	162(24)	82(18)	35(15)	-5(13)	-21(17)	-28(16)
C(221)	85(17)	31(12)	36(13)	2(9)	6(12)	-1(11)
C(232)	49(15)	114(20)	73(16)	16(14)	8(13)	-19(16)
C(233)	74(21)	103(22)	103(20)	23(17)	-4(15)	-15(15)
C(234)	73(18)	106(22)	96(20)	-8(17)	-20(15)	-3(17)
C(235)	122(24)	74(19)	129(23)	9(17)	-39(20)	-7(19)
C(236)	81(20)	98(23)	117(22)	5(18)	-31(16)	-22(15)
C(231)	71(15)	31(12)	43(12)	0(10)	-11(11)	13(11)
SI(3)	55(4)	44(4)	38(3)	-1(3)	-2(3)	0(3)
O(3)	79(10)	49(9)	53(9)	2(7)	5(8)	-3(7)
C(312)	90(17)	78(18)	56(17)	-11(14)	-2(13)	-1(13)
C(313)	135(23)	94(21)	66(19)	-10(16)	3(17)	27(17)

Table 5.6 ctd.

C(314)	94(18)	127(23)	40(15)	-15(17)	-1(13)	13(17)
C(315)	261(37)	103(23)	55(19)	-17(17)	46(21)	-97(23)
C(316)	233(33)	76(19)	56(18)	-9(15)	24(19)	-81(20)
C(311)	49(12)	63(14)	42(12)	-10(12)	-9(10)	6(11)
C(322)	67(16)	100(19)	91(18)	-38(15)	-11(15)	16(16)
C(323)	136(27)	73(18)	103(21)	-45(16)	0(18)	9(17)
C(324)	26(13)	149(27)	101(20)	-5(18)	4(13)	6(15)
C(325)	85(19)	88(19)	135(24)	-30(17)	3(19)	34(18)
C(326)	90(20)	72(17)	96(19)	-35(15)	-8(15)	-17(15)
C(321)	77(15)	54(14)	32(12)	3(10)	-6(11)	-23(12)
C(332)	89(17)	60(17)	66(16)	-20(13)	-3(14)	-13(13)
C(333)	75(18)	71(17)	94(20)	-41(16)	-1(15)	6(14)
C(334)	58(16)	120(23)	69(19)	-39(17)	3(14)	5(17)
C(335)	68(18)	142(26)	55(16)	5(17)	-9(14)	16(16)
C(336)	46(14)	110(19)	54(15)	2(15)	-2(12)	3(13)
C(331)	61(13)	47(13)	34(12)	-10(10)	-6(10)	1(11)
SI(4)	42(3)	62(4)	39(4)	-2(3)	-4(3)	0(3)
O(4)	51(9)	111(12)	34(8)	-2(8)	4(7)	3(8)
C(412)	54(15)	78(16)	68(15)	-1(13)	-4(13)	-8(14)
C(413)	67(20)	114(23)	89(19)	0(17)	-14(15)	-16(15)
C(414)	39(15)	156(26)	59(16)	-1(17)	1(12)	14(17)
C(415)	109(23)	156(26)	69(18)	-46(17)	-2(17)	0(23)
C(416)	63(18)	127(23)	77(18)	-48(16)	0(13)	9(15)
C(411)	73(16)	70(15)	28(12)	-2(11)	-2(11)	-12(13)
C(422)	119(21)	106(21)	66(16)	5(16)	-26(15)	-53(17)
C(423)	153(26)	80(20)	111(23)	11(18)	-39(20)	-45(18)
C(424)	78(17)	91(22)	92(20)	-35(16)	-19(15)	-14(15)
C(425)	81(18)	97(20)	73(17)	-14(17)	-8(14)	-14(15)
C(426)	74(15)	56(15)	59(15)	2(12)	-13(12)	-21(12)
C(421)	73(14)	29(12)	51(14)	6(10)	-6(11)	-7(10)
C(432)	129(21)	67(17)	41(15)	0(12)	-6(15)	-24(15)
C(433)	158(28)	94(22)	53(17)	3(17)	-8(17)	-31(19)
C(434)	109(22)	85(19)	87(21)	1(18)	-40(16)	-16(18)
C(435)	80(19)	106(25)	125(26)	-26(19)	4(18)	-7(17)
C(436)	69(16)	46(14)	98(18)	-23(14)	6(14)	2(12)
C(431)	48(13)	61(13)	43(13)	-7(11)	-22(10)	-2(11)
O(1G)	104(15)	244(24)	100(15)	87(15)	22(12)	43(15)

References.

5.1. P. Schuster; G. Zundel; C. Sanderfy (Eds.) '*The Hydrogen Bond II, Structure and Spectroscopy.*' Chapter 8. North-Holland Publishing Co., Amsterdam, (1976).

5.2. E. Weber; K. Skobridis; I. Goldberg. *J. Chem. Soc., Chem. Commun.*, 1195, (1989).

5.3. W. C. Hamilton. *Acta Crystallogr.*, **18**, 502, (1965).

5.4. M. Braun; H. Reuter; H. Puff. Personal communication.

5.5. L. Pauling. '*The Nature of the Chemical Bond.*' Cornell University Press, New York, (1960).

5.6. W. H. Baur. *Acta Crystallogr.*, **B**28, 1456, (1972).

5.7. D. H. Williams; I. Fleming. '*Spectroscopic methods in Organic Chemistry.*' 3rd edition, McGraw-Hill, London, (1980).

5.8. E. Bye; W. B. Schweizer; J. D. Dunitz. *J. Am. Chem. Soc.* **104**, 5893, (1982).

CHAPTER 6 : CRYSTAL AND MOLECULAR STRUCTURE - CLASS D.

The host to guest ratios, space group and cell parameters are summarised at the beginning of the discussion about each structure. Fractional atomic coordinates, thermal parameters and details of hydrogen bonding are given in Tables 6.2 - 6.9 at the end of this chapter.

The atom labelling scheme for the host, tri-1-naphthylsilanol, is given in Figure 6.1. The labelling used for the guest is shown at the beginning of the discussion about each compound. The geometry of the host is discussed in detail at the end of this chapter.

DUNCAN : $(C_{30}H_{22}OSi)$. dmso

Space group : $P\bar{1}$	H:G 1:1
a = 9.122(2)Å	α = 61.75(2)°
b = 12.852(3)Å	β = 87.79(2)°
c = 12.873(2)Å	γ = 83.49(2)°
Z = 2	

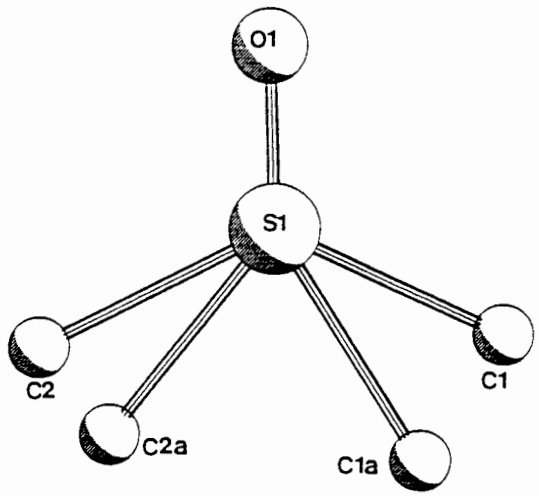

Direct methods, in this case, found 34 atoms, *i.e.* the silicon, oxygen and carbon atoms of the host as well as the sulphur and oxygen of the guest. Refinement proceeded in the usual way. After several least-squares cycles, four peaks of relatively high electron density were generated. These were assigned to the methyl carbons of the dmso, each

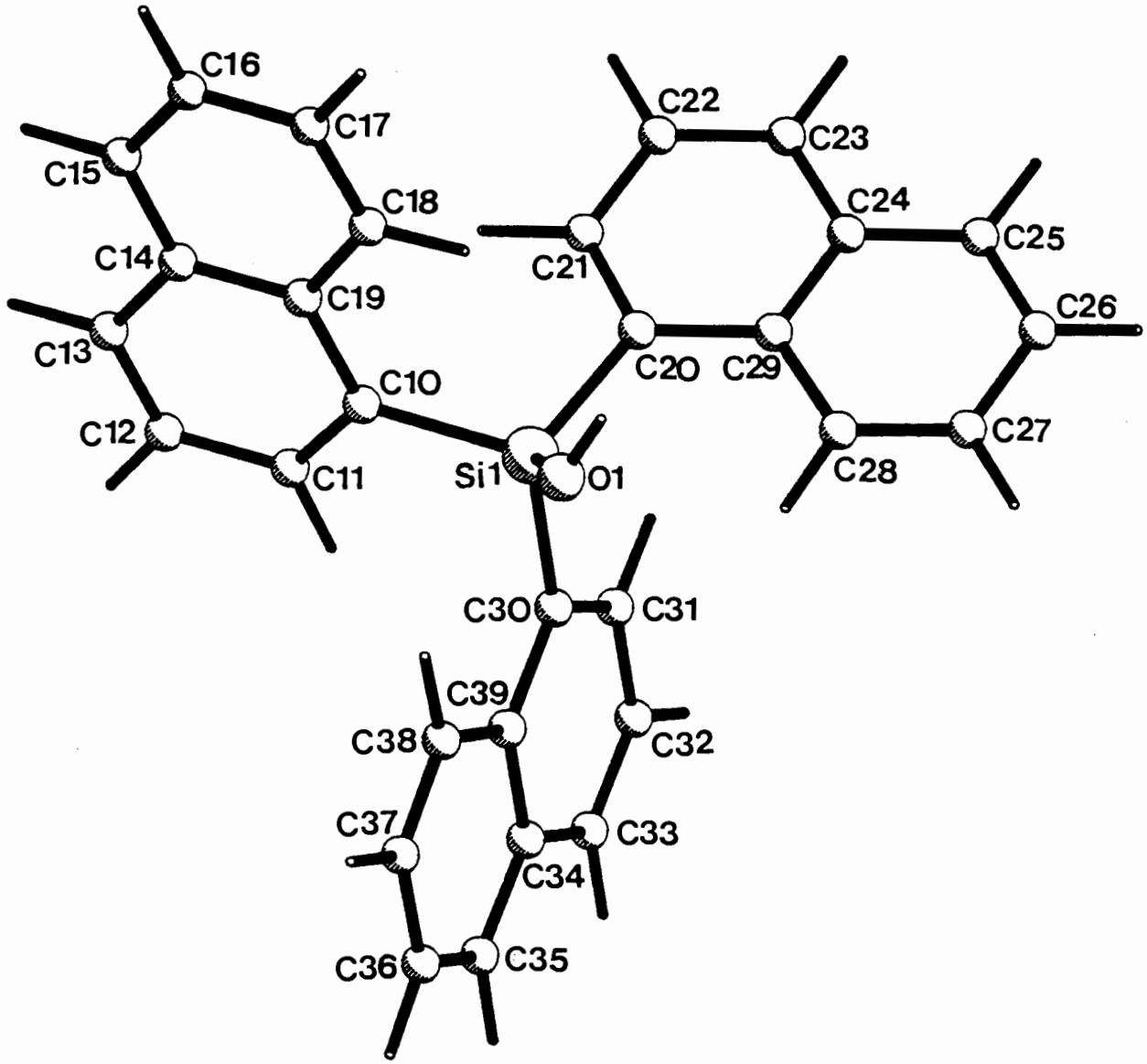

Figure 6.1. Atom labelling scheme for tri-1-naphthylsilanol (Class D).

methyl being statistically disordered over two positions. The four "partial" carbons were inserted into the model, with site occupancies, as shown below, in proportion to the heights at which they had appeared in the difference Fourier map :

Atom	S.O.F.
C(1G)	0.70
C(1GA)	0.30
C(2G)	0.54
C(2GA)	0.46

All non-hydrogen atoms were treated anisotropically. Hydrogens were geometrically placed at 1.00 Å from the host's naphthyl carbons and linked to a common temperature factor. Because of the disorder in the dmso's methyl carbons, no attempt was made to model the methyl hydrogens.

The hydroxyl hydrogen was found in a difference Fourier map and constrained to its parent oxygen as well as to the dmso's oxygen.

There was one peak of high electron density (0.55 $eÅ^{-3}$) remaining after the final refinement. This was in the region of the dmso methyls and was probably due to further disorder. Final coordinates and thermal parameters are listed in Table 6.3.

Molecular structure.

The dmso guest is disordered as shown in Figure 6.2 which also shows the relationship between the host and guest molecules in the asymmetric unit.

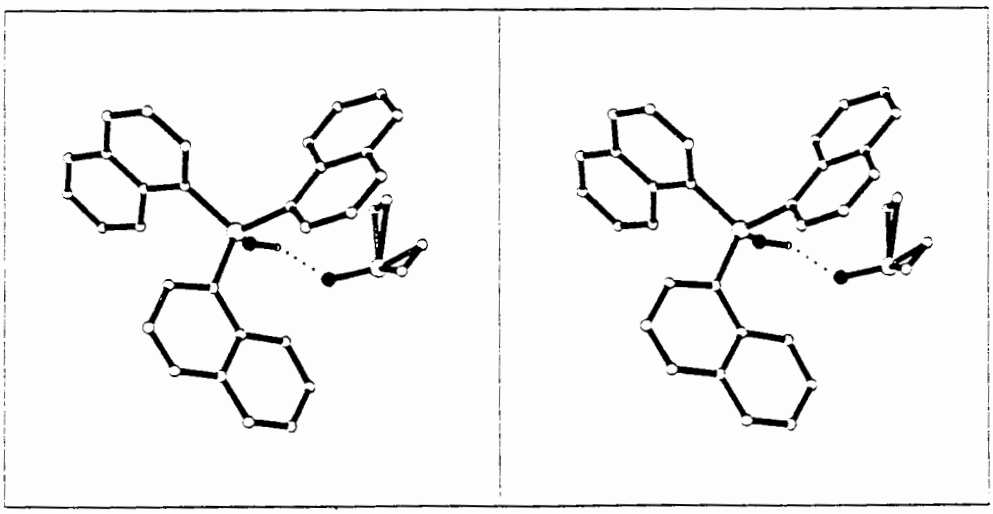

Figure 6.2. Molecular structure of **DUNCAN**, showing the disorder of the guest.

Dmso molecules are found in an approximately hourglass-shaped pocket, as shown in Figure 6.3. For clarity, C(1GA) and C(2GA) have been omitted. The cavity is approximately 5 x 4 x 6 Å in dimension at its maximum cross-section.

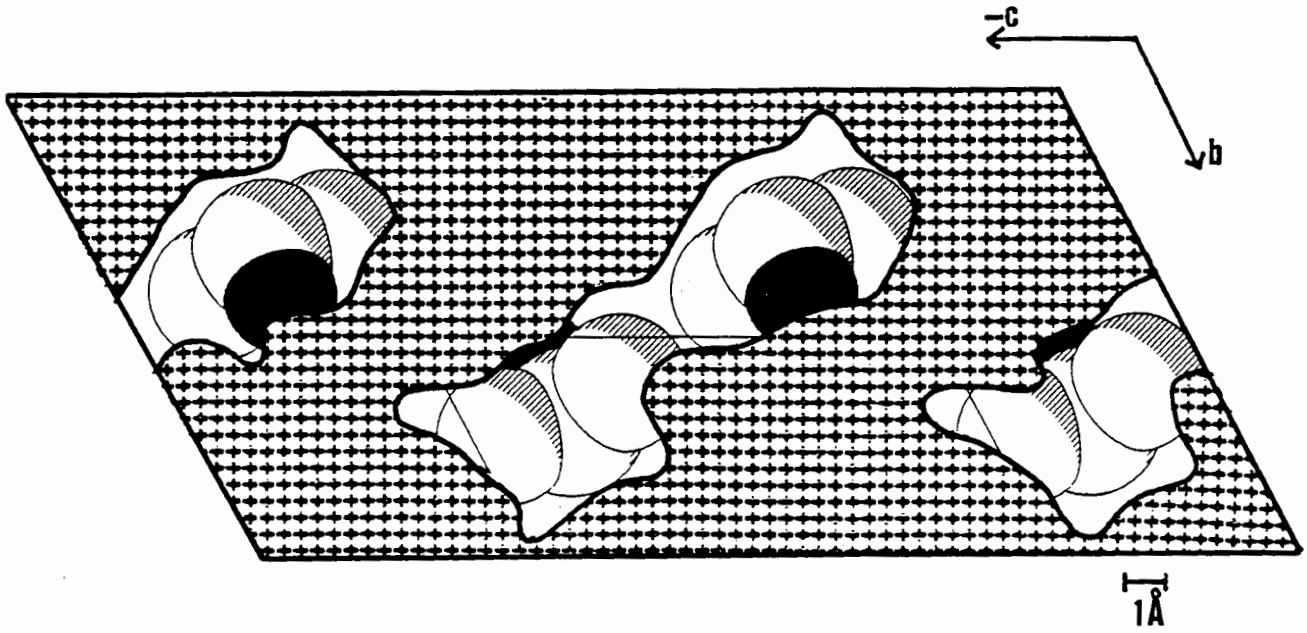

Figure 6.3. Cross-section through **DUNCAN** at x = 0.1. Only one of the guest's orientations is shown.

A packing diagram of **DUNCAN**, viewed down [100], (Figure 6.4) shows the way in which each dmso is placed among naphthyl moieties of neighbouring hosts. The molecules are hydrogen bonded in units of one host and one guest with hydrogen bonds which are almost parallel to [010].

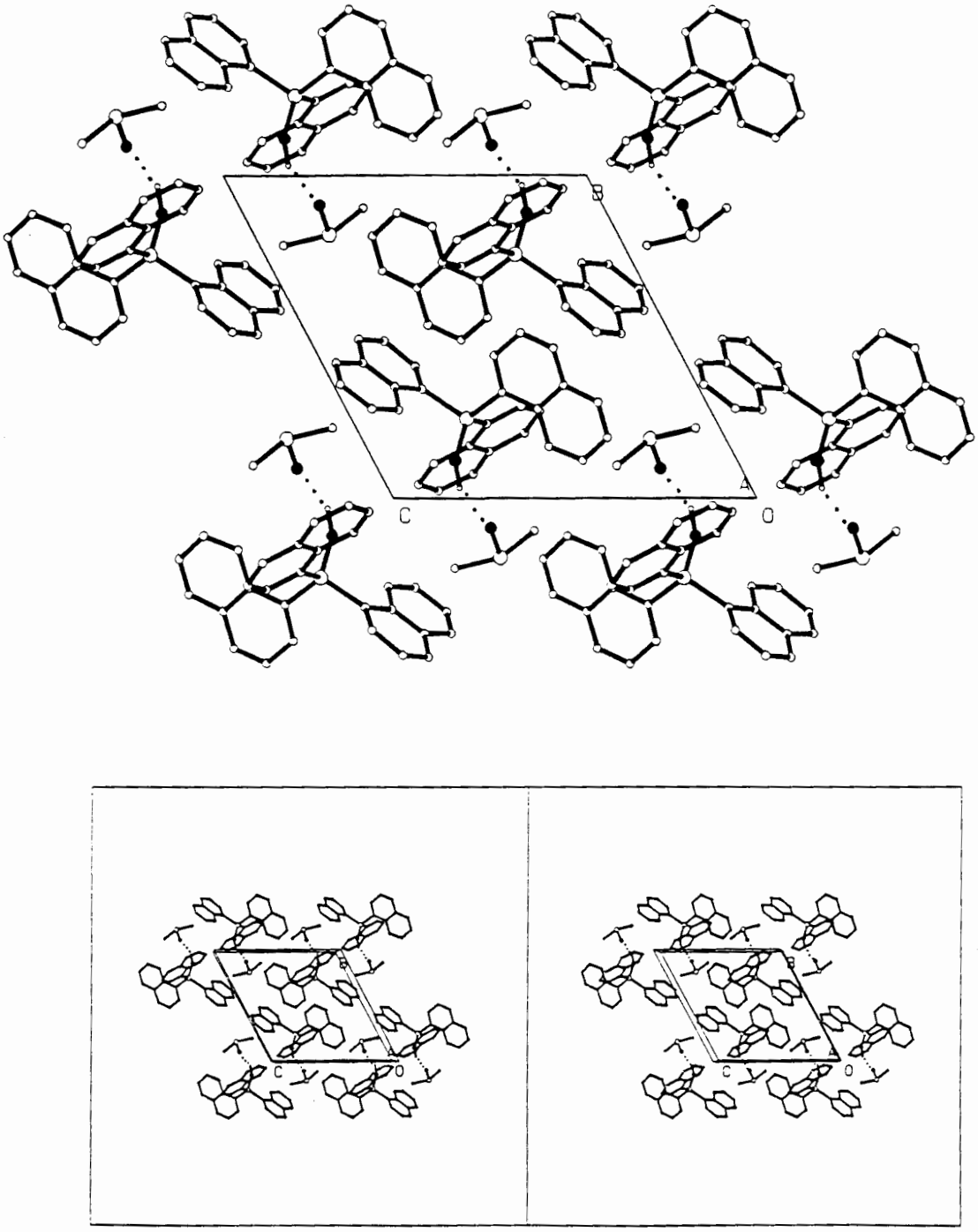

Figure 6.4. Packing diagram of **DUNCAN** viewed along [100]. Only one orientation of the guest is shown, oxygen atoms are shaded.

NADIO : ($C_{30}H_{22}OSi$) . dioxane

Space group : $P\bar{1}$	H:G = 1:1
a = 9.298(4) Å	α = 115.63(5)°
b = 12.577(9) Å	β = 90.99(3)°
c = 12.859(6) Å	γ = 92.34(5)°
Z = 2	

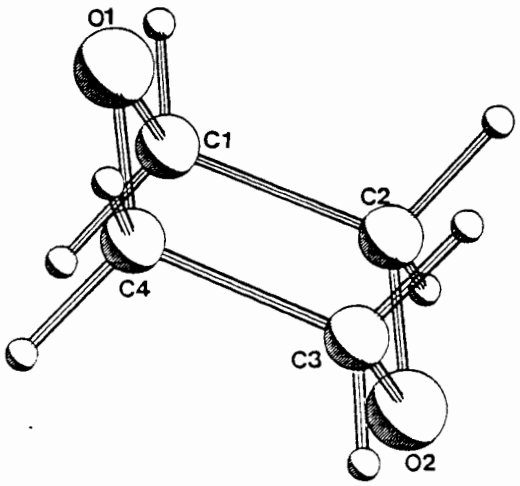

Structure solution and refinement for this compound were routine. After all the non-hydrogen atoms had been refined anisotropically and the hydrogens treated in the usual manner, the R factor was 0.038.

Although the guest was well-ordered, its atomic temperature factors were, on average, twice as high as those of similar host atoms. The maximum shift/e.s.d. in the final cycle was 0.002 and no feature on the electron density map was greater than 0.23 or less than -0.17 $eÅ^{-3}$. Final coordinates and thermal parameters are listed in Table 6.4

Molecular structure.

This structure shares many features in common with **W1DIOX**. The relationship between host and guest is almost identical (cf Figure 6.5 with Figure 5.2)

The dioxane molecule adopts a chair conformation, according to the parameters described by Duax and Norton.[6.1] Each dioxane is held within the host lattice in a "pocket", thus allowing this compound to be classified an *aediculate*.[6.2]

The guest's O - C and C - C distances, as well as the ring's internal angles are all within accepted limits.

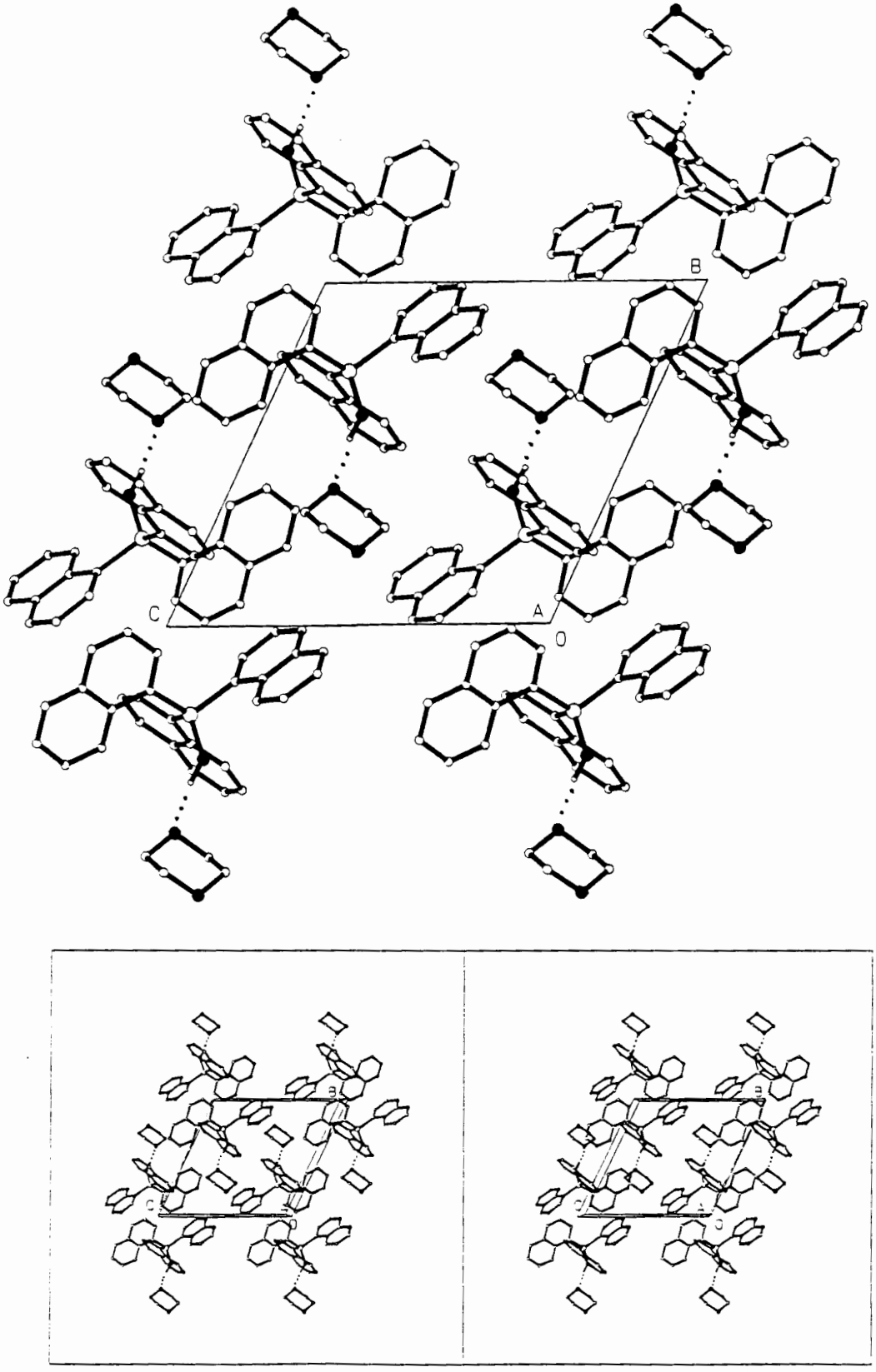

Figure 6.5. Packing diagram of **NADIO** viewed along [100]. Oxygen atoms are shaded.

NATOL : ($C_{30}H_{22}OSi$) . toluene

Space group : $P\bar{1}$	H:G = 1:1
a = 9.465(3) Å	α = 116.07(2)°
b = 12.424(2) Å	β = 91.67(2)°
c = 13.344(4) Å	γ = 92.77(2)°
Z = 2	

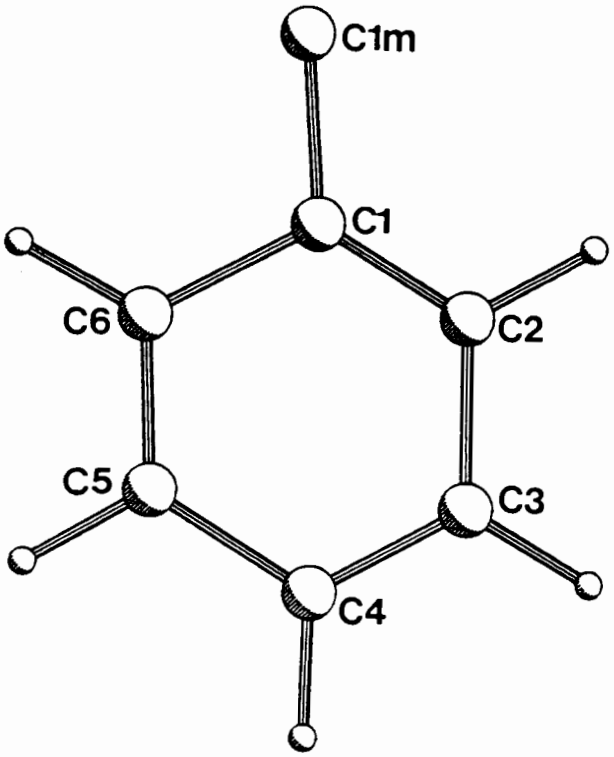

Refinement of the host molecule proved uneventful. The aromatic ring of the guest was easily located and refined anisotropically with hydrogens geometrically fixed. The methyl carbon of the toluene however, emerged only late in the refinement. Its temperature factor was higher than those of the ring carbons and it was treated isotropically. The max shift/e.s.d. in the final cycle was 0.005; although there was a peak of residual electron density of 0.83 $eÅ^{-3}$, this was in the region of the guest and was ascribed to an imperfect model of the toluene. An attempt was made to include this peak, but doing so did not produce a sensible model of toluene (angles around the sp^2 carbon ranged from 90° to 150°). Final coordinates and thermal parameters are listed in Table 6.5. The molecular structure of **NATOL** is discussed along with that of the next compound.

ODIN : ($C_{30}H_{22}OSi$) . o-xylene

Space group : $P\bar{1}$	H:G = 1:1
a = 9.399(5) Å	α = 115.96(4)°
b = 12.475(6) Å	β = 90.37(4)°
c = 13.577(5) Å	γ = 92.71(4)°
Z = 2	

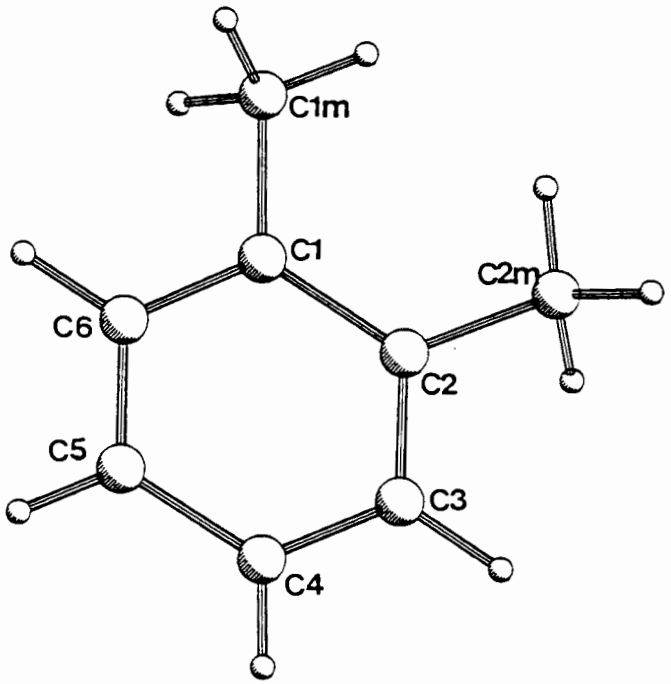

This structure is very similar to that of **NATOL.**

Although the crystal was of an approximately uniform size (0.25 x 0.22 x 0.31 mm), its absorption was high. The average transmission was 69.79% with maxima and minima of 99.50% and 47.18%. The data were corrected for absorption using these values, and two parallel refinements followed, one using the absorption corrected data and one using the uncorrected data.

After the structure had been fully refined using both data sets, the final models were compared by performing the Hamilton test [6.3] on the R_G factors obtained from the two final runs. This indicated, that at the 95% significance level, the uncorrected data set gave a better model. All parameters reported for **ODIN** are those obtained using this data set.

The *o*-xylene molecule was located in the same position and orientation as the toluene in **NATOL** and proved to be well-ordered. Even the methyl carbons had relatively low thermal parameters (U_{equiv} = 0.06 Å^2), close to U_{equiv} of the ring carbons. Hydrogens were placed in calculated positions on the ring and methyl carbons.

The final shift/e.s.d. was 0.006 and there were no peaks on the final electron density map greater than 0.23 eÅ^{-3} or less than -0.36 eÅ^{-3}. Final coordinates and thermal parameters are listed in Table 6.6.

Molecular structure.
Since **NATOL** and **ODIN** are very similar, their packing will be discussed together.

The guest molecules (either toluene of *o*-xylene) lie in hour-glass shaped channels parallel to [100] which have approximately circular constrictions of ≈1.5 Å at x = 0. The positions of guest molecules relative to host are shown in Figure 6.6 ,a packing diagram down [100]. In this view the guests are seen edge-on.

There is evidence of hydrogen bonding between the hydroxyl group of the host and the aromatic π electrons of the guest molecules. The centroid•••O distance is 3.40 Å, with a centroid•••H - O angle of 160° (see Table 6.2). Further evidence for this hydrogen bonding is found on examining the infrared spectra of these compounds (see Table 3.4). The shift in ν from the non-hydrogen-bonded α-phase to each of these compounds is -65 and -60 cm^{-1} for **NATOL** and **ODIN** respectively.

A similar situation has recently been reported.[6.4] An X-ray diffraction study of Na_4[calix[4]arene sulphonate] • 13.5 H_2O, found a water molecule embedded in the cavity of four aromatic groups. The oxygen atom was 3.16 and 3.19 Å from the centroids of the nearest aromatic rings, with centroid•••H - O angles of 133° and 127°.

In Figure 6.7, the channel has been mapped using OPEC. The "shallowness" of the channel in y is obvious, as it is seen to widen between y = 0 and y = 0.2 and then to narrow again until it is almost closed at y = 0.4.

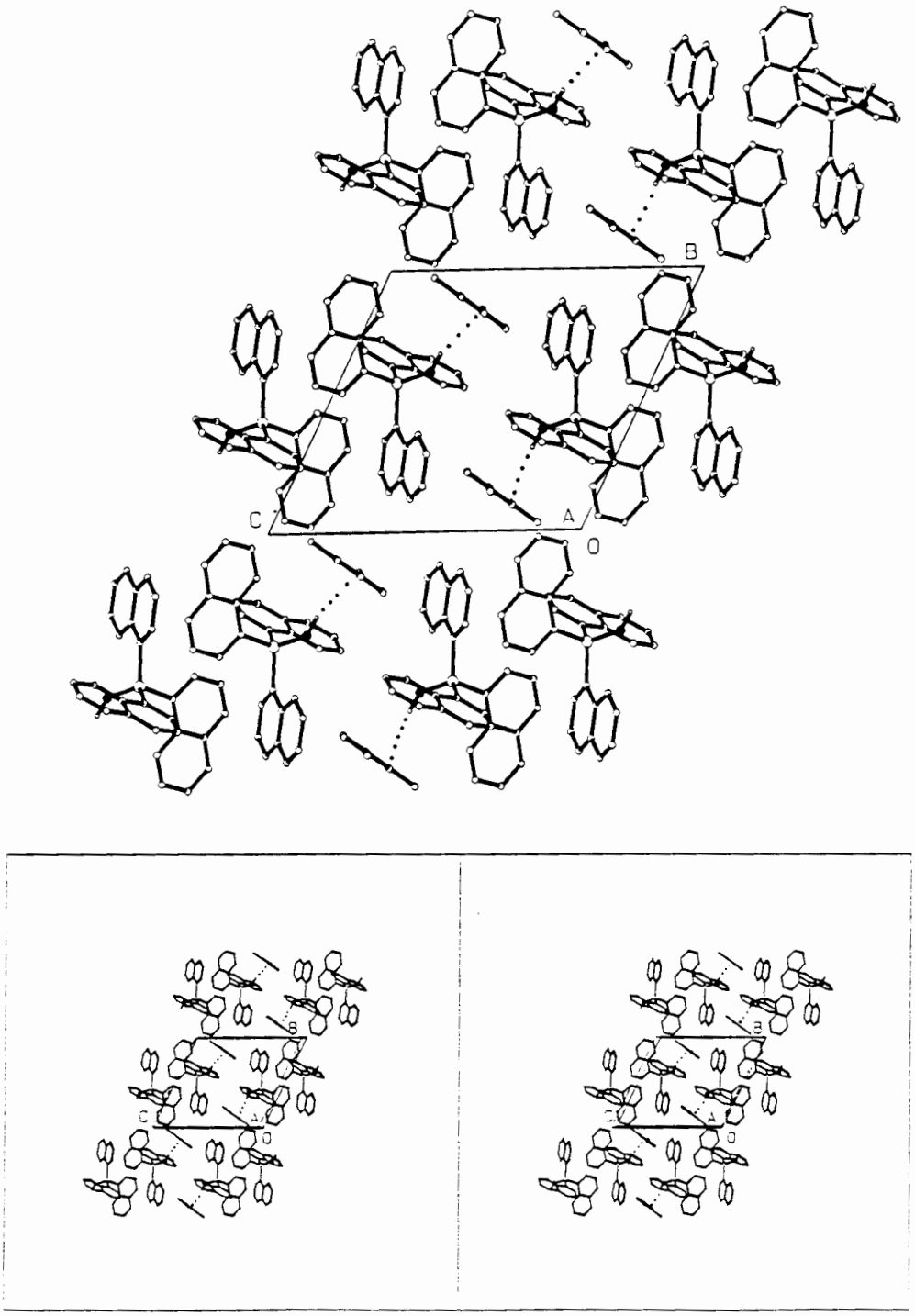

Figure 6.6. Packing diagram of **ODIN** viewed along [100]. Xylene molecules are seen edge-on. Dotted lines indicate O-H···aryl hydrogen bonds.

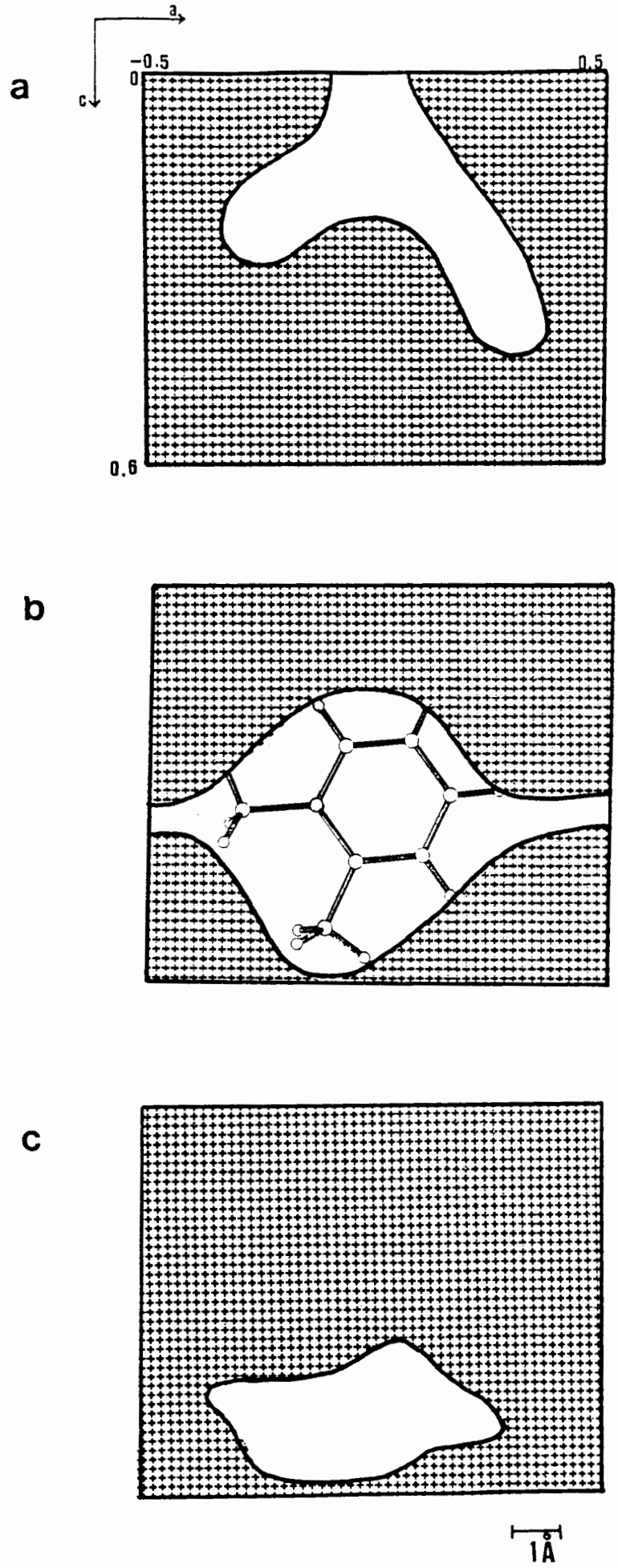

Figure 6.7. Cross-sections through **ODIN** at (a) y = 0, (b) y = 0.15 and (c) y = 0.3. An *o*-xylene molecule is shown in (b).

MAXINE : ($C_{30}H_{22}OSi$) . m-xylene

Space group : $P\bar{1}$	H:G = 1:1
a = 11.974(3) Å	α = 65.16(1)°
b = 12.243(2) Å	β = 72.50(2)°
c = 12.317(2) Å	γ = 61.85(2)°
Z = 2	

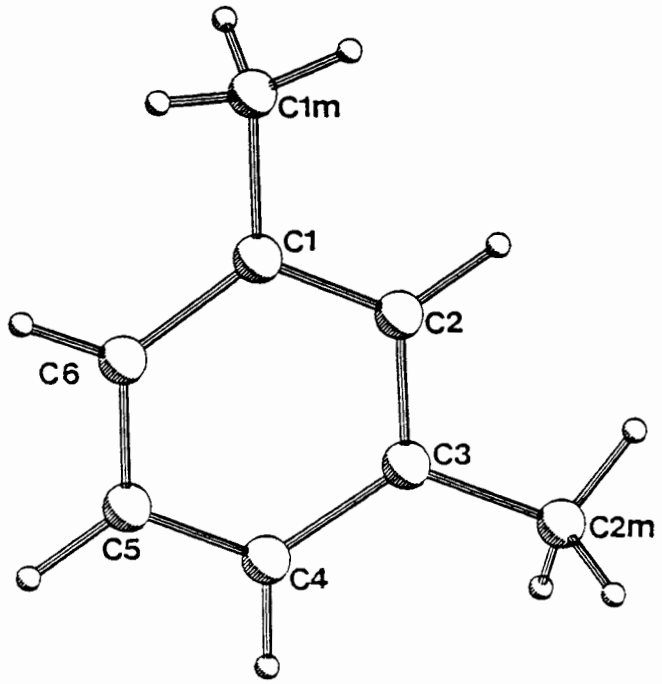

Although the empirical formula of this compound and that of the previous one, **ODIN**, are identical, the structures are not isomorphous.

The structure was refined in the same way as before, to a final R factor of 0.038. The methyl hydrogens of the *m*-xylene had U_{iso} = 0.19 and 0.13 $Å^2$ which were much higher than U_{iso} for the ring hydrogens (0.08 $Å^2$). There were no peaks in the electron density map higher than 0.20 nor lower than -0.25 $eÅ^{-3}$. Final coordinates and thermal parameters are listed in Table 6.7.

Molecular structure.

The manner in which this structure packs is quite different from that displayed in **NATOL** and **ODIN**, as Figure 6.8 shows.

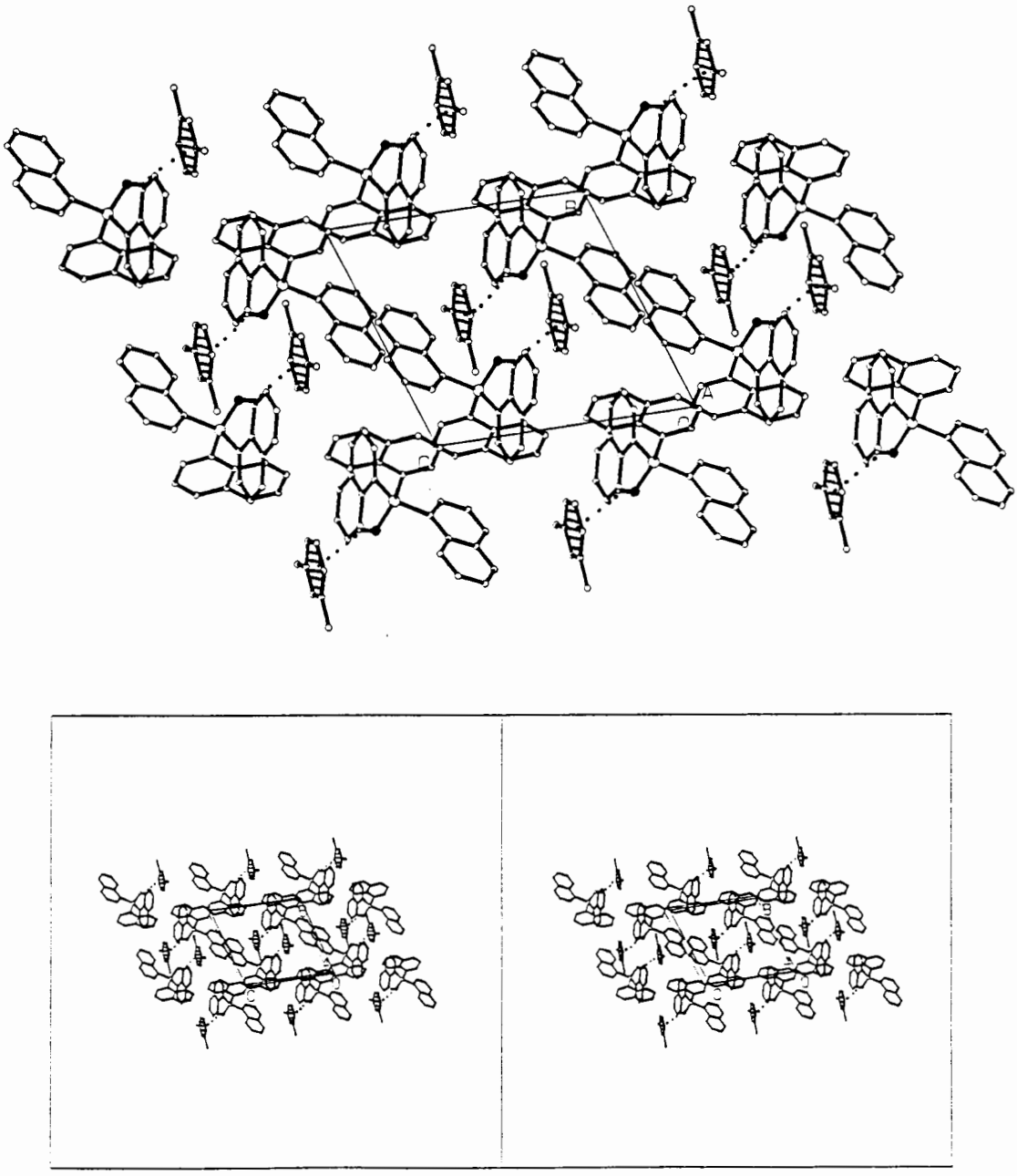

Figure 6.8. Packing diagram of **MAXINE** viewed along [100]. Xylene molecules are shaded.

The major stabilizing factor in this structure appears to be an O - H···aryl hydrogen bond of the type seen in **NATOL** and **ODIN**. Details are given in Table 6.4.

m-Xylene molecules are found in cavities, centred at z = 0.3 and z = 0.7, and connected by narrow channels. A guest is shown in such a cavity in Figure 6.9.

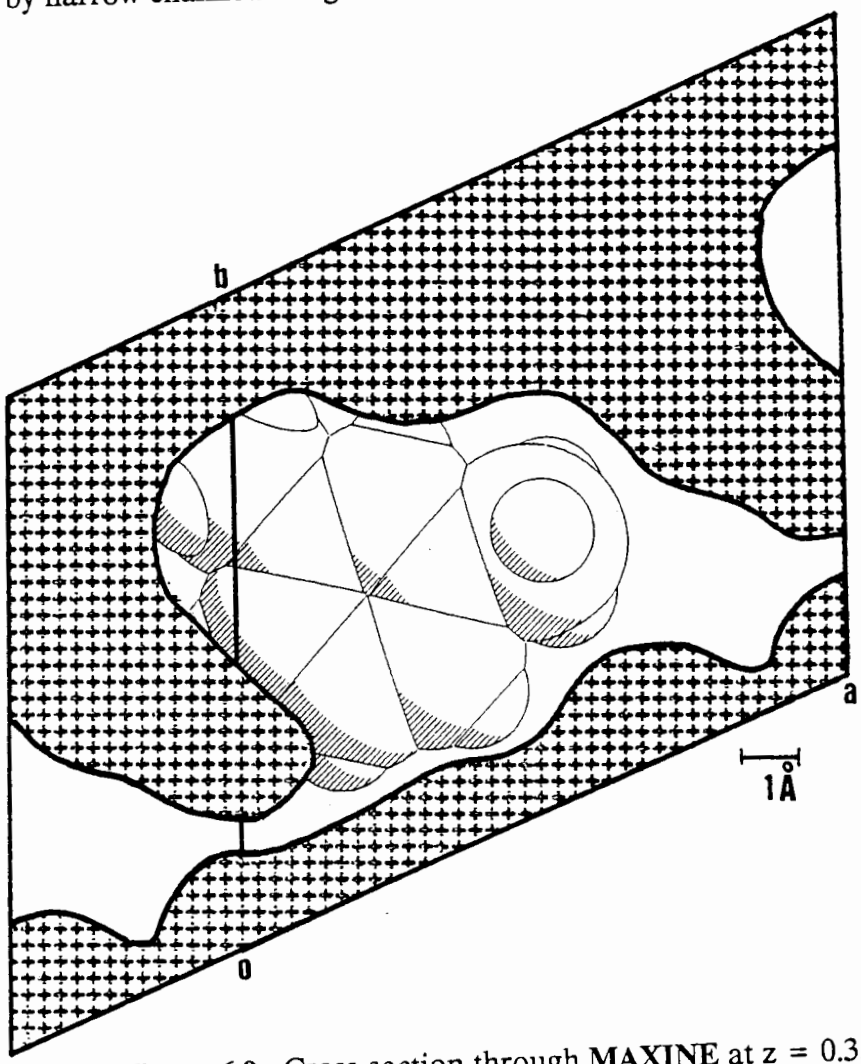

Figure 6.9. Cross-section through **MAXINE** at z = 0.3.

An examination of the channel in **ODIN** was made to explain the differences in the structures of **ODIN** and **MAXINE**. Figure 6.10 shows space-filled molecules of toluene, *o*-xylene, *m*-xylene and *p*-xylene. The orientation chosen was that of the *o*-xylene molecule in **ODIN**. Superimposed on each molecule is a cross-section of the widest part of the channel. (taken from Figure 6.7 (b)). It is clear that while toluene and *o*-xylene can be easily accomodated in this channel, *m*- and *p*-xylene cannot. The shallowness of the channel in y (<4.5 Å) precludes the re-orientation of these molecules in a way that would allow them to be accommodated. It is therefore necessary for the lattice made of host molecules to rearrange itself in order to include these guests.

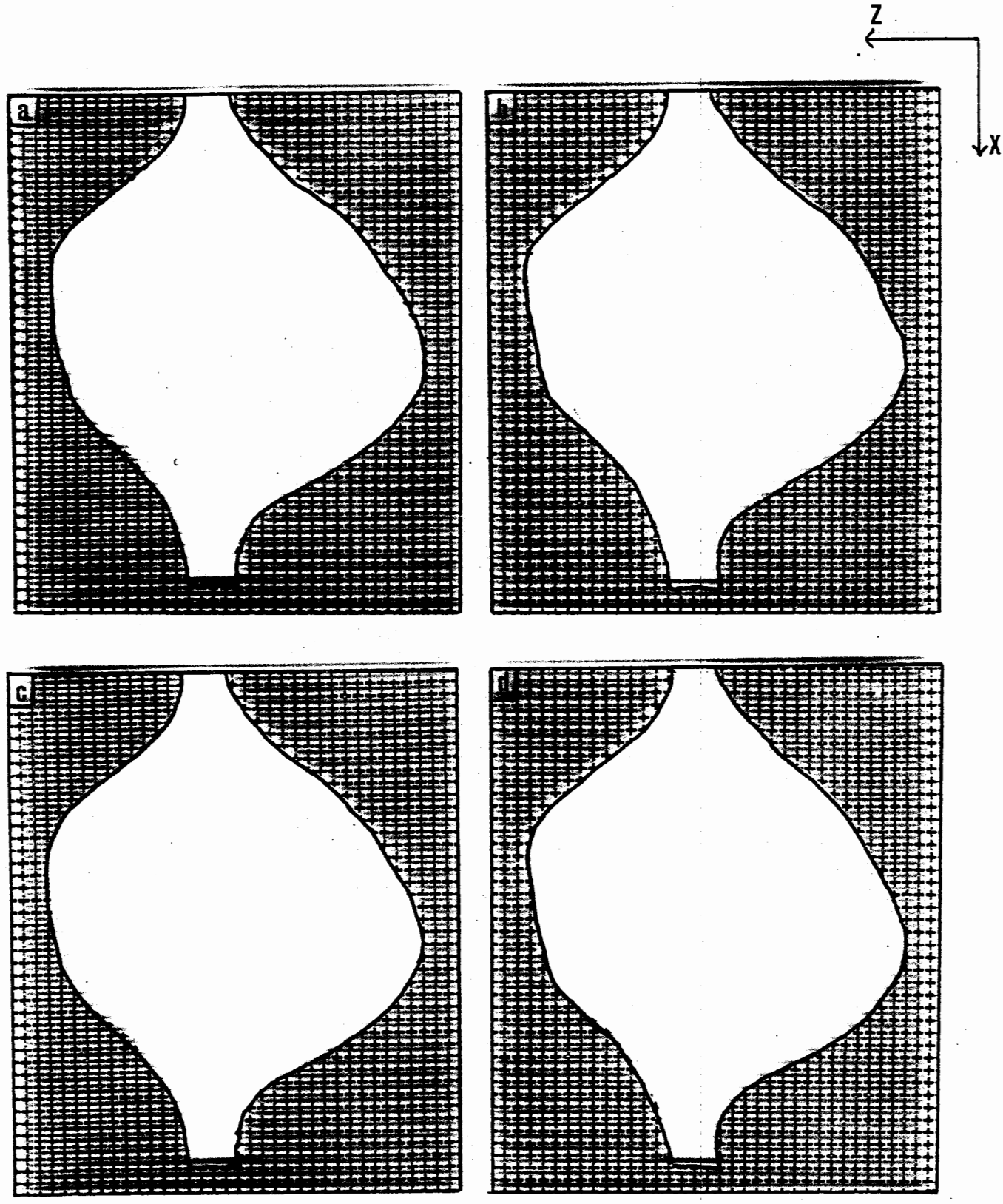
Z
X
a
b
c
d

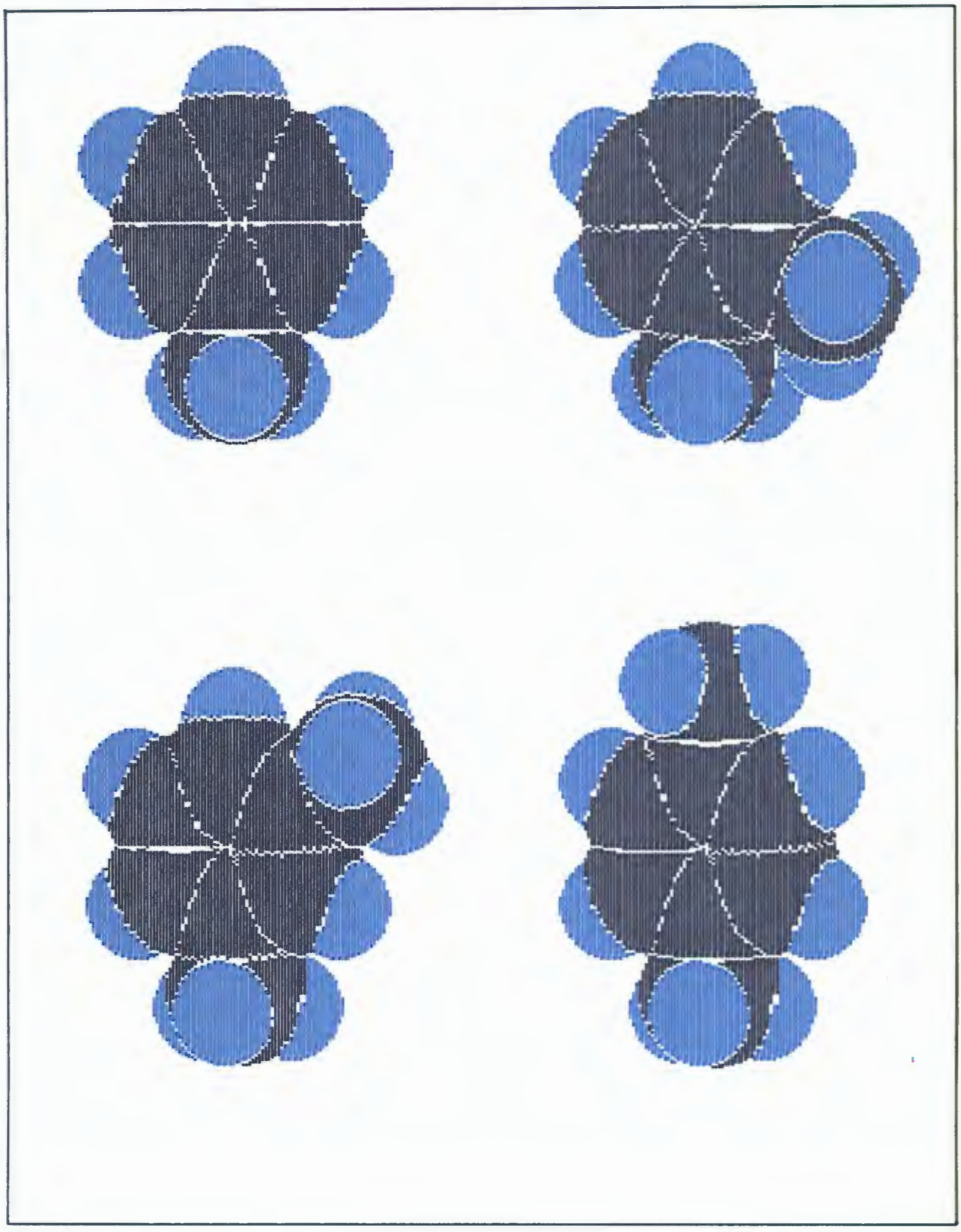

Figure 6.10. Cross-section through **ODIN** at y = 0.15 superimposed on molecules of (a) toluene, (b) *o*-xylene, (c) *m*-xylene and (d) *p*-xylene.

NAPPY : ($C_{30}H_{22}OSi$) . 2(p-xylene)

Space group : $P\bar{1}$	H:G = 1:2
a = 9.315(6) Å	α = 82.51(2)°
b = 12.462(1) Å	β = 82.08(4)°
c = 15.901(4) Å	γ = 87.25(5)°
Z = 2	

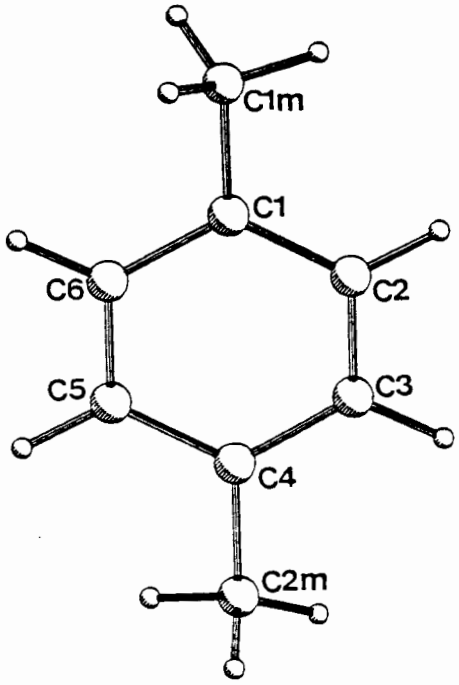

The host-guest stoichiometry of **NAPPY** had been determined by NMR, TG and density to be 1:2. When the structure was solved by direct methods, only 1½ guests were located. These atoms were refined for several cycles before the peaks corresponding to the missing "half-guest" were seen.

There are three crystallographically independent sites for the guest molecules, only one of which (guest A) does not fall on a centre of inversion. Guests B and C are located on centres of inversion at (½ ½ ½) and (½ 0 ½), which are Wyckoff positions *h* and *f* respectively.

All non-hydrogen atoms were refined anisotropically and all hydrogens, except the hydroxyl, were modelled by fixing them geometrically to their parent atoms. The hydroxyl hydrogen was found in a difference Fourier map and constrained to 0.93 Å from its oxygen.

The final max. shift/e.s.d. was 0.042 and the maximum and minimum residual densities were 0.30 and -0.20 $eÅ^{-3}$. Final coordinates and thermal parameters are listed in Table 6.8.

Molecular structure.
This compound differs from the previous three in that the host : guest ratio is 1:2. Within the crystal structure, guest molecules occupy three crystallographically different sites, which are shown in Figure 6.11, a packing diagram viewed down [100], with guests removed and their sites labelled. Figure 6.12 indicates the orientations of the *p*-xylene molecules within these sites.

The centre of the ring in guest A is 3.28 Å from the oxygen atom of the host, and the centroid•••H -O angle is 148°, thus identifying this as another hydrogen bond. Details are given in Table 6.2.

Figure 6.13 is an OPEC analysis of the empty volume in the cell. The entire asymmetric unit is shown, sectioned at intervals of 0.93 Å. The space occupied by host molecules is relatively small, leaving a great deal of space for guest molecules.

Tri-1-naphthylsilanol almost invariably forms compounds with host to guest ratios of 1:1. **NAPPY** is the only known exception. The change in cell parameters in going from **ODIN** to **NAPPY** involves an elongation of the c-axis with small changes in cell angles. Thus, the packing observed in these two structures was compared to try to establish how an extra xylene molecule could have been included.

Guest A may be compared with the *o*-xylene in **ODIN**, since both are held in position by O - H• • •aryl interactions.

The planar, narrow *p*-xylene molecule is able to insinuate itself between the naphthyl moieties of two neighbouring hosts, thus forcing the hosts further apart (guest C). This is far less likely for the lower-symmetry *o*- or *m*-xylene molecules. This process is probably stabilized by π - π interactions or by methyl• • •aryl interactions. In fact, one of guest C's methyl hydrogens is 2.95 Å from a naphthyl ring and pointed at its centre.

The resultant increase in volume, caused by the forcing-apart of the host molecules, opens up another site, that occupied by guest B.

To test this hypothesis, the potential energy environments of the *p*-xylene molecules in the lattice were evaluated using EENY. The minimisation for a given guest was carried out by surrounding it by an appropriate number of host and other guest molecules. These were held at constant positions while the guest under study was allowed to find its minimum energy environment by incremental translations and rotations. The minimum potential energies thus obtained, were -73.0, -47.0 and -67.0 $kJmol^{-1}$ for guests A, B and C respectively. Since guest A is stablized by hydroxyl • • • aryl hydrogen bonding and guest C by methyl • • • aryl interactions, it follows that the expected potential energy would be :

more stable A > C > B *less stable*

which is the order found by EENY.

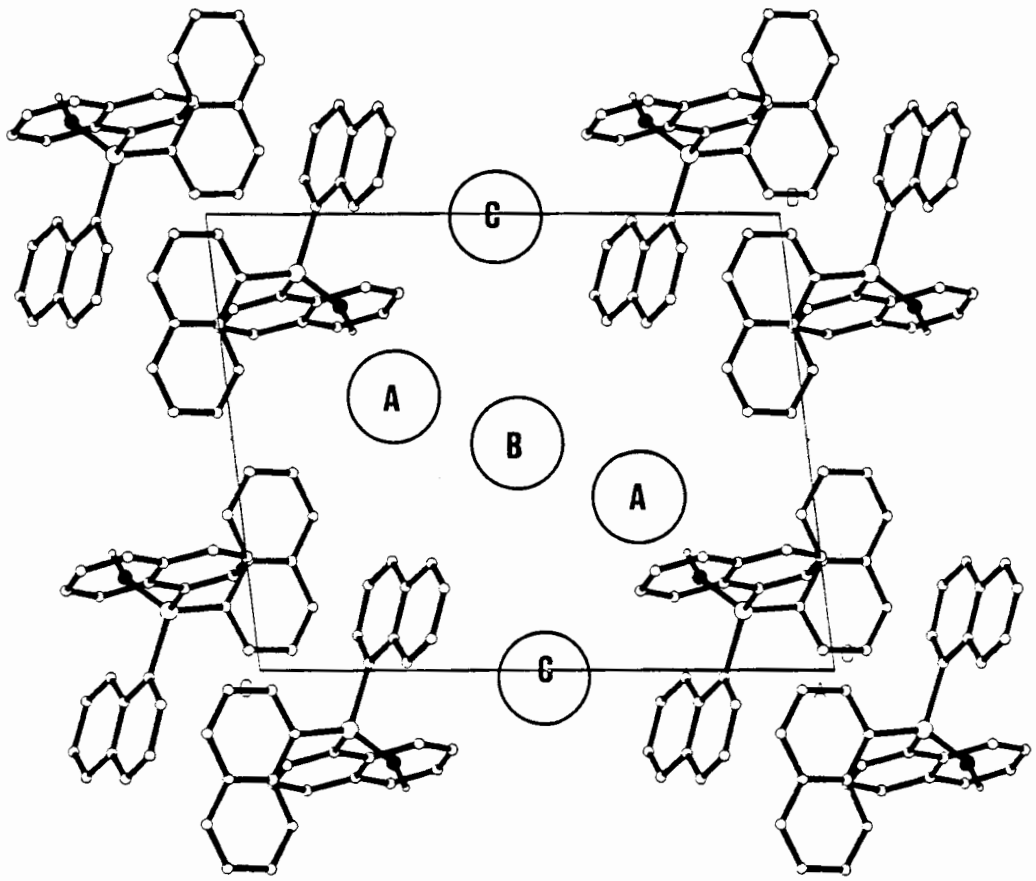

Figure 6.11. The three crystallographically distinct guest sites are indicated by the labels A, B and C.

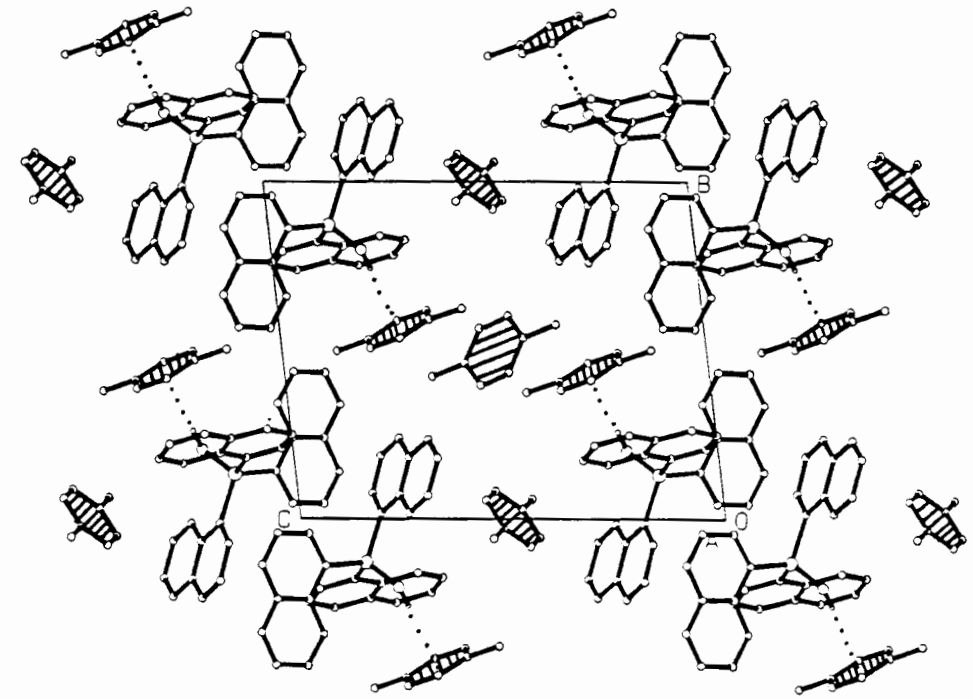

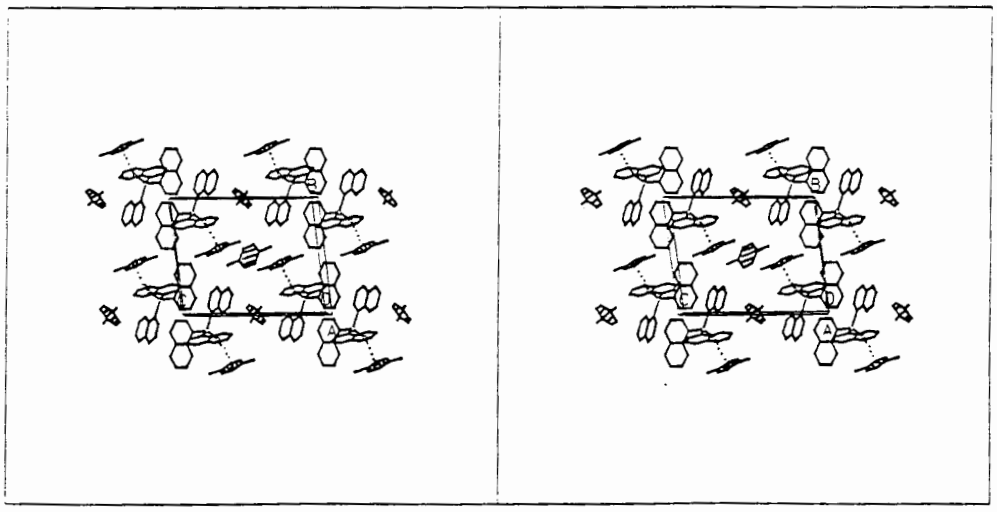

Figure 6.12. Packing diagram of **NAPPY** viewed along [100]. Guest molecules are shaded and H-bonds indictated by dotted lines.

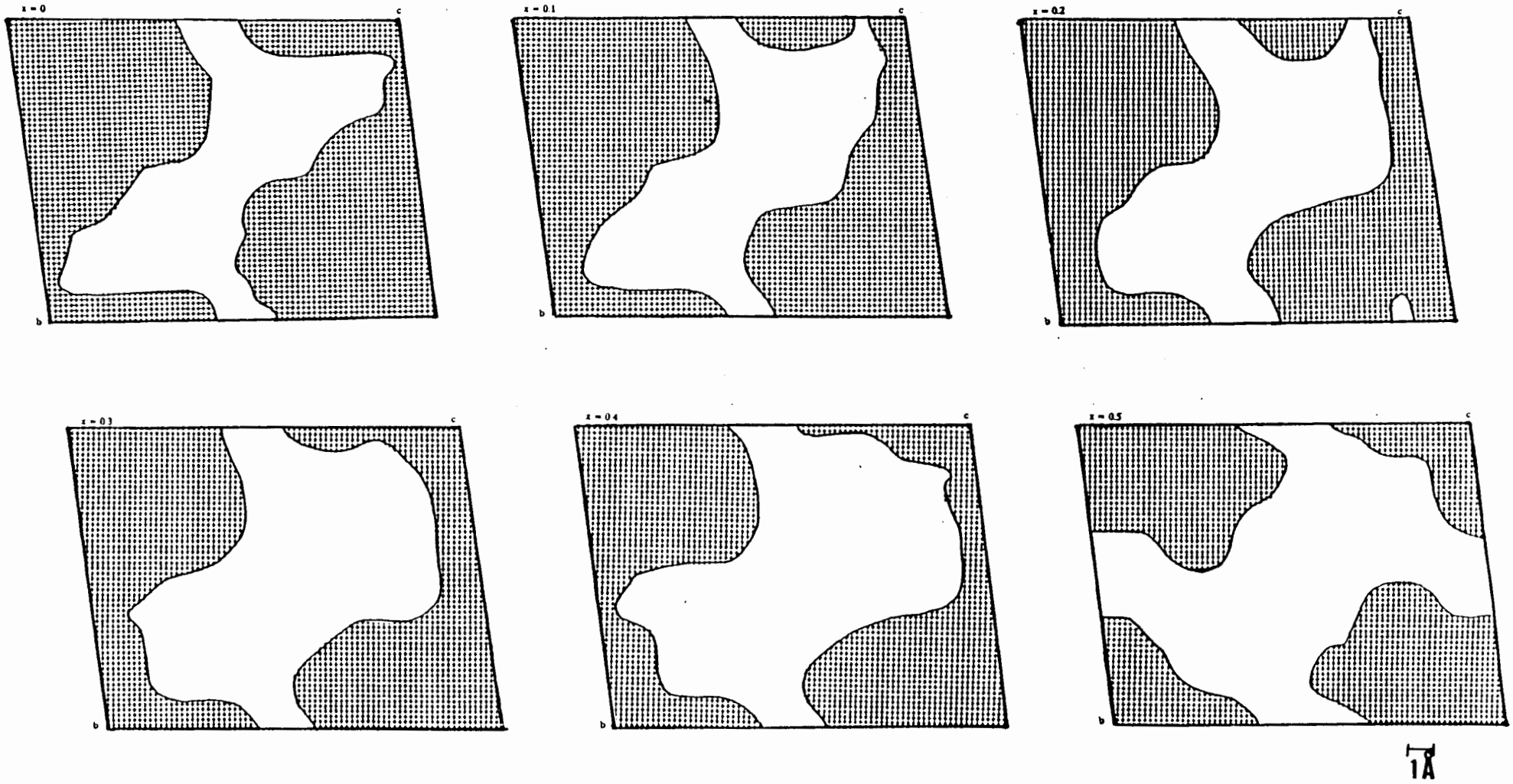

Figure 6.13. OPEC analysis of the asymmetric unit of **NAPPY**. Hatched areas are those occupied by host molecules. Blank areas indicate the space available to guests.

NATRET : $(C_{30}H_{22}OSi)$. triethylamine

Space group : $P\bar{1}$	H:G = 1:1
a = 12.254(6) Å	α = 119.51(5)°
b = 12.472(11) Å	β = 107.35(5)°
c = 12.675(7) Å	γ = 99.07(5)°
Z = 2	

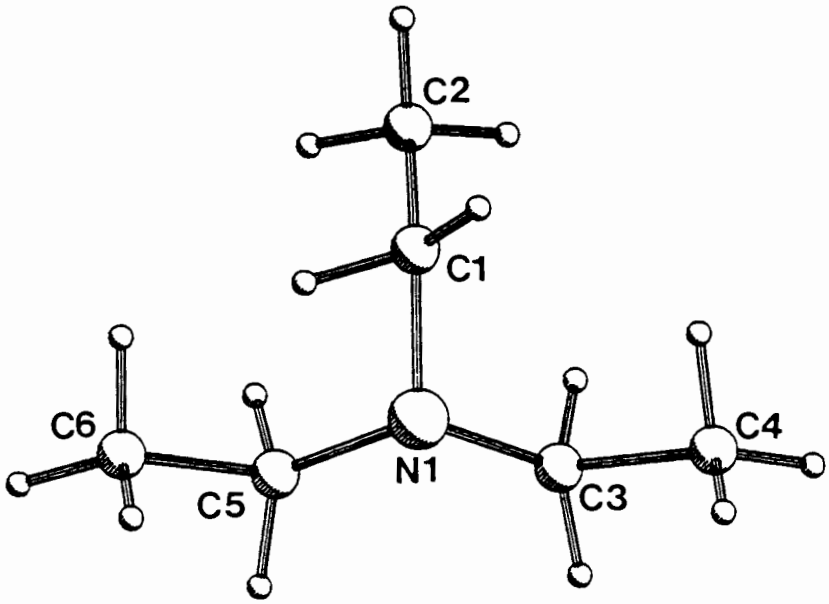

One host and one guest molecule were found by direct methods solution. (R_E = 0.31) The structure was refined in the usual way to a final R factor of 0.050. The ethyl moieties of the guest displayed marked thermal motion. U_{equiv} for the ethyl carbons averaged 0.136 $Å^2$ while the U_{iso} for the CH_2 hydrogens was 0.143 $Å^2$ and that of the CH_3 hydrogens was 0.190 $Å^2$. The final maximum shift/e.s.d. was 0.008 and the highest and lowest peaks in the final electron density map were 0.21 and -0.22 $eÅ^{-3}$ respectively. Final coordinates and thermal parameters are listed in Table 6.9.

Molecular structure.

The host and guest molecule in the asymmetric unit are shown as a hydrogen bonded unit in Figure 6.14.

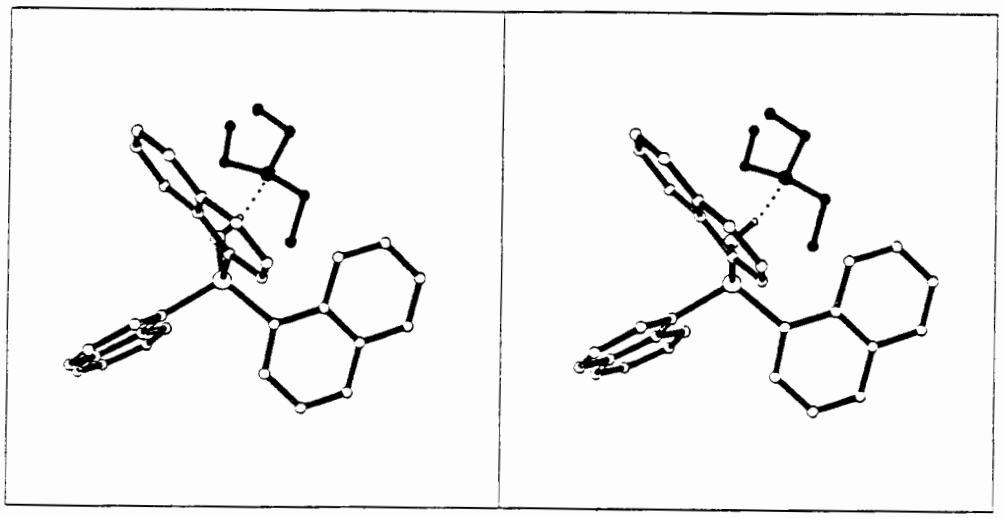

Figure 6.14. Molecular structure of **NATRET**.

These units pack with the hydrogen bond approximately parallel to [010]. Two guests lie in a centrosymmetric cavity about (0 ½ 0). The cavity is approximately 9 x 9 x 10 Å in size. Bond lengths and angles of the triethylamine were within normal ranges. These features are shown in Figure 6.15, a packing diagram viewed down [100].

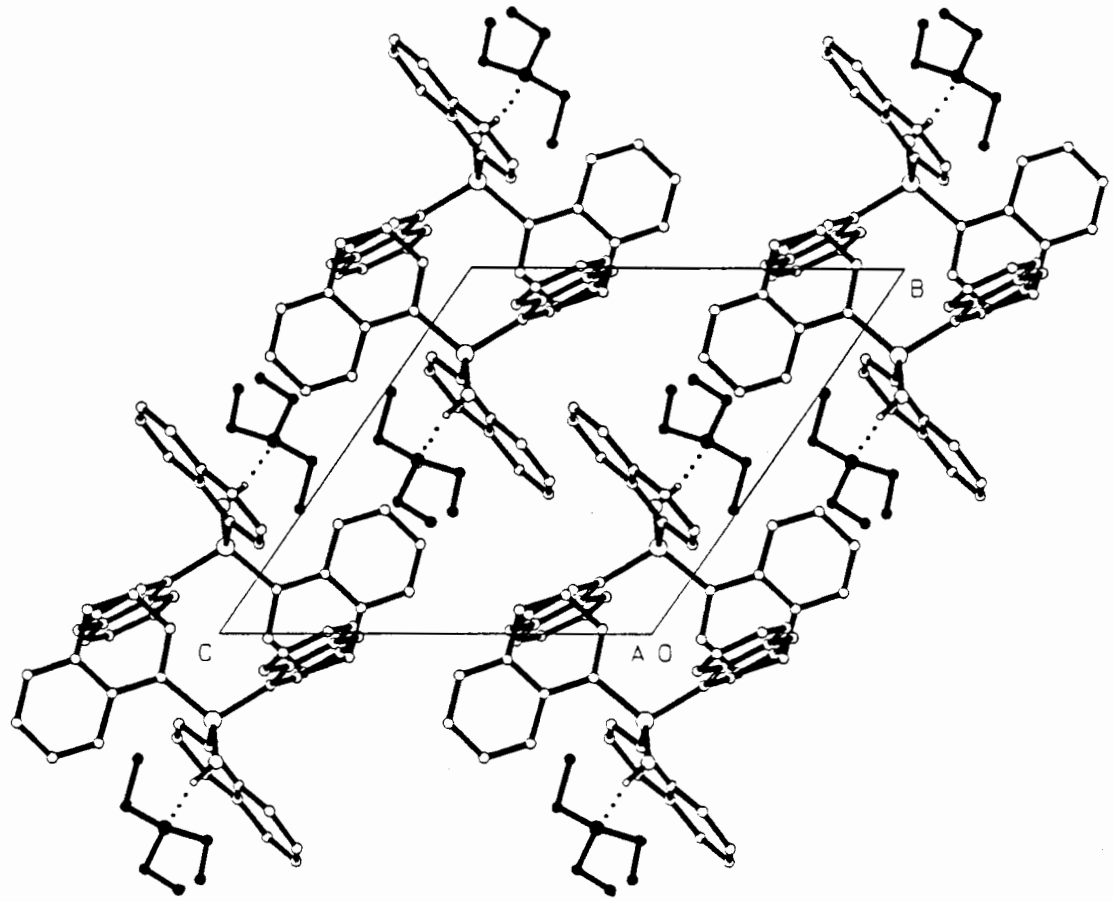

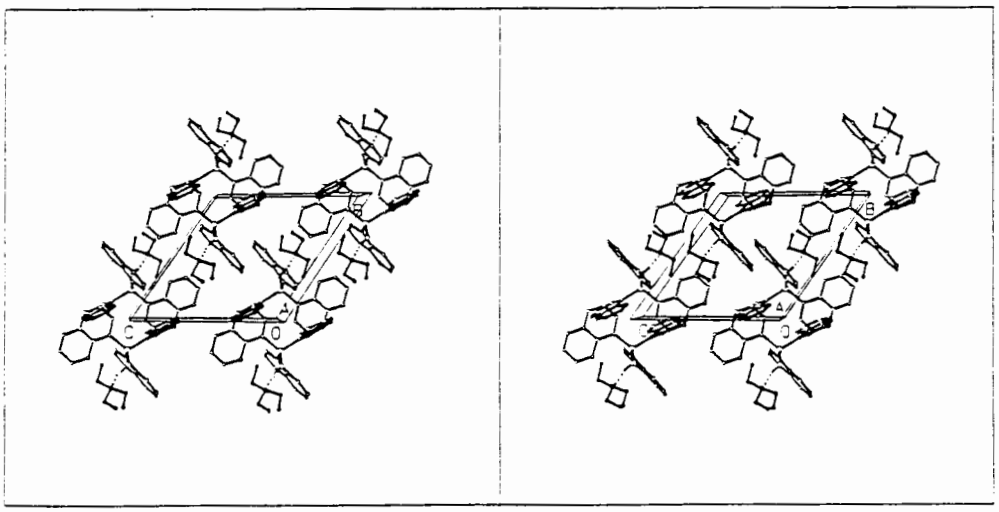

Figure 6.15. Packing diagram of **NATRET** viewed down [100]. Guest atoms are shaded.

Host conformation in Class D structures.

The design of this host, tri-1-naphthylsilanol, was based on the shape of the triphenylalcohol hosts of Classes B and C. Thus it is expected to show similar conformational behaviour to that described in Chapter 5.

Bond lengths and angles.

No major deviations from the expected values are seen for these parameters, a summary of which is given in Table 6.1.

Table 6.1. Bond lengths and angles.

O - Si	1.610(3) - 1.642(3) Å
Si - C_{ring}	1.857(5) - 1.887(5) Å
C_{ring} - C_{ring}	1.314(15) - 1.453(7) Å
Si - C_{ring} - C_{ring}	116.5(3) - 122.8(1)°
Angles inside ring	119.4(3) - 121.7(6)°

Geometry of the central atom.

This angle always falls within the range 105.5 - 113.7° as shown in Figure 6.16. The distribution is skewed with a maximum number of angles between 107 and 108°, owing to the crowding of the bulky naphthyl groups around the silicon atom.

The planarity of the aromatic rings.

The maximum deviation from the mean plane in any of the rings of one molecule was never greater than 0.05 Å.

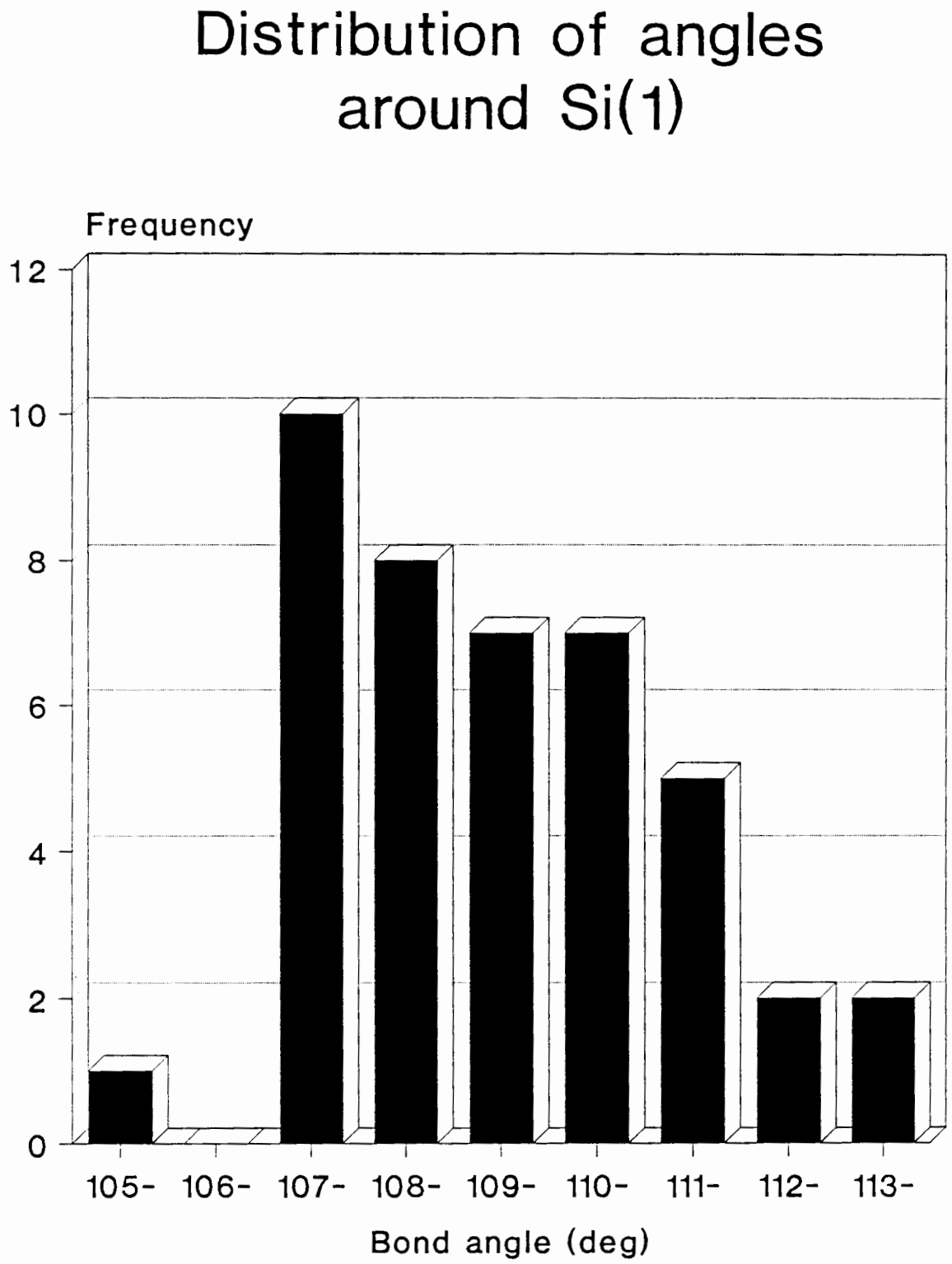
Distribution of angles around Si(1)
Frequency
12
10
8
6
4
2
0
105-
106-
107-
108-
109-
110-
111-
112-
113-
Bond angle (deg)

Figure 6.16.

The orientation of the aromatic rings.

A procedure similar to that described in Chapter 5 was used to analyse the conformation of this host. The torsion angles chosen were τ_i = O(1)-Si(1)-C(X0)-C(X9) where X = 1 - 3. This is the angle to the "inner" portion of the naphthyl ring (see Figure 6.1). As before, the torsion angles were chosen so that the majority within a structure are positive, and the ring associated with the largest value of τ is defined as ring A.

The values of τ_A, τ_B and τ_C obtained for the seven host molecules in this class are displayed as a bar chart in Figure 6.17. Also included in Figure 6.17 are the values obtained from a molecule of tri-1-naphthylsilanol energy-minimized using ALCHEMY II (initial values of τ_i = 40°). This molecule is shown in space-filled form in Figure 6.18.

All molecules in Class D have $\tau_A \approx \tau_B \approx \tau_C \approx 40°$ which corresponds to the ideal propeller conformation. The bulkiness of the naphthyl rings probably makes it difficult for any other conformation to be adopted.

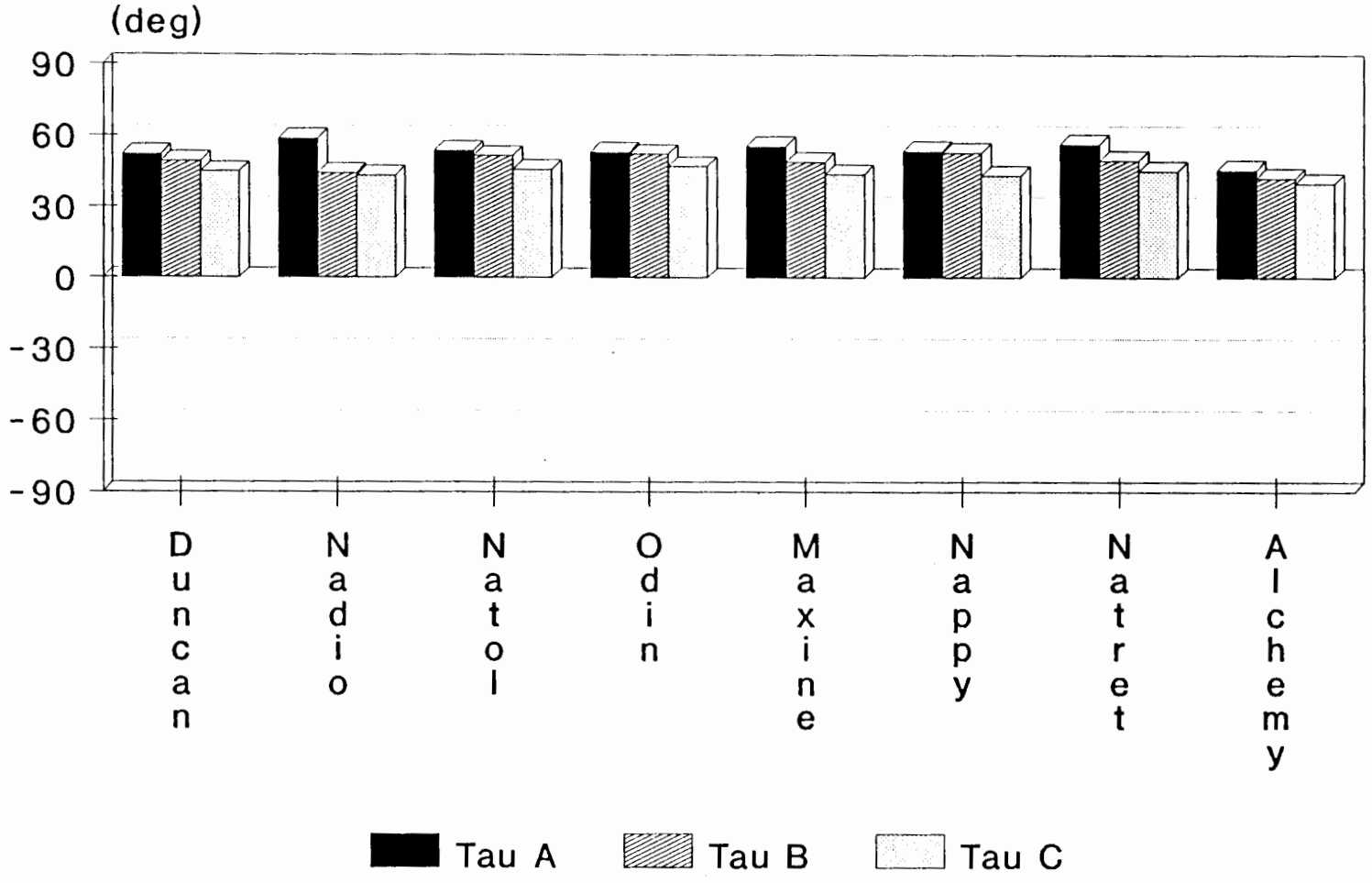

Figure 6.17. Orientation of the naphthyl rings.

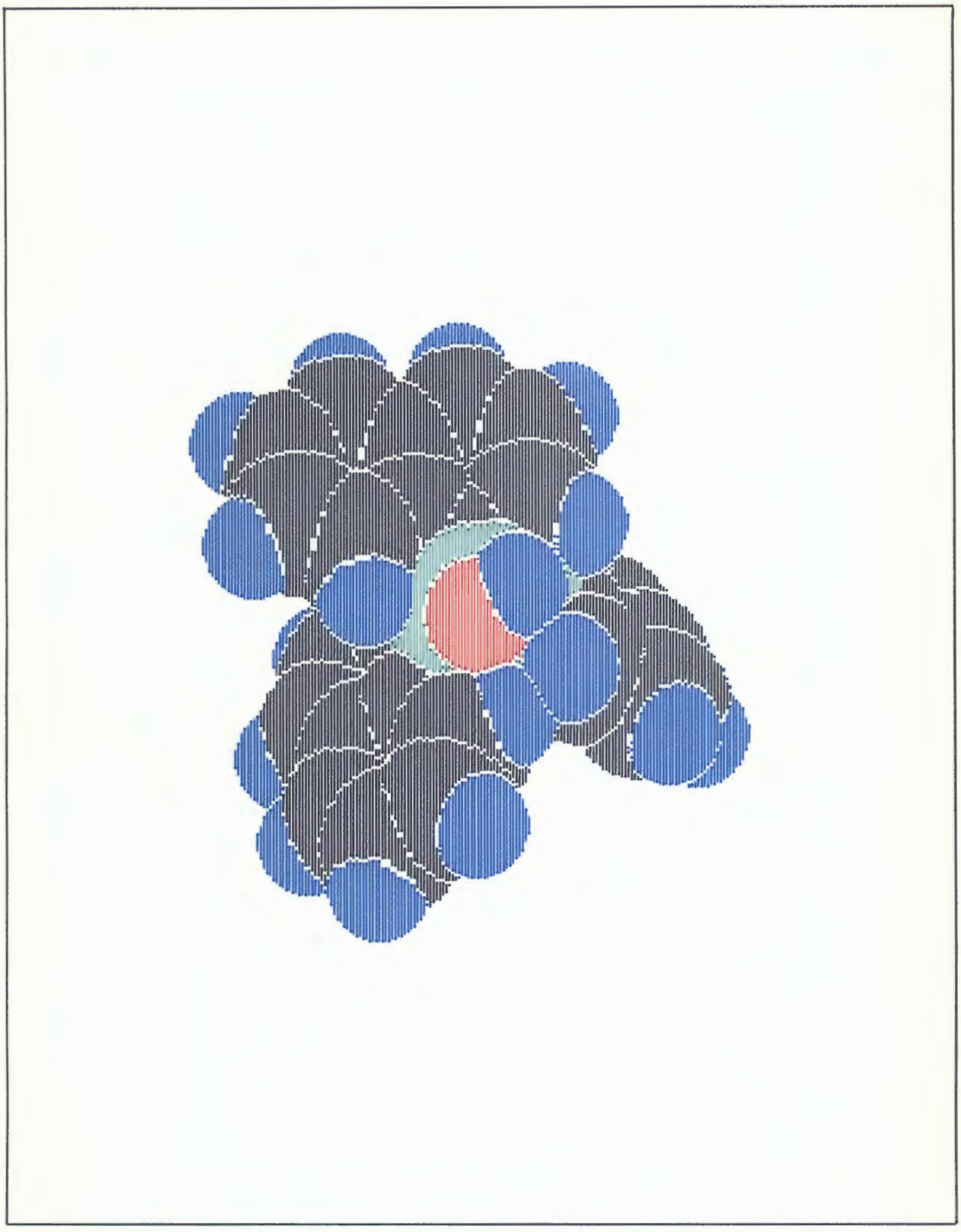

Figure 6.18. Space-filled diagram of the host molecule (Class D).

Table 6.2. Details of Hydrogen bonding in Class D.

Compound	Donor-H	Donor···Acceptor	D-H···Acceptor
DUNCAN			
O(1)-H(1)···O(1G)	0.98(3)	2.647(12)	145.5(92)
NADIO			
O(1)-H(1)···O(1G)	0.90(3)	2.736(3)	169.7(23)
NATOL			
O(1)-H(1)···Centroid	0.85(8)	3.396(4)	159.8
ODIN			
O(1)-H(1)···Centroid	0.91(5)	3.396(4)	159.8
MAXINE			
O(1)-H(1)···Centroid	0.87(4)	3.659(4)	142.5
NAPPY			
O(1)-H(1)···Centroid	0.90(5)	3.281(4)	147.7
NATRET			
O(1)-H(1)···N(1)	0.87(6)	2.701(5)	157.8(48)

TABLE 6.3 Fractional atomic coordinates (x 10^4) and Thermal Parameters ($Å^2$ x 10^3) with e.s.d. s in parentheses for DUNCAN

Atom	x/a	y/b	z/c	U_{iso}/U_{equiv}(*)
SI(1)	1509(2)	2466(2)	6855(1)	36(1) *
O(1)	2322(5)	1163(4)	7767(4)	48(2) *
C(10)	-324(7)	2318(6)	6369(5)	37(2) *
C(11)	-671(8)	2860(7)	5175(6)	47(3) *
C(12)	-1974(8)	2725(7)	4719(7)	53(4) *
C(13)	-2958(9)	2036(7)	5461(7)	54(4) *
C(14)	-2723(8)	1461(7)	6706(7)	51(4) *
C(15)	-3777(9)	775(8)	7465(9)	64(5) *
C(16)	-3508(10)	256(9)	8671(10)	80(6) *
C(17)	-2284(10)	451(8)	9121(8)	69(4) *
C(18)	-1238(9)	1083(7)	8406(6)	57(3) *
C(19)	-1420(7)	1635(6)	7155(6)	40(3) *
C(20)	2596(7)	3294(6)	5484(6)	37(3) *
C(21)	2875(8)	4419(6)	5187(6)	47(3) *
C(22)	3639(8)	5118(7)	4135(6)	52(3) *
C(23)	4144(8)	4642(7)	3441(6)	54(3) *
C(24)	3917(8)	3491(7)	3696(6)	49(3) *
C(25)	4484(10)	2986(9)	2976(7)	67(4) *
C(26)	4237(11)	1891(9)	3236(7)	71(5) *
C(27)	3525(10)	1175(8)	4240(8)	65(4) *
C(28)	2966(9)	1615(7)	4976(7)	53(3) *
C(29)	3158(7)	2771(6)	4749(6)	43(3) *
C(30)	1273(8)	3386(6)	7643(6)	44(3) *
C(31)	-31(9)	4101(7)	7492(7)	57(4) *
C(32)	-251(11)	4872(8)	7962(8)	71(4) *
C(33)	834(12)	4924(8)	8641(8)	70(5) *
C(34)	2150(10)	4205(7)	8872(6)	53(4) *
C(35)	3286(12)	4190(9)	9613(8)	73(5) *
C(36)	4569(13)	3547(9)	9785(8)	77(5) *
C(37)	4864(10)	2773(8)	9283(7)	65(4) *
C(38)	3794(8)	2744(7)	8579(6)	52(4) *
C(39)	2394(8)	3450(6)	8350(5)	44(3) *
S(1G)	1439(3)	-1831(2)	7932(3)	83(2) *
O(1G)	2365(10)	-908(7)	7787(10)	122(6) *
C(1G)	339(20)	-1003(20)	6609(21)	108(15) *
C(1GA)	-444(49)	-1434(50)	7205(41)	112(28) *
C(2G)	617(35)	-2145(25)	9379(26)	104(15) *
C(2GA)	-270(49)	-1890(32)	8833(34)	158(23) *

Anisotropic atoms have thermal parameters ($Å^2$ x 10^3) of the form :
$\exp[-2\pi^2(U_{11}h^2a^{*2} + U_{22}k^2b^{*2} + U_{33}l^2c^{*2} + 2U_{23}klb^*c^* + 2U_{13}hla^*c^* + 2U_{12}hka^*b^*)]$

Atom	U_{11}	U_{22}	U_{33}	U_{23}	U_{13}	U_{12}
SI(1)	40(1)	37(1)	31(1)	-15(1)	0(1)	-6(1)
O(1)	50(3)	40(3)	46(3)	-14(2)	-7(2)	-1(2)
C(10)	43(4)	34(3)	30(3)	-12(3)	-8(3)	5(3)
C(11)	49(4)	49(4)	37(3)	-14(3)	4(3)	-10(3)
C(12)	43(4)	63(5)	52(4)	-25(4)	-14(4)	5(4)
C(13)	47(4)	58(5)	66(5)	-35(4)	-7(4)	-4(4)
C(14)	47(4)	48(4)	62(5)	-27(4)	12(4)	-4(3)
C(15)	49(5)	56(5)	98(7)	-42(5)	24(5)	-18(4)
C(16)	53(6)	73(6)	105(8)	-32(6)	33(5)	-18(5)
C(17)	60(5)	67(6)	62(5)	-15(4)	19(4)	-2(4)
C(18)	56(5)	59(5)	40(4)	-11(4)	-1(3)	-4(4)
C(19)	38(4)	33(3)	44(4)	-13(3)	0(3)	0(3)
C(20)	35(3)	40(3)	37(3)	-18(3)	-3(3)	-2(3)
C(21)	50(4)	44(4)	49(4)	-21(3)	6(3)	-7(3)
C(22)	56(5)	49(4)	47(4)	-16(4)	1(4)	-11(4)
C(23)	53(5)	55(5)	39(4)	-7(3)	2(3)	-16(4)
C(24)	45(4)	60(5)	41(4)	-23(3)	6(3)	-4(3)
C(25)	65(5)	91(7)	44(4)	-32(4)	13(4)	-4(5)
C(26)	92(7)	84(7)	51(5)	-43(5)	19(5)	-8(5)
C(27)	74(6)	64(5)	69(5)	-41(5)	5(5)	-10(4)
C(28)	58(5)	49(4)	58(4)	-27(4)	1(4)	-16(3)

Table 6.3 ctd.

C(29)	34(3)	50(4)	45(4)	-21(3)	0(3)	-6(3)
C(30)	55(4)	37(4)	36(3)	-14(3)	4(3)	-5(3)
C(31)	56(5)	62(5)	54(4)	-27(4)	-6(4)	-1(4)
C(32)	80(6)	55(5)	64(5)	-21(4)	8(5)	13(5)
C(33)	110(8)	53(5)	57(5)	-32(4)	18(5)	-19(5)
C(34)	81(6)	48(4)	37(4)	-22(3)	14(4)	-24(4)
C(35)	99(8)	90(7)	57(5)	-51(5)	21(5)	-41(6)
C(36)	96(8)	85(7)	52(5)	-25(5)	-12(5)	-36(6)
C(37)	69(5)	65(5)	55(5)	-18(4)	-9(4)	-24(4)
C(38)	54(5)	57(5)	41(4)	-18(4)	-1(3)	-14(4)
C(39)	62(4)	43(4)	34(3)	-21(3)	13(3)	-18(3)
S(1G)	98(2)	53(1)	104(2)	-42(1)	20(2)	-14(1)
O(1G)	113(7)	82(5)	193(10)	-80(6)	3(7)	-17(5)
C(1G)	76(11)	139(17)	167(21)	124(17)	-21(12)	18(11)
C(1GA)	76(27)	169(45)	90(28)	-57(29)	-51(23)	0(28)
C(2G)	129(24)	76(17)	95(20)	-34(15)	48(17)	-5(16)
C(2GA)	169(38)	95(23)	111(28)	13(20)	112(28)	38(24)

TABLE 6.4 Fractional atomic coordinates (x 10^4)
and Thermal Parameters ($Å^2$ x 10^3)
with e.s.d. s in parentheses for NADIO

Atom	x/a	y/b	z/c	U_{iso}/U_{equiv}(*)
SI(1)	979(0)	7424(0)	8303(0)	35(0) *
O(1)	1558(1)	6140(1)	7433(1)	47(1) *
C(10)	1018(2)	8384(2)	7521(1)	38(1) *
C(11)	-121(2)	9074(2)	7615(2)	47(1) *
C(12)	-182(2)	9826(2)	7066(2)	56(1) *
C(13)	902(3)	9868(2)	6390(2)	55(1) *
C(14)	2114(2)	9189(2)	6256(1)	45(1) *
C(15)	3261(3)	9225(2)	5560(2)	58(1) *
C(16)	4426(3)	8590(2)	5452(2)	63(1) *
C(17)	4540(2)	7884(2)	6045(2)	58(1) *
C(18)	3449(2)	7810(2)	6713(2)	47(1) *
C(19)	2194(2)	8451(1)	6833(1)	39(1) *
C(20)	2160(2)	8144(2)	9647(1)	38(1) *
C(21)	2798(2)	9242(2)	9925(2)	48(1) *
C(22)	3667(2)	9858(2)	10939(2)	59(1) *
C(23)	3895(2)	9363(2)	11668(2)	63(1) *
C(24)	3277(2)	8234(2)	11439(2)	53(1) *
C(25)	3491(3)	7710(3)	12201(2)	74(1) *
C(26)	2910(3)	6631(3)	11971(2)	84(2) *
C(27)	2061(3)	5995(2)	10957(2)	73(1) *
C(28)	1810(2)	6481(2)	10208(2)	54(1) *
C(29)	2410(2)	7611(2)	10418(2)	42(1) *
C(30)	-912(2)	7294(2)	8733(1)	37(1) *
C(31)	-1245(2)	7940(2)	9870(2)	46(1) *
C(32)	-2637(2)	7914(2)	10268(2)	58(1) *
C(33)	-3710(2)	7224(2)	9523(2)	60(1) *
C(34)	-3450(2)	6538(2)	8349(2)	48(1) *
C(35)	-4568(2)	5811(2)	7562(2)	63(1) *
C(36)	-4308(2)	5161(2)	6436(2)	67(1) *
C(37)	-2945(3)	5211(2)	6018(2)	61(1) *

C(38)	-1842(2)	5906(2)	6747(2)	48(1) *
C(39)	-2056(2)	6581(2)	7942(2)	39(1) *
O(1G)	620(2)	3982(1)	7271(2)	78(1) *
O(2G)	2347(2)	2160(2)	5904(2)	85(1) *
C(1G)	1373(4)	3318(2)	7745(3)	85(1) *
C(2G)	2683(3)	2843(3)	7075(3)	92(2) *
C(3G)	1632(4)	2836(3)	5459(2)	89(1) *
C(4G)	304(4)	3262(2)	6078(3)	93(2) *

Anisotropic atoms have thermal parameters ($Å^2 \times 10^3$) of the form :
$\exp[-2\pi^2(U_{11}h^2a^{*2} + U_{22}k^2b^{*2} + U_{33}l^2c^{*2} + 2U_{23}klb^*c^* + 2U_{13}hla^*c^* + 2U_{12}hka^*b^*)]$

Atom	U_{11}	U_{22}	U_{33}	U_{23}	U_{13}	U_{12}
SI(1)	34(0)	34(0)	35(0)	15(0)	0(0)	-1(0)
O(1)	48(1)	35(1)	53(1)	15(1)	9(1)	0(1)
C(10)	42(1)	34(1)	34(1)	12(1)	0(1)	0(1)
C(11)	49(1)	44(1)	48(1)	20(1)	4(1)	5(1)
C(12)	61(1)	46(1)	63(1)	27(1)	0(1)	10(1)
C(13)	74(1)	43(1)	52(1)	27(1)	-5(1)	0(1)
C(14)	62(1)	36(1)	33(1)	13(1)	-1(1)	-6(1)
C(15)	77(2)	53(1)	45(1)	23(1)	5(1)	-12(1)
C(16)	71(2)	61(1)	51(1)	18(1)	19(1)	-13(1)
C(17)	53(1)	51(1)	61(1)	16(1)	15(1)	0(1)
C(18)	47(1)	43(1)	51(1)	19(1)	6(1)	0(1)
C(19)	46(1)	33(1)	31(1)	9(1)	-1(1)	-4(1)
C(20)	34(1)	40(1)	38(1)	16(1)	1(1)	0(1)
C(21)	45(1)	45(1)	47(1)	16(1)	0(1)	-4(1)
C(22)	53(1)	53(1)	53(1)	6(1)	-5(1)	-9(1)
C(23)	50(1)	75(2)	41(1)	3(1)	-8(1)	4(1)
C(24)	43(1)	70(1)	37(1)	15(1)	3(1)	17(1)
C(25)	76(2)	102(2)	45(1)	30(1)	-3(1)	32(2)
C(26)	99(2)	110(2)	68(2)	60(2)	8(2)	39(2)
C(27)	83(2)	81(2)	78(2)	54(2)	13(1)	20(1)
C(28)	56(1)	60(1)	55(1)	33(1)	3(1)	5(1)
C(29)	36(1)	52(1)	38(1)	19(1)	4(1)	9(1)
C(30)	38(1)	36(1)	39(1)	19(1)	0(1)	0(1)
C(31)	46(1)	49(1)	42(1)	18(1)	4(1)	5(1)
C(32)	55(1)	66(1)	56(1)	28(1)	19(1)	14(1)
C(33)	41(1)	70(1)	79(2)	42(1)	18(1)	10(1)
C(34)	35(1)	48(1)	70(1)	36(1)	0(1)	2(1)
C(35)	37(1)	64(1)	99(2)	47(1)	-10(1)	-4(1)
C(36)	53(1)	63(1)	90(2)	40(1)	-31(1)	-15(1)
C(37)	66(1)	55(1)	59(1)	25(1)	-23(1)	-7(1)
C(38)	49(1)	48(1)	47(1)	22(1)	-8(1)	-2(1)
C(39)	37(1)	38(1)	48(1)	24(1)	-2(1)	1(1)
O(1G)	96(1)	42(1)	97(1)	28(1)	19(1)	11(1)
O(2G)	98(1)	75(1)	86(1)	36(1)	32(1)	22(1)
C(1G)	122(3)	63(2)	78(2)	37(1)	24(2)	14(2)
C(2G)	78(2)	103(2)	116(3)	69(2)	-3(2)	4(2)
C(3G)	141(3)	59(2)	66(2)	26(1)	0(2)	0(2)
C(4G)	96(2)	52(2)	119(3)	26(2)	-29(2)	-1(1)

TABLE 6.5 Fractional atomic coordinates ($\times 10^4$)
and Thermal Parameters ($Å^2 \times 10^3$)
with e.s.d. s in parentheses for NATOL

Atom	x/a	y/b	z/c	U_{iso}/U_{equiv}(*)
SI(1)	1180(1)	5677(1)	8125(1)	42(1) *
O(1)	1828(3)	6078(3)	7205(2)	56(1) *
C(10)	939(4)	4003(3)	7481(3)	45(2) *
C(11)	-277(5)	3473(4)	7649(3)	58(2) *
C(12)	-528(5)	2220(4)	7222(4)	70(2) *
C(13)	460(6)	1482(4)	6623(4)	73(2) *
C(14)	1734(5)	1953(4)	6409(3)	61(2) *
C(15)	2773(7)	1205(5)	5777(4)	84(3) *
C(16)	3973(7)	1655(5)	5559(5)	94(3) *
C(17)	4246(5)	2899(5)	5988(4)	79(3) *
C(18)	3285(4)	3660(4)	6610(4)	58(2) *
C(19)	1991(4)	3215(3)	6835(3)	50(2) *

Table 6.5 ctd.

C(20)	-566(4)	6343(3)	8584(3)	43(2) *
C(21)	-758(4)	6948(3)	9702(3)	50(2) *
C(22)	-2037(5)	7483(3)	10108(4)	58(2) *
C(23)	-3118(4)	7398(3)	9382(4)	59(2) *
C(24)	-3001(4)	6779(3)	8234(4)	51(2) *
C(25)	-4129(5)	6671(4)	7461(5)	68(3) *
C(26)	-4010(5)	6082(4)	6348(5)	76(3) *
C(27)	-2761(5)	5540(4)	5926(4)	73(2) *
C(28)	-1647(4)	5608(4)	6634(4)	58(2) *
C(29)	-1720(4)	6238(3)	7813(3)	46(2) *
C(30)	2423(4)	6178(3)	9390(3)	43(2) *
C(31)	2766(4)	5351(4)	9768(3)	54(2) *
C(32)	3626(5)	5662(4)	10741(4)	64(2) *
C(33)	4150(5)	6814(4)	11361(4)	64(2) *
C(34)	3845(4)	7706(3)	11023(3)	50(2) *
C(35)	4387(5)	8910(4)	11662(4)	69(2) *
C(36)	4101(5)	9769(4)	11330(4)	75(2) *
C(37)	3279(5)	9473(4)	10361(4)	66(2) *
C(38)	2722(4)	8325(3)	9730(4)	56(2) *
C(39)	2997(4)	7399(3)	10043(3)	44(2) *
C(1)	9292(8)	1027(6)	2561(6)	97(4) *
C(2)	7905(7)	921(5)	2595(5)	84(3) *
C(3)	7194(7)	1591(5)	3580(6)	95(3) *
C(4)	7950(8)	2304(6)	4497(5)	102(4) *
C(5)	9432(8)	2399(6)	4463(6)	99(4) *
C(6)	10129(8)	1817(7)	3571(7)	110(4) *
C(1M)	10087(10)	420(8)	1599(8)	153(3)

Anisotropic atoms have thermal parameters ($Å^2 \times 10^3$) of the form :
$\exp[-2\pi^2(U_{11}h^2a^{*2} + U_{22}k^2b^{*2} + U_{33}l^2c^{*2} + 2U_{23}klb^*c^* + 2U_{13}hla^*c^* + 2U_{12}hka^*b^*)]$

Atom	U_{11}	U_{22}	U_{33}	U_{23}	U_{13}	U_{12}
SI(1)	43(1)	40(1)	47(1)	23(1)	3(0)	5(0)
O(1)	61(2)	58(2)	64(2)	38(2)	12(1)	11(1)
C(10)	51(2)	45(2)	45(2)	24(2)	1(2)	5(2)
C(11)	66(3)	52(2)	56(3)	25(2)	8(2)	2(2)
C(12)	80(3)	54(3)	79(3)	34(3)	1(3)	-13(2)
C(13)	114(4)	42(2)	67(3)	27(2)	0(3)	-2(3)
C(14)	92(3)	45(2)	53(3)	26(2)	3(2)	16(2)
C(15)	133(5)	53(3)	71(3)	28(3)	22(3)	32(3)
C(16)	120(5)	89(4)	91(4)	49(3)	44(4)	60(4)
C(17)	77(3)	95(4)	90(4)	60(3)	30(3)	39(3)
C(18)	55(3)	63(3)	67(3)	38(2)	12(2)	18(2)
C(19)	63(3)	49(2)	42(2)	24(2)	0(2)	11(2)
C(20)	46(2)	38(2)	50(2)	23(2)	2(2)	2(2)
C(21)	53(2)	46(2)	54(3)	23(2)	6(2)	2(2)
C(22)	63(3)	48(2)	62(3)	22(2)	21(2)	9(2)
C(23)	48(3)	49(2)	87(4)	35(2)	16(2)	11(2)
C(24)	45(2)	40(2)	75(3)	31(2)	4(2)	2(2)
C(25)	44(3)	60(3)	105(4)	42(3)	-7(3)	6(2)
C(26)	56(3)	73(3)	97(4)	40(3)	-27(3)	-2(2)
C(27)	80(4)	70(3)	68(3)	32(3)	-24(3)	-5(3)
C(28)	57(3)	55(3)	63(3)	28(2)	-3(2)	4(2)
C(29)	45(2)	38(2)	58(3)	25(2)	0(2)	1(2)
C(30)	37(2)	44(2)	55(2)	28(2)	4(2)	3(2)
C(31)	55(3)	54(2)	59(3)	32(2)	-3(2)	-1(2)
C(32)	65(3)	73(3)	74(3)	52(3)	-2(2)	7(2)
C(33)	59(3)	74(3)	62(3)	35(3)	-15(2)	0(2)
C(34)	43(2)	54(2)	53(2)	23(2)	1(2)	-1(2)
C(35)	63(3)	68(3)	64(3)	20(3)	-11(2)	-6(2)
C(36)	79(3)	49(3)	79(3)	14(3)	0(3)	-7(2)
C(37)	74(3)	46(3)	81(3)	31(2)	3(3)	2(2)

Table 6.5 ctd.

C(38)	57(3)	46(2)	67(3)	29(2)	-3(2)	1(2)
C(39)	35(2)	47(2)	54(2)	27(2)	5(2)	2(2)
C(1)	120(5)	92(4)	109(5)	69(4)	37(4)	32(4)
C(2)	115(5)	70(3)	72(4)	37(3)	3(3)	-5(3)
C(3)	106(5)	89(4)	100(5)	54(4)	-7(4)	-8(3)
C(4)	134(6)	89(4)	83(4)	37(4)	7(4)	18(4)
C(5)	104(5)	106(5)	92(5)	51(4)	-29(4)	-8(4)
C(6)	120(6)	111(5)	124(6)	76(5)	-12(5)	1(4)

TABLE 6.6 Fractional atomic coordinates (x 10^4)
and Thermal Parameters ($Å^2$ x 10^3)
with e.s.d. s in parentheses for ODIN

Atom	x/a	y/b	z/c	U_{iso}/U_{equiv}(*)
SI(1)	1189(2)	5705(1)	8130(1)	31(1) *
O(1)	1888(4)	6109(3)	7234(3)	44(2) *
C(10)	-580(5)	6342(4)	8533(4)	32(2) *
C(11)	-860(6)	6955(5)	9652(4)	41(2) *
C(12)	-2154(6)	7447(5)	10024(5)	48(3) *
C(13)	-3229(6)	7357(5)	9303(5)	47(3) *
C(14)	-3037(6)	6729(4)	8165(5)	40(2) *
C(15)	-4166(6)	6598(5)	7404(6)	54(3) *
C(16)	-3971(7)	6014(6)	6315(6)	64(4) *
C(17)	-2689(7)	5500(6)	5913(6)	63(3) *
C(18)	-1574(6)	5605(5)	6619(5)	46(3) *
C(19)	-1726(5)	6226(4)	7774(4)	36(2) *
C(20)	2387(5)	6199(4)	9385(4)	33(2) *
C(21)	2709(6)	5365(5)	9742(5)	43(2) *
C(22)	3565(7)	5664(6)	10709(5)	54(3) *
C(23)	4073(7)	6788(6)	11285(5)	53(3) *
C(24)	3799(6)	7702(5)	10991(4)	40(2) *
C(25)	4327(6)	8883(5)	11586(5)	52(3) *
C(26)	4077(7)	9745(6)	11270(5)	56(3) *
C(27)	3240(6)	9470(5)	10324(5)	50(3) *
C(28)	2685(6)	8339(5)	9720(5)	44(2) *
C(29)	2945(5)	7406(4)	10013(4)	35(2) *
C(30)	988(6)	4032(4)	7496(4)	36(2) *
C(31)	-230(7)	3507(5)	7664(5)	48(3) *
C(32)	-428(8)	2267(5)	7288(6)	59(3) *
C(33)	622(8)	1543(5)	6752(5)	59(3) *
C(34)	1914(7)	2026(5)	6553(5)	48(3) *
C(35)	3019(9)	1274(6)	5972(6)	64(3) *
C(36)	4242(9)	1755(7)	5773(6)	68(4) *
C(37)	4431(7)	2977(6)	6120(5)	56(3) *
C(38)	3398(6)	3723(5)	6689(5)	46(3) *
C(39)	2121(6)	3273(4)	6908(4)	39(2) *
C(1A)	9200(6)	1004(5)	2582(4)	43(3) *
C(2A)	10056(6)	1615(5)	3543(5)	45(2) *
C(3A)	9394(7)	2250(5)	4514(5)	56(3) *
C(4A)	7950(8)	2297(6)	4564(6)	66(4) *
C(5A)	7095(7)	1681(6)	3628(6)	59(3) *
C(6A)	7729(7)	1051(5)	2651(5)	53(3) *
C(1MA)	9884(8)	320(6)	1511(5)	64(3) *
C(2MA)	11625(7)	1531(6)	3508(6)	64(3) *

Anisotropic atoms have thermal parameters ($Å^2$ x 10^3) of the form :
$\exp[-2\pi^2(U_{11}h^2a^{*2} + U_{22}k^2b^{*2} + U_{33}l^2c^{*2} + 2U_{23}klb^*c^*$
$+ 2U_{13}hla^*c^* + 2U_{12}hka^*b^*)]$

Atom	U_{11}	U_{22}	U_{33}	U_{23}	U_{13}	U_{12}
SI(1)	33(1)	35(1)	22(1)	8(1)	-4(1)	0(1)
O(1)	54(2)	47(2)	36(2)	24(2)	1(2)	5(2)
C(10)	35(3)	33(3)	25(3)	10(2)	-6(2)	0(2)
C(11)	45(3)	45(3)	26(3)	9(3)	-3(3)	4(3)
C(12)	54(4)	46(3)	38(4)	12(3)	4(3)	8(3)
C(13)	40(4)	46(3)	56(4)	23(3)	12(3)	10(3)
C(14)	34(3)	38(3)	47(4)	17(3)	-2(3)	0(2)
C(15)	34(3)	54(4)	70(5)	24(4)	-10(3)	0(3)

Table 6.6 ctd.

C(16)	54(4)	64(4)	69(5)	25(4)	-34(4)	-7(3)
C(17)	75(5)	61(4)	39(4)	10(3)	-27(4)	-1(3)
C(18)	45(4)	54(3)	30(3)	9(3)	-7(3)	5(3)
C(19)	38(3)	35(3)	34(3)	14(2)	-9(3)	0(2)
C(20)	32(3)	42(3)	23(3)	12(2)	-3(2)	1(2)
C(21)	49(4)	45(3)	32(3)	15(3)	-7(3)	-5(3)
C(22)	63(4)	62(4)	46(4)	31(3)	-14(3)	3(3)
C(23)	60(4)	73(4)	29(3)	26(3)	-11(3)	3(3)
C(24)	38(3)	55(3)	22(3)	12(3)	-2(3)	-2(2)
C(25)	52(4)	58(4)	35(4)	11(3)	-12(3)	-7(3)
C(26)	50(4)	53(4)	45(4)	3(3)	-7(3)	-8(3)
C(27)	51(4)	43(3)	51(4)	15(3)	-6(3)	0(3)
C(28)	46(4)	42(3)	40(4)	14(3)	-11(3)	-2(2)
C(29)	31(3)	44(3)	26(3)	13(3)	-2(2)	2(2)
C(30)	48(3)	39(3)	20(3)	12(2)	-1(3)	0(2)
C(31)	58(4)	46(3)	36(4)	14(3)	0(3)	-3(3)
C(32)	75(5)	51(4)	53(4)	26(3)	2(4)	-15(3)
C(33)	90(5)	40(3)	43(4)	14(3)	0(4)	-4(3)
C(34)	71(4)	42(3)	31(3)	16(3)	0(3)	8(3)
C(35)	96(6)	48(4)	44(4)	15(3)	4(4)	21(4)
C(36)	89(6)	72(5)	45(4)	24(4)	13(4)	45(4)
C(37)	56(4)	74(4)	46(4)	31(4)	6(3)	24(3)
C(38)	48(4)	53(3)	34(3)	18(3)	0(3)	12(3)
C(39)	54(4)	42(3)	19(3)	10(2)	-4(3)	8(3)
C(1A)	60(4)	40(3)	29(3)	16(3)	-5(3)	0(3)
C(2A)	53(4)	42(3)	36(3)	16(3)	-12(3)	-7(3)
C(3A)	68(5)	60(4)	25(3)	6(3)	-5(3)	-3(3)
C(4A)	75(5)	71(4)	40(4)	13(4)	14(4)	16(4)
C(5A)	60(4)	73(4)	49(4)	30(4)	0(4)	7(3)
C(6A)	56(4)	65(4)	40(4)	25(3)	-16(3)	-7(3)
C(1MA)	76(5)	66(4)	30(4)	4(3)	-3(3)	1(4)
C(2MA)	58(4)	72(4)	50(4)	18(4)	-13(4)	-4(3)

TABLE 6.7 Fractional atomic coordinates (x 104)
and Thermal Parameters (Å2 x 103)
with e.s.d. s in parentheses for MAXINE

Atom	x/a	y/b	z/c	Uiso/ Uequiv(*)
SI(1)	4001(0)	2102(0)	7469(0)	33(0) *
O(1)	3398(1)	3250(1)	6242(1)	44(1) *
C(10)	5736(2)	1049(2)	7158(1)	35(1) *
C(11)	6154(2)	-290(2)	7734(2)	41(1) *
C(12)	7453(2)	-1138(2)	7653(2)	46(1) *
C(13)	8348(2)	-641(2)	7007(2)	47(1) *
C(14)	7991(2)	719(2)	6391(2)	40(1) *
C(15)	8914(2)	1252(2)	5700(2)	51(1) *
C(16)	8556(2)	2549(2)	5071(2)	57(1) *
C(17)	7253(2)	3403(2)	5105(2)	54(1) *
C(18)	6345(2)	2930(2)	5781(2)	45(1) *
C(19)	6674(2)	1576(2)	6445(2)	35(1) *
C(20)	3870(2)	2953(2)	8491(2)	36(1) *
C(21)	4890(2)	2435(2)	9116(2)	46(1) *
C(22)	4874(2)	2949(2)	9950(2)	56(1) *
C(23)	3829(2)	3994(2)	10165(2)	56(1) *
C(24)	2755(2)	4579(2)	9558(2)	44(1) *
C(25)	1661(2)	5672(2)	9773(2)	56(1) *
C(26)	629(2)	6230(2)	9195(2)	60(1) *
C(27)	625(2)	5718(2)	8370(2)	54(1) *
C(28)	1659(2)	4661(2)	8138(2)	46(1) *
C(29)	2763(2)	4060(2)	8716(2)	37(1) *
C(30)	3093(2)	1018(2)	8252(2)	35(1) *
C(31)	2567(2)	879(2)	9434(2)	43(1) *
C(32)	1863(2)	100(2)	10075(2)	53(1) *
C(33)	1663(2)	-537(2)	9523(2)	52(1) *
C(34)	2160(2)	-433(2)	8305(2)	42(1) *
C(35)	1949(2)	-1070(2)	7707(2)	55(1) *

Table 6.7 ctd.

C(36)	2440(2)	-974(2)	6536(2)	58(1) *
C(37)	3186(2)	-243(2)	5906(2)	53(1) *
C(38)	3415(2)	388(2)	6456(2)	43(1) *
C(39)	2898(2)	333(2)	7666(2)	36(1) *
C(1A)	3491(2)	4335(2)	3093(2)	52(1) *
C(2A)	2504(2)	5570(2)	2820(2)	53(1) *
C(3A)	1232(2)	5741(2)	3076(2)	56(1) *
C(4A)	955(2)	4636(2)	3634(2)	65(1) *
C(5A)	1922(3)	3403(2)	3890(2)	69(1) *
C(6A)	3172(2)	3250(2)	3620(2)	59(1) *
C(1MA)	4859(2)	4179(3)	2827(3)	78(2) *
C(2MA)	177(3)	7098(3)	2755(3)	83(2) *

Anisotropic atoms have thermal parameters (Å2 x 103) of the form :

exp [-2p2(U11h2a*2 + U22k2b*2 + U3312c*2 + 2U23klb*c* +
2U13hla*c* + 2U12hka*b*)]

Atom	U11	U22	U33	U23	U13	U12
SI(1)	34(0)	29(0)	34(0)	-11(0)	-4(0)	-9(0)
O(1)	54(1)	37(1)	39(1)	-9(1)	-12(1)	-12(1)
C(10)	39(1)	33(1)	34(1)	-12(1)	-3(1)	-12(1)
C(11)	44(1)	32(1)	41(1)	-11(1)	-2(1)	-11(1)
C(12)	48(1)	32(1)	47(1)	-11(1)	-7(1)	-5(1)
C(13)	38(1)	44(1)	48(1)	-18(1)	-5(1)	-4(1)
C(14)	41(1)	46(1)	36(1)	-19(1)	-2(1)	-15(1)
C(15)	40(1)	64(1)	55(1)	-27(1)	1(1)	-22(1)
C(16)	57(1)	68(1)	58(1)	-22(1)	5(1)	-40(1)
C(17)	61(1)	46(1)	58(1)	-12(1)	-3(1)	-29(1)
C(18)	47(1)	38(1)	51(1)	-14(1)	-5(1)	-16(1)
C(19)	38(1)	34(1)	36(1)	-15(1)	-4(1)	-12(1)
C(20)	39(1)	33(1)	35(1)	-10(1)	-3(1)	-13(1)
C(21)	49(1)	44(1)	46(1)	-13(1)	-14(1)	-12(1)
C(22)	64(1)	58(1)	51(1)	-15(1)	-23(1)	-18(1)
C(23)	77(2)	58(1)	44(1)	-23(1)	-11(1)	-26(1)
C(24)	58(1)	40(1)	36(1)	-14(1)	0(1)	-21(1)
C(25)	71(2)	46(1)	51(1)	-27(1)	5(1)	-22(1)
C(26)	56(1)	42(1)	65(1)	-23(1)	7(1)	-10(1)
C(27)	43(1)	46(1)	59(1)	-19(1)	-1(1)	-6(1)
C(28)	43(1)	43(1)	48(1)	-18(1)	-4(1)	-11(1)
C(29)	43(1)	31(1)	35(1)	-9(1)	0(1)	-15(1)
C(30)	32(1)	33(1)	36(1)	-11(1)	-5(1)	-8(1)
C(31)	40(1)	46(1)	38(1)	-14(1)	-1(1)	-15(1)
C(32)	49(1)	61(1)	42(1)	-13(1)	3(1)	-24(1)
C(33)	43(1)	50(1)	56(1)	-9(1)	0(1)	-23(1)
C(34)	34(1)	37(1)	52(1)	-9(1)	-10(1)	-11(1)
C(35)	52(1)	45(1)	78(2)	-16(1)	-16(1)	-23(1)
C(36)	65(1)	53(1)	71(2)	-25(1)	-23(1)	-20(1)
C(37)	63(1)	47(1)	51(1)	-21(1)	-13(1)	-13(1)
C(38)	49(1)	39(1)	41(1)	-14(1)	-7(1)	-14(1)
C(39)	31(1)	29(1)	42(1)	-9(1)	-9(1)	-6(1)
C(1A)	58(1)	55(1)	37(1)	-13(1)	-12(1)	-14(1)
C(2A)	64(1)	49(1)	48(1)	-12(1)	-15(1)	-20(1)
C(3A)	59(1)	57(1)	52(1)	-20(1)	-19(1)	-11(1)
C(4A)	64(2)	74(2)	66(2)	-24(1)	-13(1)	-30(1)
C(5A)	88(2)	63(2)	65(2)	-15(1)	-14(1)	-38(1)
C(6A)	76(2)	47(1)	48(1)	-14(1)	-16(1)	-13(1)
C(1MA)	59(2)	83(2)	79(2)	-18(2)	-13(1)	-19(1)
C(2MA)	70(2)	70(2)	92(2)	-30(2)	-30(2)	0(1)

TABLE 6.8 Fractional atomic coordinates (x 10^4) and Thermal Parameters ($Å^2$ x 10^3) with e.s.d. s in parentheses for NAPPY

Atom	x/a	y/b	z/c	U_{iso}/U_{equiv}(*)
SI(1)	3360(1)	1293(1)	1449(1)	38(0) *
O(1)	2450(2)	2016(2)	2149(1)	50(1) *
C(10)	5251(3)	1794(2)	1133(2)	40(1) *
C(11)	5737(4)	2078(2)	280(2)	48(1) *
C(12)	7128(4)	2493(3)	-6(2)	55(1) *
C(13)	8026(4)	2639(3)	570(3)	56(1) *
C(14)	7613(3)	2361(2)	1451(2)	49(1) *
C(15)	8553(4)	2487(3)	2051(3)	66(2) *
C(16)	8150(5)	2186(3)	2898(3)	74(2) *
C(17)	6797(4)	1742(3)	3198(3)	69(2) *
C(18)	5850(4)	1612(3)	2632(2)	55(1) *
C(19)	6225(3)	1918(2)	1741(2)	44(1) *
C(20)	3416(3)	-164(2)	1927(2)	41(1) *
C(21)	4690(4)	-756(3)	1782(2)	52(1) *
C(22)	4809(4)	-1864(3)	2077(2)	62(1) *
C(23)	3657(5)	-2381(3)	2543(2)	62(1) *
C(24)	2322(4)	-1826(3)	2727(2)	51(1) *
C(25)	1113(5)	-2349(3)	3227(2)	65(2) *
C(26)	-152(5)	-1805(3)	3393(3)	74(2) *
C(27)	-326(4)	-707(3)	3072(2)	62(1) *
C(28)	815(3)	-186(3)	2597(2)	48(1) *
C(29)	2181(3)	-710(2)	2414(2)	40(1) *
C(30)	2429(3)	1382(2)	469(2)	39(1) *
C(31)	2175(3)	435(2)	158(2)	48(1) *
C(32)	1543(4)	428(3)	-593(2)	55(1) *
C(33)	1159(4)	1367(3)	-1044(2)	56(1) *
C(34)	1392(3)	2372(3)	-771(2)	46(1) *
C(35)	1000(4)	3359(3)	-1237(2)	58(1) *
C(36)	1197(4)	4314(3)	-967(2)	61(1) *
C(37)	1817(4)	4340(3)	-216(2)	59(1) *
C(38)	2214(4)	3402(2)	247(2)	48(1) *
C(39)	2017(3)	2383(2)	-11(2)	39(1) *
C(1A)	3685(4)	4684(3)	2086(3)	65(2) *
C(2A)	2218(5)	4926(3)	2113(3)	69(2) *
C(3A)	1266(5)	4615(3)	2828(3)	72(2) *
C(4A)	1713(5)	4066(3)	3556(3)	71(2) *
C(5A)	3184(6)	3820(4)	3529(3)	85(2) *
C(6A)	4154(5)	4122(3)	2807(3)	75(2) *
C(1MA)	4750(5)	5018(4)	1314(3)	91(2) *
C(2MA)	650(7)	3740(5)	4348(4)	117(3) *
C(1B)	4048(5)	4615(4)	5719(3)	79(2) *
C(2B)	3872(5)	5650(4)	5292(3)	84(2) *
C(3B)	4799(6)	6028(4)	4589(3)	85(2) *
C(1MB)	3006(7)	4220(6)	6514(4)	126(3) *
C(1C)	3621(5)	269(4)	4760(3)	74(2) *
C(2C)	4167(5)	815(4)	5342(3)	77(2) *
C(3C)	5495(5)	553(4)	5583(3)	77(2) *
C(1MC)	2130(6)	571(5)	4503(3)	109(3) *

Anisotropic atoms have thermal parameters ($Å^2$ x 10^3) of the form :

$$\exp[-2\pi^2(U_{11}h^2a^{*2} + U_{22}k^2b^{*2} + U_{33}l^2c^{*2} + 2U_{23}klb^*c^* + 2U_{13}hla^*c^* + 2U_{12}hka^*b^*)]$$

Atom	U_{11}	U_{22}	U_{33}	U_{23}	U_{13}	U_{12}
SI(1)	37(1)	37(0)	40(1)	-4(0)	-2(0)	-3(0)
O(1)	46(1)	51(1)	53(1)	-16(1)	1(1)	-7(1)
C(10)	38(2)	37(2)	45(2)	-2(1)	-2(1)	-1(1)
C(11)	49(2)	43(2)	49(2)	-2(1)	0(2)	0(1)
C(12)	50(2)	45(2)	61(2)	4(2)	9(2)	0(2)
C(13)	39(2)	42(2)	81(3)	-2(2)	5(2)	-3(1)
C(14)	38(2)	36(2)	74(2)	-7(2)	-7(2)	1(1)
C(15)	45(2)	57(2)	101(3)	-14(2)	-21(2)	-3(2)
C(16)	68(3)	75(3)	91(3)	-16(2)	-38(2)	-1(2)
C(17)	72(3)	77(3)	61(2)	-5(2)	-24(2)	0(2)

Table 6.8 ctd.

C(18)	54(2)	59(2)	53(2)	-1(2)	-10(2)	-4(2)
C(19)	40(2)	39(2)	53(2)	-3(1)	-5(1)	1(1)
C(20)	45(2)	40(2)	39(2)	-8(1)	-6(1)	0(1)
C(21)	49(2)	49(2)	57(2)	-1(2)	-2(2)	2(2)
C(22)	67(2)	51(2)	63(2)	-3(2)	-2(2)	14(2)
C(23)	87(3)	41(2)	59(2)	-3(2)	-11(2)	4(2)
C(24)	71(2)	43(2)	39(2)	-4(1)	-6(2)	-10(2)
C(25)	91(3)	47(2)	53(2)	0(2)	0(2)	-19(2)
C(26)	81(3)	73(3)	64(3)	-5(2)	8(2)	-35(2)
C(27)	54(2)	70(2)	61(2)	-15(2)	4(2)	-16(2)
C(28)	48(2)	51(2)	46(2)	-8(2)	-3(2)	-10(2)
C(29)	50(2)	40(2)	31(2)	-3(1)	-4(1)	-7(1)
C(30)	33(2)	40(2)	43(2)	-5(1)	-2(1)	-3(1)
C(31)	50(2)	42(2)	54(2)	-10(2)	-4(2)	-1(1)
C(32)	64(2)	53(2)	56(2)	-22(2)	-13(2)	-4(2)
C(33)	55(2)	73(2)	46(2)	-19(2)	-12(2)	-2(2)
C(34)	37(2)	57(2)	42(2)	-7(2)	0(1)	2(1)
C(35)	52(2)	73(3)	45(2)	2(2)	-7(2)	2(2)
C(36)	62(2)	58(2)	60(2)	10(2)	-8(2)	4(2)
C(37)	60(2)	47(2)	66(2)	0(2)	-5(2)	1(2)
C(38)	51(2)	42(2)	52(2)	-4(2)	-9(2)	-1(1)
C(39)	30(2)	44(2)	42(2)	-5(1)	0(1)	-1(1)
C(1A)	73(3)	52(2)	78(3)	-21(2)	-20(2)	0(2)
C(2A)	74(3)	61(2)	75(3)	-11(2)	-18(2)	11(2)
C(3A)	70(3)	73(3)	80(3)	-22(2)	-16(2)	9(2)
C(4A)	89(3)	69(3)	62(3)	-26(2)	-16(2)	0(2)
C(5A)	108(4)	75(3)	84(3)	-14(3)	-52(3)	-1(3)
C(6A)	68(3)	70(3)	95(3)	-24(3)	-28(3)	1(2)
C(1MA)	81(3)	83(3)	110(4)	-21(3)	1(3)	-14(2)
C(2MA)	142(5)	122(5)	86(4)	-23(3)	-3(4)	-5(4)
C(1B)	75(3)	98(4)	70(3)	-5(3)	-19(2)	-22(3)
C(2B)	79(3)	96(4)	84(3)	-18(3)	-23(3)	0(3)
C(3B)	93(4)	87(3)	80(3)	-5(3)	-28(3)	-14(3)
C(1MB)	108(4)	172(6)	96(4)	3(4)	-8(3)	-48(4)
C(1C)	76(3)	93(3)	53(2)	-11(2)	-6(2)	-13(2)
C(2C)	90(3)	85(3)	61(3)	-19(2)	-9(2)	-4(2)
C(3C)	93(3)	89(3)	54(2)	-17(2)	-11(2)	-16(3)
C(1MC)	88(4)	161(5)	85(4)	-24(3)	-24(3)	1(4)

TABLE 6.9 Fractional atomic coordinates (x 10^4)
and Thermal Parameters ($Å^2$ x 10^3)
with e.s.d. s in parentheses for NATRET

Atom	x/a	y/b	z/c	U_{iso}/U_{equiv}(*)
SI(1)	4075(1)	2363(1)	1236(1)	44(1) *
O(1)	3549(2)	3485(2)	1963(2)	58(2) *
C(10)	5704(3)	3062(3)	1555(3)	44(2) *
C(11)	6035(3)	2458(3)	519(4)	55(2) *
C(12)	7250(4)	2833(4)	694(4)	64(3) *
C(13)	8159(4)	3825(4)	1946(5)	67(3) *
C(14)	7893(3)	4493(3)	3048(4)	53(2) *
C(15)	8825(3)	5528(4)	4351(4)	68(3) *
C(16)	8556(4)	6179(4)	5399(4)	76(3) *
C(17)	7338(4)	5827(4)	5215(4)	67(3) *
C(18)	6416(3)	4823(3)	3987(4)	56(3) *
C(19)	6657(3)	4123(3)	2864(3)	46(2) *
C(20)	4065(3)	1409(3)	2017(3)	42(2) *
C(21)	5123(3)	1202(3)	2499(3)	51(2) *
C(22)	5188(3)	530(3)	3124(4)	58(3) *
C(23)	4223(4)	87(3)	3294(4)	61(3) *
C(24)	3114(3)	270(3)	2830(3)	53(3) *
C(25)	2089(4)	-190(4)	2984(4)	75(3) *
C(26)	1015(4)	-55(4)	2498(4)	81(3) *
C(27)	902(3)	522(4)	1790(4)	69(3) *
C(28)	1876(3)	1009(3)	1636(4)	56(2) *
C(29)	3024(3)	902(3)	2148(3)	45(2) *
C(30)	3098(3)	1199(3)	-629(3)	45(2) *
C(31)	2615(3)	-134(3)	-1207(3)	51(2) *
C(32)	1849(3)	-1063(4)	-2587(4)	62(2) *

Table 6.9 ctd.

C(33)	1555(3)	-651(4)	-3411(4)	65(3) *
C(34)	2026(3)	699(4)	-2898(4)	58(3) *
C(35)	1747(4)	1141(5)	-3750(4)	80(3) *
C(36)	2222(5)	2432(6)	-3248(6)	101(5) *
C(37)	3000(4)	3368(5)	-1876(5)	86(4) *
C(38)	3283(4)	2979(4)	-1027(4)	68(3) *
C(39)	2809(3)	1628(3)	-1507(4)	50(3) *
N(1)	2633(3)	5273(3)	1835(3)	67(2) *
C(1)	2411(4)	5617(4)	3007(5)	90(4) *
C(2)	1832(5)	6667(5)	3468(7)	134(5) *
C(3)	1522(5)	4699(5)	601(5)	128(5) *
C(4)	675(5)	3402(6)	122(8)	198(6) *
C(5)	3512(5)	6397(4)	2039(6)	106(5) *
C(6)	4728(5)	6958(6)	3132(7)	157(6) *

Anisotropic atoms have thermal parameters ($Å^2 \times 10^3$) of the form :
$\exp[-2\pi^2(U_{11}h^2a^{*2} + U_{22}k^2b^{*2} + U_{33}l^2c^{*2} + 2U_{23}klb^*c^* + 2U_{13}hla^*c^* + 2U_{12}hka^*b^*)]$

Atom	U_{11}	U_{22}	U_{33}	U_{23}	U_{13}	U_{12}
SI(1)	49(1)	42(1)	45(1)	26(1)	19(1)	20(1)
O(1)	72(2)	54(2)	59(2)	34(1)	30(1)	37(1)
C(10)	57(2)	38(2)	44(2)	27(2)	23(2)	20(2)
C(11)	61(3)	47(2)	57(3)	31(2)	26(2)	19(2)
C(12)	79(3)	62(3)	71(3)	41(3)	46(3)	33(2)
C(13)	58(3)	66(3)	91(4)	50(3)	39(3)	25(2)
C(14)	54(3)	46(2)	65(3)	37(2)	23(2)	18(2)
C(15)	52(2)	63(3)	78(3)	43(3)	15(2)	13(2)
C(16)	65(3)	66(3)	64(3)	33(3)	6(3)	9(2)
C(17)	77(3)	63(3)	47(3)	27(2)	20(2)	22(2)
C(18)	63(2)	52(2)	46(3)	26(2)	19(2)	17(2)
C(19)	57(2)	39(2)	49(3)	30(2)	20(2)	18(2)
C(20)	48(2)	40(2)	40(2)	22(2)	20(2)	19(2)
C(21)	52(2)	51(2)	60(3)	36(2)	27(2)	25(2)
C(22)	63(3)	55(2)	66(3)	40(2)	25(2)	30(2)
C(23)	85(3)	54(2)	57(3)	39(2)	32(2)	29(2)
C(24)	63(3)	43(2)	50(2)	24(2)	28(2)	16(2)
C(25)	92(3)	69(3)	75(3)	45(3)	48(3)	21(3)
C(26)	71(3)	82(3)	87(4)	41(3)	49(3)	16(3)
C(27)	49(3)	76(3)	63(3)	28(3)	25(2)	20(2)
C(28)	46(2)	57(2)	54(3)	27(2)	19(2)	17(2)
C(29)	51(2)	37(2)	39(2)	16(2)	21(2)	16(2)
C(30)	46(2)	42(2)	48(2)	25(2)	20(2)	20(2)
C(31)	48(2)	52(2)	50(3)	28(2)	20(2)	19(2)
C(32)	52(2)	50(2)	59(3)	19(2)	20(2)	15(2)
C(33)	49(2)	76(3)	44(3)	20(2)	15(2)	24(2)
C(34)	52(2)	82(3)	48(3)	37(2)	26(2)	37(2)
C(35)	83(3)	118(4)	51(3)	54(3)	28(2)	51(3)
C(36)	130(5)	142(5)	96(4)	97(4)	59(4)	81(4)
C(37)	125(4)	91(3)	88(4)	71(3)	57(3)	56(3)
C(38)	91(3)	72(3)	66(3)	51(3)	38(2)	40(2)
C(39)	52(2)	60(2)	52(3)	35(2)	26(2)	31(2)
N(1)	75(2)	56(2)	75(3)	38(2)	32(2)	38(2)
C(1)	119(4)	85(3)	102(4)	58(3)	71(4)	59(3)
C(2)	171(6)	112(4)	173(6)	75(4)	125(5)	96(4)
C(3)	136(5)	122(5)	98(4)	47(4)	22(4)	95(4)
C(4)	83(4)	88(4)	231(8)	11(5)	-11(5)	36(4)
C(5)	148(5)	75(4)	145(5)	74(4)	90(5)	63(4)
C(6)	91(5)	85(4)	231(8)	60(5)	56(5)	23(4)

References.

6.1. W. L. Duax; D. A. Norton (Eds.) *Atlas of Steroid Structure, Vol. 1.* Plenum Press, London, (1975).

6.2. E. Weber; H-P. Josel. *J. Incl. Phenom.* **1**, 79, (1983).

6.3. W. C. Hamilton. *Acta Crystallogr.* **18**, 502, (1965).

6.4. J. L. Atwood; F. Hamada; K. D. Robinson; G. W. Orr; R. L. Vincent. *Nature*. **349**, 683, (1991).

CHAPTER 7 : THERMAL ANALYSIS.

Thermal analysis involves the measurement of physical properties of a substance as a function of temperature while the substance is subjected to a controlled temperature-change programme. [7.1] Several books are available on the techniques and applications of thermal analysis. [7.1-7.3] The description below covers only a very small part of the field.

The physical properties which can be measured by thermal techniques include mass, temperature and enthalpy, as well as mechanical, acoustic, optical, electrical and magnetic properties. It is usual to apply two or more complementary techniques to a sample, in order to obtain several types of data under the same thermal conditions. The techniques applied in this study were thermogravimetry (TG) and differential scanning calorimetry (DSC).

The thermal behaviour of a sample is highly dependent on sample preparation. Differences arise out of structural differences in solids (even though they have the same chemical composition) such as the defect content, porosity and surface properties. An example of the differences that may be observed by varying the particle size is shown in Figure 7.1 which shows the TG and DSC curves of **W1DIOX**.

In addition, as the sample size increases, problems occur, such as the non-uniformity of sample temperature, caused by slow heat transfer. Therefore, samples were crushed as uniformly as possible and spread thinly in the container. Because of the instability of the inclusion compounds, sample preparation time had to be kept to a minimum. It was impossible to ensure that the crystals were crushed to the same degree (for example, by sieving) for every analysis, so some irreproducibility remained.

Thermogravimetry (TG).

TG determines the change in sample mass as a function of either temperature or time. In order to obtain useful information using TG, the sample must evolve a volatile product, whose mass loss can be determined.

The Perkin Elmer TGA7 uses a small platinum wound microfurnace which functions both as a heater and a resistance thermometer, detecting its own temperature and supplying power to heat the sample. A chromel-alumel thermocouple passes through the base of the furnace and is located close to the sample holder.

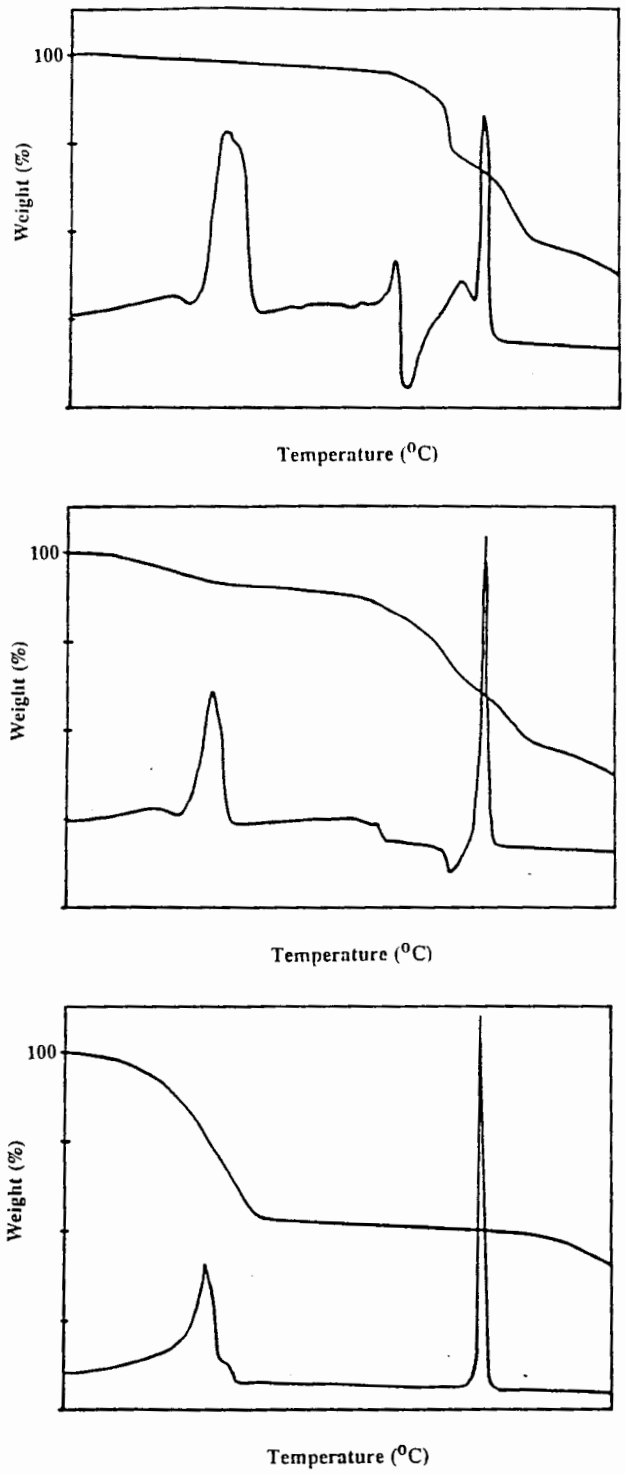

Figure 7.1. The effect of particle size on TG and DSC traces of **W1DIOX**.
(a) Single crystal ≈2 x 2 x 1 mm.
(b) Several small crystals.
(c) Crystals crushed to a powder.
Sample weights were approximately the same.

A null-point balance is used. A detector with an optical sensor measures the deflection of the beam supporting the sample pan and uses current to return the beam to its original position. The amount of current needed is a direct measure of the weight on the beam. Null-point mechanisms are favoured in TG because they ensure that the sample remains in the same zone of the furnace irrespective of changes in mass.

The sample is placed in platinum pan and suspended from the balance. The furnace is placed within the balance housing as shown schematically below in Figure 7.2.

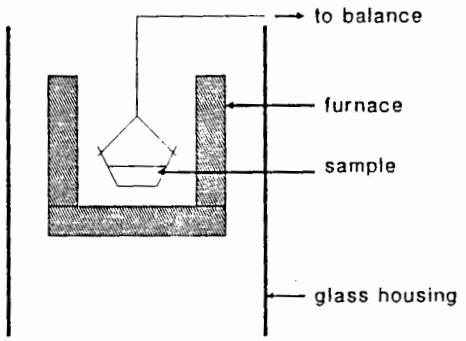

Figure 7.2. The arrangement of furnace, sample and housing in the Perkin-Elmer TGA7.

A constant flow of pure, dry nitrogen was passed through the housing in order to :

(i) reduce condensation of reaction products,
(ii) flush out corrosive products,
(iii) reduce secondary reactions and
(iv) act as a coolant for the balance mechanism.

The pressure of nitrogen flowing over the sample was kept higher than that flowing over the balance to prevent volatile products from travelling up into the balance mechanism.

Temperature calibration of the furnace used the Curie points of some metals and alloys. A ferromagnetic material loses its ferromagnetism at a characteristic temperature (the Curie point). If a magnet is placed below the sample (as shown in Figure 7.3) the total downward force on the sample, at temperatures below the Curie point, is the sum of the sample weight and the magnetic force. At the Curie point the magnetic force decreases to zero and an apparent mass loss is seen. By using several ferromagnetic materials, a multi-point temperature calibration is obtained.

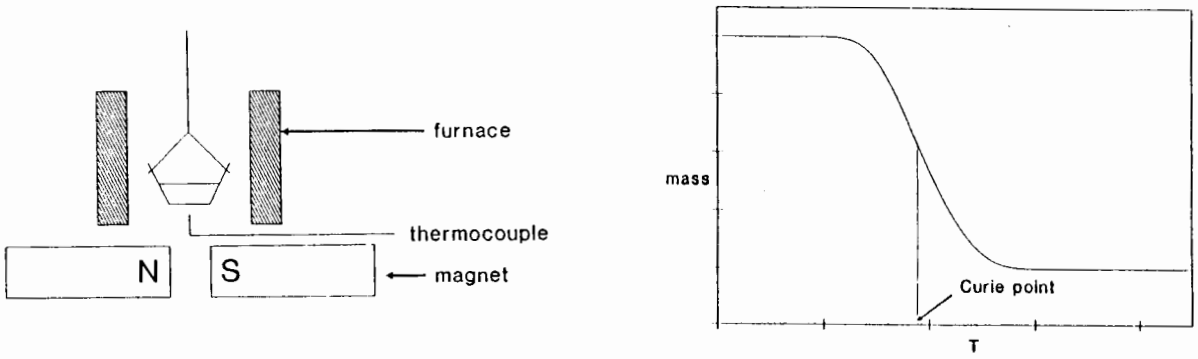

Figure 7.3. Curie-point method of temperature calibration.[7.2]

Typical TG curves which may be obtained are shown in Figure 7.4. They are classified as follows :

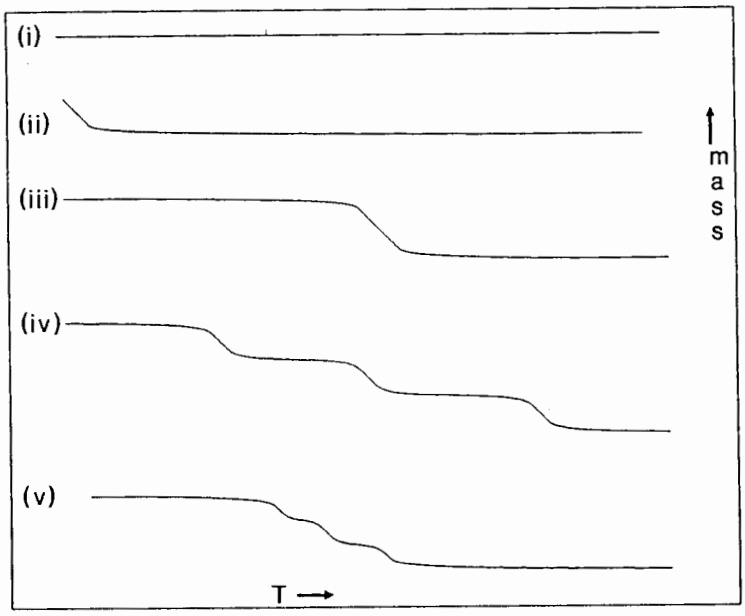

Figure 7.4. Main types of TG curves (adapted from ref. 7.2).

(i) The sample is stable over the temperature range shown. No information is gained about phase transitions or other reactions which do not evolve volatile products.
(ii) The initial mass loss indicates surface drying or desorption.
(iii) A single stage decomposition of the sample generates curves such as this.
(iv) This curve is indicative of a multi-stage decomposition with relatively stable intermediates, while the intermediates formed in the type (v) curve are not stable.
It is also possible to obtain curves which show a mass gain over temperature, but these were not observed in this study so have been omitted.

TG is generally only useful for following desorption and decomposition processes. When the process occurring is clearly defined however, the kinetics of the reaction can be determined. Details are given in a later section.

Differential Scanning Calorimetry (DSC).

In power-compensated DSC, the sample and a reference are maintained at the same temperature ($\Delta T = \Delta T_s - \Delta T_r = 0$) throughout the temperature programme by the input of electrical energy.

The Perkin-Elmer DSC7 operates on a "null-balance" principle; energy absorbed or evolved by the sample is compensated by adding or subtracting an equivalent amount of energy to a heater located in the sample holder. Measurement of this energy is made directly in milliwatts, providing a direct measurement of peak area.

Thermal events in the sample appear as deviations from the DSC baseline. They can be either endo- or exothermic, depending on whether more or less energy has to be supplied to the sample relative to the reference material. In DSC, endothermic events are conventionally represented as positive, *i.e.* above the baseline, corresponding to an increase in enthalpy. Endo- and exotherms are characterised by their onset temperature, T_{on}, which is the temperature quoted for any event. Figure 7.5 shows the main features of a DSC curve.

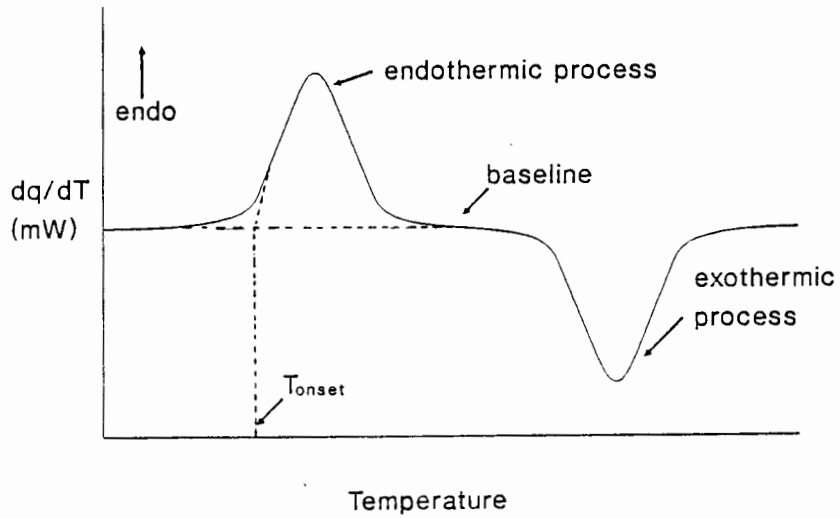

Figure 7.5. Main features of a typical DSC curve.

Sample preparation, as far as possible, was identical to that of samples for TG. Samples were then placed in vented aluminium pans and lids were crimped into place. The reference material was simply an empty pan. DSC was performed in vented rather than open pans because they reduce the rate of escape of vapour, thus giving a sharper trace. Because TG was performed using an open sample pan, the TG and DSC traces do not always coincide, particularly if the guest is very volatile.

The sample holder was purged by high-purity, dry nitrogen at a flow rate of 30 $mlmin^{-1}$.

A stable baseline is crucial in DSC as all thermal events are measured as deviations from the baseline. A baseline, run by matching empty sample and reference holders was subtracted from each sample run. The area of the endotherms or exotherms is measured as the amount of energy needed to maintain the sample and reference at the same temperature. The measured area, A, is related to the enthalpy change, ΔH, by

$$\Delta H = AK/m$$

where m is the sample mass and K the calibration factor. The calibration factor is specific to an instrument and must be determined by relating a known enthalpy change to a measured peak area. In DSC, K is virtually independent of temperature, allowing calibration for the full temperature range to be performed over a narrow range of temperatures.

DSC was used, in conjunction with TG, to follow thermal events in the inclusion compounds whose structures had been studied. Generally these events were:

(i) desorption of the guest species (endothermic)

(ii) other molecular rearrangements, or solid-solid phase transitions in the remaining host lattice (either endo- or exothermic)

(iii) melting of the host species (endothermic).

Results of TG and DSC.

The results of the thermogravimetric and differential scanning calorimetry analyses are summarized in Table 7.1 and the thermal analysis curves are shown in Figures 7.6 - 7.25. The thermal analyses of all four α-phases have been included, even though the crystal structures of triphenylmethanol and tri-1-naphthylsilanol are not known. Also included for the sake of comparision are the curves for the complexes of triphenylmethanol with dmso (2:1) and methanol (1:1) whose structures have been reported elsewhere.[7.4] The inclusion compounds of the four hosts with dmso exhibit some unusual behaviour and they have been dealt with separately.

The observed weight losses (TG) were used to calculate the true stoichiometries of the inclusion compounds (reported in Chapter 3). The calculated weight losses reported in Table 7.1 are for the integral stoichiometries used in the crystal structure analyses. The differences between the two are always < 3%.

The enthalpy values observed for all processes are low (< 100 $kJmol^{-1}$). This is in agreement with the low stability of the compounds, most of which decompose within an hour if removed from their mother liquor, even at room temperature.

The host 1,1,2,2-tetraphenylethane-1,2-diol, (**PEDIL**) decomposes at its melt point. This is seen as an exotherm immediately following the melting endotherm at ≈190°C in Figures 7.6 - 7.12. This made analysing the peak area corresponding to the melt more difficult and explains the wide range of ΔH observed for this process (12.0 - 37.1 $kJmol^{-1}$). The range of ΔH values for the other hosts are much narrower. They are given below.

$C_{19}H_{16}O$	20.5 - 28.6 $kJmol^{-1}$
$C_{18}H_{16}OSi$	17.3 - 24.5 $kJmol^{-1}$
$C_{30}H_{22}OSi$	23.5 - 27.1 $kJmol^{-1}$

When an inclusion compound is heated and the guest allowed to escape, the host may revert to the non-porous α-phase, or the host framework may hold, giving rise to an empty clathrate, or β_0 phase. [7.5] In the majority of inclusion compounds where hosts are discrete organic molecules the latter process is rare and the structure of the inclusion compound (or β-phase) usually collapses to the α-phase on guest loss.

The reason that such large deviations in the ΔH of melting are observed is that the host-guest compound first loses the guest, and in doing so, generally changes from the β- to α-phase. This phase change dramatically changes the physical properties of the host compound which remains. In particular, the crystallite size becomes smaller, with a concomitant change in the area of the melting endotherm.

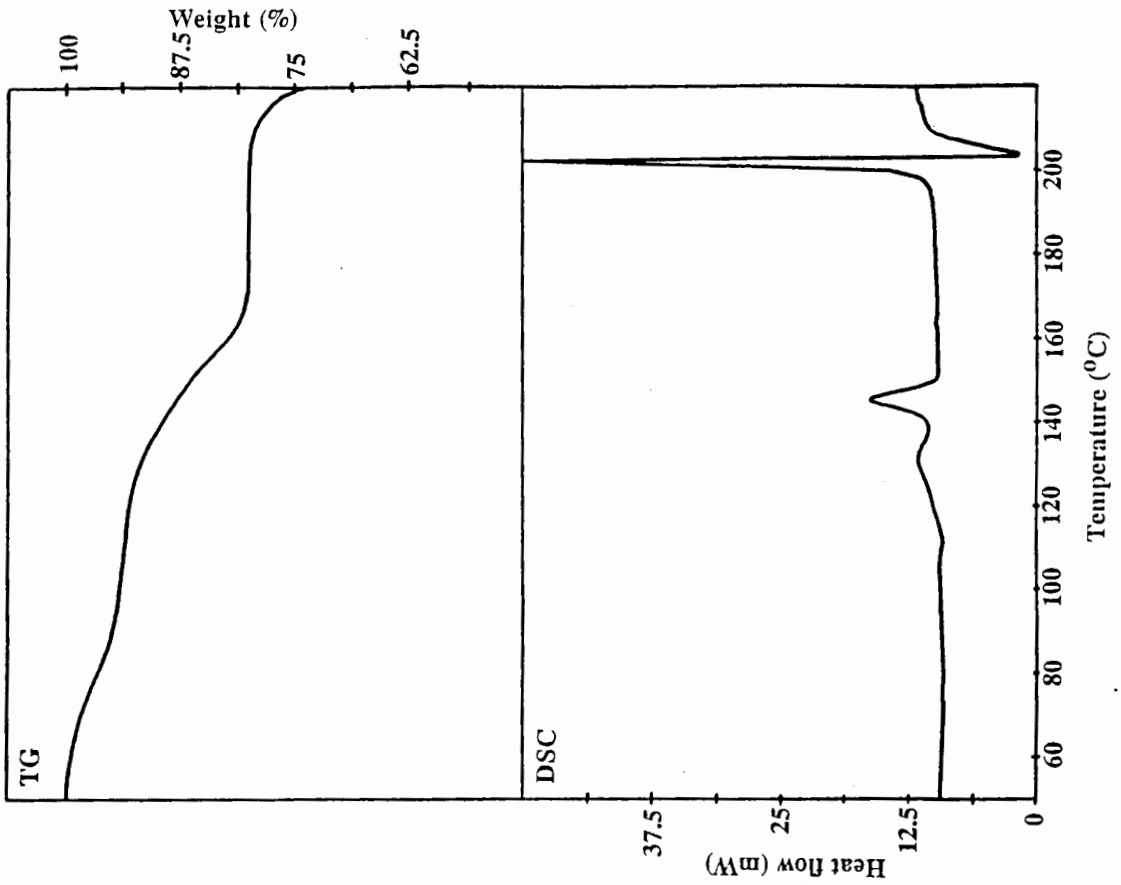

Figure 7.7. TG and DSC curves of **PEDIOX.**

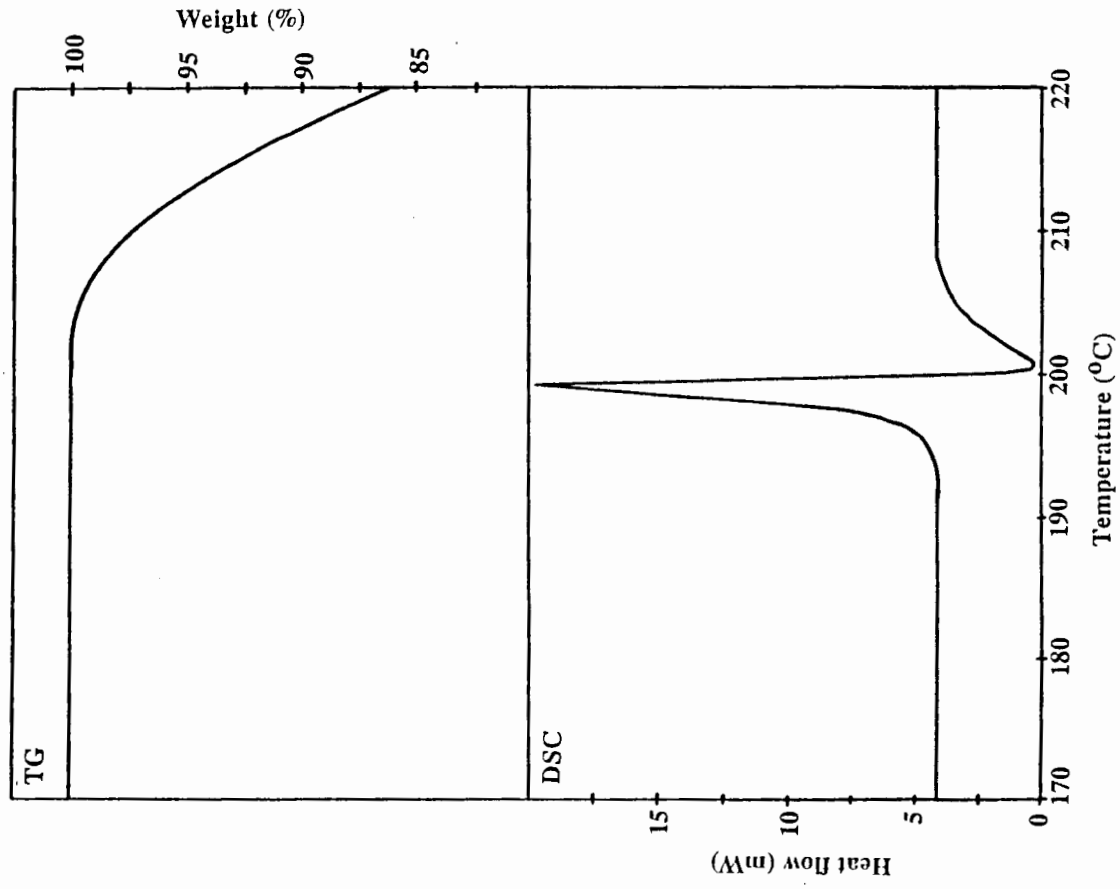

Figure 7.6. TG and DSC curves of **PEDIL.**

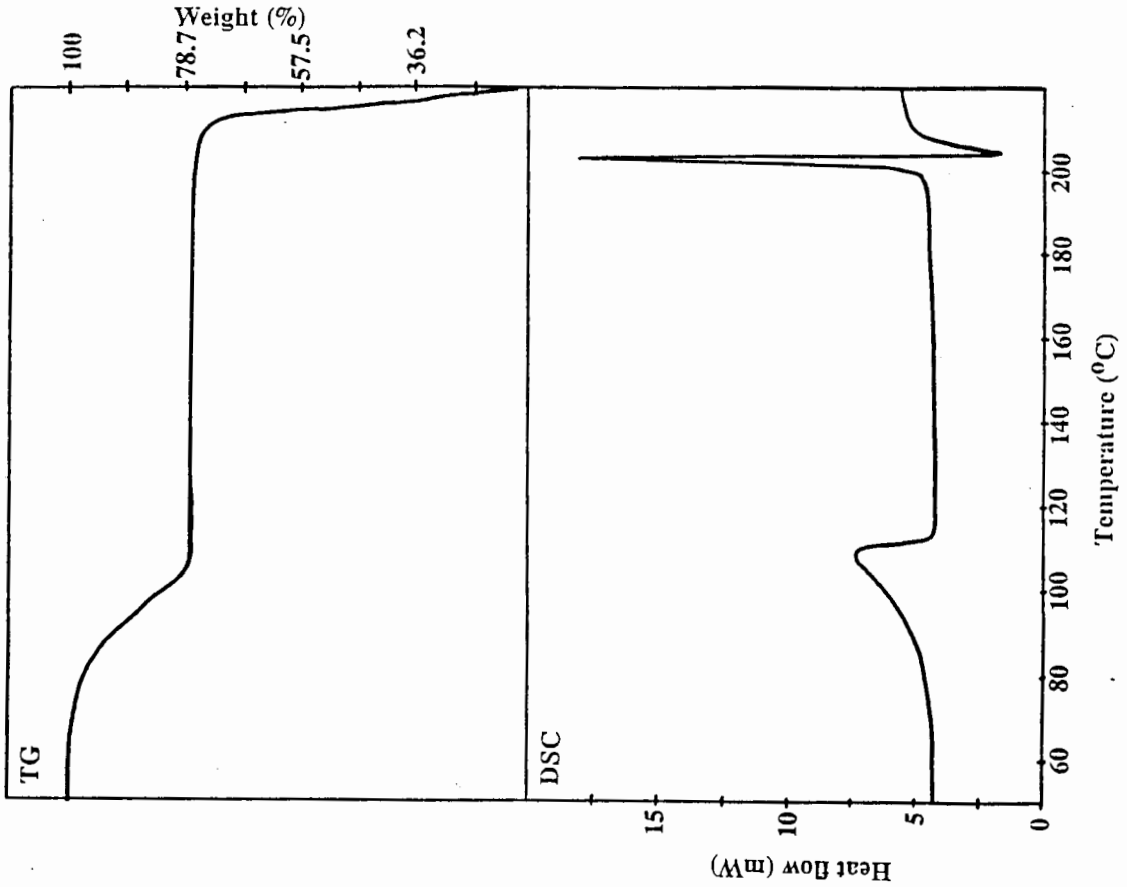

Figure 7.9. TG and DSC curves of DINM.

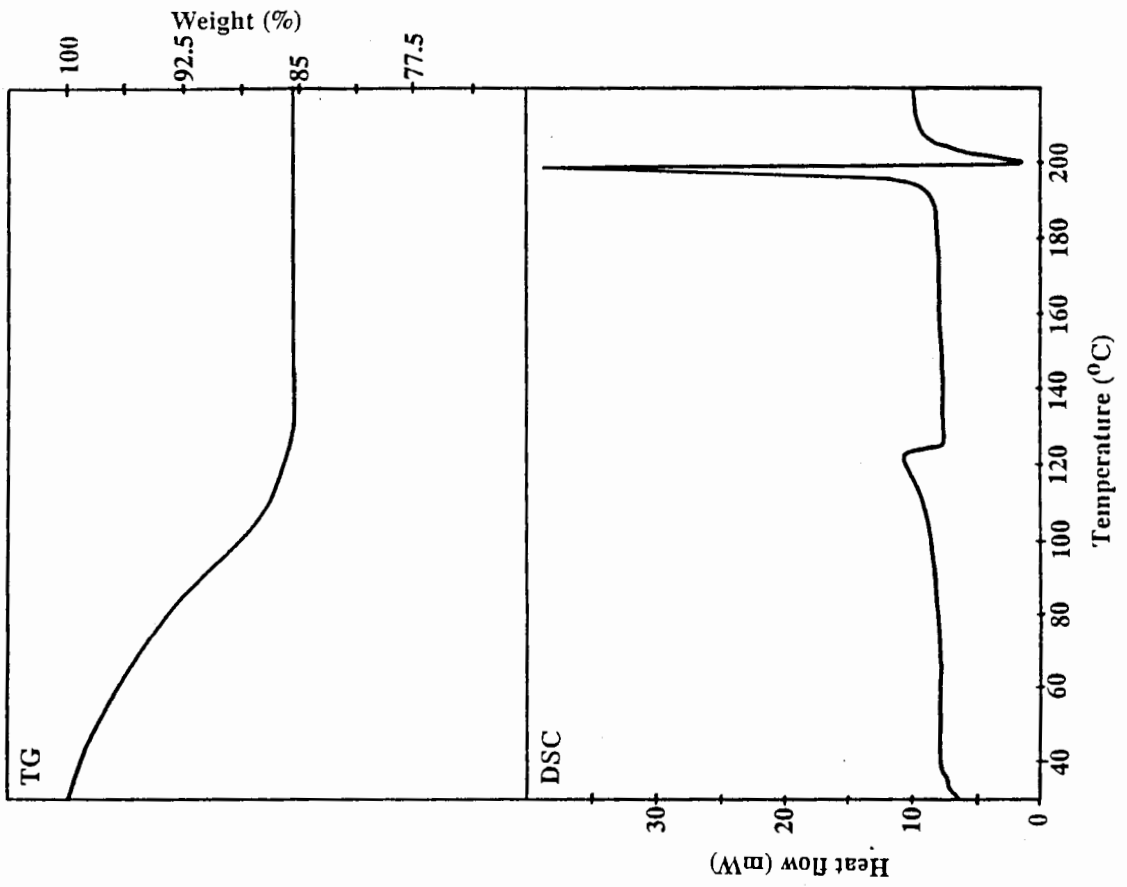

Figure 7.8. TG and DSC curves of PECTIL.

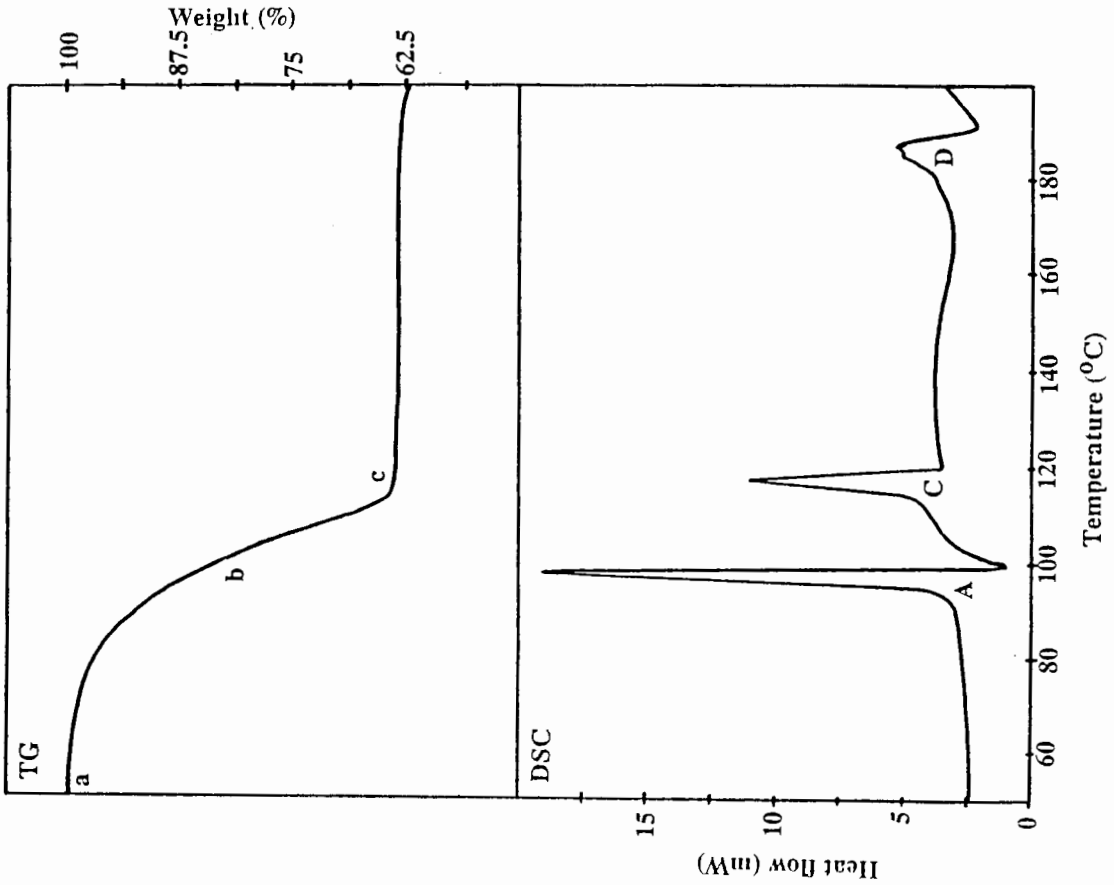

Figure 7.11. TG and DSC curves of **DINO.**

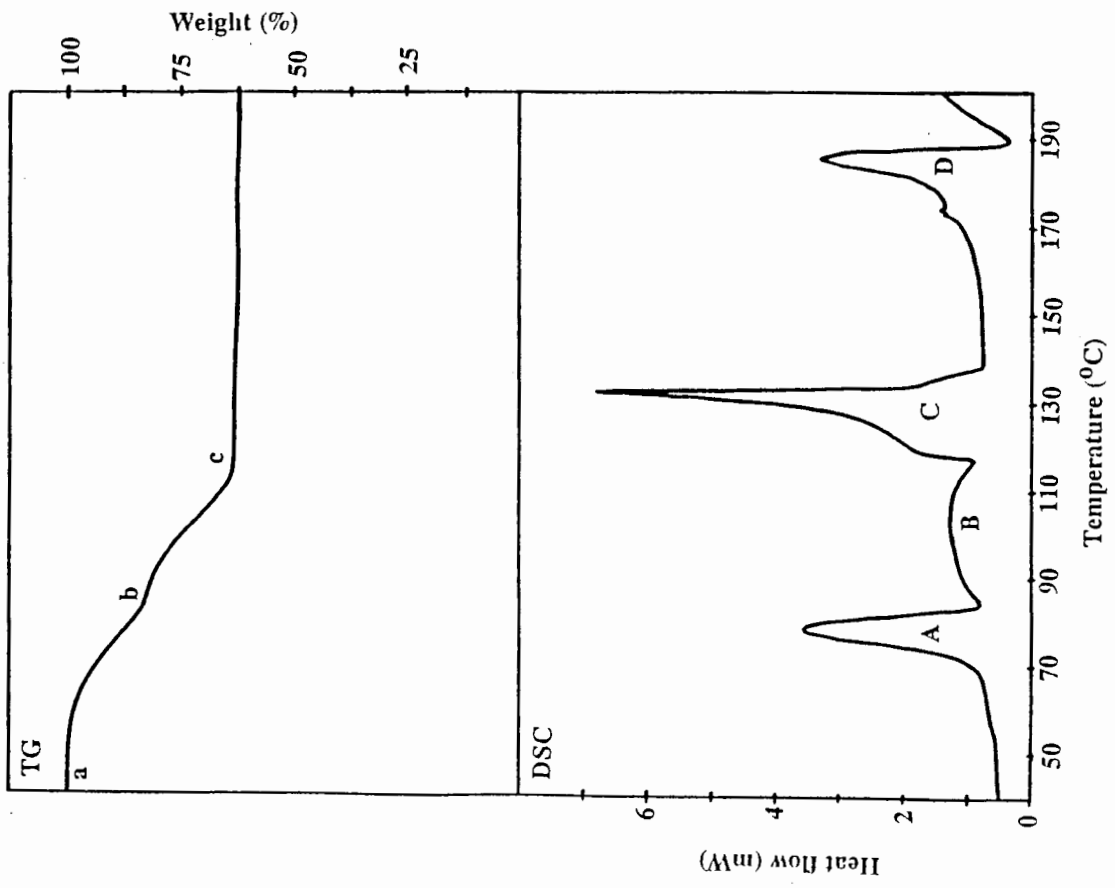

Figure 7.10. TG and DSC curves of **LUTI.**

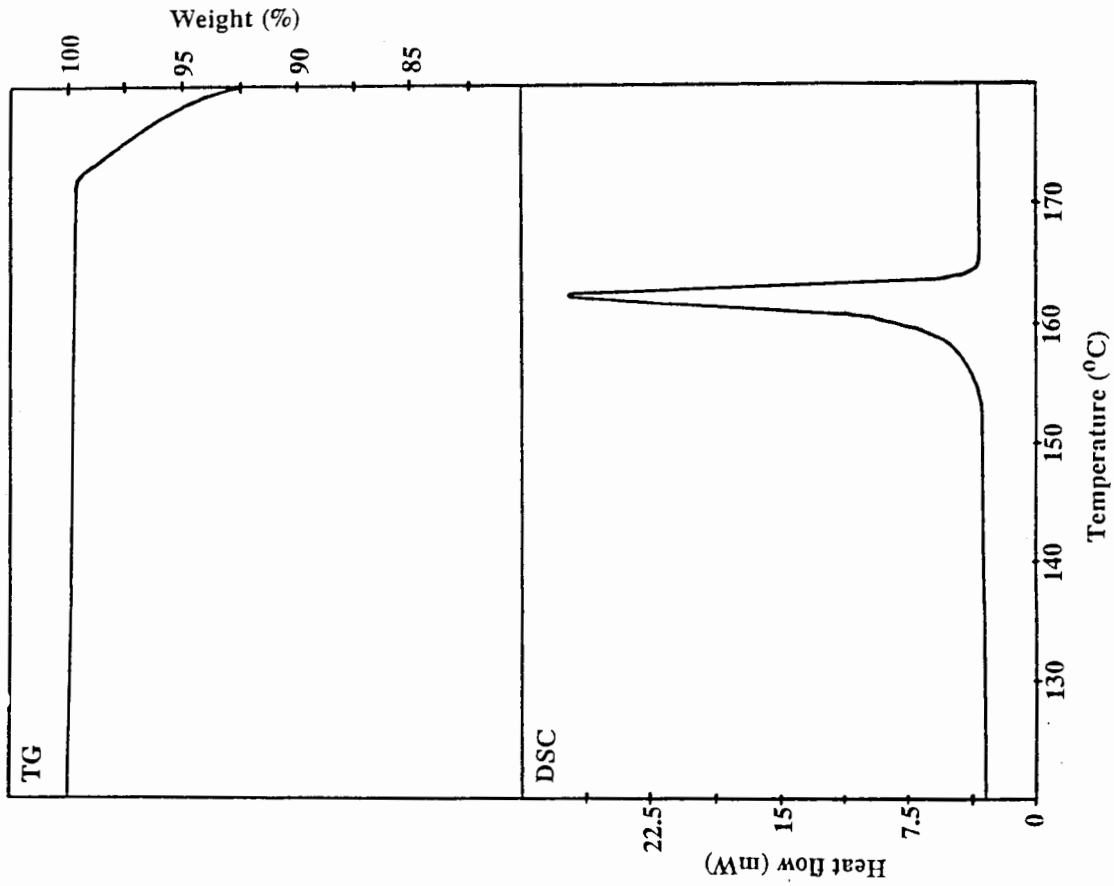

Figure 7.13. TG and DSC curves of Ph_3COH

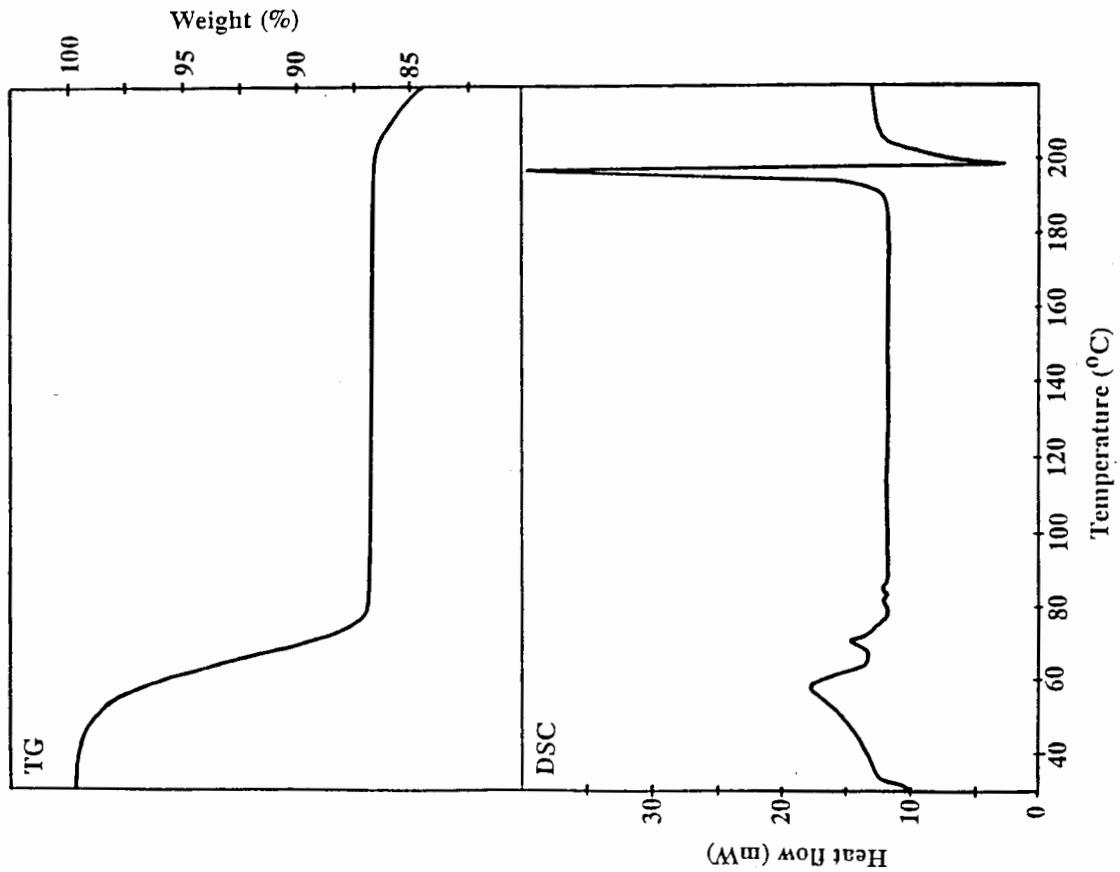

Figure 7.12. TG and DSC curves of **PEACH.**

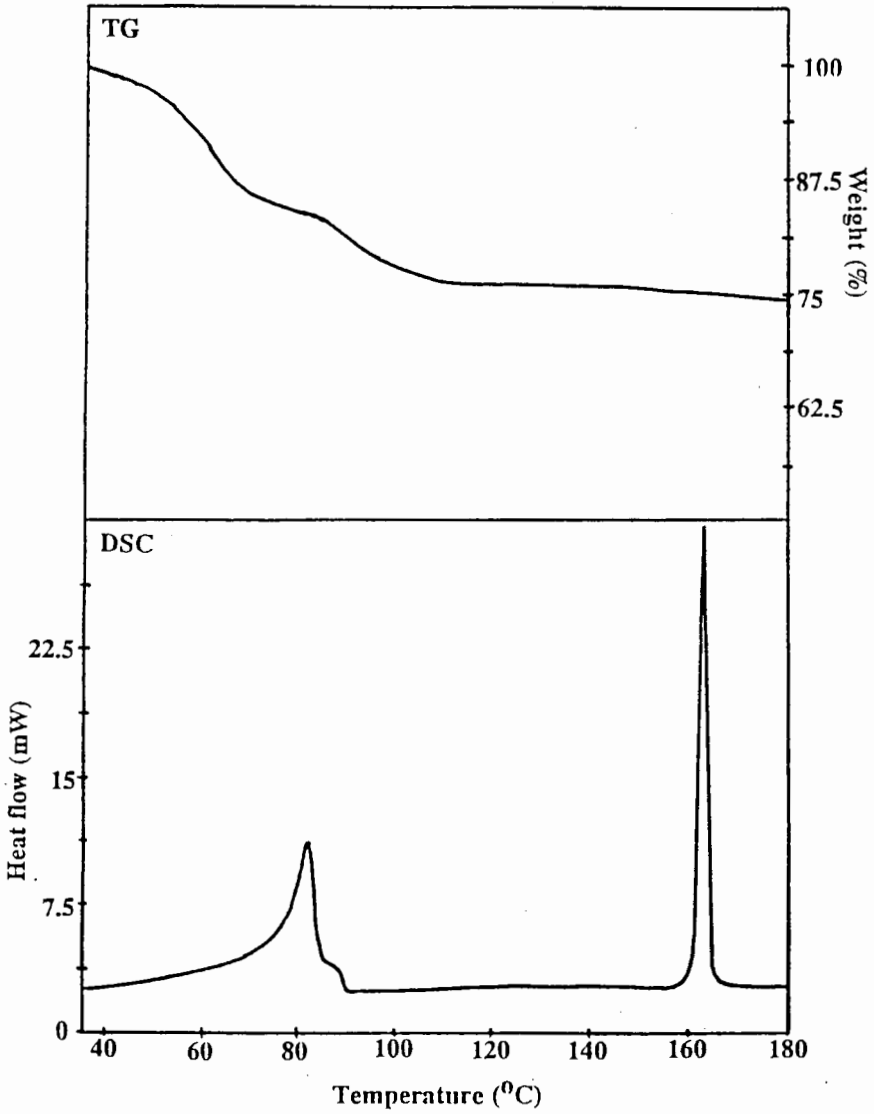

Figure 7.14. TG and DSC curves of **W1DIOX.**

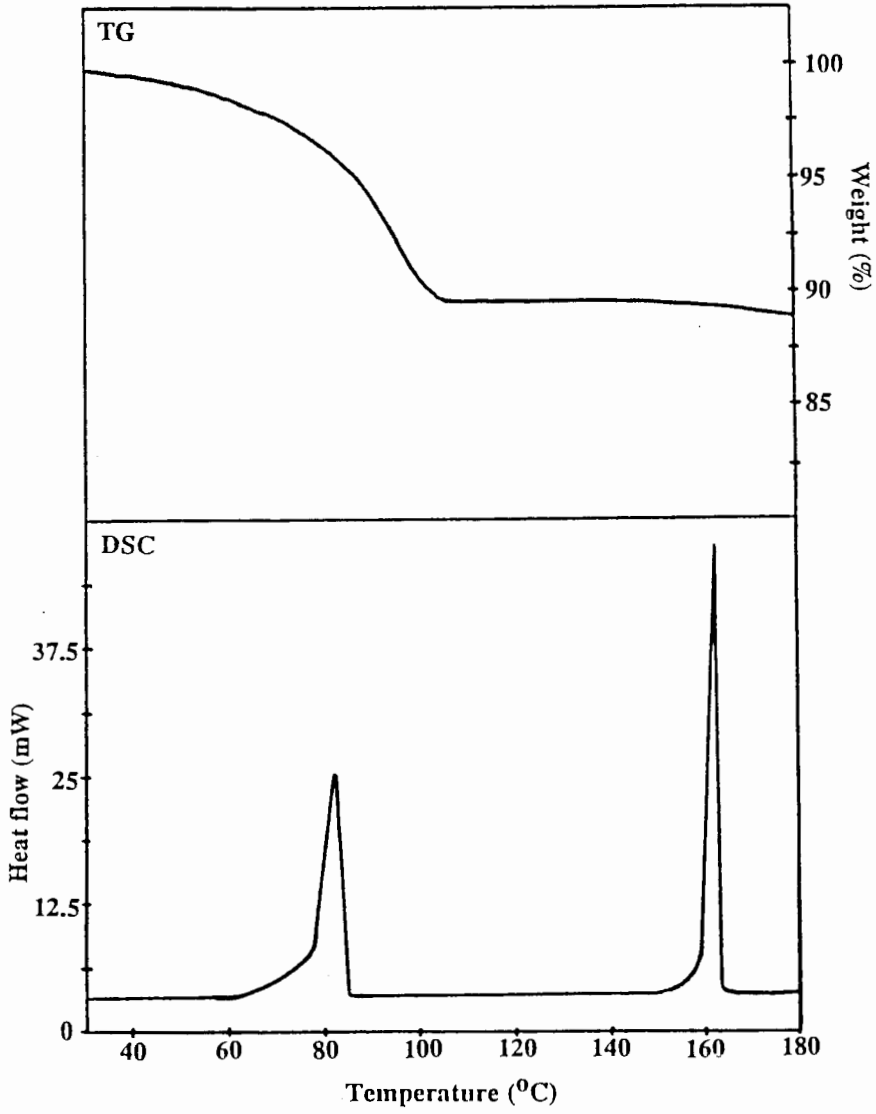

Figure 7.15. TG and DSC curves of $Ph_3COH \cdot MeOH$.

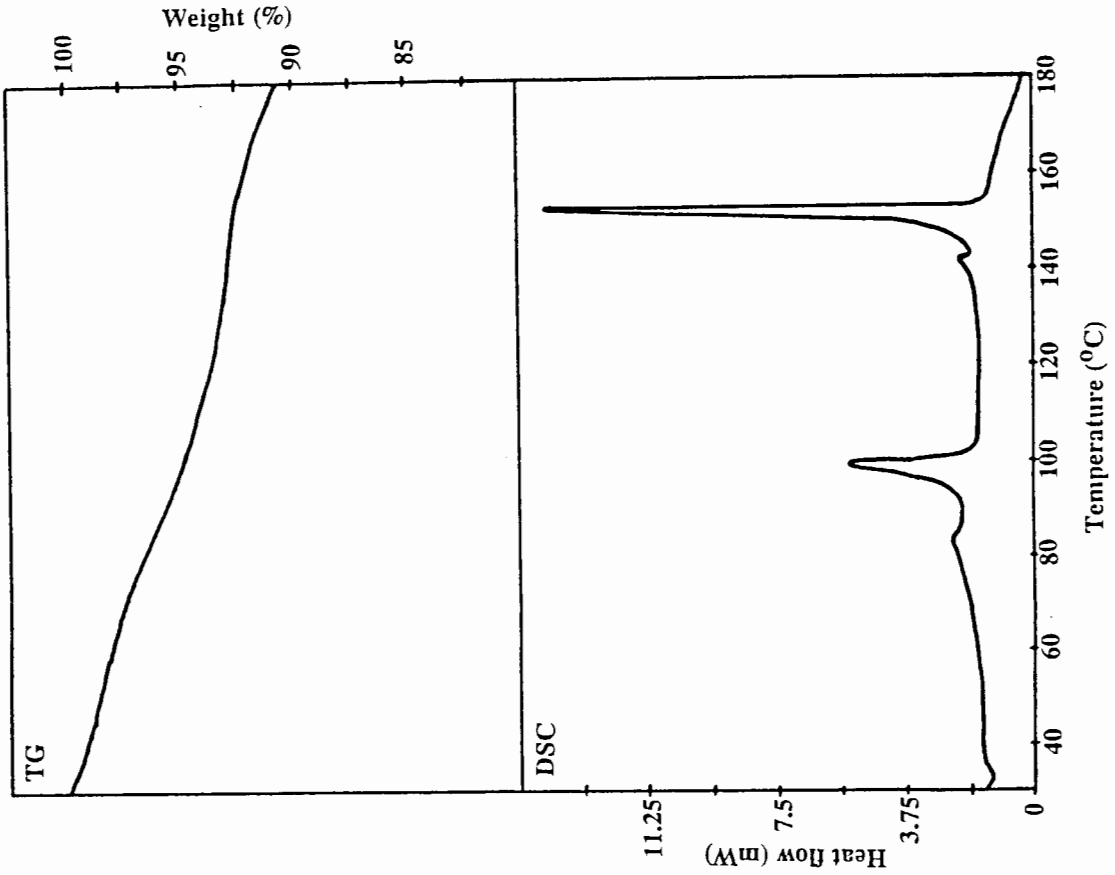

Figure 7.17. TG and DSC curves of **BASIL.**

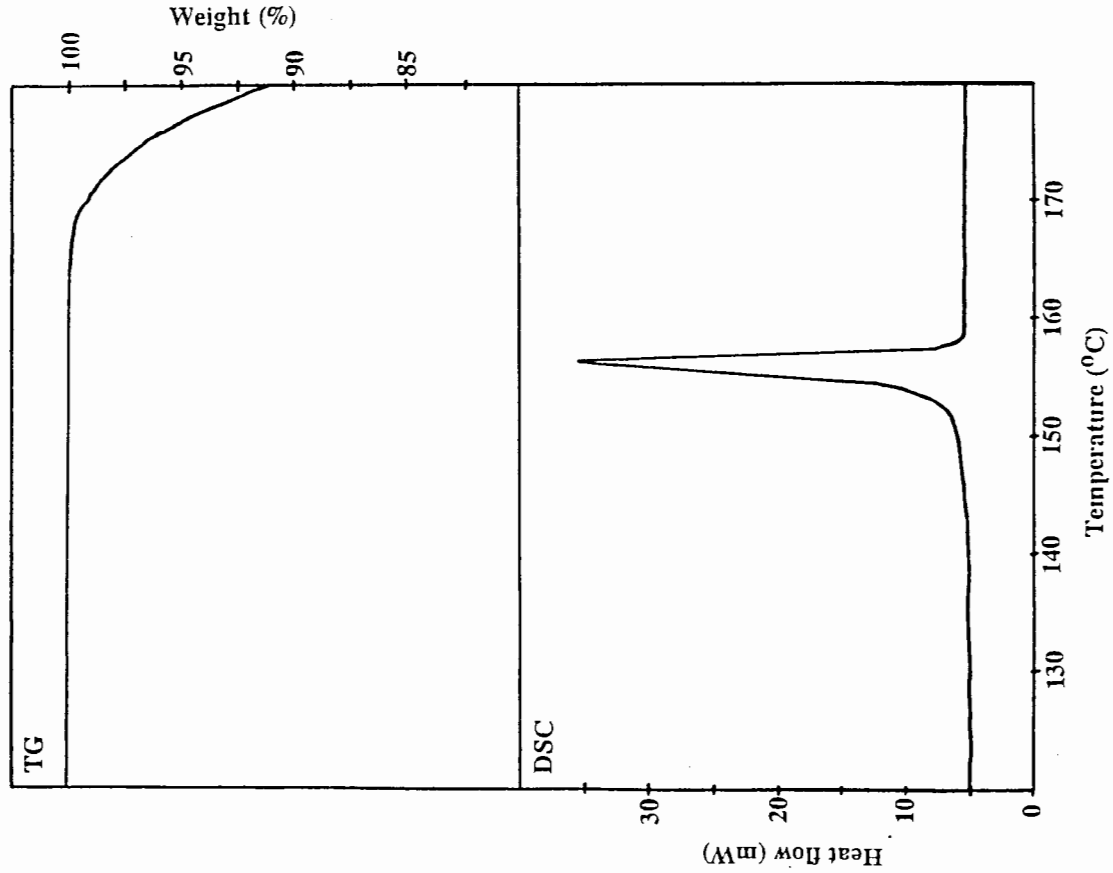

Figure 7.16. TG and DSC curves of **WEB2.**

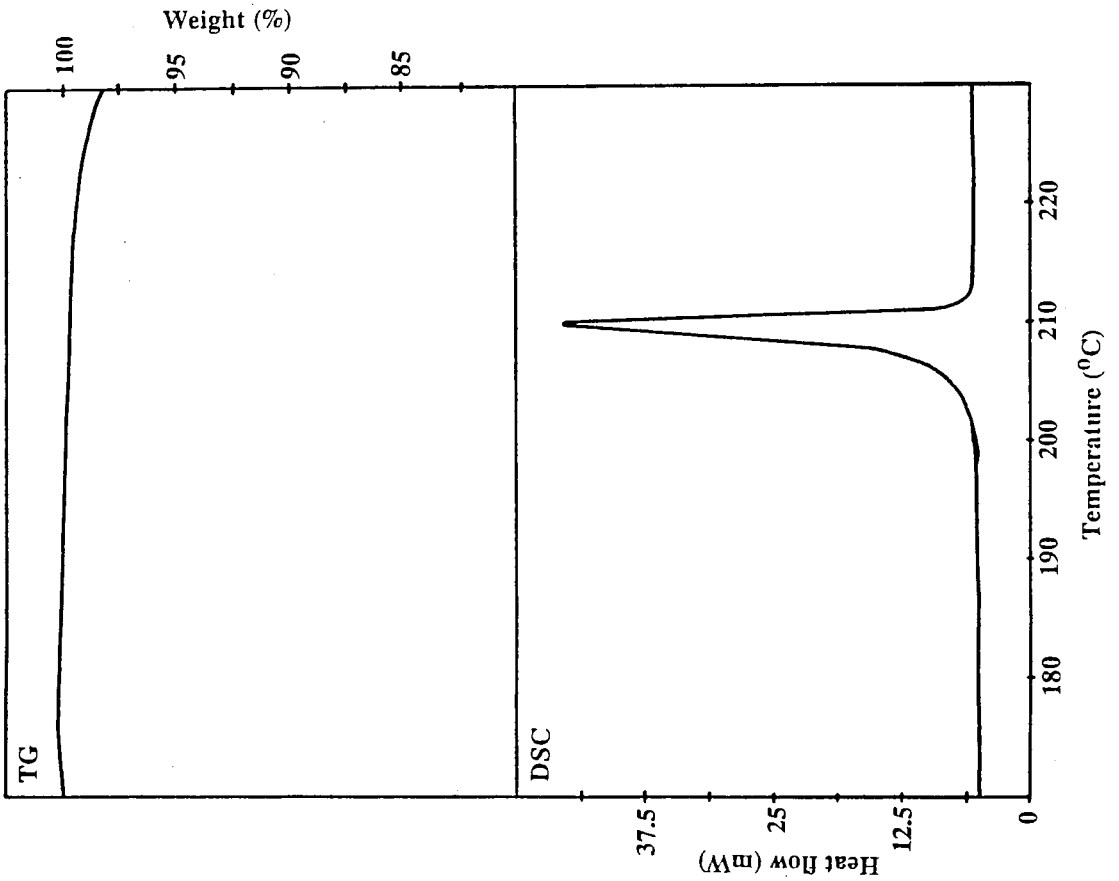

Figure 7.19. TG and DSC curves of $(C_{10}H_7)_3SiOH$.

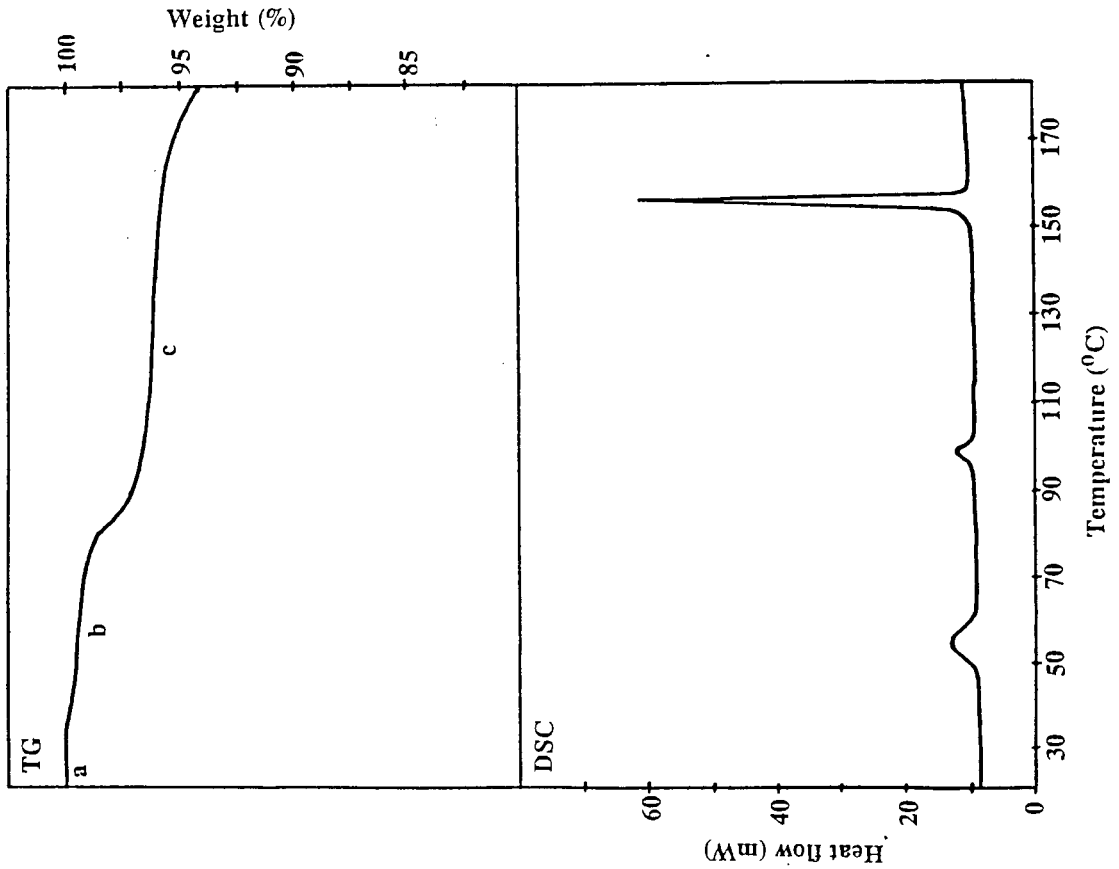

Figure 7.18. TG and DSC curves of SETH.

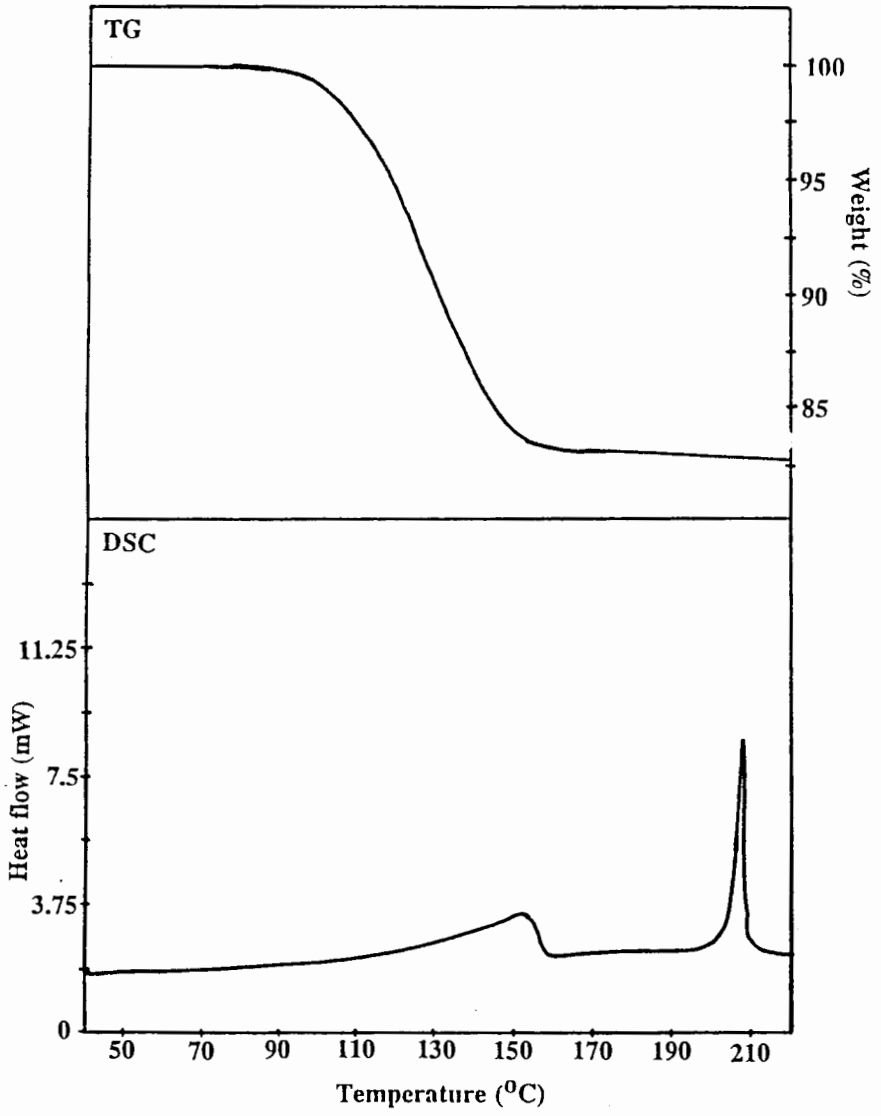

Figure 7.20. TG and DSC curves of **NADIO.**

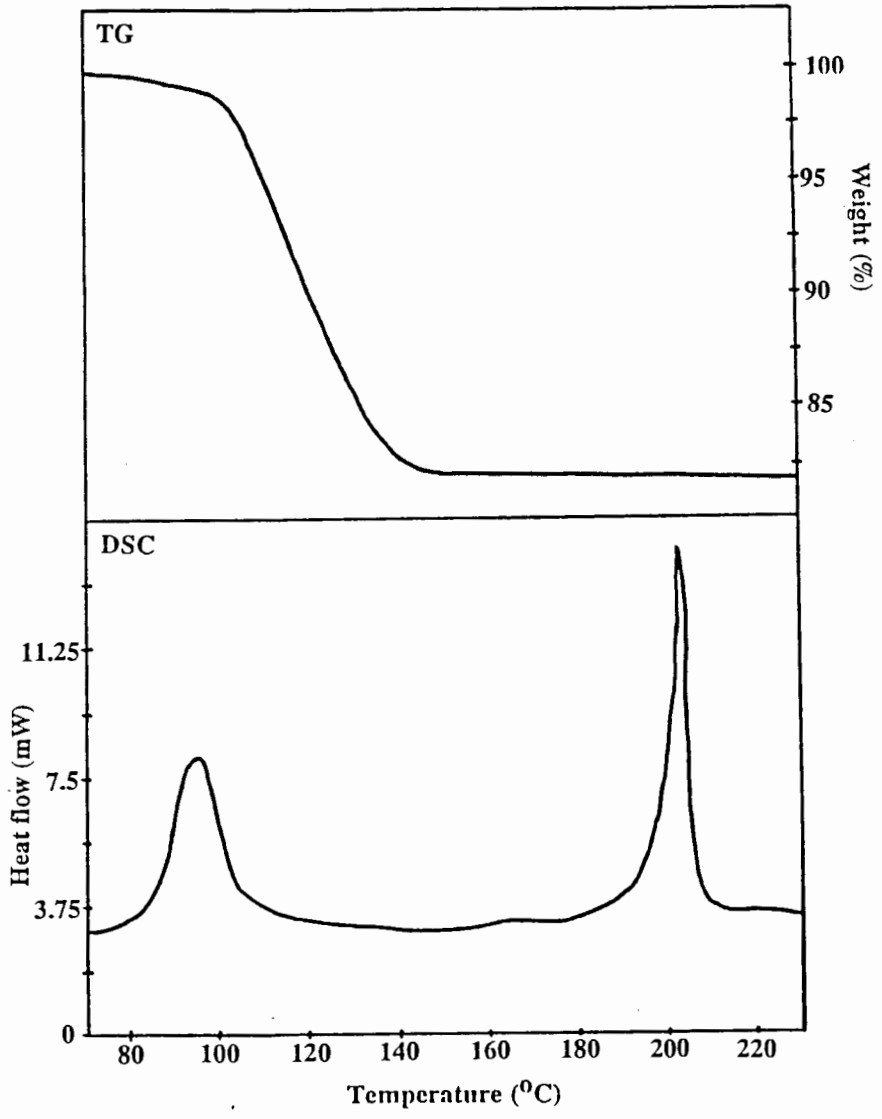

Figure 7.21. TG and DSC curves of **NATOL.**

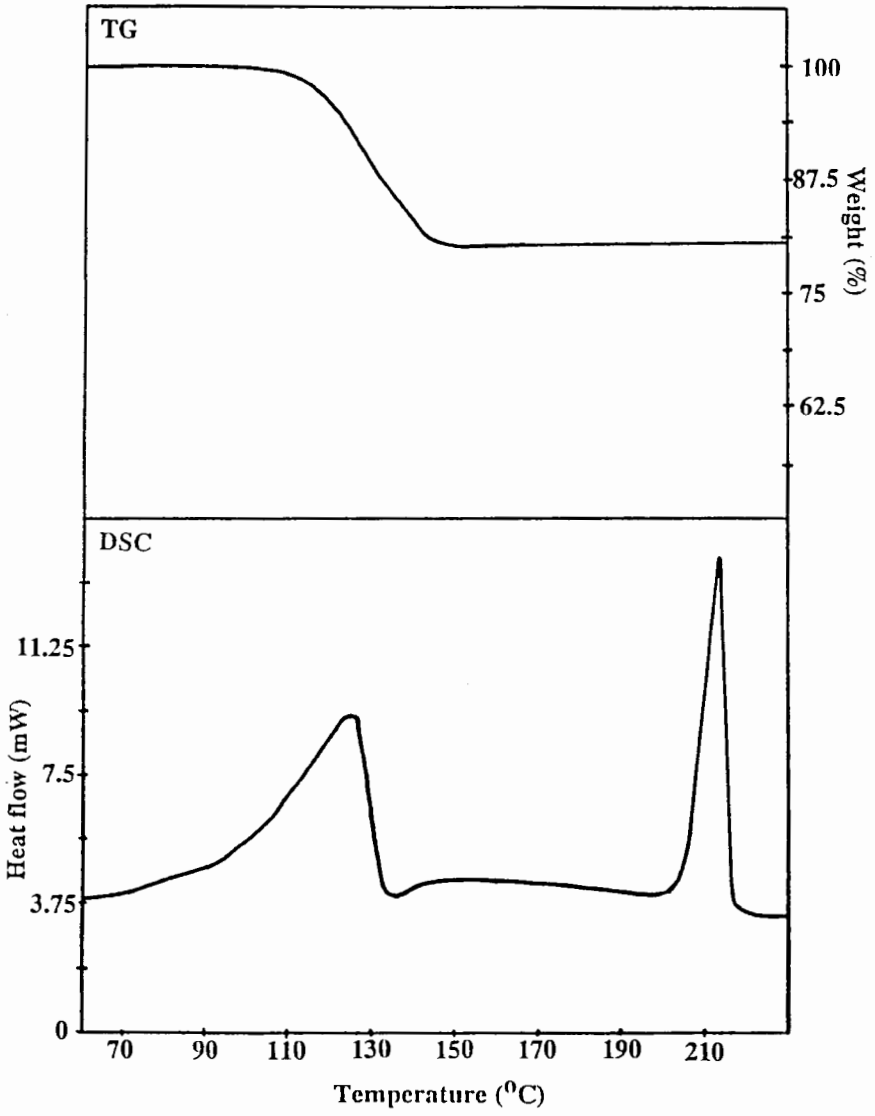

Figure 7.22. TG and DSC curves of **ODIN.**

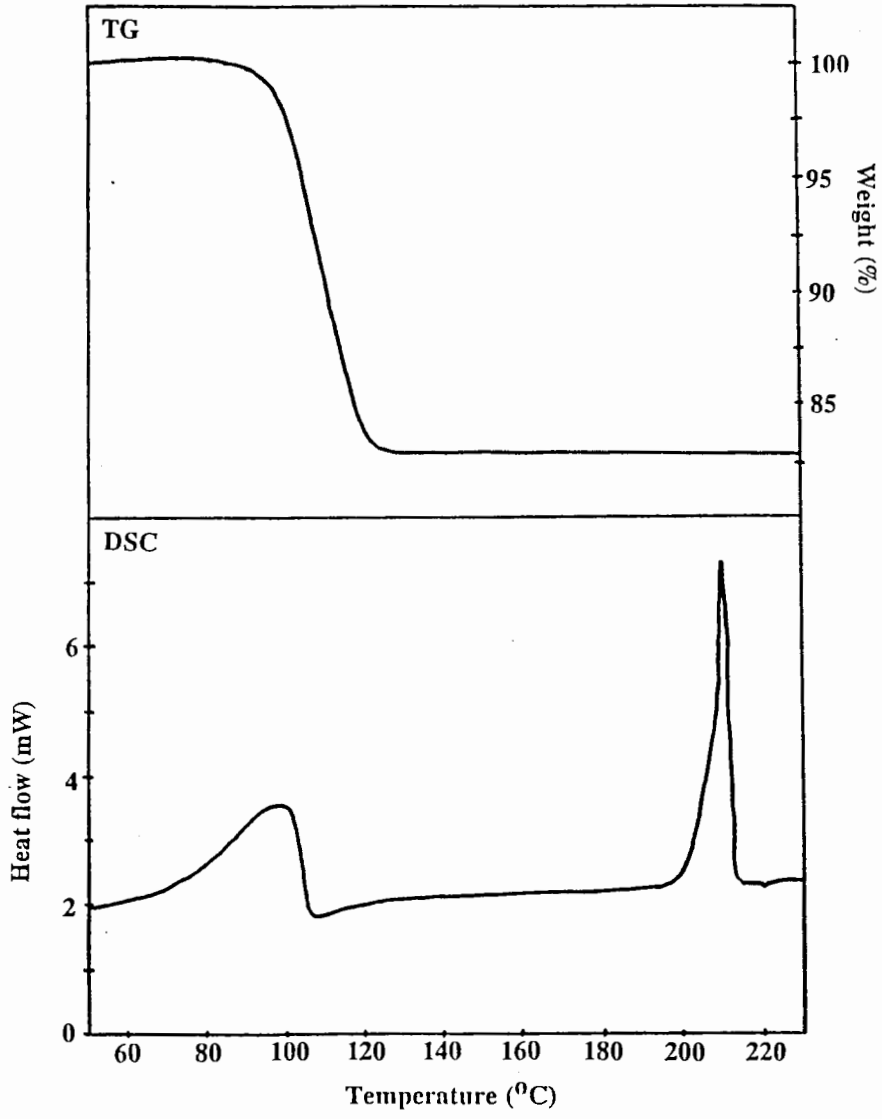

Figure 7.23. TG and DSC curves of **MAXINE.**

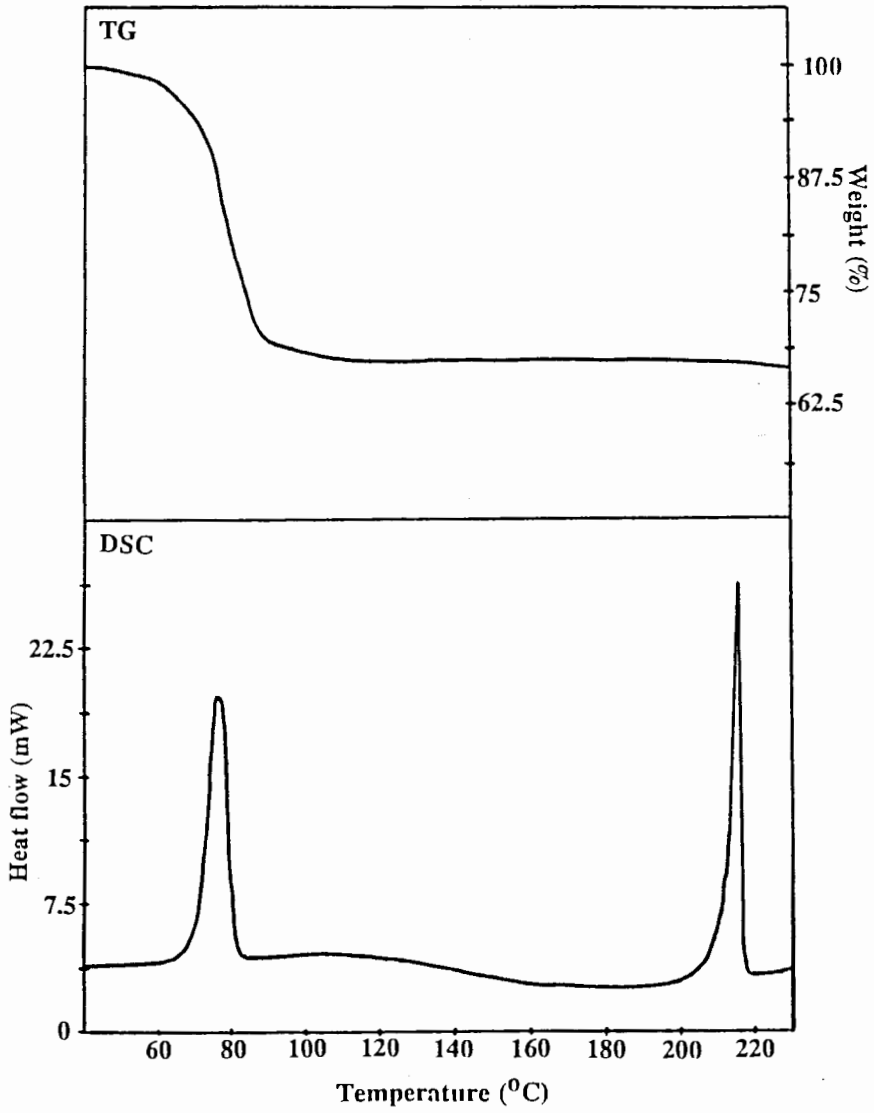

Figure 7.24. TG and DSC curves of **NAPPY.**

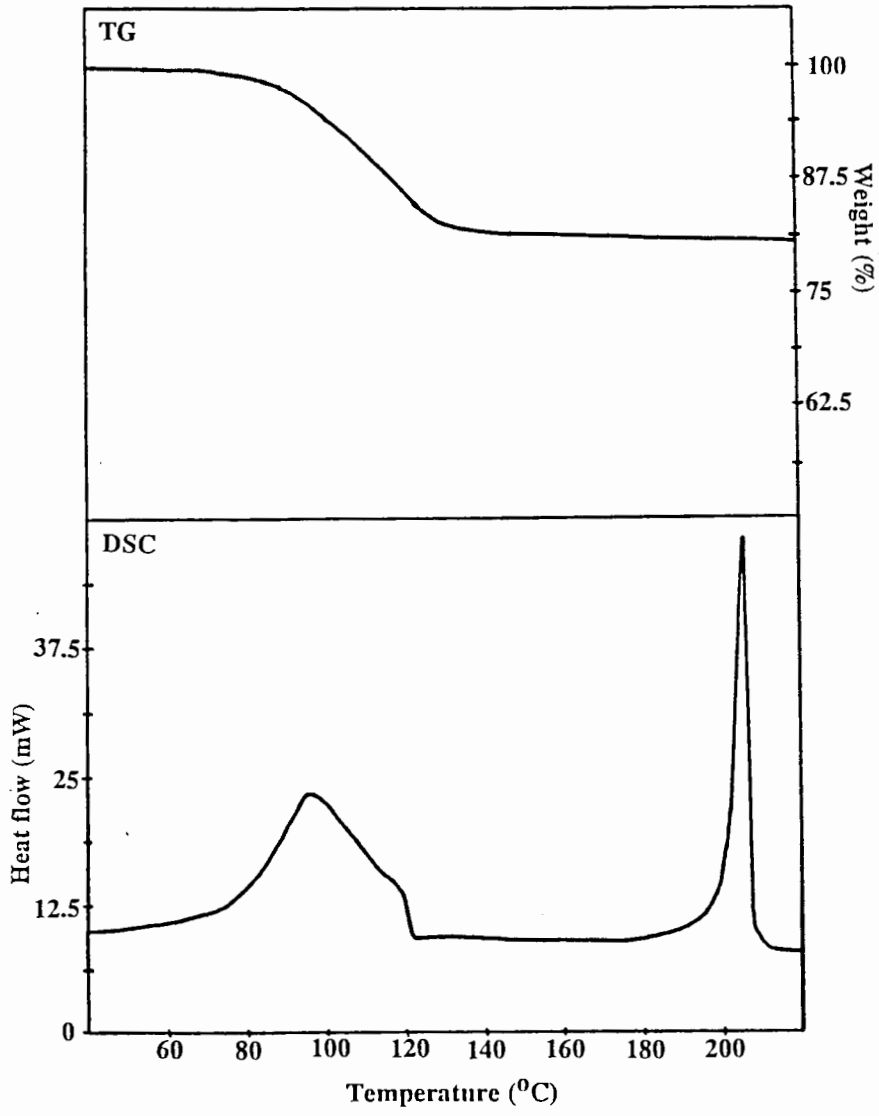

Figure 7.25. TG and DSC curves of **NATRET.**

Table 7.1. Results of thermal analyses.

Compound	Weight loss calculated (%)	Weight loss observed (%)	|Δ| (%)	T_{on} (°C)	Peak area (J/g)	ΔH (kJmol^{-1})
PEDIL	0	0		197.4	101.3	37.1
PEDIOX	19.38	19.80	0.42	140.4	64.6	29.4
				200.9	99.0	36.3
PECTIL	14.73	14.38	0.35	105.8	65.1	28.0
				197.0	97.4	35.7
DINM	22.62	22.42	0.20	91.6	139.0	65.8
				201.5	79.3	29.1
LUTI	36.90	36.83	0.07	72.2	64.5	36.5
				127.8	91.0	33.3
				179.5	55.8	20.5
DINO	36.90	36.35	0.55	95.5	87.9	51.1
				114.7	39.4	14.4
				183.4	32.8	12.0
PEACH	13.68	13.01	0.67	45.3	76.6	32.5
				194.9	98.0	35.9
Ph_3COH	0	0		160.6	102.5	26.7
W1DIOX	25.29	23.40	1.89	76.1	149.0	51.9
				161.7	78.7	20.5
$Ph_3COH \cdot MeOH$	10.96	10.17	0.79	79.1	151.9	44.4
				162.0	102.3	26.6

Table 7.1 ctd.

Compound	Weight loss calculated (%)	Weight loss observed (%)	$\|\Delta\|$ (%)	T_{on} (°C)	Peak area (J/g)	ΔH (kJmol^{-1})
WEB2	0	0		154.4	88.0	24.3
BASIL	7.38	6.78	0.60	96.2	195.6	58.4
				150.3	62.5	17.3
SETH	4.00	3.99	0.01	49.1	38.3	11.0
				96.1		
				154.6	88.8	24.5
$(C_{10}H_7)_3SiOH$	0	0		206.1	63.6	27.1
NADIO	17.11	16.81	0.30	132.5	113.0	58.2
				206.3	61.5	26.3
NATOL	17.76	17.55	0.21	87.8	63.9	33.2
				200.5	60.8	26.0
ODIN	19.93	19.50	0.43	98.9	115.7	61.6
				210.7	59.3	25.3
MAXINE	19.93	17.53	2.40	76.9	92.5	49.3
				207.9	59.4	25.3
NAPPY	33.23	32.80	0.43	70.5	66.3	42.3
				212.5	53.4	22.8
NATRET	17.00	17.54	0.54	83.3	111.4	57.2
				203.7	55.0	23.5

X-ray powder diffraction patterns prove that most of the compounds listed in Table 7.1 change from their respective β-phases to the α-phase on guest loss.

The *p*-chlorotoluene complex with 1,1,2,2-tetraphenylethane-1,2-diol (**PECTIL**) is the only inclusion compound in this series where no host-guest hydrogen bonding occurs. For this reason, it seemed possible that the guest might escape by means of the channels described in Chapter 4, leaving the host framework undamaged. XRD studies however did not reveal this β_0-phase. Figure 7.26 shows that the α-phase changes directly into the β-phase when **PECTIL** crystals are maintained at 120°C *in vacuo* for 1 hour to ensure complete loss of guest. A typical example of a host-guest hydrogen bonded structure (**DINM**) is shown in Figure 7.27. Figure 7.27(a) shows the pattern obtained from **DINM** crystals, freshly removed from their mother liquor, blotted dry and crushed (β-phase); (b) is the pattern obtained after **DINM** crystals were crushed and maintained at 120°C *in vacuo* for 24 hours to ensure complete guest loss. This is quite different from (a) but is essentially the same pattern as that obtained for the pure host recrystallised from diethyl ether (α-phase) which is shown in (c).

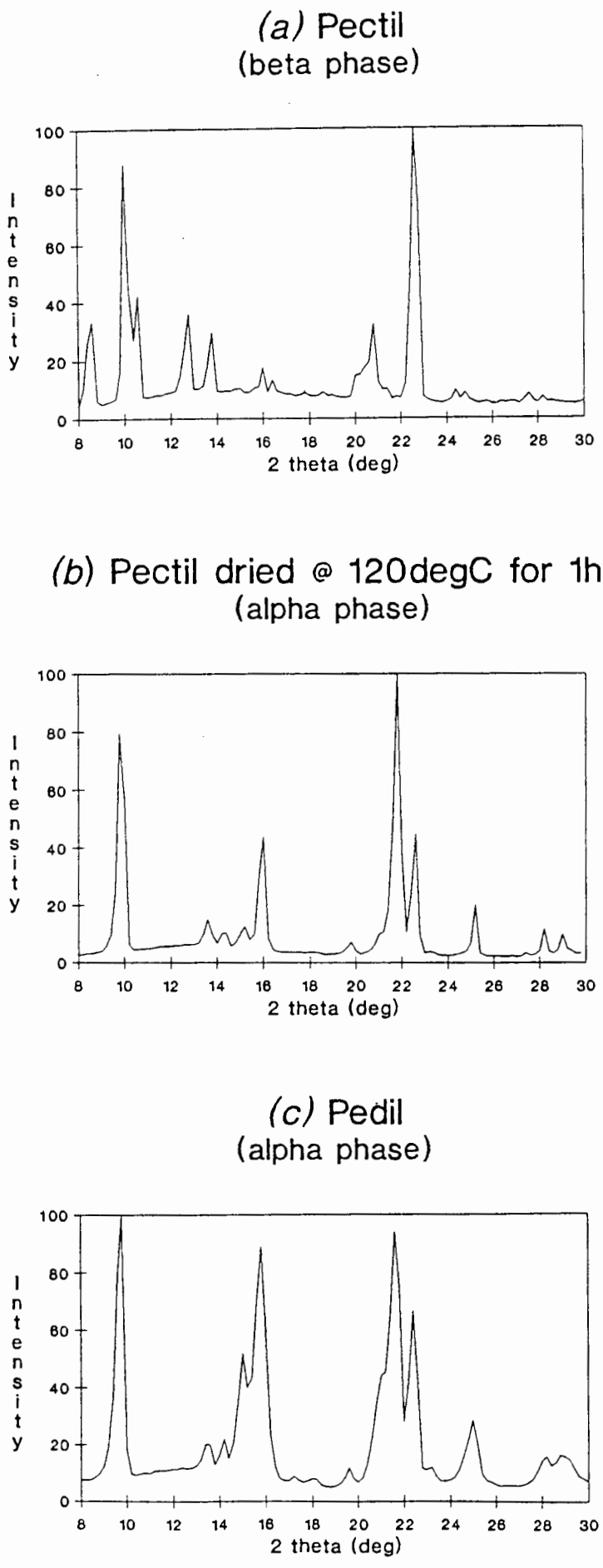

Figure 7.26. X-ray powder diffraction patterns of **PECTIL** (a) β-phase; (b) after guest loss; (c) α-phase.

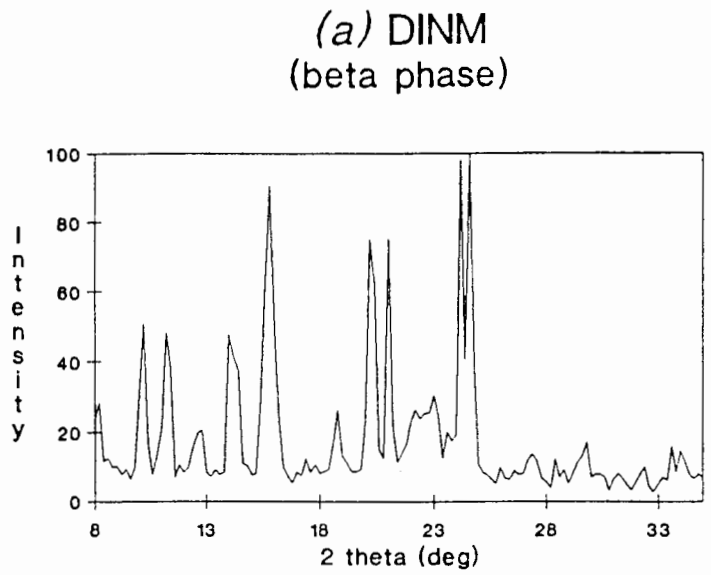

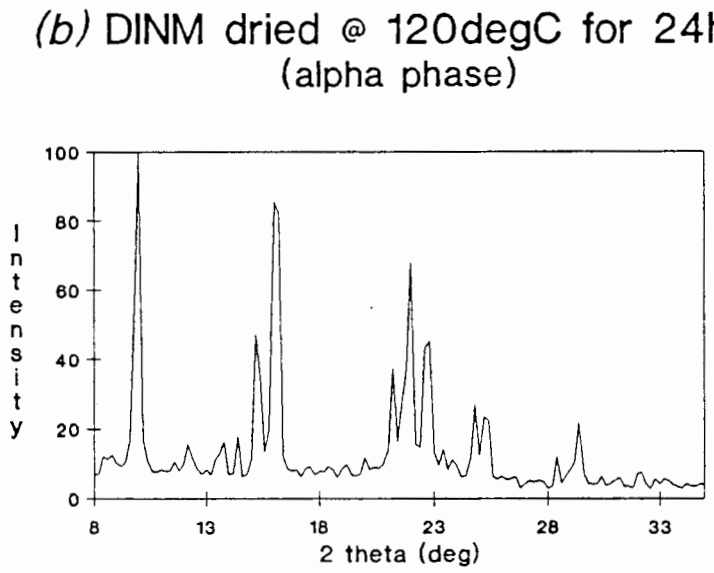

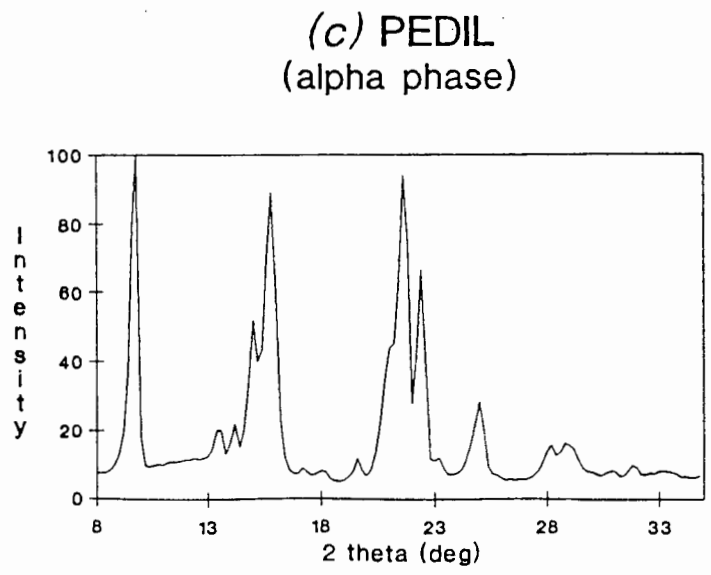

Figure 7.27. X-ray powder diffraction patterns of **DINM** (a) β-phase; (b) after guest loss; (c) α-phase.

LUTI displays a different decomposition pattern. Figure 7.10 shows a mass loss with an inflection in the TG which, with its corresponding endotherms in the DSC (labelled A and B), is caused by the guest release reaction. This is followed by a third endotherm, C, which is not associated with any weight loss, and which is caused by a structural phase change of the remaining host lattice. The fourth endotherm, D, is associated with the melting of the host compound.

The same processes were observed when **LUTI** was heated on the hot stage microscope. The clear crystals showed the appearance of bubbles at 60 - 75°C and discoloured to brown (endotherms A and B). Between 120 and 140°C feather-like crystallites appeared on the surface of the crystal (endotherm C) and the complex melted with further discolouration and decomposition at ≈ 180°C. These events are shown in the photographs in Figure 7.28.

The powder diffraction patterns, Figure 7.29, show the various phases of **LUTI** after it had been (a) removed from its mother liquor, blotted dry and crushed; (b) crushed and maintained at 87°C for 1 hour *in vacuo*; (c) crushed and maintained at 120°C *in vacuo* for 24 hours, which yielded the same pattern as (d), the pattern obtained from the pure host crystallised from diethyl ether (α-phase). The pattern shown in Figure 7.29(b) is different from the other patterns, and corresponds to a new structure, labelled the γ-phase.

(a)

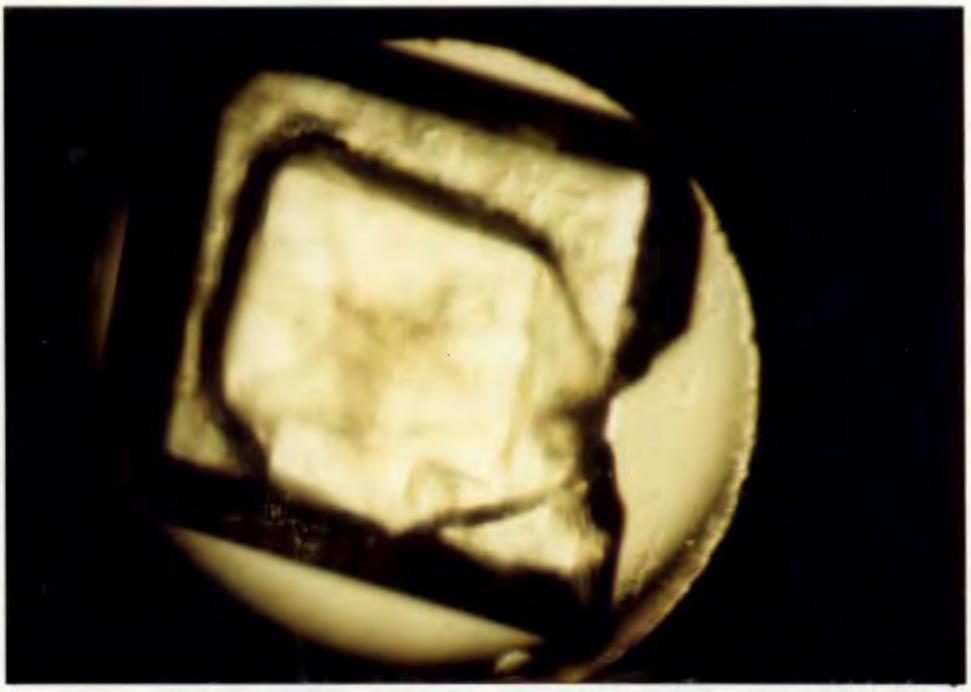

(b)

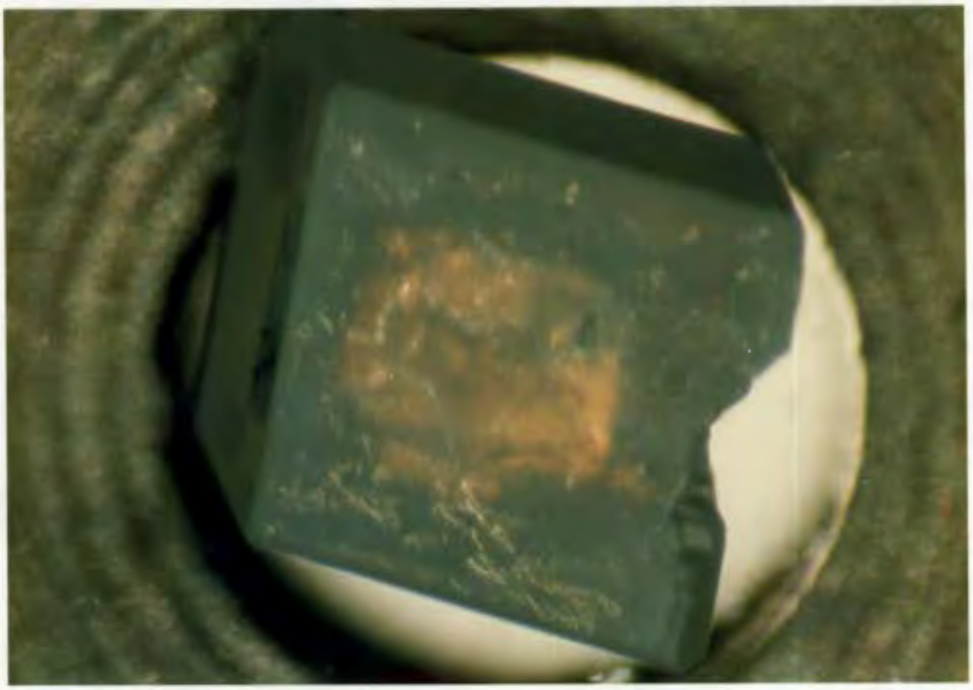

(c)

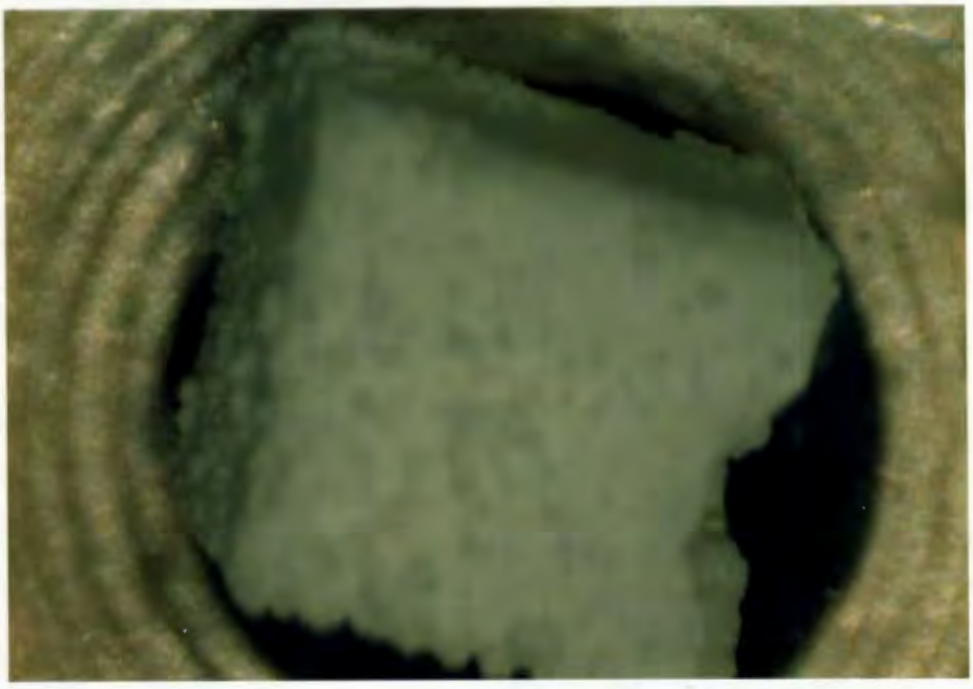

Figure 7.28. Thermal decomposition of **LUTI** crystal (see text).
(a) T = 25°C; (b) T = 70°C; (c) T = 151°C.

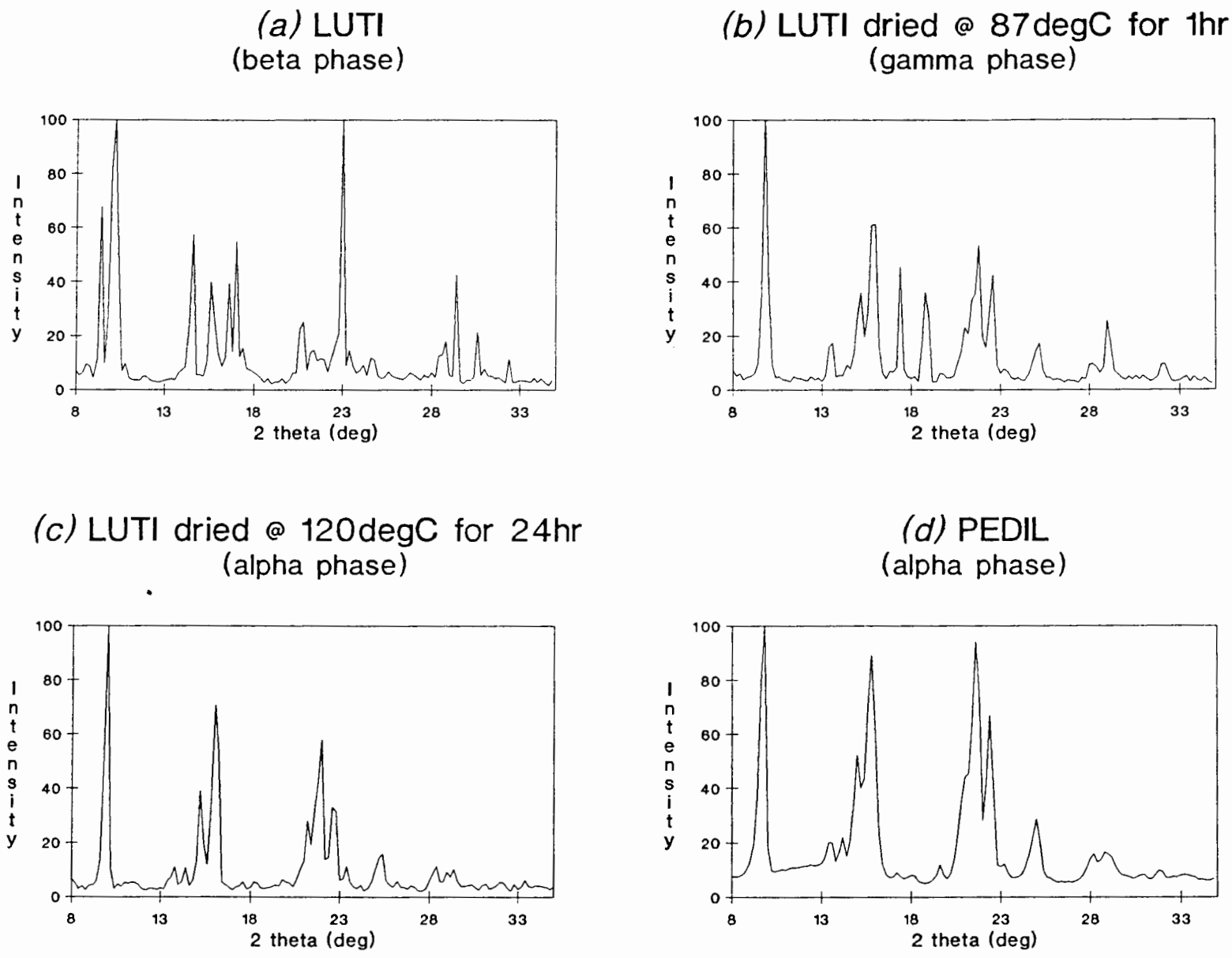

Figure 7.29. X-ray diffraction patterns of **LUTI** at different stages of decomposition (see text). (a) β-phase; (b) after 1 hour at 87°C; (c) after complete guest loss; (d) α-phase.

The decomposition of **DINO** (Figure 7.11) is similar to that of **LUTI**.
The endotherm, C, corresponding to a structural phase change, appears again immediately after the guest release (which occurs in a single step in this case). This was confirmed by visual observation of feather-like crystals growing between 105 and 120°C. Powder diffraction patterns are given in Figure 7.30 and again show the presence of a new γ-phase which occurs after the guest loss, but before the reversion to the α-phase.

Competition experiment.

2,6-Lutidine and 3,5-lutidine are very similar in shape and size. A competition experiment was carried out to determine which of the two isomers would be most readily included by the host. The method used was described in Chapter 2. Varying mole fractions of 2,6- and 3,5-lutidine were added to the host, 1,1,2,2-tetraphenylethane-1,2-diol, which had been dissolved in Et_2O. The solutions were left for several weeks until crystals formed. These were dissolved in acetone and analyzed by gas chromatography using a Pye Unicam PU4500 Chromatograph which was equipped with a Flame Ionizer Detector; output was plotted on a pen recorder. The columns used were glass tubing packed with 10% (w/w) Squalane on Chromosorb W (80/100 mesh) at a temperature of 180°C. Nitrogen was used as the carrier gas (30 $mlmin^{-1}$) and the flame of the detector was supported by an air/hydrogen mixture. The injector and detector temperatures were 250°C and the sample aliquot was 5 μl. X-ray powder diffraction studies were performed to determine the phase changes in the crystals.

The result is shown in Figure 7.31. 3,5-Lutidine is preferentially included; at compositions of $X_{3,5\text{-Lutidine}} \geq 0.5$, it is the only guest species included in the host lattice. X-ray powder diffraction studies showed that only two phases are possible in this series - those of **DINM** and **LUTI**. For $X_{3,5\text{-Lutidine}} = 0$ to 0.3, the crystals exist in the same phase as **DINM**, while from $X_{3,5\text{-Lutidine}} = 0.4$ to 1, the phase is the same as that of **LUTI**.

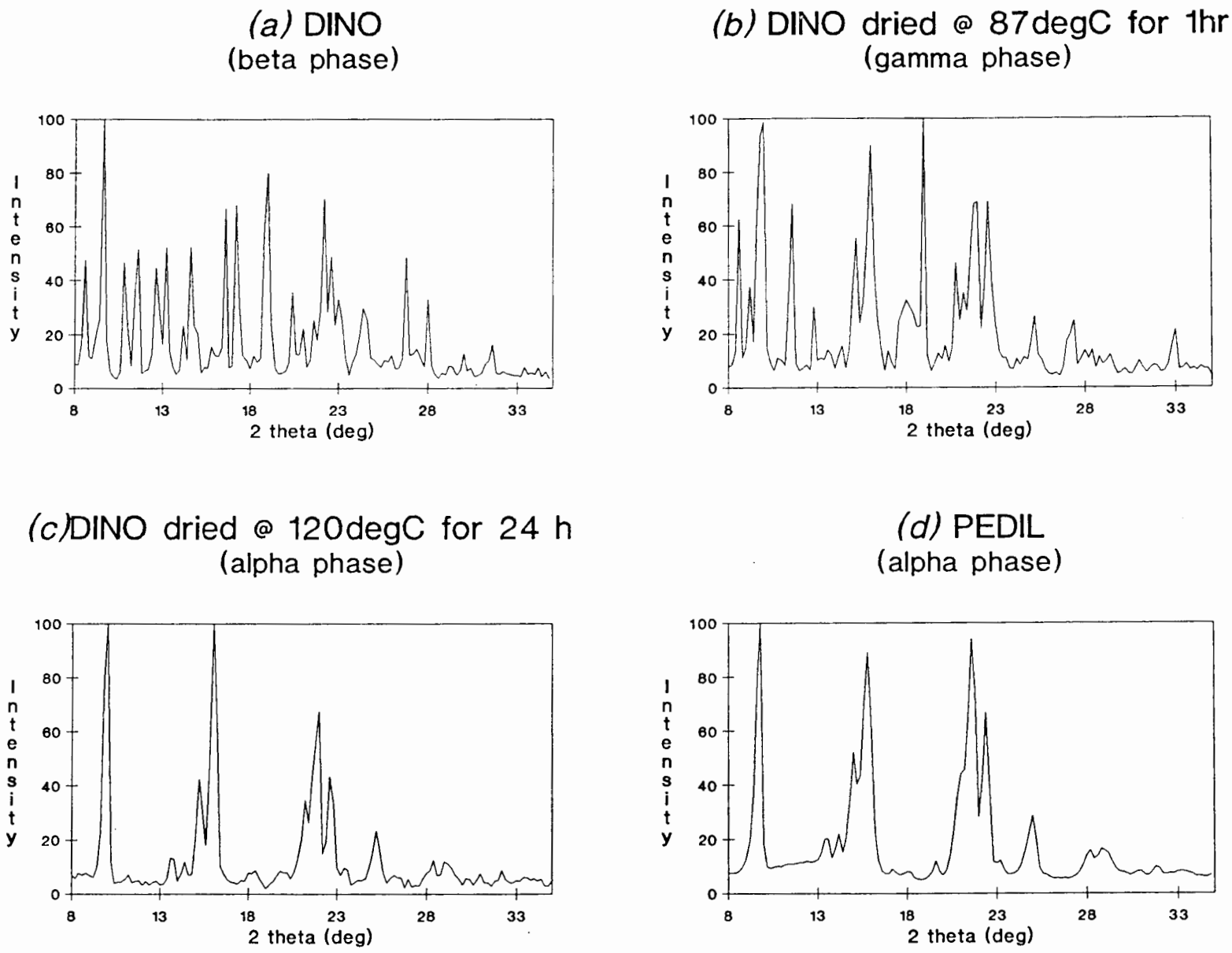

Figure 7.30. X-ray diffraction patterns of **DINO** at different stages of decomposition (see text). (a) β-phase; (b) after 1 hour at 87°C; (c) after complete guest loss; (d) α-phase.

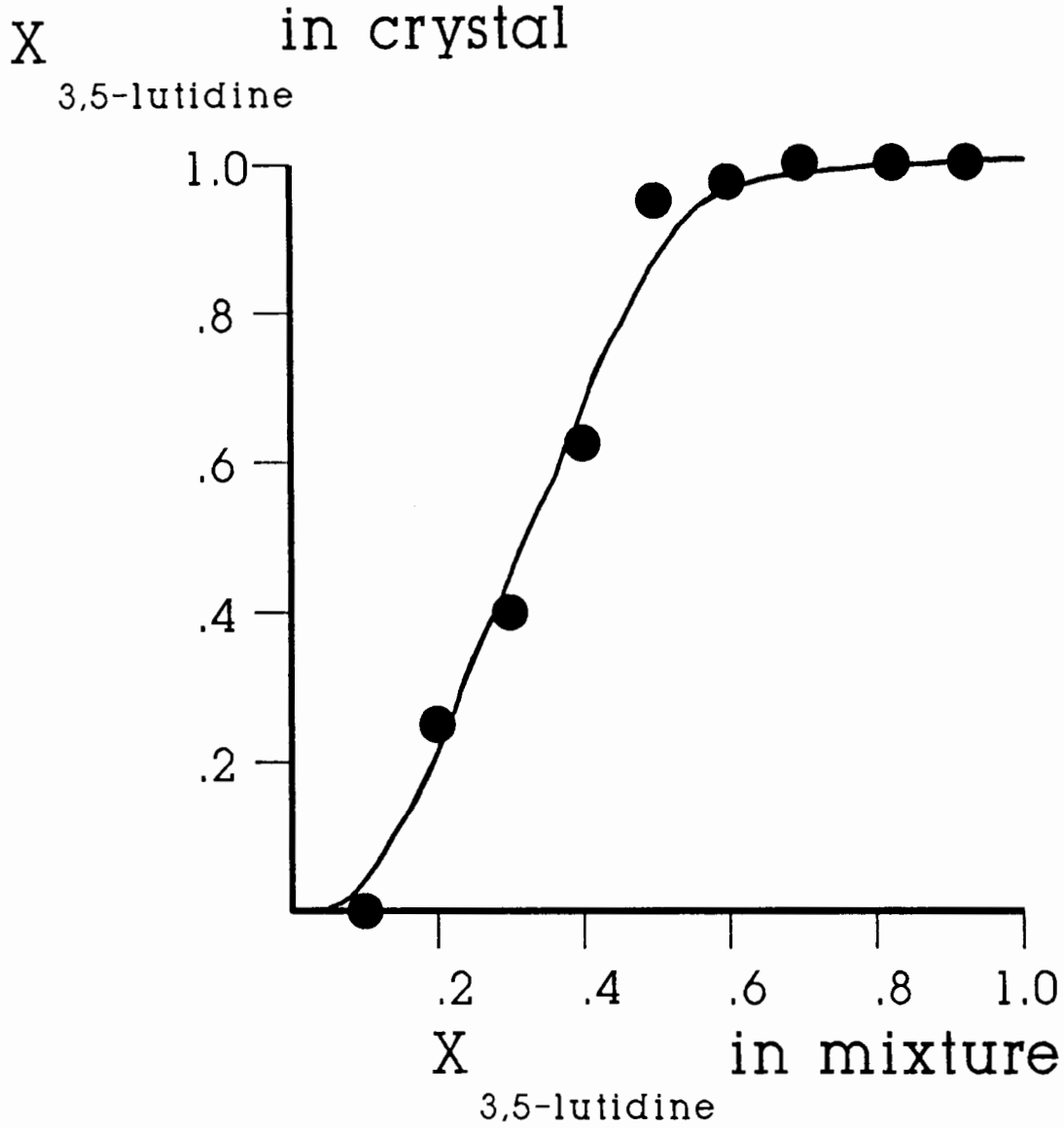

Figure 7.31. Separation of 3,5-lutidine from 2,6-lutidine by inclusion formation with 1,1,2,2-tetraphenylethane-1,2-diol.

The complex of triphenylsilanol with ethanol (**SETH**) also decomposes via an intermediate γ-phase. TG (Figure 7.18) indicates that the ethanol is removed in two distinct steps. The total measured weight loss of 3.99% is in excellent agreement with that required for the 4:1 complex (4.00%). The DSC curve shows two endotherms with onset temperatures of 49.1°C and 96.1°C while the third peak with onset at 154.6°C is caused by the melting of the triphenylsilanol. The formation of a new phase was confirmed by X-ray powder diffraction. Figure 7.32 shows the diffraction patterns obtained : (a) **SETH** crystals freshly removed from their mother liquor and crushed (β-phase); (b) crushed and exposed to air until they had shown a 1.02% weight loss; (c) crushed and dried at 110°C for 6 hours *in vacuo*, which yields the same pattern as (d) which was obtained from triphenylsilanol recrystallised from diethyl ether (α-phase). The pattern shown in (b) has been labelled the γ-phase of this compound.

In all of the above cases, differences in the intensities of peaks in two patterns were not judged to be significant since they are probably caused by different degrees of alignment of the crystals (a preferred orientation effect). The equivalence of two spectra was rather determined by the d-spacings of the peaks, since these are unique for each crystal structure.

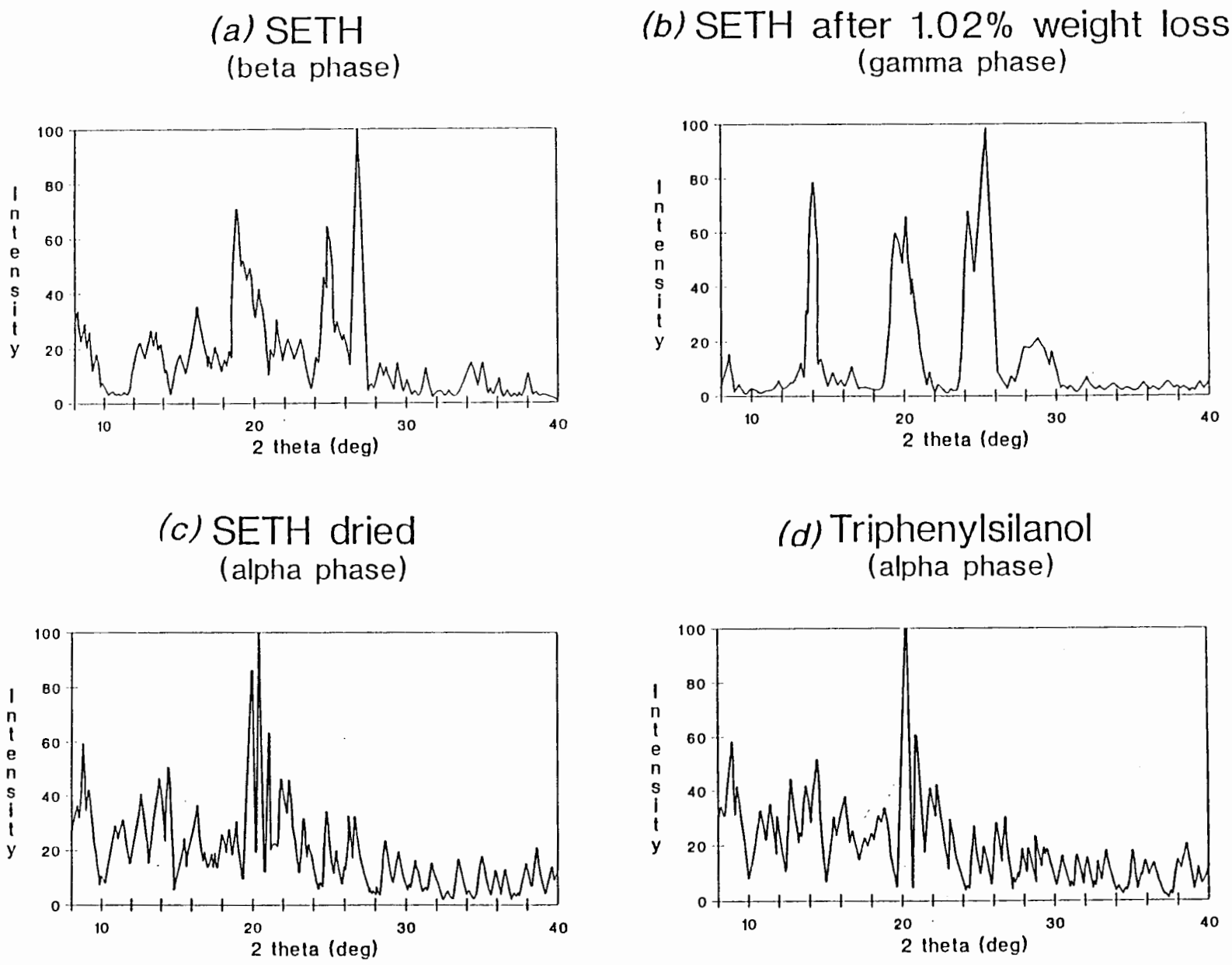

Figure 7.32. X-ray powder diffraction patterns of **SETH** at different stages of decomposition (see text). (a) β-phase; (b) after 1.02% weight loss; (c) after complete guest loss; (d) α-phase.

Thermal analysis of the dmso complexes **DEMPE**, Ph_3COH • dmso, **TRIPSID** and **DUNCAN** showed some unusual features, so these compounds will be treated separately. Results for these complexes are summarized in Table 7.2.

When the samples were heated at 10°Cmin^{-1} only one endotherm appeared in the DSC, while the TG showed a continuous loss of mass over the temperature ranges scanned. The curves obtained for **TRIPSID**, which are typical, are given in Figure 7.33.

The four samples were rerun at 5°Cmin^{-1} which yielded more familiar traces. These are shown as Figures 7.34 - 7.37. The results obtained for **DEMPE** and **DUNCAN** now fit the trends seen in their respective classes. However, for Ph_3COH • dmso and **TRIPSID**, the onset temperatures of their second peaks were about 10°C lower than the melting points of their hosts. Also, the ΔH values obtained for the melts were 7.6 and 5.6 kJmol^{-1} which were thought unreasonable. These two complexes were again analysed using DSC, this time using open sample pans. (Figures 7.38 and 7.39). This meant that the escaping guest could be more efficiently removed by the purge gas. The results obtained for all of these analyses are shown in Table 7.2. The values for Ph_3COH • dmso and **TRIPSID** however, did not reveal definite weight losses which could account for the stoichiometry observed in the crystal structures and confirmed by density measurements and NMR.

The decomposition of these four compounds was followed visually on the hot stage microscope. Analogous results were obtained as follows:
At heating rates of 10°Cmin^{-1} or higher, the following events were noted :

(i) Liquid droplets appeared on the surface of the crystals. Liquid could be seen escaping through cracks in the crystal surface.

(ii) The crystals broke up explosively into a pile of crystallites which immediately began to dissolve in the released liquid.

(iii) The crystallites were completely dissolved before the melt point of the host compound was reached.

At a slower heating rate (2 - 5°Cmin^{-1}), a different sequence of events was seen :

(i) Liquid droplets appeared at surface defects, as before.

(ii) The breakup of the crystals was more gradual. A constant movement and rearrangement of crystallites in the pool of liquid dmso could be seen until

(iii) the melt point of the host compound was reached, at which point the crystallites melted.

The temperatures noted for all these events are listed in Table 7.3.

Dmso has a boiling point of 189°C ; since it escapes in each of these cases before its boiling point, it is released as a liquid. The host compounds are all soluble in dmso. At slow heating rates, an equilibrium is set up between the dmso being released from the crystals and the host dissolving in the dmso. This allows the host compounds to remain solid until their melting points are reached. Performing the DSC analyses in open pans for Ph_3COH • dmso and **TRIPSID** was probably necessary to aid the removal of dmso by the purge gas, since these two hosts melt at temperatures lower than 189°C. The effect of the liquid dmso is also noted in the TG where a mass is still registered for some of the dmso after the endotherm in the DSC indicates that all the guest has been released.

Thus, when we carry out thermal analysis of inclusion compounds which entrap high boiling guests, different techniques must be applied. In particular, in order to obtain sensible guest-release endotherms, which are well separated from the subsequent melt of the host, an appropriate heating rate must be found. In this case, it was also necessary to change from vented to open pans.

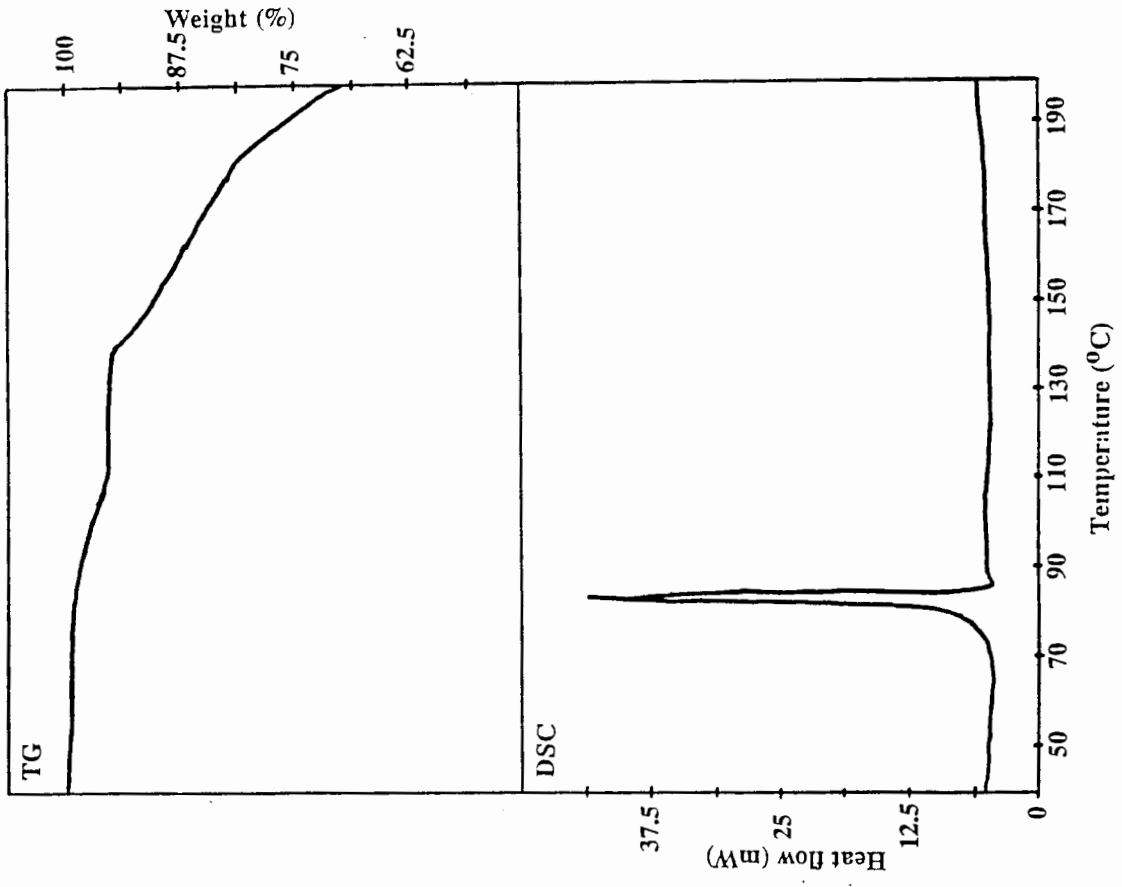

Figure 7.33. TG and DSC curves of **TRIPSID**, 10 °C min^{-1}, vented pan.

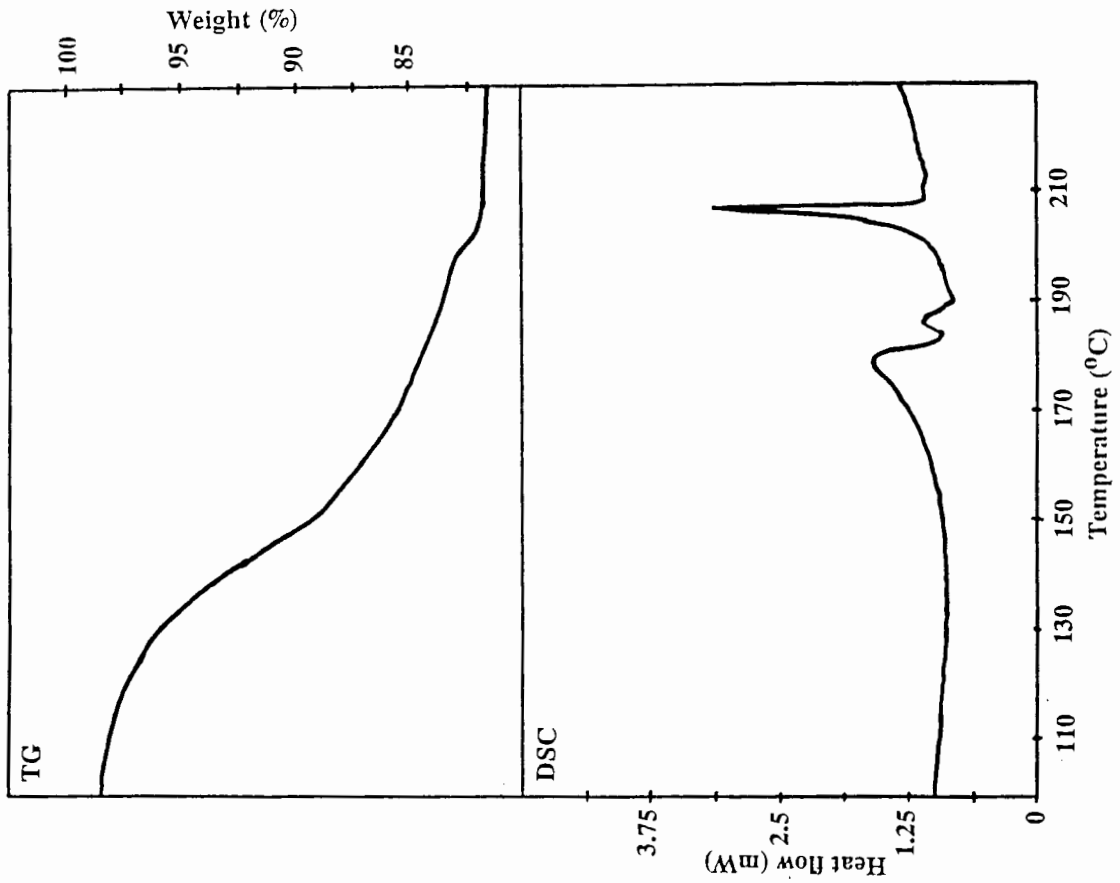

Figure 7.35. TG and DSC curves of **DUNCAN**, 5 °C min^{-1}, vented pan.

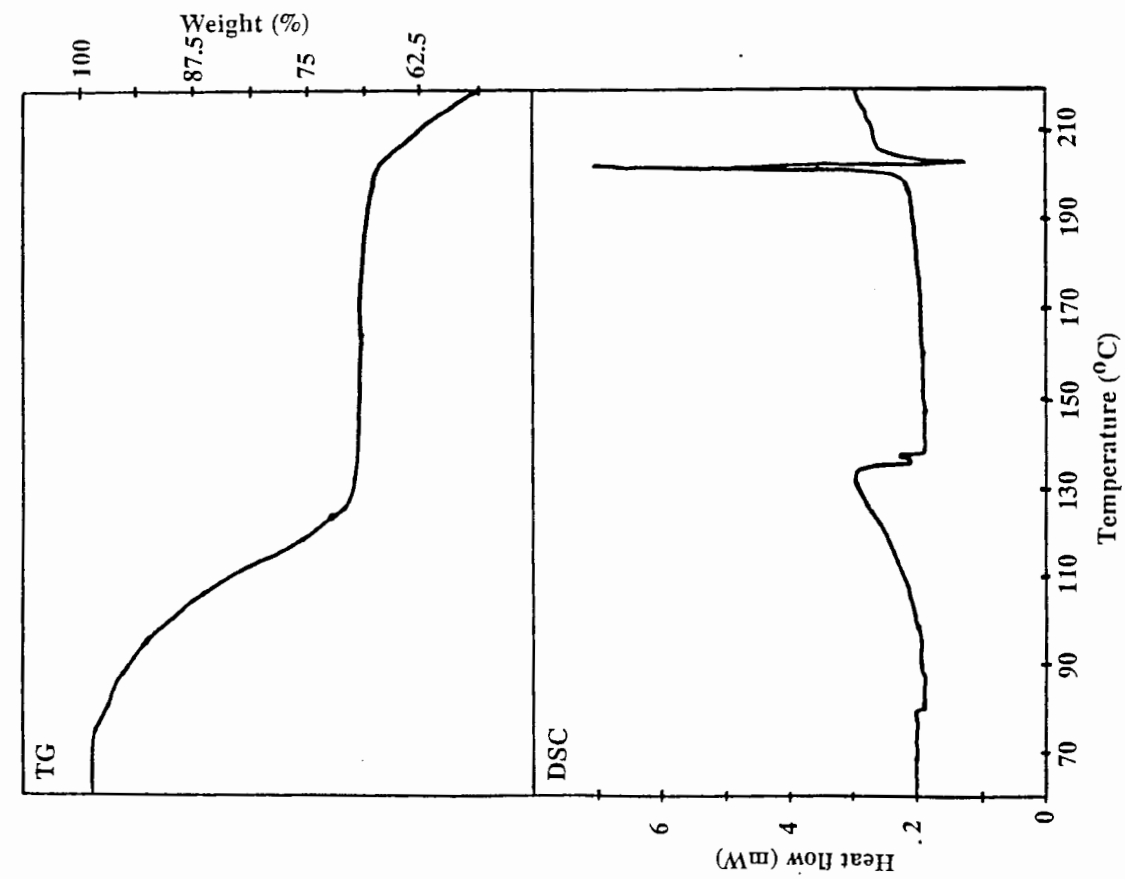

Figure 7.34. TG and DSC curves of **DEMPE**, 5 °C min^{-1}, vented pan.

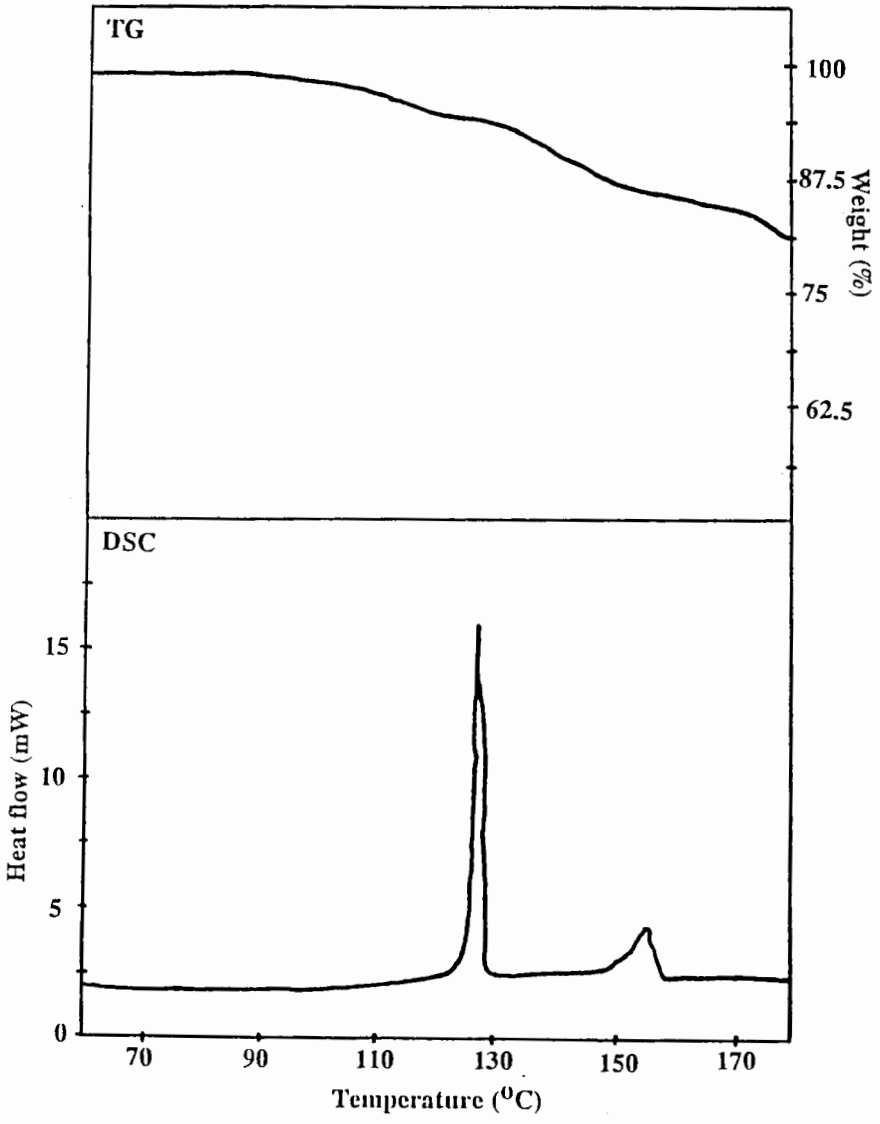

Figure 7.36. TG and DSC curves of $Ph_3COH \cdot$ dmso, 5°C min^{-1}, vented pan.

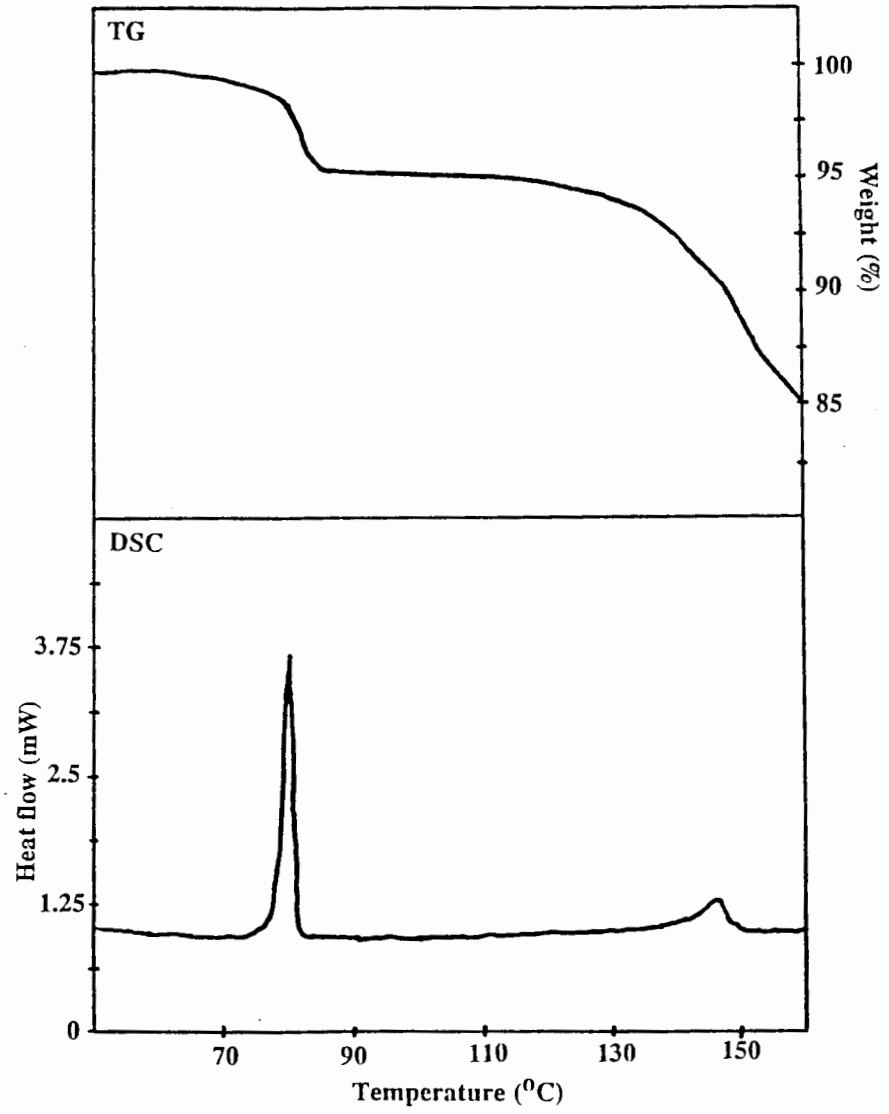

Figure 7.37. TG and DSC curves of **TRIPSID**, 5°C min^{-1}, vented pan.

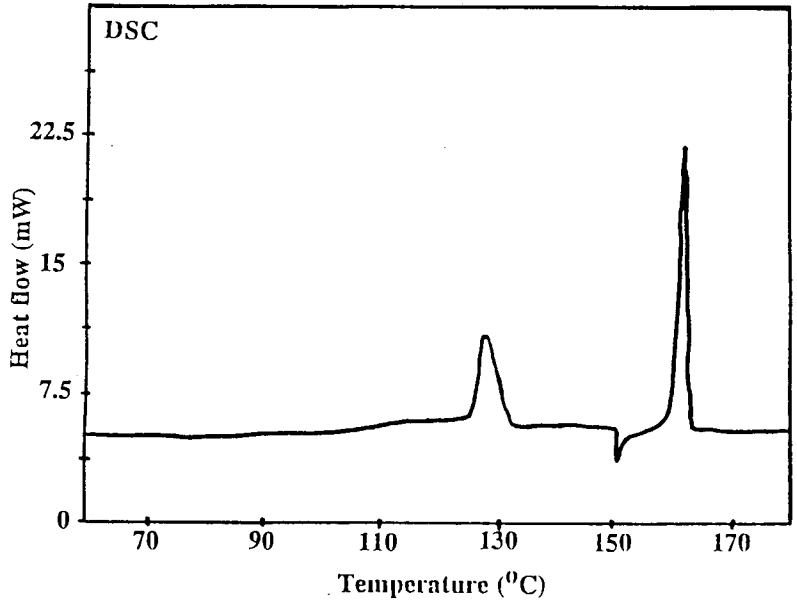

Figure 7.38. TG and DSC curves of $Ph_3COH \cdot$ dmso, 5°C min^{-1}, open pan.

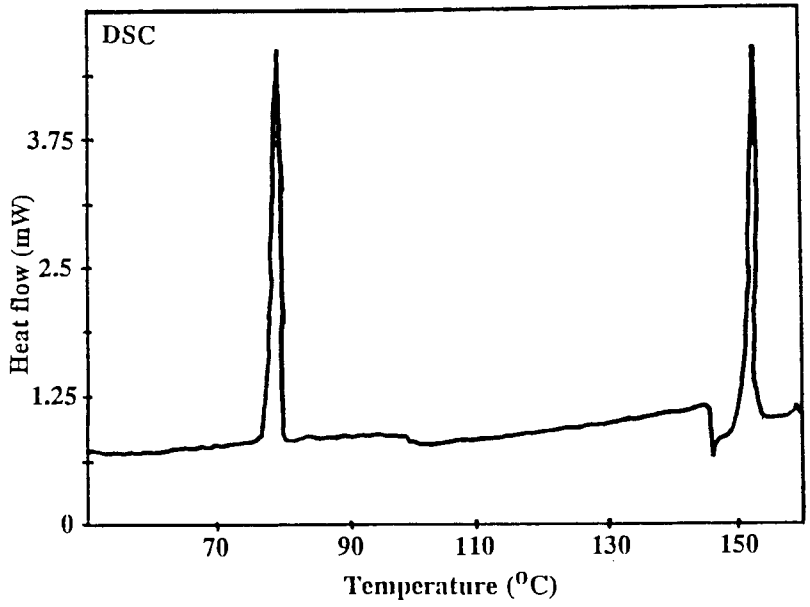

Figure 7.39. TG and DSC curves of **TRIPSID**, 5°C min^{-1}, open pan.

Table 7.2. Results of thermal analyses of dmso complexes.

Compound	Weight loss calculated (%)	Weight loss observed (%)	T_{on} (°C)	Peak area (J/g)	ΔH (kJmol^{-1})
10°Cmin-1					
DEMPE			138.1[a]	99.2	51.8
Ph_3COH · dmso			129.3	95.5	28.6
TRIPSID			80.8	61.2	19.3
DUNCAN			183.8	112.2	56.6
5°Cmin-1 (vented pans)					
DEMPE	29.89	29.51	97.5	103.5	54.2
			201.4	61.2	22.4
Ph_3COH · dmso	13.05	-[b]	126.4	95.7	28.7
			151.9	29.2	7.6
TRIPSID	12.38	-[b]	78.5	68.0	21.5
			141.6	20.1	5.6
DUNCAN	15.48	15.08	170.5	91.0	45.9
			204.9	48.2	20.6

[a] This peak corresponds to the "melting point" reported for this complex in reference 7.8.
[b] No sensible value for weight loss in TG was obtained (see text).

Table 7.2 ctd.

Compound	Weight loss calculated (%)	Weight loss observed (%)	T_{on} (°C)	Peak area (J/g)	ΔH(kJmol^{-1})
5°Cmin^{-1} (open pans)					
Ph_3COH · dmso			77.9	62.6	19.7
			151.1	60.2	16.7
TRIPSID			126.2	93.5	28.0
			160.9	93.3	24.3

Table 7.3. Visual observation of dmso complexes.

	DEMPE	$Ph_3COH \cdot dmso$	TRIPSID	DUNCAN
Fast heating rates ($> 10°Cmin^{-1}$)				
Liquid droplets appear on crystal surface (°C)	90	112	65	125
Crystal breaks up into crystallites, starting at	135	126	81	174
Crystal completely dissolved by	160	139	93	217
Slow heating rates ($2 - 5\ °Cmin^{-1}$)				
Liquid droplets appear, starting at	74	100	68	138
Crystal breaks up but doesn't fully dissolve, constant movement and rearrangement in liquid dmso, until melt of host begins at	196	158	154	205

Potential energy studies.

It should, in principle, be possible to correlate the measured enthalpy of the guest release reaction with the host-guest interactions which are found in the crystal structure. These interactions can be either van der Waals forces or hydrogen bonds. The potential energy environment of guest molecules in the host lattice was evaluated by the method of atom-atom potentials using EENY or HEENY as described in Chapter 2.

For each compound, the guest molecule was completely surrounded by host molecules. The positions of the latter were held constant while the guest, placed at the coordinates established in the crystal structure, was allowed to find its minimum energy environment by incremental rotations and translations. The position of the guest after minimization was expected to be very close to that at which it had been placed, both because EENY (or HEENY) finds only the local minimum and because the crystal structure is expected to be close to the most stable environment. Table 7.4 lists the results obtained from the thermal analysis and energy calculations for the relevant compounds.

Table 7.4. Potential energy of guest molecules.

Compound	ΔH (kJmol^{-1})	V_{min} (kJmol^{-1})
NATOL	33.2	-68.4
ODIN	61.6	-74.7
MAXINE	49.3	-63.1
NAPPY	42.3	-73.0, -47.0, -67.0
PEDIOX	29.4	-75.1
W1DIOX	51.9	-77.6
BASIL	58.4	-87.3
NADIO	58.2	-96.9
DEMPE	54.2	-75.2, -81.0, -76.1, -83.4
Ph_3COH · dmso	19.7	-54.3
TRIPSID	28.0	-68.2
DUNCAN	45.9	-77.6

Energy values obtained for different guest molecules cannot be compared directly, because the atom-atom potential method depends on the summation of atomic interactions of the guest with atoms surrounding it. In addition, the H:G ratio should be the same for structures to be compared. Thus, in the comparison of structures of tri-1-naphthylsilanol with toluene and xylene, only **ODIN** (*o*-xylene) and **MAXINE** (*m*-xylene) may be compared directly. **ODIN** has the higher value of ΔH and the lower value of U_{min}, thus allowing it to be classified the more stable compound.

In order to compare structures of the same guest with different hosts, care was taken to ensure that a single guest molecule was surrounded by host molecules (and other guests, if necessary). This approach gave at least a qualitative correlation between ΔH and V_{min} for the series of compounds with dioxane as guest :

more stable	ΔH	**NADIO ≈ BASIL > W1DIOX > PEDIOX**	*less stable*
	V_{min}	**NADIO > BASIL > W1DIOX > PEDIOX**	

In the series containing dmso several points arose :

(i) difficulty in obtaining sensible values for ΔH, especially for the complexes of Ph_3COH and Ph_3SiOH. These values are likely to have relatively large errors associated with them.

(ii) although the H:G ratio is 1:2 in **DEMPE**, there are in fact four crystallographically distinct guests. Each of these was minimized separately, by surrounding it with host and other guest molecules.

The following tentative order of stability is suggested :

more stable	ΔH	**DUNCAN > TRIPSID > Ph_3COH · dmso**	*less stable*
	V_{min}	**DUNCAN > TRIPSID > Ph_3COH · dmso**	

Since it is difficult to find an appropriate average potential energy for **DEMPE**, and its ΔH is also more complex, arising from the loss of more than one guest, this compound was omitted from the analysis.

Determination of the activation energy of guest desorption.

Information on the kinetics or mechanism by which an inclusion compound decomposes is of value in understanding the nature of the inclusion compound. Several methods, using TG, for establishing the kinetics of such reactions have been proposed. [7.2]

The rate of a homogenous reaction :

$$A \rightarrow B + C$$

is measured by following the change in concentration of one of the reactants or products.

For a heterogenous reaction :

$$A(s) \rightarrow B(s) + C(g)$$

concentration no longer has the same significance. It is replaced rather by such geometrical concepts as crystal structure or defects in crystal structure.

Decomposition of solid reactants is often initiated at defective regions in the crystal such as the surface or at dislocations on the surface. The gaseous product escapes and the resulting disruption causes strain in the neighbouring regions, resulting in further decomposition. Reaction is localised at the reactant/product interface and diffusion processes may become rate-controlling.

The loss of mass of the sample or the heat absorbed or evolved during decomposition may be measured and related to the dimensionless extent of decomposition, C : *eg.*

$$C = (m_o - m)/(m_o - m_f)$$ where m_o and m_f are initial and final masses.

C may be measured as a function of time (at constant temperature) which corresponds to the conventional concentration *vs* time curve of homogeneous kinetics. C may instead be measured as a function of temperature, which is increased according to a linear heating programme, $\beta = dT/dt$.

In either case, the observed C, t or C, T results are fitted to a small set of models based on a geometrical form of progress at the reactant/product interface. The expressions derived from these models can all be written in their integral forms (at constant T) as :

$$f(C) = k(t - t_0)$$

or differential forms as :

$$dC/ct = k\, g(C).$$

The effect of temperature is introduced by the Arrhenius equation, $k = Ae^{-E/RT}$ so :

$$dC/dt = Ae^{-E/RT} g(C).$$

The validity of the Arrhenius equation in this context is questionable but the parameters E and A do have practical value even if they are not interpretable theoretically. [7.2]

For dynamic measurements, the expression above is written :

$$dC/dT = (dC/dt)(dt/dT) = (1/\beta)(dC/dt)$$

Then, $dC/dT = (A/\beta)e^{-E/RT} g(C)$.

Flynn and Wall [7.6] rearranged the above equation and differentiated it with respect to C. They assumed that A, g(C) and E are independent of temperature and that A and E are independent of g(C). Using finite differences, rather than the derivative, they arrived at the following equation :

$$d(\log \beta)/d(1/T) \approx (0.457/R)E$$

Thus, from weight loss *vs* temperature curves at several heating rates, β, the corresponding temperatures at a constant weight loss (or degree of conversion, C) may be read off. A plot of $\log \beta$ *vs* $1/T$ yields a straight line with slope = $(R/0.457)E$. The procedure is repeated at several values of C, to give a more precise average value of E and to establish the validity of the method for each sample.

This method was originally developed for the degradation of polymers, but has also been applied to the decomposition of inorganic complexes. [7.7]

Results.

It was observed during these experiments that the starting temperature and shape of the decomposition curves are highly sensitive to sample preparation. The instability of the inclusion compounds made it impossible to ensure completely uniform particle size. Thus, although every effort was made to keep the sample preparation identical for each analysis, the $-\log \beta$ *vs* $1/T$ plots for most compounds showed only fair correlation.

Some compounds were impossible to analyse by this method as varying the heating rate led to different decomposition pathways. One such example is shown in Figure 7.40, the decomposition curves of **PECTIL**.

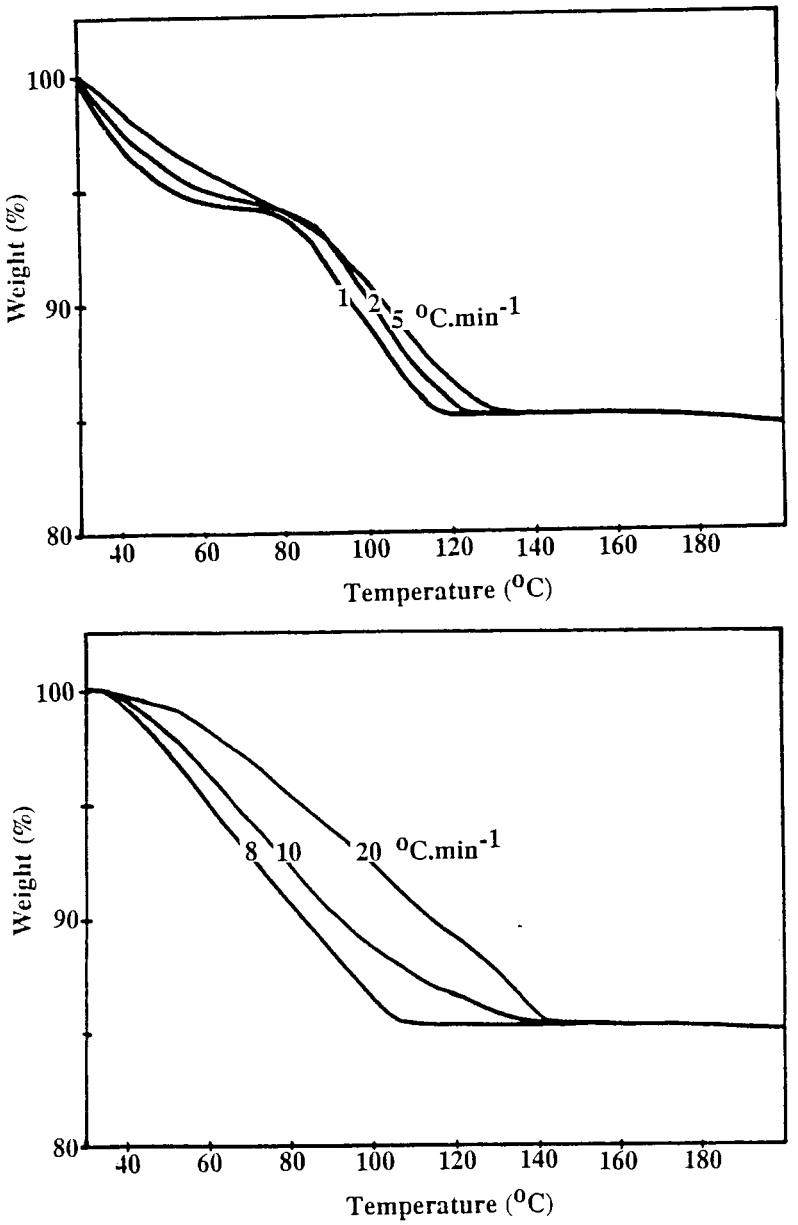

Figure 7.40. Desorption curves of **PECTIL**.

At heating rates of up to 5°Cmin^{-1}, a two-step decomposition occurs. As the heating rate is increased however, the curve smooths out into a single step. For both sets of curves, kinetic plots were found to be non-linear. This implies that the guest desorption process is non-uniform so no value for the activation energy can be obtained.

The weight losses observed in **BASIL** (6.78%) and **SETH** (3.99%) were too small for any meaningful analysis to be made. TG had not proved to be a reliable method of analysis for **TRIPSID** (previous section), so this compound was also excluded.

The desorption curves for **W1DIOX** are shown in Figure 7.41, along with the corresponding kinetic plot.

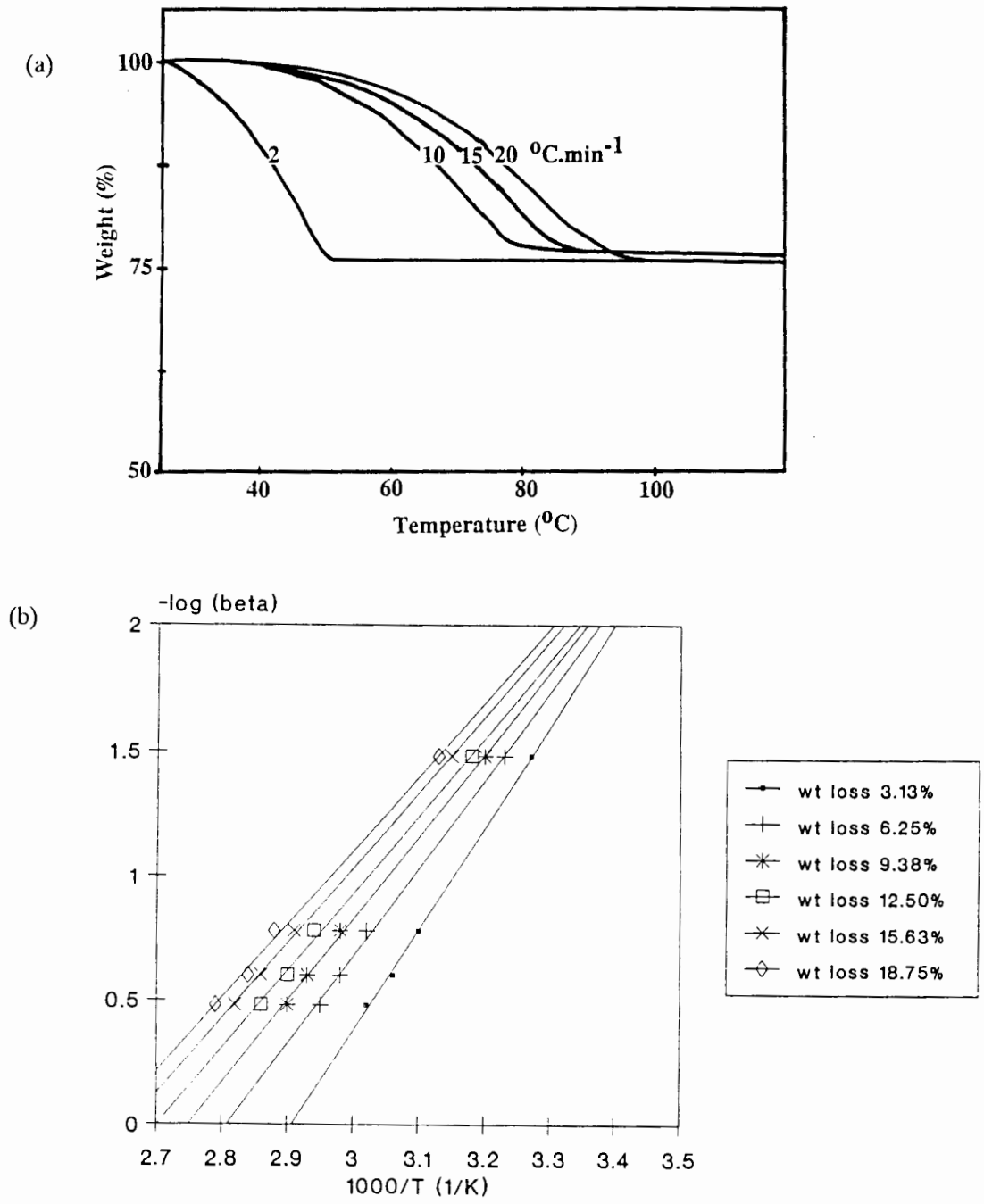

Figure 7.41. (a) Desorption and (b) kinetic curves of **W1DIOX.**

The desorption process shown is obviously not uniform. The individual -log β *vs* 1/T plots change continuously, giving rise to values for the activation energy in the range 54 - 74 kJmol^{-1}. One or more of the assumptions made by Flynn and Wall do not hold in this case.

The plots for the loss of dmso from **DEMPE** at heating rates of 2, 5, 10, 20 and 30 °Cmin^{-1} and the corresponding -log β *vs* 1/T plots are shown in Figure 7.42.

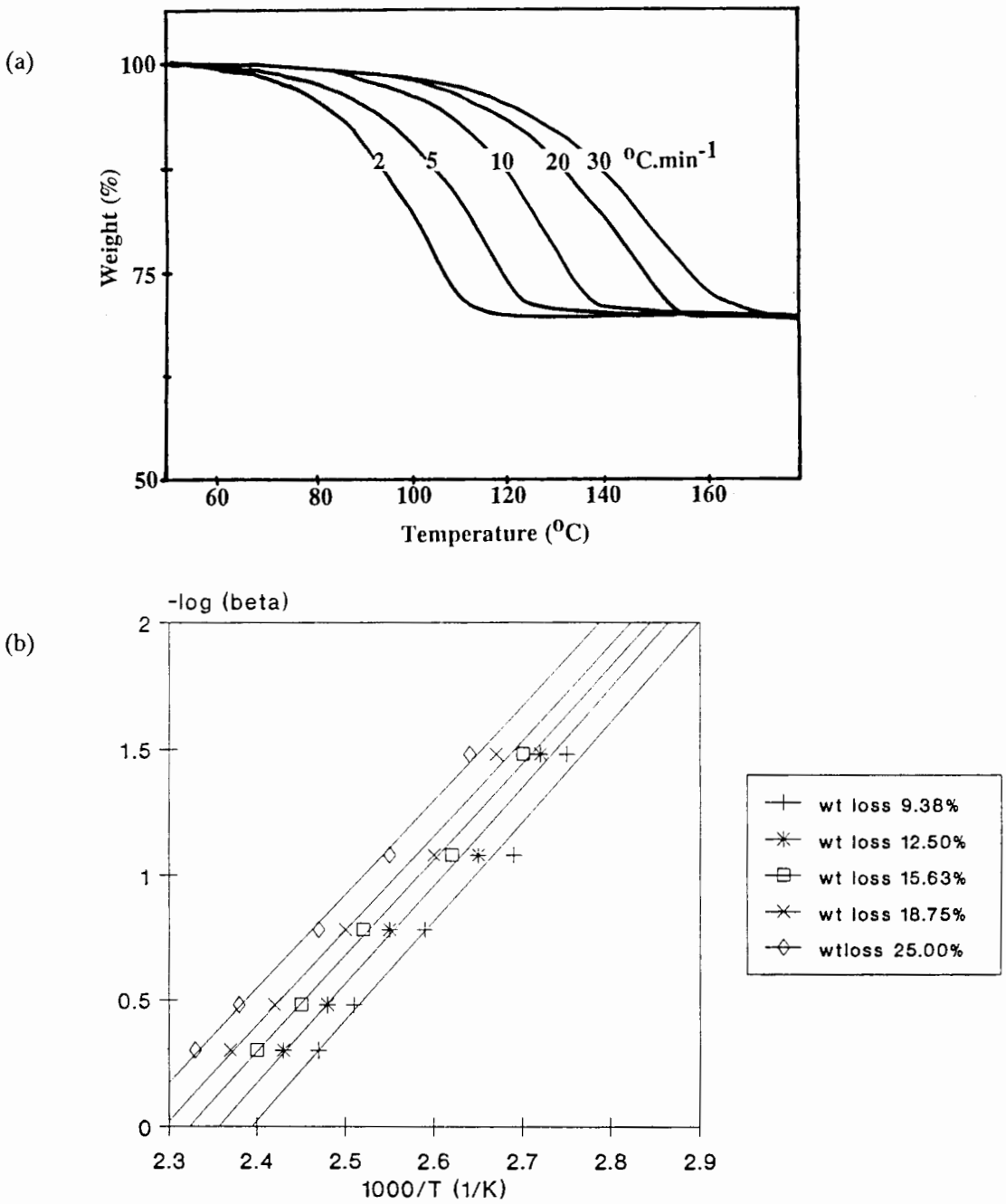

Figure 7.42. (a) Desorption and (b) kinetic curves of **DEMPE.**

Good correlation between the points allowed an activation energy of 71 ±2 kJmol^{-1} to be calculated.

Surprisingly, given the high lability of the acetone guest, the curves observed for **PEACH** (Figure 7.43) show good correlation.

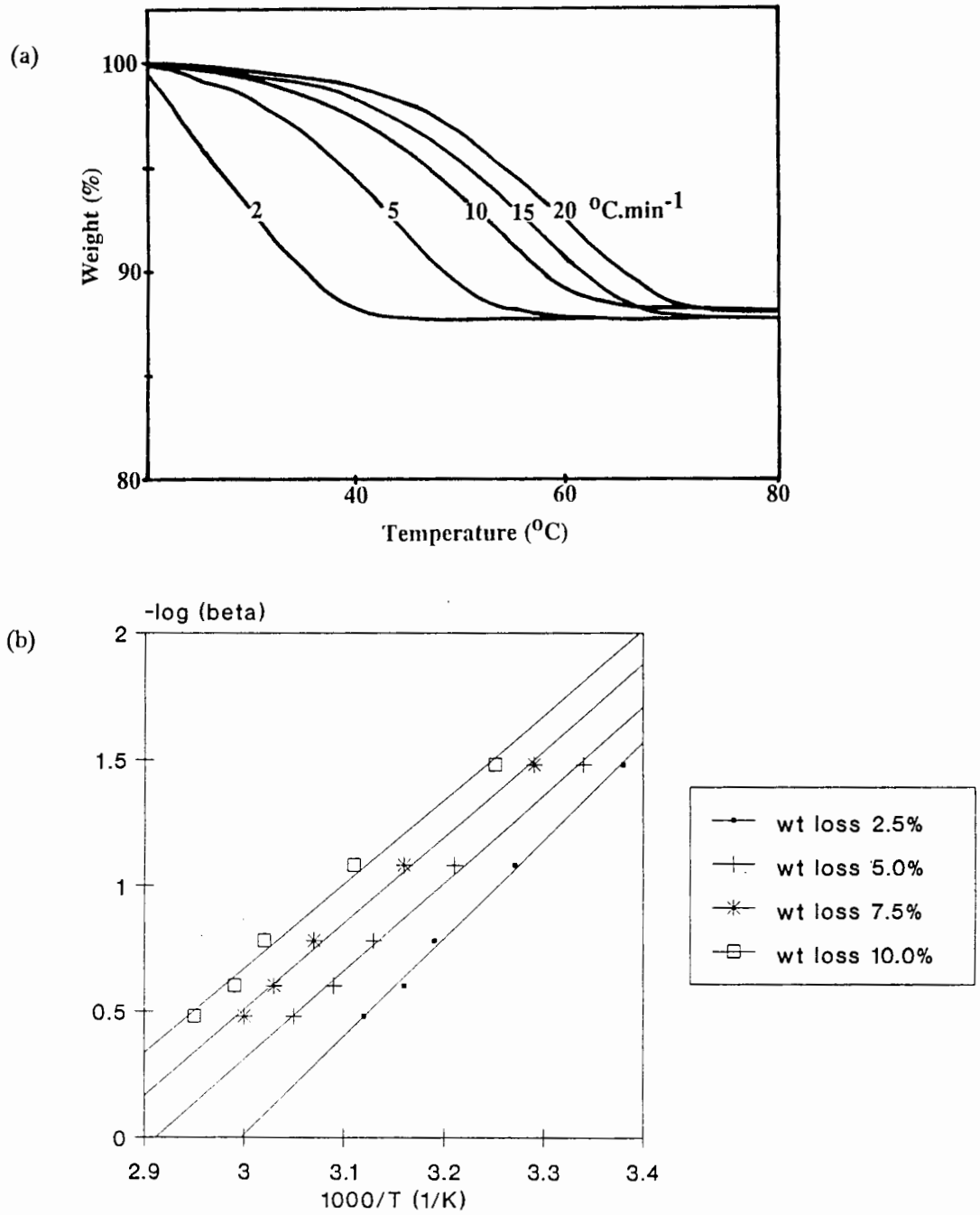

Figure 7.43. (a) Desorption and (b) kinetic curves of **PEACH**.

A relatively low activation energy of 64 ±4 kJmol^{-1} was calculated. This accords with the extremely fast decay observed once **PEACH** crystals were removed from their mother liquor.

Desorption and kinetic curves for the compounds of 1,1,2,2-tetraphenylethane-1,2-diol with three lutidine isomers (**DINM**, **LUTI** and **DINO**) are shown as Figures 7.44 - 7.46.

LUTI and **DINO** each lose their guests in two distinct steps. The incomplete separation of the two processes leads to difficulties in interpretation, particularly at high heating rates, where the second desorption process begins to overlap the first.

In each case, the two processes were analysed separately. The values obtained for these compounds are listed below.

Compound	**E ($kJmol^{-1}$)**
DINM	74 ±3
LUTI, 1st step	64 ±4
LUTI, 2nd step	64 ±1
DINO, 1st step	69 ±4
DINO, 2nd step	57±3

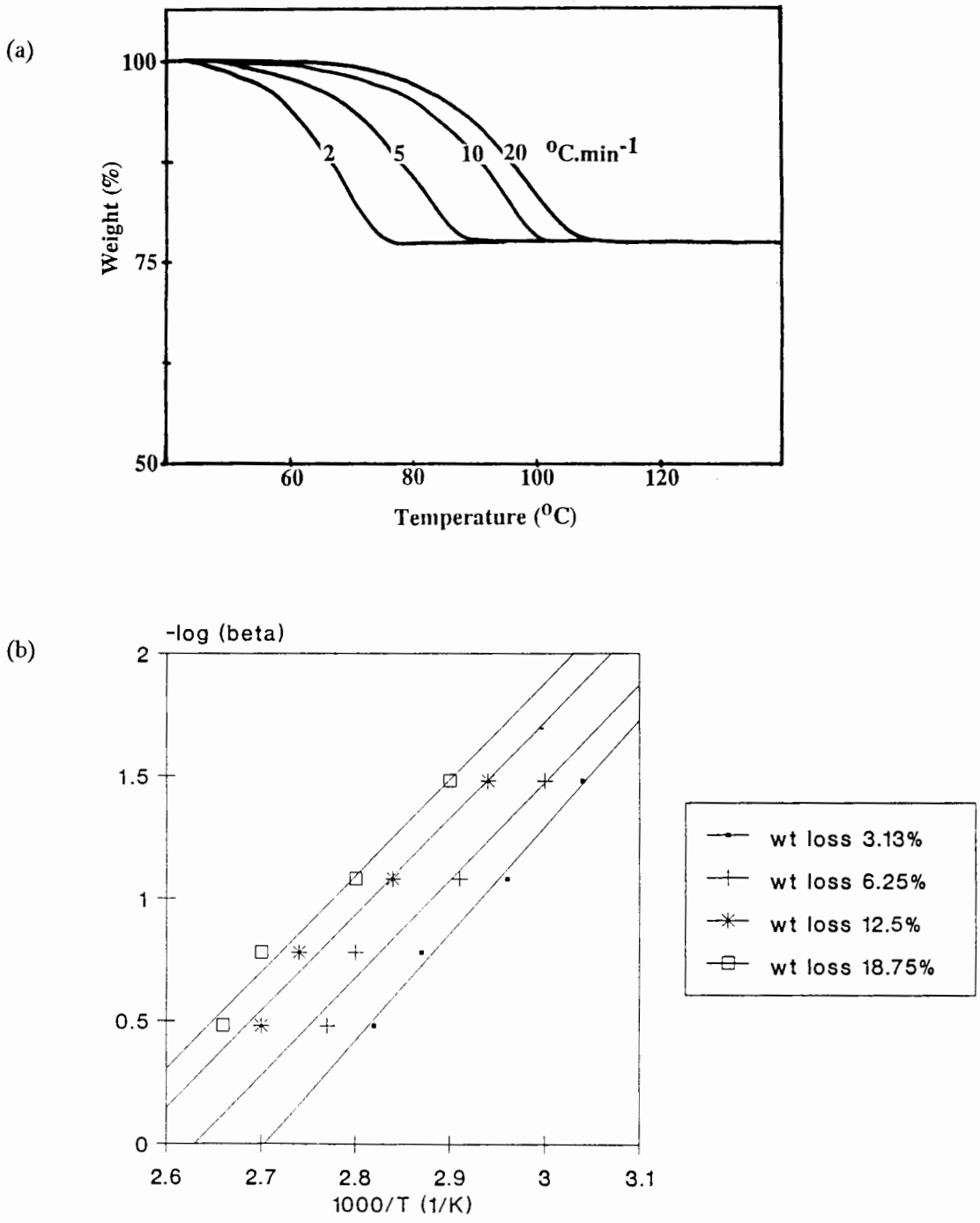

Figure 7.44. (a) Desorption and (b) kinetic curves of **DINM**.

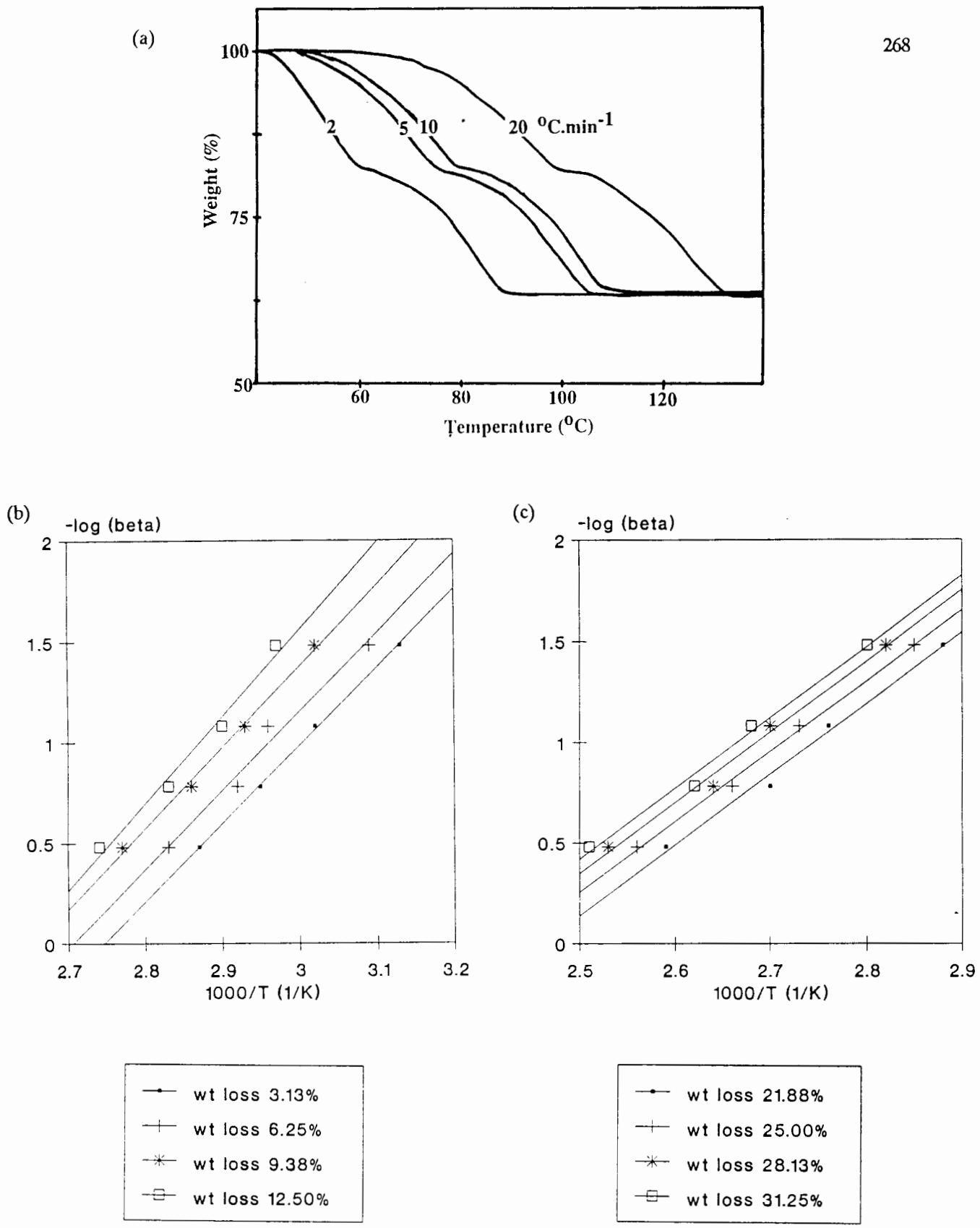

Figure 7.45. (a) Desorption curve of **LUTI**. (b) and (c) kinetic curves for the two-stage decomposition of **LUTI.**

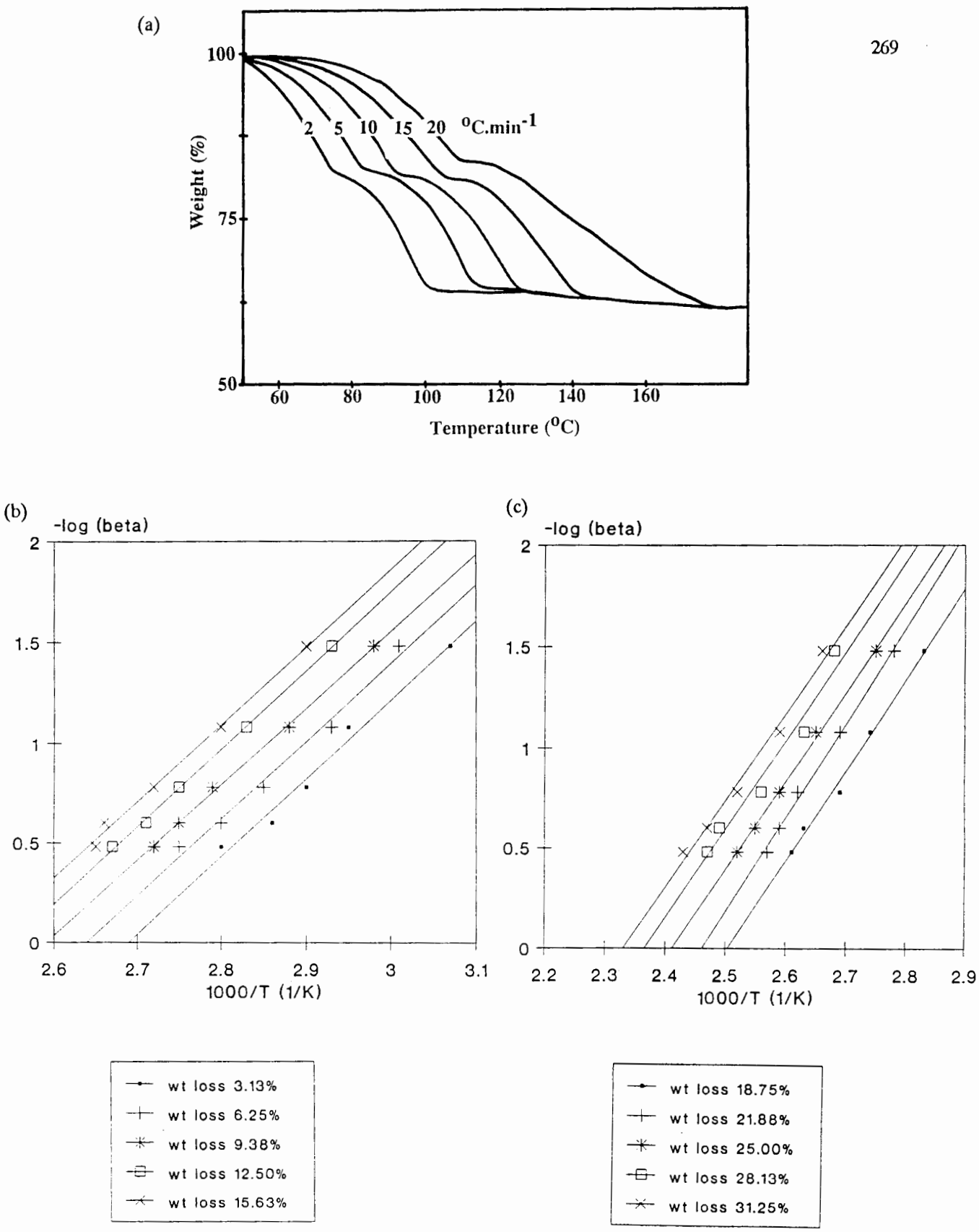

Figure 7.46. (a) Desorption curve of **DINO**. (b) and (c) kinetic curves for the two-stage decomposition of **DINO.**

Another series of related compounds is that of tri-1-naphthylsilanol with toluene, *o*-, *m*- and *p*-xylene. Desorption and kinetic curves for these four compounds are shown in Figures 7.47 -7.50. In all cases, the guest desorption occurs as a single step, even for **NAPPY**, where the host to guest ratio is 1:2. Good correlations were observed in the kinetic plots and the activation energies obtained for the guest desorption are listed below.

Compound	**E ($kJmol^{-1}$)**
NATOL	94 ±2
ODIN	89 ±2
MAXINE	100 ±4
NAPPY	102 ±7

These values fall within a narrow range, but are higher than the energies calculated for the other inclusion compounds. These four compounds are relatively stable, taking several hours to decompose at room temperature. Hence visual observations correlate, at least qualitatively, with the values obtained for the activation energies.

Similar values to those found in this study have been obtained by Iwamoto *et al.* for the release of benzene from Hofmann-type clathrates[7.9] and for the release of nitriles and substituted pyridines from *trans*-9,10-dihydroxy-9,10-diphenyl-9,10-dihydroanthracene.[7.10]

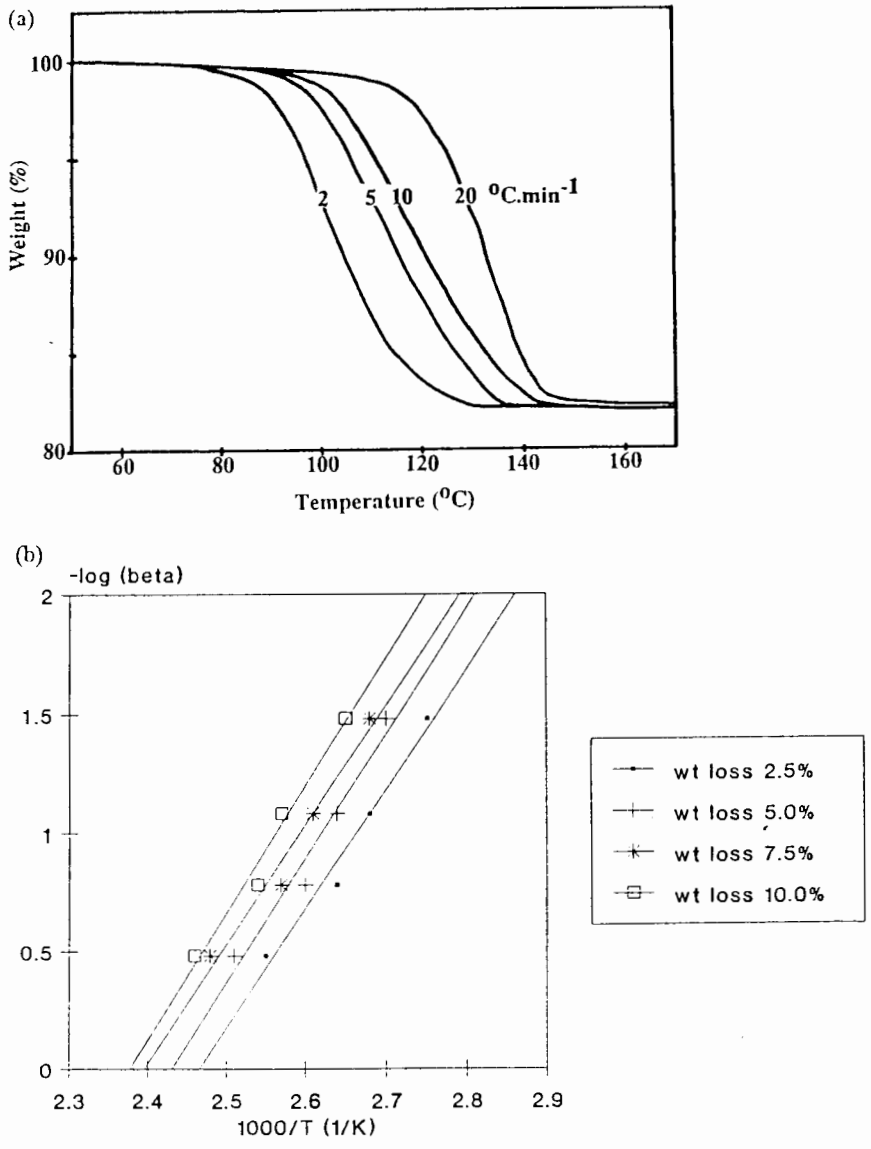

Figure 7.47. (a) Desorption and (b) kinetic curves of NATOL.

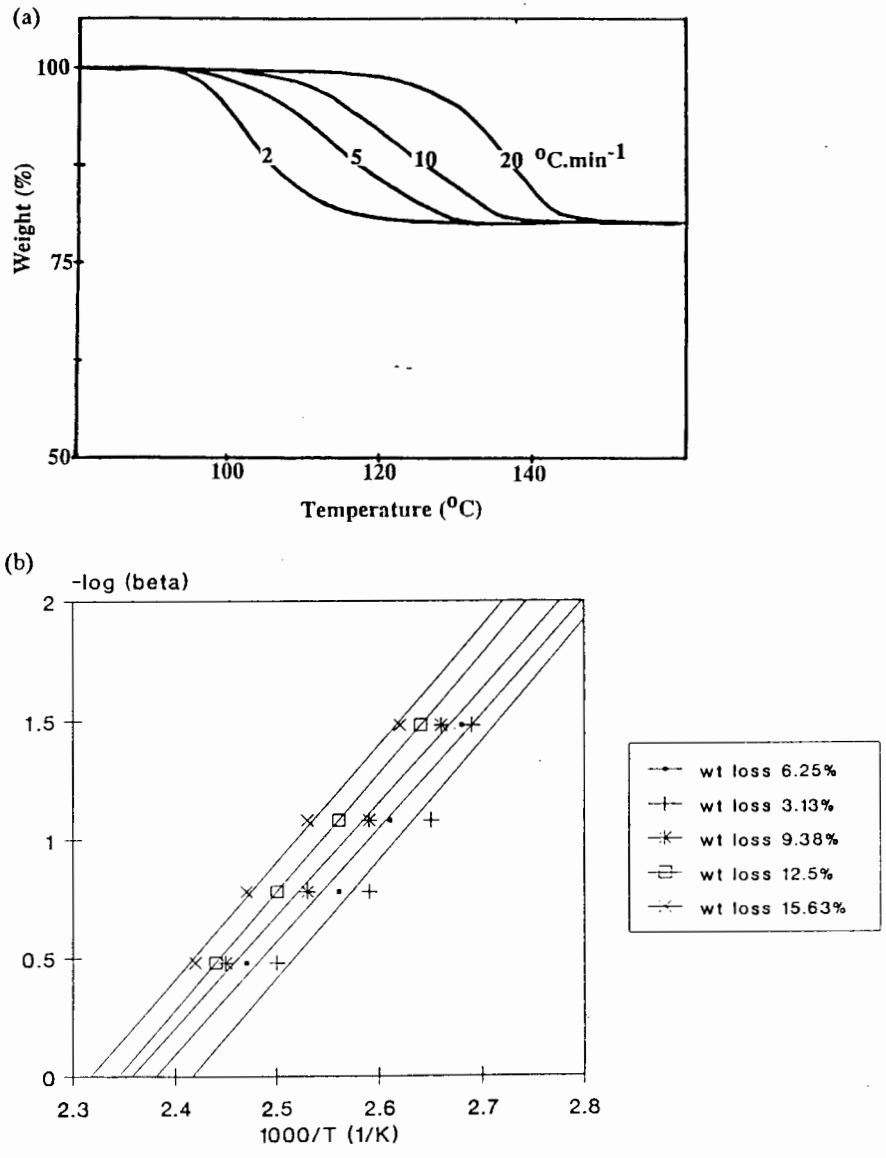

Figure 7.48. (a) Desorption and (b) kinetic curves of ODIN.

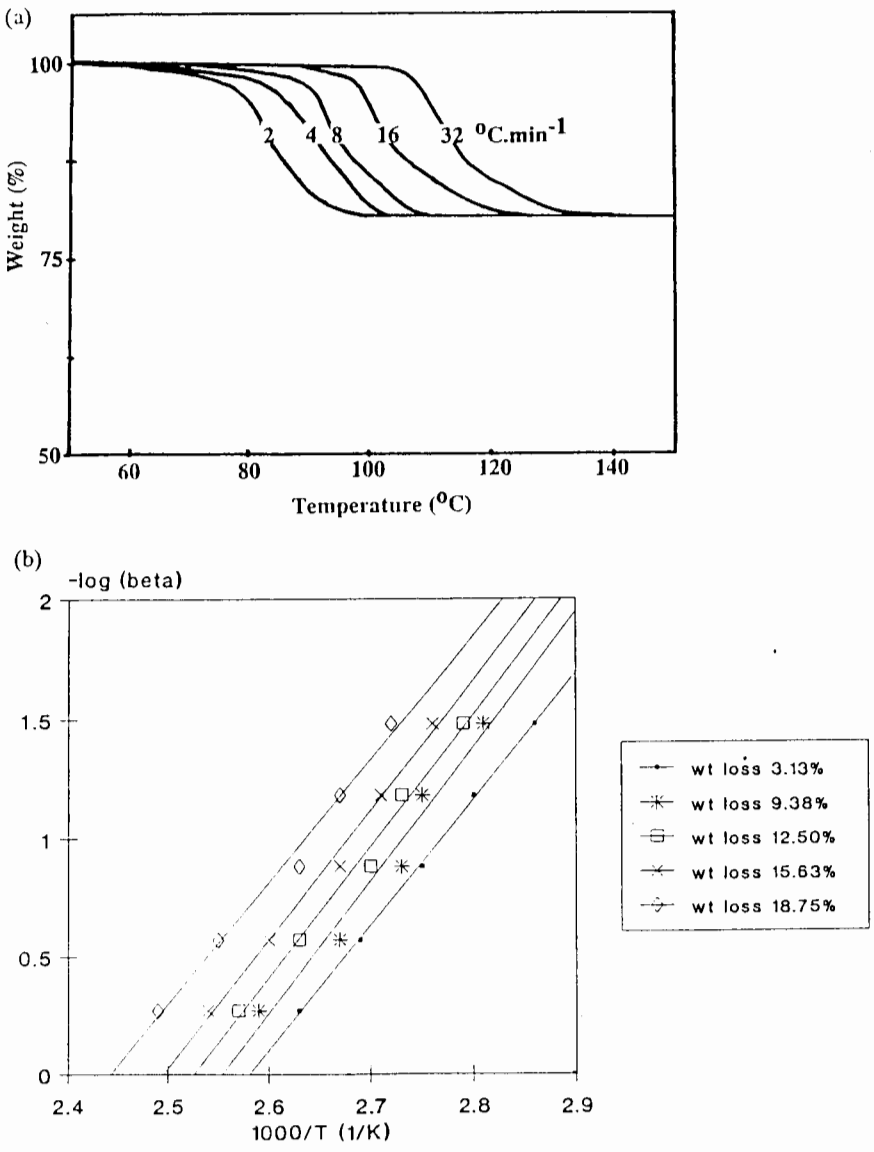

Figure 7.49. (a) Desorption and (b) kinetic curves of **MAXINE**.

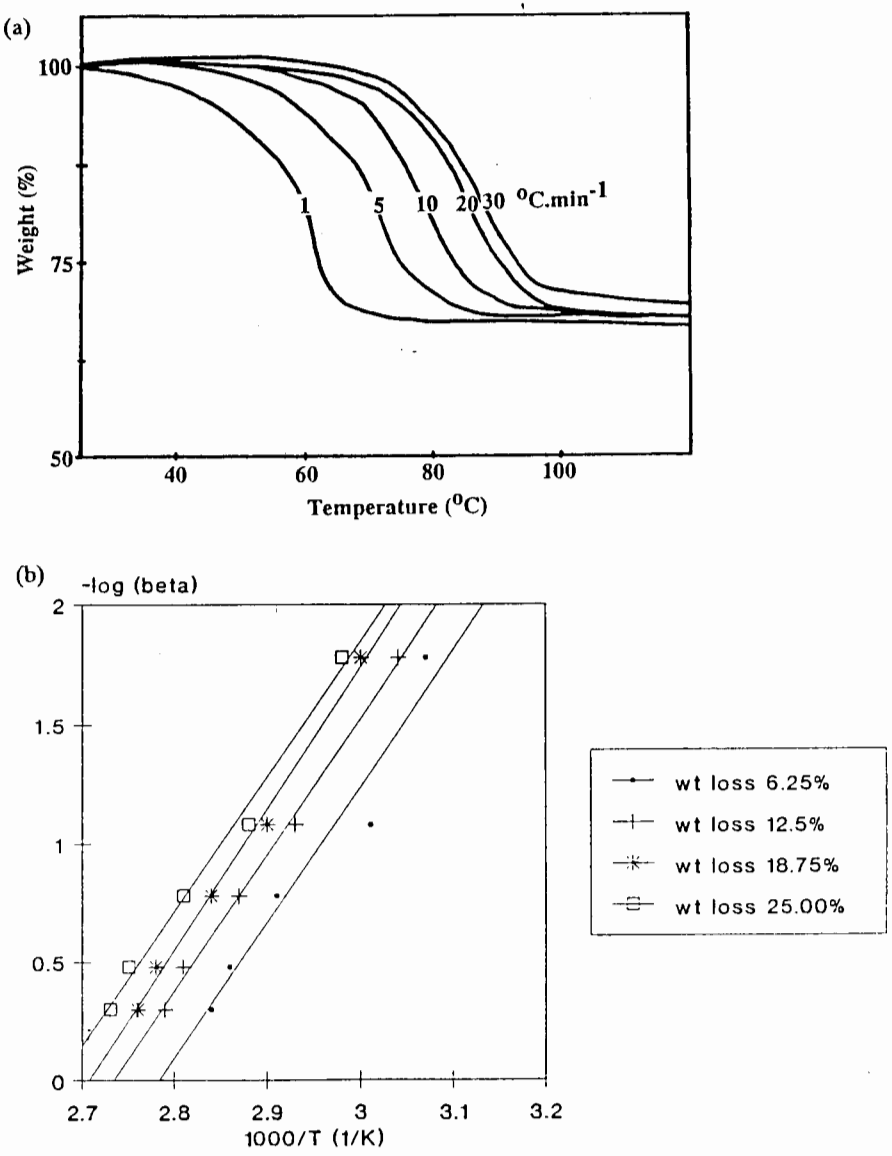

Figure 7.50. (a) Desorption and (b) kinetic curves of **NAPPY**.

References.

7.1. W. W. Wendlandt. *Thermal Analysis.* 3rd edition. John Wiley and Sons, London. (1986).

7.2. M. E. Brown. *Introduction to Thermal Analysis.* Chapman and Hall, (1988).

7.3. B. Wunderlich. *Thermal Analysis.* Academic Press, (1990).

7.4. E. Weber; K. Skobridis; I. Goldberg. *J. Chem. Soc., Chem. Commun.* 1195, (1989).

7.5. D. R. Bond; M. R. Caira; G. A. Harvey; L. R. Nassimbeni; F. Toda. *Acta Crystallogr.* **B46**, 771, (1990).

7.6. J. H. Flynn; L. A. Wall. *Polymer letters.* **4**, 323, (1966).

7.7. M. A. Herman; H. Hoffmans; H. O. Desseyn. *Thermochimica Acta.* **85**, 63, (1985).

7.8. F. Toda; K. Tanaka; Y. Wang; G-H. Lee. *Chem. lett.* 109, (1986).

7.9. T. Kitazawa; Y. Mizushima; J. Shiraha; R. Taguchi; A. Katoh; T. Hasegawa; S-I. Nishikiori; T. Iwamoto. *J. Incl. Phenom. and Mol. Recogn. in Chem.* **10**, 29, (1991).

7.10. W-D. Schubert. MSc. thesis, University of Cape Town, 1991.

CHAPTER 8 : CONCLUSION.

The ability of the four related hydroxy molecules A - D to form inclusion compounds has been studied.

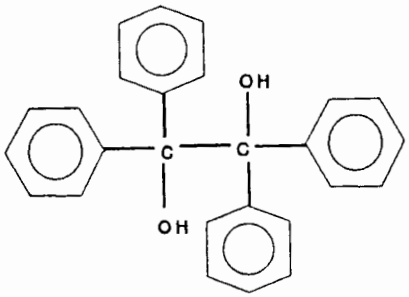

A

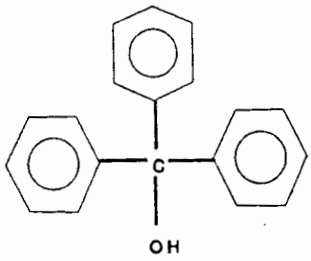

B

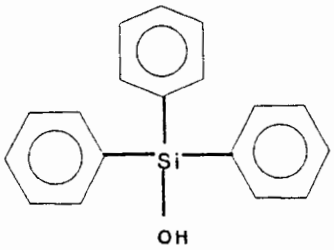

C

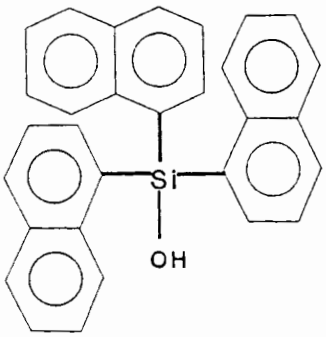

D

These hosts have a common feature : each has a tetrahedral atom (either C or Si) bonded to a hydroxyl group and shielded by at least two bulky aromatic moieties. The aromatic groups make these compounds difficult to crystallize in their non-porous α-phases. This, together with their "probe" hydroxyl groups, allows for the formation of topologically and chemically varied inclusion compounds.

The host : guest ratios observed ranged from 4:1 to 1:2 testifying to the versatility of these compounds as host molecules.

Hydrogen bonding proved to be the greatest stabilizing force in these compounds. Host···Host, Host···Guest, or a combination of these hydrogen bonds were observed. Host-guest aggregates took a number of forms :

multimolecular chains were the most common form; chain length varied from two to up to five molecules,

infinite ribbons were seen in **PEDIOX**,

a ring was found in **SETH**.

An infinite chain of host molecules in **PECTIL** provided the frame into which the guest fitted.

The thermal decomposition of the inclusion compounds was studied, to determine the forces holding the guest within the structure and to understand the changes in the host lattice as the guest was desorbed. To this end, DSC and XRD were used to observe and confirm phase changes in the compounds as the guest was lost.

The enthalpies of guest desorption ranged between 11.0 and 100.9 $kJmol^{-1}$. In most cases, the guest was released from the crystals before the boiling point of the pure guest compound. This is not unexpected; if the guests are held in the lattice in such a way that they are isolated (more than 5 Å from another guest molecule), they can be regarded as being in the gaseous phase already.

Since, in most cases the guest was intimately involved in the structure's framework, it was expected that the removal of the guest would severely disrupt the packing. The only example of a β-phase compound in which the guest was not hydrogen bonded to the host was **PECTIL** (the *p*-chlorotoluene complex of 1,1,2,2-tetraphenylethane-1,2-diol). This compound might have been expected to lose its guest without disruption of the host framework (leaving behind an empty host lattice, or β_0-phase). XRD studies however, revealed that the loss of the *p*-chlorotoluene results in the collapse of the host lattice to the α-phase.

Similar collapse to their respective α-phases was observed for all compounds. In some cases, (**LUTI** and **DINO** the 3,5- and 3,4-lutidine complexes with 1,1,2,2-tetraphenylethane-1,2-diol, and in **SETH**, the ethanol complex of triphenylsilanol), an intermediate, or γ-phase, was seen. The DSC in these cases showed an endotherm which corresponded to the phase change from γ- to α-phase.

TG was used to determine the activation energy of the guest desorption process. Limitations in the method used as well as complex desorption processes and difficulties in sample preparation, meant that only nine of the eighteen inclusion compounds yielded reasonable results. The values obtained for the activation energy were between 54 and 102 $kJmol^{-1}$ which are within the same range as those reported for similar compounds.

The results of a preliminary competition experiment between 2,6- and 3,5-lutidine indicated that 3,5-lutidine is preferentially included in the structure of the host 1,1,2,2-tetraphenylethane-1,2-diol.

Selectivity studies of the triphenylsilanol host gave the following results :

Mixture of liquid solvents (ratio)	Inclusion compound formed (H : G)
MeOH/EtOH (1:1)	EtOH (4:1)
PrOH/EtOH (1:1)	EtOH (4:1)
H_2O/EtOH (up to 40% H_2O)	EtOH (4:1)
Dmso/EtOH (1:1)	Dmso (2:1)
Dioxane/EtOH (1:1)	Dioxane (4:1)
Dmso/Dioxane (1:1)	Dmso (2:1)

The compounds of tri-1-naphthylsilanol with the three isomers of xylene and with toluene had some interesting features. An unusual form of hydrogen bonding (between the host's hydroxyl group and the aromatic π electrons of the guests) was observed. The presence of this hydrogen bonding was inferred from the distances of the hydroxyl group from the centres of the aromatic rings and confirmed by the shifts in the infrared spectra of these four compounds.

One might expect that the compound of greatest stability would have the lowest crystal potential energy, U_{min} (evaluated by EENY) and the highest value of ΔH (obtained from DSC). The results of the intermolecular energy calculation must however be treated with caution because comparison of host-guest interactions should be carried out only between guests which are geometrical isomers and among compounds which have the same H:G ratio. This allows only **ODIN** (the *o*-xylene complex) and **MAXINE** (the *m*-xylene complex) to be compared. The results are listed below ; **ODIN** has both the lower potential energy and the higher value of ΔH, thus it is the more stable compound of the two.

	NATOL	ODIN	MAXINE	NAPPY
H : G	1:1	1:1	1:1	1:2
ΔH (kJmol^{-1})	33.2	61.6	49.3	42.3
U_{min} (kJmol^{-1})	-68.4	-74.7	-63.1	-73.0, -47.0, -67.0

Each of the four hosts was found to form inclusion compounds with dioxane. The topology of these compounds fell into two categories. The triarylalcohols entrapped dioxane in pockets and could be classified as aediculates, while the complex with the diol host was a tubulate with the dioxane molecules lying in channels. There was a qualitative correlation between the minimum potential energy (HEENY) and the enthalpy of the guest release reaction (DSC) :

	PEDIOX	W1DIOX	BASIL	NADIO
H:G	1:1	1:1	4:1	1:1
ΔH (kJmol^{-1})	29.4	51.9	58.4	58.2
V_{min} (kJmol^{-1})	-75.1	-77.6	-87.3	-96.9

The following stability pattern applies :

more stable ΔH **NADIO ≈ BASIL > W1DIOX > PEDIOX** *less stable*

V_{min} **NADIO > BASIL > W1DIOX > PEDIOX**

Dmso was another guest which formed inclusion compounds with all four hosts. As was observed in the dioxane structures, the triarylalcohol complexes (Ph_3COH·dmso, **TRIPSID**, **DUNCAN**) were aediculates while the diol complex (**DEMPE**) was a tubulate. The high boiling point of dmso made determination of sensible thermal analyses for these compounds quite difficult. Each of the four crystallographically distinct dmso molecules in **DEMPE** was minimized separately by surrounding it with host and other guest molecules.

	DEMPE	Ph_3COH·dmso	**TRIPSID**	**DUNCAN**
H:G	1:2	2:1	2:1	1:1
ΔH ($kJ.mol^{-1}$)	54.2	19.7	28.0	45.9
V_{min} ($kJ.mol^{-1}$)	-75.2, -81.0, -76.1, -83.4	-54.3	-68.2	-77.6

Since it is difficult to find an appropriate average potential energy for **DEMPE**, and its ΔH is caused by the loss of more than one guest, this compound was not included in a comparison of these values.

The following order of stability is proposed for the remaining three compounds :

more stable ΔH **DUNCAN** > **TRIPSID** > Ph_3COH·dmso *less stable*

V_{min} **DUNCAN** > **TRIPSID** > Ph_3COH·dmso

Thus, as the host increases in size, its complex with dmso becomes more stable.

A better understanding of the stability of these inclusion compounds has been obtained, in that the energy between host and guest entities can be correlated, at least qualitatively, with their structures.

The inclusion of a small organic molecule into the framework of a host compound is a complex process. Better understanding of this process can best be obtained by studying the molecular environment of the guest - the size and shape of the cavity, the types of moieties that surround it and the energies involved in both the inclusion and desorption of the guest. In addition, competition and selectivity studies may lead to the design of more efficient and specific hosts.

Compounds studied.

Host	Guest	Host:Guest	Code name
Class A.			
1,1,2,2-Tetraphenyl-	-	-	**PEDIL**
ethane-1,2-diol	dmso	1:2	**DEMPE**
	dioxane	1:1	**PEDIOX**
	p-chlorotoluene	2:1	**PECTIL**
	2,6-lutidine	1:1	**DINM**
	3,5-lutidine	1:2	**LUTI**
	3,4-lutidine	1:2	**DINO**
	acetone	1:1	**PEACH**
Class B.			
Triphenylmethanol	dioxane	1:1	**W1DIOX**
Class C.			
Triphenylsilanol	-	-	**WEB2**
	dmso	2:1	**TRIPSID**
	dioxane	4:1	**BASIL**
	ethanol	4:1	**SETH**
Class D.			
Tri-1-naphthylsilanol	dmso	1:1	**DUNCAN**
	dioxane	1:1	**NADIO**
	toluene	1:1	**NATOL**
	o-xylene	1:1	**ODIN**
	m-xylene	1:1	**MAXINE**
	p-xylene	1:2	**NAPPY**
	triethylamine	1:1	**NATRET**

APPENDIX 1.

Runstreams used for Cambridge Structural Database searches.

a) To find Ph - X - OH ••• O where X may be any atom in systems containing only C, H, O, N, S, Si.

```
T1 *ELEM 4M
T2 *ELEM 8A
T3 *ELEM 7A
T4 *ELEM SE
T5 *ELEM AS
T6 *ELEM TE
T7 *ELEM P
T8 *ELEM B
T9 *CONN
AT1 AA 2
AT2 O 1 1 E
AT3 O 1
AT4 C 3 0
AT5 C 2 1
AT6 C 2 1
AT7 C 2 1
AT8 C 2 1
AT9 C 2 1
BO 1 2 1 A
BO 1 4 1 A
BO 4 5 5 C
BO 5 6 5 C
BO 6 7 5 C
BO 7 8 5 C
BO 8 9 5 C
BO 4 9 5 C
NOL
END
SAVE 3
QUEST T9 - T1 - T2 - T3 - T4 - T5 - T6 - T7 - T8
```

b) Test, using GSTAT, to identify all possible hydrogen bonds in the file created in part (a).

```
CALC INTER FROM O 1.6 TO O 1.6 EXT
FRAG O-H...O
AT1 O 2
AT2 H 1
AT3 O 2
BO 1 2 0.70 1.15
BO 1 3 2.30 3.10
BO 2 3 1.10 2.50
END
DEF O...O 1 3
DEF O-H 1 2
DEF H...O 2 3
DEF HANG 1 2 3
SCAT O...O  O-H
SCAT H...O  O-H
SCAT O...O HANG
SCAT H...O HANG
END
```

c) To find Ph - X - OH ••• N where X may be any atom in systems containing only C, H, O, N, S, Si.

```
T1 *ELEM 4M
T2 *ELEM 8A
T3 *ELEM 7A
T4 *ELEM SE
T5 *ELEM AS
T6 *ELEM TE
T7 *ELEM P
T8 *ELEM B
T9 *CONN
AT1 AA 2
AT2 O 1 1 E
AT3 N 1
AT4 C 3 0
AT5 C 2 1
AT6 C 2 1
AT7 C 2 1
AT8 C 2 1
AT9 C 2 1
BO 1 2 1 A
BO 1 4 1 A
BO 4 5 5 C
BO 5 6 5 C
BO 6 7 5 C
BO 7 8 5 C
BO 8 9 5 C
BO 4 9 5 C
NOL
END
SAVE 3
QUEST T9 - T1 - T2 - T3 - T4 - T5 - T6 - T7 - T8
```

d) Test, using GSTAT, to identify all possible hydrogen bonds in the file created in part (c).

```
CALC INTER FROM O 1.6 TO N 1.5 EXT
FRAG O-H...N
AT1 O 2
AT2 H 1
AT3 N 2
BO 1 2 0.70 1.15
BO 1 3 2.30 3.10
BO 2 3 1.10 2.50
END
DEF O...N 1 3
DEF O-H 1 2
DEF H...N 2 3
DEF HANG 1 2 3
SCAT O...N  O-H
SCAT H...N  O-H
SCAT O...N HANG
SCAT H...N HANG
END
```